Escola de Camins
Escola Tècnica Superior d'Enginyeria de Camins, Canals i Ports
UPC BARCELONATECH

DOCTORAL THESIS

Article-based Ph.D. Thesis:

Sustainability, Durability, and Mechanical Characterization of a New Recycled Textile-Reinforced Strain-Hardening Cementitious Composite for Building Applications

Doctoral Program:

Construction Engineering

Doctoral Candidate:

Payam Sadrolodabaee

Thesis Supervisors:

Prof. Albert De La Fuente Antequera
Prof. Josep Claramunt

Barcelona, May 2022

ACKNOWLEDGMENT

I have a great deal of thanks to the many people who have helped me and encouraged me over these past four years during my work on this Ph.D. project and dissertation.

First and foremost, I would like to express my deepest gratitude to Dr. Albert de la Fuente and Dr.Josep Claramunt, my supervisors, for providing me with this opportunity and for their unending support throughout my dissertation work. Their endless efforts in monitoring me and their tremendous contributions and motivations are highly appreciated. I am of course indebted to them for lending their precious time on alleviating all of my concerns regarding the details of this study. Aside from the research, their affirmative and cheerful characters also positively influenced me.

I also owe a special debt of gratitude to Dr. Monica Ardunay for her support, encouragement, valuable guidance, and supervision provided throughout the period of the research. Although not being officially my supervisor, her guidance helped me significantly during this research.

I am also most thankful to Dr. Amin. Hosseini, a former Post-Doc researcher at the Civil and Environmental Engineering Department of UPC, Dr.Laia Haurie, and Dr.Ana Lacasta, both from the Department of Building Construction and Architecture of UPC, for their support and sharing of useful data.

Thanks are due to the directors, researchers, and staff of the various departments and campuses of UPC including Civil and Environmental Engineering at Campus North-Barcelona, Building Construction and Architecture at Campus South-Barcelona, Materials Science and Engineering at Terrassa Campus, and Agri-Food Engineering and Biotechnology at Castelldefels Campus for sharing generously their time in responding to this research.

Further, thanks to Dr.Ilenia Farina, from the University of Naples Parthenope, who has provided me with the opportunity of being a visiting researcher for a few months before my graduation in Naples.

Last but not least, I would like to give my special thanks to my family and my parents, who gently offer me unconditional love and support throughout my studies and life. And also to my friends in Barcelona who have got my back during these years being far from my family and hometown.

ABSTRACT (ENGLISH)

Cementitious materials have one of the highest compressive strength-to-weight ratios compared to other construction materials. Nonetheless, both tensile strength capacity and toughness result to be an order of magnitude less respect to the former, which thereby leads to cracking under tensile stresses caused by service loads. This lack of tensile strength capacity of the material leads to cracking and fragile failure in case the material is insufficiently reinforced. Within this context, fibers can be used in cementitious matrices aiming at enhancing the toughness, energy absorption capacity, post-cracking behavior as well as flexural and tensile strength.

Although during the past decades, various types of fibers such as asbestos, steel, glass, and polymeric have been tested in brittle matrices, there have been some disadvantages such as detrimental health effects, high cost, and specifically, substantial environmental footprint. Likewise, based on the statistics, the construction sector is responsible for about 40% of the European Union's total final energy consumption, 35% of its total CO_2 emissions, and 45% of waste generation. That is why significant efforts should be devoted to applying the '3Rs' concept of reducing, reusing, and recycling in the building sector and material fabrication.

On the other hand, textile leftover is one of the predominant wastes resources worldwide while only less than 20% is being recycled. The textile industry produces textile wastes (TW) from the primary stages of garment production (pre-consumer waste such as fiber, yarn, and fabric) to the end of its useful life (post-consumer waste: discarded clothes). Thus, the reuse of this textile waste in construction is becoming interesting and convenient due to the shortage of natural mineral resources and increasing waste disposal costs.

Recently, sustainable fibers produced from renewable, biodegradable, waste, recycled, available, and low-cost resources becoming a focal point. In this sense, vegetable and cellulosic fibers have already been used as reinforcement in cementitious materials for low- to medium-performance structural applications. TW fiber could be another sustainable alternative for reinforcement in cementitious composites.

In view of the abovementioned, this research comprehensively verifies, by means of physical, mechanical, and durability-based material characterization tests, the possibility of incorporation of short TW fiber as well as the nonwoven TW fabric in the cementitious composites as internal reinforcement to produce a sustainable, ductile, and durable composite to be used in building applications. In this regard, several experimental tests were carried out on different mix design samples to characterize the mechanical, microstructural, durability, thermal, acoustic, fire, and shrinkage properties.

The results have shown that the recycled TW fiber, especially in the form of nonwoven fabric, could be a technically feasible, sustainable, and durable reinforcement to be used in the cementitious mortar for low to medium-performance structural applications (e.g., façade panels, roofing, raised floors, and masonry structures). Further, the sustainability of the optimum composite as a façade cladding panel (as an example of one projected application) was assessed through the MIVES, a new comprehensive and integrated Multi-Criteria Decision-Making method that embraces the three pillars of sustainability: economic, environmental, and social.

Future works on this kind of fiber-reinforced cementitious mortar could be to develop a numerical model simulation or produce a 3D concrete printing (3DCP) prototype by employing additive manufacturing technology.

ABSTRACT (SPANISH)

Los materiales cementosos tienen una de las más altas resistencias a la compresión comparada con la de otros materiales de construcción. No obstante, tanto la capacidad de resistencia a la tracción como la tenacidad resultan ser un orden de magnitud menor que la primera, lo que conduce a la fisuración bajo los esfuerzos de tracción provocados por las bajas cargas de servicio. Esta falta de capacidad de resistencia a la tracción puede provocar grietas y roturas frágiles.. Por esta razón, las fibras se han utilizado predominantemente en matrices cementosas con el objetivo de mejorar la tenacidad, la capacidad de absorción de energía, el comportamiento posterior al agrietamiento y la resistencia a la flexión y a la tracción.

Aunque durante las últimas décadas, se han probado varios tipos de fibras como asbesto, acero, vidrio y polímeros en matrices frágiles. Algunas de ellas presentan algunas desventajas como efectos perjudiciales para la salud, alto costo y, específicamente, una huella ambiental sustancial. Asimismo, según las estadísticas, el sector de la construcción es responsable de cerca del 40% del consumo total de energía final de la Unión Europea, el 35% de sus emisiones totales de CO_2 y el 45% de la generación de residuos. Es por eso que se deben dedicar esfuerzos significativos a aplicar el concepto de las '3R' de reducción, reutilización y reciclaje en el sector de la construcción y la fabricación de materiales.

Por otro lado, el sobrante textil es uno de los residuos predominantes a nivel mundial del cual se recicla menos del 20%. La industria textil produce residuos textiles (TW) desde las etapas primarias de la producción de prendas de vestir (restos previos al consumo, como fibras, hilados y telas) hasta el final de su vida útil (excedentes posteriores al consumo: ropa desechada). Así, la reutilización de estos residuos textiles en la construcción se está volviendo interesante y conveniente debido a la escasez de recursos minerales naturales y al aumento de los costes de eliminación de residuos.

Recientemente, las fibras sostenibles producidas a partir de recursos renovables, biodegradables, de desecho, reciclados, disponibles y de bajo costo estan adquiriendo protagonismo. En este sentido, las fibras vegetales y celulósicas ya se han utilizado como refuerzo en materiales cementosos para aplicaciones de baja y media resistencia. La fibra TW podría ser otra alternativa sostenible para el refuerzo en compuestos cementosos.

En vista de lo anterior, esta investigación verifica exhaustivamente la posibilidad de incorporar fibra corta de TW, así como fieltros de TW en los compuestos cementosos como refuerzo interno para producir un compuesto sostenible, dúctil y duradero para ser utilizado en aplicaciones de construcción. Se realizaron varios ensayos experimentales sobre diferentes muestras para caracterizar las propiedades mecánicas, microestructurales, de durabilidad, térmicas, acústicas, al fuego y de contracción.

Los resultados han demostrado que la fibra de TW reciclada, especialmente en forma de fieltro, podría ser un refuerzo técnicamente factible, sostenible y duradero para ser utilizado en el mortero cementoso para aplicaciones estructurales de rendimiento bajo a medio (por ejemplo, paneles de fachada, techos, pisos elevados y estructuras de mampostería). Además, la sostenibilidad del compuesto óptimo destinado a panel de revestimiento para fachada ventilada (como ejemplo de aplicación) se evaluó a través de MIVES, un nuevo método integral e integrado de toma de decisiones de criterios múltiples que abarca los tres pilares de la sostenibilidad: económico, ambiental y social.

La investigación futura en este tipo de mortero cementoso reforzado con fibra podría ser el desarrollo de modelos de simulación numérica o la formulación específica de material para impresión de hormigón 3D mediante el empleo de tecnología de fabricación aditiva.

Table of Contents

1. CHAPTER ° I

INTRODUCTION

This chapter presents a general introduction and state-of-the-art review of fiber-reinforced cement (FRC) composite materials, specifically those reinforced with sustainable natural-based fibers. The new promising recycled fiber from waste textiles is introduced. Moreover, this chapter describes the general and specific objectives of this thesis. Additionally, it includes the list of publications derived from this work and the structure of this document.

1.1 Scope

Incorporating fibers into cementitious matrices is long known to improve various properties of the composite such as flexural strength, toughness, and shrinkage, among others. Next to steel, cement-based matrices have demonstrated one of the highest strength-to-weight ratios among building materials but suffer from one shortcoming; failure in a brittle manner under tensile stresses or impact loads owes to the lack of tensile strength once cracking occurs. The use of fibers in different forms and shapes is an effective method of strengthening brittle materials against cracking under tensile stress. Cracks are deflected in the presence of fibers, and thus the toughness or ductility can be increased.

Fiber/textile reinforced mortars (FRM/TRM) are growingly used in many components of the building technologies like facade and precast architectural cladding panels, cover plates for buildings, pavements, reinforcement of structures, masonry applications, urban furniture, etc. These composite materials can be constituted of various kinds of fibers -steel, synthetic, or vegetable- together with a cementitious matrix which can be in the form of cement paste, lime binder, mortar, or concrete. One of the promising kinds of fiber can be recycled textile waste originating from the garment industry.

Nowadays, the disposal of solid wastes is a major problem worldwide. Recycling or reusing these waste materials is motivating, especially in construction. Using recycled materials and wastes in construction is becoming more popular due to shortages of natural mineral resources and increasing waste disposal costs. However, with the increasing use of wastes in engineering applications, a need for further understanding of their mechanical and durability performance is required. Studies have indicated that fibers recovered from various waste streams could be suitable for mortar reinforcement. The advantages of using such waste fibers include generally lower cost to process than virgin fibers and the elimination of the need for waste disposal in landfills. Thus, due to the influx of these voluminous wastes in our environment, turning them into useful materials serves a dual function: elimination of wastes, and introduction of a new product.

In view of the abovementioned, the objective of this thesis is to research further on the mechanical, durability and microstructural characterization of the novel recycled Textile Waste (TW) fiber originated from the cloths and garments, see Figure 1, as internal reinforcement in cement composites. Further, the sustainability of using those in a proper function in the building and construction sector is quantified.

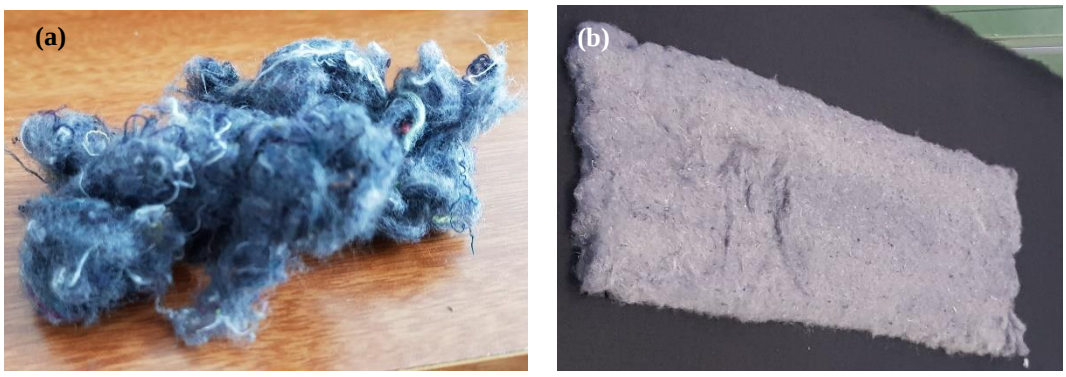

Figure 1. a) Recycled shredded TW fiber; b) nonwoven fabric TW

1.2 State-of-the-Art

1.2.1 Introduction

The fiber-reinforced cement (FRC) composites are considered the next generation of materials in the building and construction sectors. Cementitious materials present the highest compressive strength to weight ratio compared to other construction materials [1]. Nonetheless, both tensile strength capacity and toughness result to be an order of magnitude less respect to the former, which thereby leads to cracking under tensile stresses caused by service loads [2]. This lack of tensile strength capacity leads to material prone to crack and fragile response in case of failure [3]. For this reason, fibers have been predominantly used in cementitious matrices aiming at enhancing the toughness, energy absorption capacity, post-cracking behavior [4], [5] as well as flexural and tensile strengths [6].

It is reported that the incorporation of fibers can also improve the shrinkage behavior of cementitious materials. Shrinkage cracks can be a problem in terms of aesthetics and durability since water, chlorides, and other harmful substances could enter those cracks, causing early deterioration and damage. Thus, controlling shrinkage cracks is of paramount importance for improving service life and minimizing repair costs. In fact, when the cementitious materials are restrained against shrinkage strains, early-age cracks could occur. These cracks reduce the capacity of load carrying and also allow aggressive agents to penetrate the mass, reducing the long-term durability of constructions. Fibers restrain shrinkage due to the bond with the matrix and specifically control the so-called plastic shrinkage cracking at early ages. Adding fibers to concrete may not affect the evaporation rate, but increases the strength and strain capacity during the early-age shrinkage against tensile cracking. The majority of available research suggests that fibers, specifically synthetic ones, have a favorable effect in minimizing the plastic and autogenous shrinkage of cement composites [7]–[11].

The incorporation of fibers has also resulted in improvements respect to durability according to several authors [12]. In this regard, the use of fibers can limit crack propagation and control the crack width, which can result in an effective reduction of the aggressive agents' ingress and the associated consequences. This is of particular interest when the use of this composite material is oriented to applications with a certain level of structural responsibility for which strength, ductility, and durability requirements are demanded.

The magnitude of the fiber effect in the post-cracking behavior of FRCs can change depending on several factors such as matrix composition, fiber type and size, fiber content, distribution, and orientation. A cementitious matrix can be in the form of cement paste, lime binder, mortar, or concrete. The matrix with the main component of Portland cement (PC) together with aggregate is still the most common. Fiber content is typically indicated by a volume fraction of fibers per unit volume of composite material and can be categorized as low volume fraction (less than 1%), moderate volume fraction (between 1% and 2%), and high volume fraction (greater than 2%) [12]. ACI committee 544 [13], suggests the following fiber size categories: macro-fibers with lengths varying from 0.5 to 2.5 inches (12.7 to 63.5 mm); micro-fibers with lengths less than 0.5 inches (12.7 mm or smaller); and nano-fibers. Fine fibers control the opening and propagation of microcracks as they are densely dispersed in cement matrix while longer fibers up to 50 or 80 mm control larger cracks and contribute to increasing the final strength of FRC. Increasing the aspect ratio (length to diameter ratio) of fibers significantly improves the mechanical performance of these composites.

Fibers are discontinued elements, which length is greater than the dimensions of the cross-section and are characterized by high tensile strength along their longitudinal direction. Fibers have been incorporated in mortars since ancient times to reduce cracking and improve the toughness and strength of brittle building materials. Since Biblical times, approximately 3,500 years ago, brittle building materials, e.g. clay sun-

baked bricks, were reinforced with horsehair, straw, and other vegetable fibers [6]. The concept of fiber reinforcement was developed in modern times and brittle cement-based paste was reinforced with asbestos fibers when in about the early 1900s the so-called Hatschek technology was invented for the production of plates for roofing, pipes, etc. The need to replace asbestos due to its detrimental influence on human health gave rise to other kinds of fibers including natural, steel, polymeric, or synthetic [14], see Figure 2.

The majority of the used fibers are synthetic ones, see Figure 2d. Nonetheless, the disadvantages of high cost and substantial environmental footprint for this kind of fiber have remained controversial [15]. For this reason, natural-based fibers (including vegetable fibers, lignocellulosic fibers, or cellulosic fibers.) have attracted great interest during the last decade. Another sustainable solution could be recycled fibers from the textile waste industry, composed of mainly natural fibers such as cotton, silk, or flax. The recycled short textile waste fiber used in this study was made up of roughly 70% cotton and 30% polyester (Figure 1a) as will be explained in the future sections. Moreover, the nonwoven fabric form (Figure 1b) was composed of 35% Flax, 45% cotton, and 20% polyester.

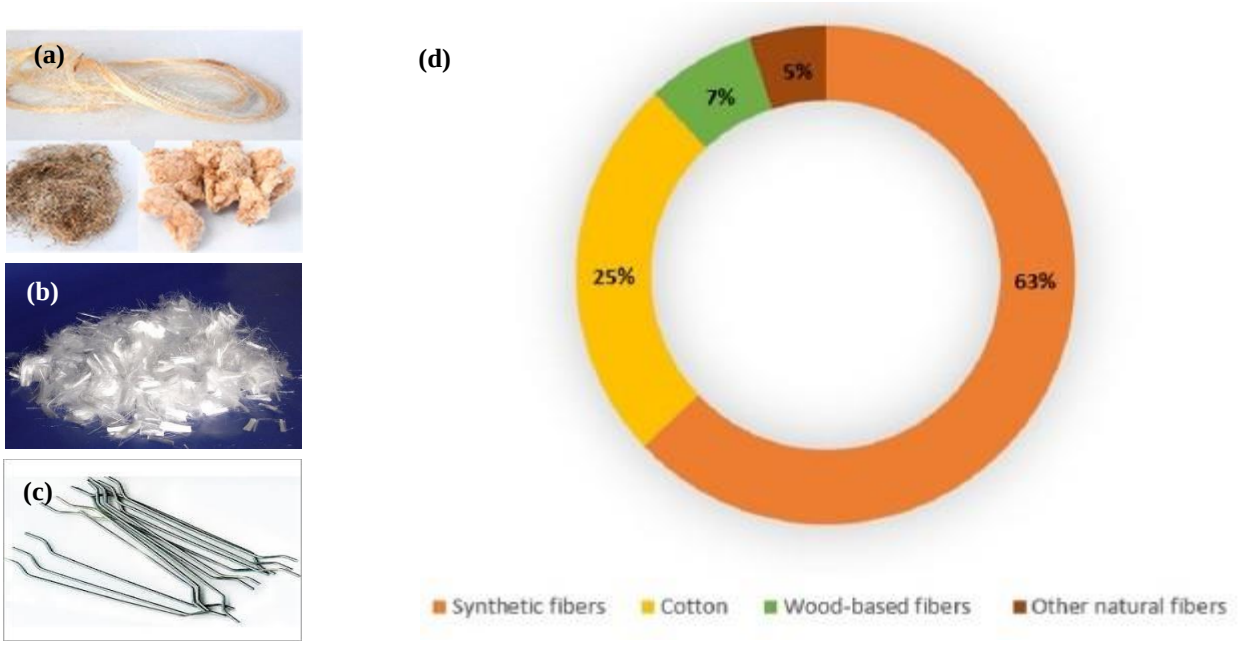

Figure 2. Various types of fibers: a) vegetable and cellulosic [4]; b) polymeric; c) steel.; d) world fiber consumption in 2019 [16].

1.2.2 Microstructure and mechanical behavior of the FRC composites

The most significant enhancement resulting from the inclusion of fibers in cementitious matrices is the improvement in post-cracking behavior, which is typically evaluated by material toughness and residual tensile/flexural strengths. Besides the fiber strength and length, the composite toughness is mainly governed by fiber-matrix bonding. A well-balanced interaction between the cement matrix and the fibers which allows fiber debonding and pull-out, as well as the stress transfer from the matrix to the fibers, is necessary to obtain composites with high toughness [4].

The addition of reinforcing fibers to a cementitious matrix can improve residual tensile and flexural strength as well as ductility and toughness. The increase in flexural strength is particularly sensitive not only to the fiber volume but also to the aspect ratio of the fibers, with higher aspect ratios leading to larger strength increases. However, both increases and decreases are recorded in compressive strength when fibers are added. It is suggested that the decrease in strength happens due to the increases in the air content of the mixture relative to plain mortar, while the increase in strength happens due to fibers oriented horizontally stitching the micro-cracks and bridging the matrix cracks, which cause the transfer of the loads [17]–[19].

The conventional cementitious matrix without fiber is characterized by an initial linear increase of stress and after the first crack opening, there is a slow decrease, the so-called softening branch. In contrast, where the fiber reinforcement is sufficient, after the first crack there is a strain hardening stage, which accompanies multiple cracking and a considerable amount of energy is absorbed that is proportional to the area under the curve [6]. In other words, the cracking phases of the strain-hardening cementitious composite under bending (or direct tensile) could be divided into three distinct branches: (A) Linearly ascending branch (the pre-cracking zone), the external load is mainly undertaken by the cement matrix while internal microcracking is occurring until a visible crack in the cement matrix is formed. The flexural stiffness of the first stage is mainly influenced by the mechanical properties of the matrix and is hardly influenced by fiber reinforcement [20]. (B) The transition zone along which both load fluctuation and cracking occur (multiple cracking is expected if the type and amount of fibers are sufficient to withstand forces superior to that generated by the crack/s). Right after the cracking onset, a load drop followed by load recovery is recorded. In the crack propagation zone, the matrix is subjected to the compression stresses on the upper part of the specimen (above the neutral axis position, if the bending moment has a positive sign) and the fiber reinforcement guarantees the equilibrium of the internal forces (bending moment) by resisting tensile stresses. Under these conditions, the stress transfer mechanism is achieved by the reinforcement-matrix adhesion in the zones between cracks. If there was insufficient matrix-reinforcement adhesion, the onset of cracking would trigger a brittle failure of the composite in flexure. On the contrary, sufficient adhesion would allow full interaction between the matrix and the textile reinforcement and a ductile response of the composite with the occurrence of multiple cracking, this proving the mechanical compatibility between both materials. (C) Another ascending branch (the post-cracking zone) usually with the lowest slope, due to the degradation of the composites' stiffness, in which the reinforcement bridge the cracks and bear the loads. No further new crack occurs in this zone and only the cracks widen. Finally, a failure happens due to the rupture or debonding of the fibers followed by further widening of the cracks and, eventually, forming the main crack that leads to the collapse (see Figure 3).

Among different kinds of fibers, short randomly distributed fibers are very popular though bring some limitations in terms of strength and specifically toughness due to the short length and the maximum quantity mixable [15]. Thereby, longer fibers in the form of strands as well as the woven and nonwoven fabrics, although representing a more difficult production procedure, have become an interesting alternative for reinforcing cement-based matrices. Owing to the higher fiber length and more contact with the cement paste, the formation of multiple micro-cracking can lead to an improvement of the tensile mechanical properties [21]–[23]. In this regard, there is already some research available regarding the cementitious mortars reinforced with long fibers including sisal strands [24], [25], and woven fabrics including alkali resistance glass fabrics [26]–[29]. However, there is still scarce, and only incipient, research on the nonwoven fabric as reinforcement for mortars. Nonetheless, all those confirmed that textile reinforced cementitious (TRC) composites oriented to thin, lightweight and sustainable structures have improved tensile and flexural performances as well as strain hardening behavior even when the reinforcing yarns have a low modulus of elasticity.

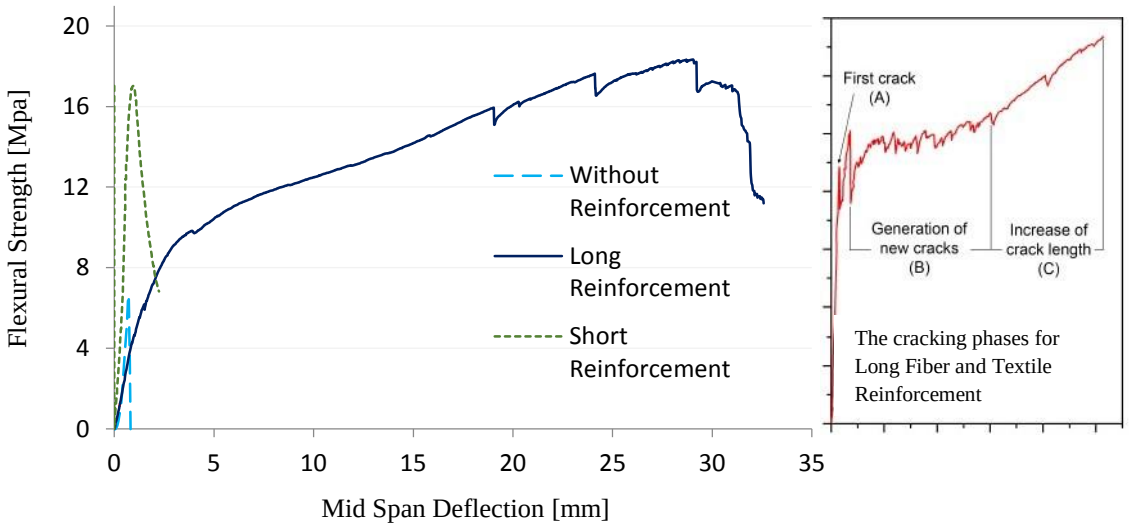

Figure 3. Representative flexural stress: deflection relationships of different types of cementitious materials [30].

1.2.3 The durability of natural-based FRC composites

The addition of fibers could significantly reduce the crack width which resulted in less penetration of various ionic species. In other words, fibers can control the cracks' propagation and limit the aperture, thereby reducing the permeability and decreasing the degradation rate which means enhanced durability. Fibers modify crack patterns, with narrower and closely spaced cracks [31].

The durability of FRC/TRC composites is related to the ability to resist both external (temperature and humidity variations, sulfate or chloride attack, among others) and internal damage (compatibility between fibers and cement matrix and volumetric changes) [32]. One important factor that should be analyzed is the degradation of bio-based and natural fibers immersed in Portland Cement (PC) due to the high calcium hydroxide (CH) content in the cement. Further, the most prevalent and critical durability test for vegetable-based composites was reported to be the exposition of the samples to accelerated wet/dry cycles [33], [34]. Indeed, when the environment is maintained constant, the transfer of OH^- ions or Ca^{2+} ions from the cement matrix to the fibers is slow. However, exposure to repeated wet/dry cycles provokes the capillary pore system of the cement matrix filled and emptied with alkaline pore water consecutively, resulting in accelerating the hydration products' migration to the fibers [32].

There are several strategies for improving the durability of vegetable FRC composites. One possibility is to modify the composition of the matrix to reduce or remove the alkaline compounds. To modify the composition of the matrix, it is necessary to add pozzolanic compounds or supplementary cementitious materials (SCMs) to promote the transformation of portlandite into calcium silicate hydrate (C-S-H) gel. In fact, the pozzolanic materials with a high amount of amorphous silica (SiO_2) and/or alumina (Al_2O_3) cause the pozzolanic reaction to promote during the hydration process which ends in the replacement of CH by C-S-H. Substituting the partial weight of PC with this kind of pozzolanic materials and by-products -like silica fume (SF), fly ash (FA), metakaolin (MK), or ground granulated blast furnace slag (GGBS)- not only leads to a reduction in alkalinity content of the matrix but also decreases the CO_2 footprint [35], [36].

Based on the literature review, see Table 1, different amounts of various SCMs have been used in vegetable-based FRC/TRC composites. In this regard, Fernández et al. [37] used 10 wt.% of SF sourced to reach the near absence of portlandite after autoclaved curing condition in the cement-based reinforced with sisal fibers. Khorami et al. [38] studied the behavior of cement boards reinforced with 8% waste Kraft pulp modified with SF. The results showed that the addition of 3-6% SF by cement weight could slightly improve flexural strength while adding more than 6% SF led to a slight reduction of strength in comparison to the control specimen. Gutierrez et al. [36] investigated the effect of SF, MK, FA, and GGBS on cement mortars reinforced by different types of natural and synthetic fibers in the proportion of 2.5% by cement weight. The conclusion was that the addition of 15% SF or MK could improve the performance of the composite while 15% FA had an adverse effect probably due to its lower degree of pozzolanic activity. Moreover, they reported that the addition of 70% GGBS had promising results. Silva et al. [22] managed to improve the durability of the Portland cementitious matrix by incorporating 30% MK and 20% calcined waste crushed clay brick to manufacture the composite laminates reinforced with long sisal fibers. Moreover, Fidelis et al. [39] and Majstorovicet al. [40] could develop a CH-free matrix by replacing almost 50% of the PC with MK in jute textile-reinforced concrete and flax textile-reinforced composites, respectively.

Table 1. *Summary of r*ecent studies on the use of SCMs in SHCCs reinforced with vegetable-based

Type and amount of SCMs	**Type of reinforcement**	**Type of mechanical test**	**Type of durability test**	**Ref**
3-9% SF	Short Kraft pulp fiber	Flexural	None	[38]
15% SF, 15% MK, 15% FA	Sisal and coconut fibers	Compressive	Chloride penetration	[36]
50% MK and calcined waste	Long sisal fibers	Tensile and flexural	None	[22]
50% MK	Jute textile	Double-sided pullout	High temperature exposure	[39]
20-40% MK	Flax woven fabrics	Flexural	None	[40]
10% SF, 40% slag	Sisal and coconut fibers	Flexural	Wet-Dry cycles, aging in water	[41]
10% SF	Flax nonwoven fabrics	Tensile and flexural	None	[42]
10-55% MK and calcined waste	Long sisal fiber	Flexural	Wet-Dry cycles	[21]
50% MK and calcined waste	Long Sisal fiber	Tensile and flexural	Hot water immersion	[43]
10-50% MK	Flax nonwoven fabrics	Flexural	Wet-Dry cycles	[44]

Alternatively, non–ordinary Portland cement matrices, in particular, those based on calcium aluminates or sulfoaluminates could be used. For those, the use of a CH-free matrix seems to be a promising alternative for increasing the durability of fiber-cement-based composites with aging [44], [45]. Moreover, accelerated carbonation can induce lower alkalinity, so using artificial carbonation in order to obtain $CaCO_3$ from $Ca(OH)_2$ leads to increased strength, low porosity, high density, good fiber-matrix interface, and reduced water absorption since calcium carbonate is denser than calcium hydroxide [46].

Another strategy to increase the durability of these composites is to modify the fibers with chemical, alkaline [47], or physical [48] treatments such as hornification -exposing the fibers to drying and rewetting

cycles- to increase their stability in the cementitious matrix. In addition to portlandite degradation, water absorption of fibers should be considered which can lead to volume changes and consequently induce cracks and loss of physical contact with the matrix [34].

1.2.4 Textile waste as a promising sustainable fiber

The building sector is one of the major consumers of natural resources and one of the biggest waste producers worldwide. Based on the statistics, in the EU the building sector accounts for 35–40% of the final total energy consumption and 25–40% of the associated carbon dioxide emission [49], [50]. Further, the construction and building sector consumes almost 40% of all raw materials extracted worldwide and is responsible for the generation of around 35% of all global waste [51]. That is why significant efforts have been devoted to applying the '3Rs' concept of reducing, reusing, and recycling in the building sector including material fabrication [52]. Thus, reusing and recycling the leftover materials with sustainable processes in material fabrication (ex., in fiber production) can mitigate the waste and environmental impacts [53], [54].

The reuse of different types of waste in the construction or rehabilitation of buildings can contribute significantly to sustainability due to the high amount of waste produced worldwide [55], [56]. The disposal of these solid wastes is a major problem throughout the world. Consequently, using recycled materials and wastes in construction is becoming more popular due to shortages of natural mineral resources and increasing waste disposal costs. However, with the increasing use of wastes in engineering applications, a need for further understanding of their engineering behavior is required since there is still skepticism about the quality of recycled materials. Thus, new research should be conducted using recycled materials to overcome these uncertainties.

World fiber production has been steadily increasing in the past few decades, now exceeding 100 million tons per year [57]. Thus, increasing interest has been garnered in the use of sustainable fibers produced from renewable, biodegradable, waste, recycled, available, and low-cost resources [58]. In this sense, vegetable and cellulosic fibers have already been used as reinforcement in cementitious materials for low- to medium-performance structural applications [59], [60]. Textile waste fiber could be another sustainable alternative for reinforcement in cementitious composites.

The global production of textiles amounts to over 110 million tons annually, which makes textile production one of the biggest industries affecting global environmental pollution through greenhouse gas emissions, depletion of natural resources, and the generation of huge amounts of waste [61], see Figure 4. Textile leftovers can be categorized as pre-or post-consumer waste, where the former includes all fiber, yarn, and fabric waste produced during garment manufacturing while the latter refers to worn-out clothing discarded by users [62]. In the EU, more than 5.8 million tons of textiles are discarded by consumers per year while only less than 25% of these textiles are recycled [63]. The remaining goes to landfills or municipal waste incinerators, this leading to substantial environmental and economic footprints. Consequently, the use of this textile waste cutting in construction may solve two problems, namely, the elimination of an environmental pollutant and the provision of an alternative material for the construction industry.

TW fibers can be made of natural or human-made fibers including cotton, silk, flax, polypropylene, nylon, and polyester, all of which have a lower elastic modulus than the matrix. According to several studies [64]–[67], TW fibers from polyester and nonwoven fabrics can be used as thermal- and sound-insulating elements. The thermal conductivity value of the woven fabric waste is reported to be similar to the values obtained for expanded polystyrene (EPS), extruded polystyrene (XPS), and mineral wool (MW). Moreover,

lightweight bricks, cement blocks, and concrete partitions containing TW fiber, namely cotton, are already being produced [68]–[70].

Regarding the mechanical properties of TW fiber-reinforced concrete, some studies have investigated concrete reinforced with nylon or polypropylene fibers recycled from carpet [71]. In most cases, tensile and flexural strengths have been enhanced whilst compressive strength, and elastic modulus have decreased [72]–[75]. The inclusion of recycled textile fibers was observed to influence the mechanical performance of concrete through a bridging action against crack propagation and redistribution of the porous matrix structure toward a more uniform structure [76]. Nonetheless, the use of a high dosage of waste fibers leads to an agglomeration effect which, in turn, could cause the formation of voids and entrapped air, thereby diminishing the concrete's properties [77].

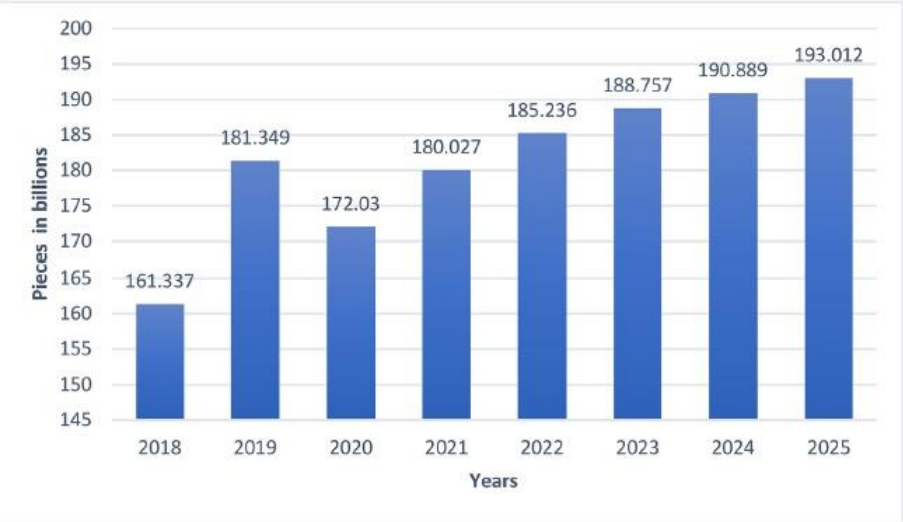

Figure 4. The volume of apparel in the global market from 2018 to 2025 [16].

1.3 Objectives of The Thesis

1.3.1 General Objectives

According to the literature review, the mechanical and durability properties of cement-based composites reinforced with textile waste fibers from garment resources of cotton and polyester are still lacking comprehensive research. Furthermore, as explained in the previous section, research on nonwoven fabric in cementitious mortars as reinforcement remains scarce. Accordingly, the *main objective of this doctoral dissertation is to characterize and analyze both the mechanical and durability performance of textile waste fiber-reinforced cement-based composites*. The results are to be used for confirming the suitability of these composites as sustainable and low-cost building construction materials for limited structural responsibility applications (i.e., facade and precast architectural cladding panels, drywall and ceiling panels, pavements, and urban furniture). Additionally, and with the same purpose, microstructural and sustainability analyses are performed in order to support the research and the outcomes derived.

1.3.2 Specific Objectives

In order to accomplish the general objectives mentioned above, several specific objectives were established:

- To find the proper fabrication method that guarantees a homogeneous dispersion of the fibers in the matrix together with a well-balanced interaction between the cement matrix and the fibers,
- To compare the composites reinforced with short randomly dispersed fibers to the ones incorporated non-woven fabrics,
- To characterize the mechanical properties of the composites such as strength, stiffness, and toughness through standard mechanical tests (flexion-tension-compression),
- To analyze the microstructural behavior of the composites,
- To quantify the durability performance of the composite and to explore mechanisms and approaches to increase it,
- To characterize the thermal and acoustic performance of the composite, as well as combustibility,
- To assess the sustainability performance of the composite when used for specific structural applications, specifically in claddings and façades.

1.4 Methodology

This Ph.D. thesis consists of a compendium of publications in JCR-indexed journals by following the regulations of the Doctoral Program in Construction Engineering of UPC. All publications derived from this thesis, both published or submitted papers, are listed below.

1.4.1 Included in the compendium

Journal Paper I:
Mechanical and durability characterization of a new Textile Waste Micro-Fiber Reinforced Cement Composite for building applications [78]
P Sadrolodabaee, J Claramunt, M Ardanuy, A de la Fuente
Case Studies in Construction Materials by ELSEVIER
(https://doi.org/10.1016/j.cscm.2021.e00492); Jan 2021
Impact factor: 3.328

Journal Paper II:
Characterization of a textile waste nonwoven fabric-reinforced cement composite for non-structural building components [79]
P Sadrolodabaee, J Claramunt, M Ardanuy, A de la Fuente
Construction and Building Materials by ELSEVIER
(https://doi.org/10.1016/j.conbuildmat.2020.122179); Jan 2021
Impact factor: 6.141

Journal Paper III:
A textile waste fiber-reinforced cement composite: comparison between short random fiber and textile reinforcement [80]
P Sadrolodabaee, J Claramunt, M Ardanuy, A de la Fuente
Materials by MDPI
(https://doi.org/10.3390/ma14133742); July 2021

Impact factor: 3.623

Journal Paper IV:
Experimental Characterization of Comfort Performance Parameters and Multi-Criteria Sustainability Assessment of Recycled Textile-Reinforced Cement Facade Cladding [81]
P Sadrolodabaee, S.M.A Hosseini, J Claramunt, M Ardanuy, L.Haurie, A.M.Lacasta, A de la Fuente
Journal of Cleaner Production by ELSEVIER
(https://doi.org/10.1016/j.jclepro.2022.131900); April 2022
Impact factor: 9.297

1.4.2 Complementary to the Ph.D. (not included in the compendium)

Research contribution for a conference I:
Preliminary study on new micro textile waste fiber reinforced cement composite [82]
P Sadrolodabaee, J Claramunt, M Ardanuy, A de la Fuente
(https://upcommons.upc.edu/handle/2117/348199); June 2021
ICBBM 2021: 4th International Conference on Bio-based Building Materials: Barcelona, Spain.

Research contribution for a conference II:
A new sustainability assessment method for Façade Cladding Panels: A case study of Fiber/Textile Reinforced Cement [83]
P Sadrolodabaee, S.M.A Hosseini, J Claramunt, M Ardanuy, A de la Fuente
(https://doi.org/10.1007/978-3-030-83719-8_69) ; September 2021
BEFIB 2021: RILEM-fib X International Symposium on Fibre Reinforced Concrete: Valencia, Spain.

Journal Paper V (Submitted for Publication):
Effect of accelerated aging and silica fume addition on the mechanical and microstructural properties of hybrid textile waste-flax fabric reinforced cement composites
P Sadrolodabaee, J Claramunt, M Ardanuy, A de la Fuente
Submitted to Journal of Cement and Concrete Composites in February 2022

A general diagram comprising the overview of the methodology and the experimental approach to reach the specific objectives of this dissertation is shown in Figure 5. As it can be seen, this study was classified into two main categories (study on the characterization of the matrix and the composite). The experimental programs and results' analyses carried out through all published or submitted papers are included in the schematic diagram.

Briefly, the matrix characterization study was done on the Portland cement paste substituted with variable SF content (0 to 30%) to reach the optimum percentage of SF that substitutes PC to improve the durability performance of the composite. This characterization program embraces the mechanical tests (flexural and compressive) and microstructure analysis techniques including thermogravimetric analysis (TGA), and X-ray diffraction (XRD). The results of this study are gathered in *Journal Paper V*.

As for the composite characterization study, several investigations were developed. Firstly, the preliminary study on this new micro textile waste FRC composite based on the 3-point flexural test and different treatments was developed. The results were published in *Research contribution for a conference I*. Then, in *Journal Paper I*, the flexural and compressive strengths of short TW fibers in different dosages (6 to 8 wt%) were compared to those obtained for composites reinforced with kraft pulp fibers. Moreover, durability tests including exposure of the samples to wet/dry cycles were also reported. Finally, scanning

electron microscopy (SEM) observations were carried out to confirm the mechanical findings. *Journal Paper II* focused on the mechanical (flexural test) and durability (against wet/dry cycles) characterization of the composites reinforced with several layers of TW nonwoven fabric (3 to 7 layers). The results were compared with those obtained for reinforced with flax nonwoven fabrics, both treated and non-treated. Further, scanning and back-scattered electron microscopy (SEM and BSEM) analyses were performed. *Journal Paper III* made a comprehensive comparison between the cement composites reinforced with short random TW fiber and those incorporated TW fabric reinforcement to select the optimum composite. Further, the drying shrinkage results were discussed.

Journal Paper IV includes the experimental results of the thermal and acoustic performance, in addition to the post-fire performance of the optimum TW composite. Further, in this paper and also in the *Research contribution for a conference II*, the sustainability index of this new material as a façade cladding panel was assessed based on the MIVES (a novel comprehensive multi-criteria decision-making method, which embraces the economic, environmental, and social aspects of sustainability). And finally, in *Journal Paper V*, in addition to the matrix characterization explained before, the tensile and flexural characterizations of the composites modified with 15 and 30% SF under the wet/dry and freeze/thaw conditions are reported and analyzed. SEM and BSEM observations were performed to study the microstructure of the composites.

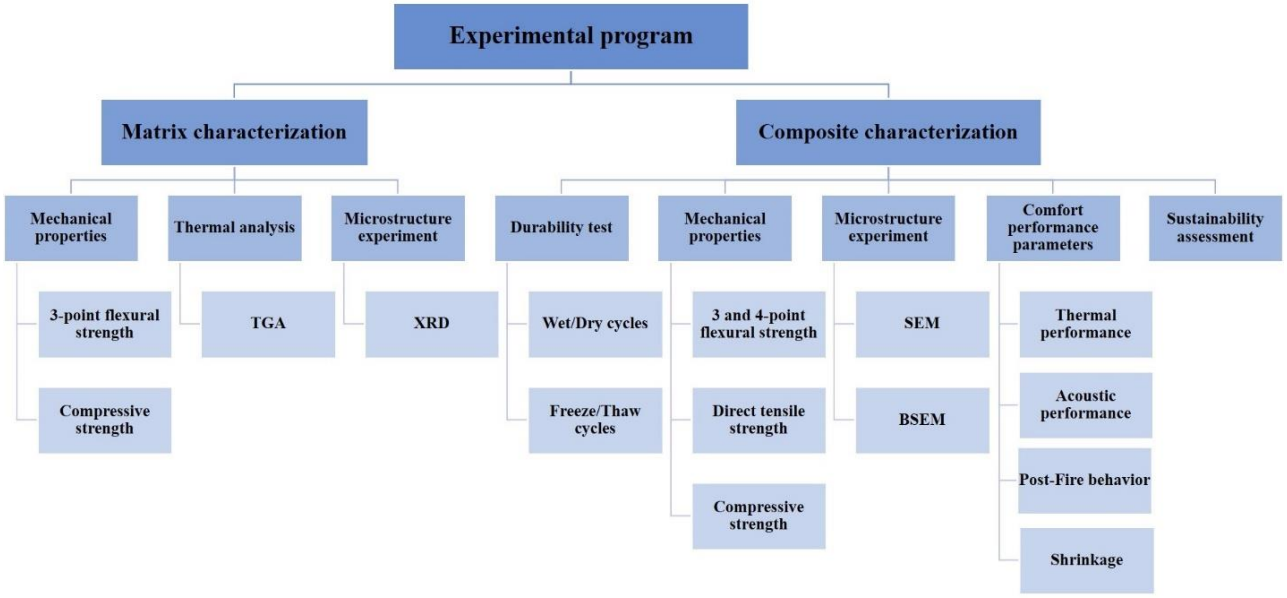

Figure 5. Schematic diagram of the experimental program of this Thesis

1.5 Structure of the Document

Aiming at presenting the results derived from this research, this document gathers a compilation of scientific contributions (scientific papers and research contributions in international conferences) written during the Ph.D. The thesis is divided into four chapters (Figure 6): Introduction (Chapter I), Body of the Thesis (Chapter II and Chapter III), and Conclusions (Chapter IV). The appendix presented the last results derived from this research work, still under review in JCR-indexed journals.

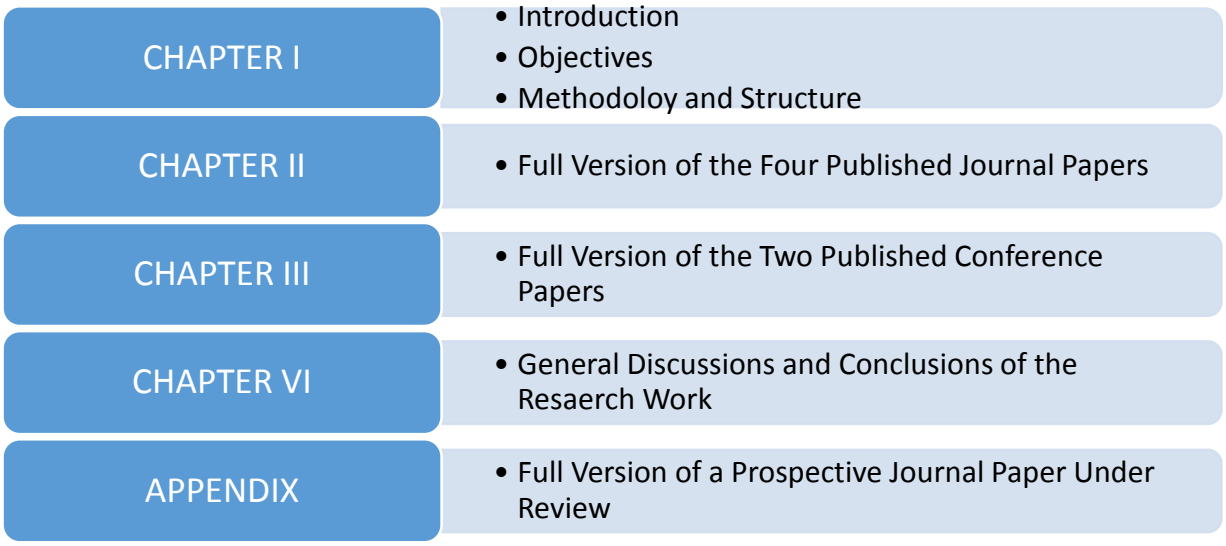

Figure 6. Ph.D. document outline

1.6 References

[1] B. Mobasher, *Mechanics of fiber and textile reinforced cement composites*. 2011.
[2] O. S. Abiola, *Natural fibre cement composites*. Elsevier Ltd, 2016.
[3] E. Erdogmus, "Use of Fiber-Reinforced Cements in Masonry Construction and Structural Rehabilitation," *Fibers*, vol. 3, no. 1, pp. 41–63, 2015.
[4] M. Ardanuy, J. Claramunt, and R. D. Toledo Filho, "Cellulosic fiber reinforced cement-based composites: A review of recent research," *Constr. Build. Mater.*, vol. 79, pp. 115–128, 2015.
[5] F. Pacheco-Torgal and S. Jalali, "Cementitious building materials reinforced with vegetable fibres: A review," *Constr. Build. Mater.*, vol. 25, no. 2, pp. 575–581, 2011.
[6] A. M. Brandt, "Fibre reinforced cement-based (FRC) composites after over 40 years of development in building and civil engineering," *Compos. Struct.*, vol. 86, no. 1–3, pp. 3–9, 2008.
[7] E. Booya, K. Gorospe, H. Ghaednia, and S. Das, "Free and restrained plastic shrinkage of cementitious materials made of engineered kraft pulp fibres," *Constr. Build. Mater.*, vol. 212, pp. 236–246, Jul. 2019.
[8] P. Soroushian and S. Ravanbakhsh, "Control of plastic shrinkage cracking with specialty cellulose fibers," *ACI Mater. J.*, vol. 95, no. 4, pp. 429–435, Jul. 1998.
[9] P. Jongvisuttisun and K. E. Kurtis, "The role of hardwood pulp fibers in mitigation of early-age cracking," *Cem. Concr. Compos.*, vol. 57, pp. 84–93, Mar. 2015.
[10] R. D. Toledo Filho, K. Ghavami, M. A. Sanjuán, and G. L. England, "Free, restrained and drying shrinkage of cement mortar composites reinforced with vegetable fibres," *Cem. Concr. Compos.*, vol. 27, no. 5, pp. 537–546, 2005.
[11] S. Kawashima and S. P. Shah, "Early-age autogenous and drying shrinkage behavior of cellulose fiber-reinforced cementitious materials," *Cem. Concr. Compos.*, vol. 33, no. 2, pp. 201–208, 2011.
[12] P. J. M. Mehta, P.K.; Montiero, *Concrete Microstructure, Properties, and Materials*, 3rd ed.; M. 2006.

[13] H. N. Marsh *et al.*, "State-of-the-Art Report on Fiber Reinforced Concrete," *J. Proc.*, vol. 70, no. 11, pp. 729–744, Nov. 1973.
[14] A. J. Majumdar and R. W. Nurse, "Glass fibre reinforced cement," *Mater. Sci. Eng.*, vol. 15, no. 2–3, pp. 107–127, Aug. 1974.
[15] J. Claramunt, L. J. Fernández-Carrasco, H. Ventura, and M. Ardanuy, "Natural fiber nonwoven reinforced cement composites as sustainableClaramunt, J., Fernández-Carrasco, L. J., Ventura, H., & Ardanuy, M. (2016). Natural fiber nonwoven reinforced cement composites as sustainable materials for building envelopes. Constructio," *Constr. Build. Mater.*, vol. 115, pp. 230–239, 2016.
[16] S. S. Rahman, S. Siddiqua, and C. Cherian, "Sustainable applications of textile waste fiber in the construction and geotechnical industries: A retrospect," *Clean. Eng. Technol.*, vol. 6, p. 100420, Feb. 2022.
[17] E. Booya, H. Ghaednia, S. Das, and H. Pande, "Durability of cementitious materials reinforced with various Kraft pulp fibers," *Constr. Build. Mater.*, vol. 191, pp. 1191–1200, Dec. 2018.
[18] J. Khedari, B. Suttisonk, N. Pratinthong, and J. Hirunlabh, "New lightweight composite construction materials with low thermal conductivity," *Cem. Concr. Compos.*, vol. 23, no. 1, pp. 65–70, 2001.
[19] M. Bentchikou, A. Guidoum, K. Scrivener, K. Silhadi, and S. Hanini, "Effect of recycled cellulose fibres on the properties of lightweight cement composite matrix," *Constr. Build. Mater.*, vol. 34, pp. 451–456, 2012.
[20] M. Saidi and A. Gabor, "Iterative analytical modelling of the global behaviour of textile-reinforced cementitious matrix composites subjected to tensile loading," *Constr. Build. Mater.*, vol. 263, p. 120130, 2020.
[21] R. D. Toledo Filho, F. de A. Silva, E. M. R. Fairbairn, and J. de A. M. Filho, "Durability of compression molded sisal fiber reinforced mortar laminates," *Constr. Build. Mater.*, vol. 23, no. 6, pp. 2409–2420, Jun. 2009.
[22] F. de A. Silva, B. Mobasher, and R. D. T. Filho, "Cracking mechanisms in durable sisal fiber reinforced cement composites," *Cem. Concr. Compos.*, vol. 31, no. 10, pp. 721–730, 2009.
[23] M. E. A. Fidelis, F. de Andrade Silva, and R. D. Toledo Filho, "The Influence of Fiber Treatment on the Mechanical Behavior of Jute Textile Reinforced Concrete," *Key Eng. Mater.*, vol. 600, pp. 469–474, Mar. 2014.
[24] F. de Andrade Silva, B. Mobasher, and R. D. T. Filho, "Fatigue behavior of sisal fiber reinforced cement composites," *Mater. Sci. Eng. A*, vol. 527, no. 21–22, pp. 5507–5513, Aug. 2010.
[25] F. de A. Silva, D. Zhu, B. Mobasher, C. Soranakom, and R. D. Toledo Filho, "High speed tensile behavior of sisal fiber cement composites," *Mater. Sci. Eng. A*, vol. 527, no. 3, pp. 544–552, Jan. 2010.
[26] I. Colombo, M. Colombo, A. Magri, G. Zani, and M. Di Prisco, "Textile reinforced mortar at high temperatures," *Appl. Mech. Mater.*, vol. 82, no. July, pp. 202–207, 2011.
[27] C. Paper, I. G. Colombo, M. Colombo, A. Magri, and G. Zani, "Tensile Behavior of Textile : Influence of Multilayer Reinforcement Tensile behaviour of Textile : influence of multilayer reinforcement," no. May 2014, 2011.
[28] G. Zani, M. Colombo, and M. Di Prisco, "High performance cementitious composites for sustainable roofing panels," *Proc. 10th fib Int. PhD Symp. Civ. Eng.*, no. February 2015, pp. 333–338, 2014.
[29] G. Promis, T. Q. Bach, A. Gabor, and P. Hamelin, "Failure behavior of E-glass fiber- and fabric-reinforced IPC composites under tension and compression loading," *Mater. Struct. Constr.*, vol. 47, no. 4, pp. 631–645, 2014.
[30] J. Claramunt, H. Ventura, L. J. Fernández-carrasco, and M. Ardanuy, "Tensile and Flexural Properties of Cement Composites Reinforced with Flax Nonwoven Fabrics," *Materials (Basel).*, pp. 1–12, 2017.

[31] G. Giaccio, M. E. Bossio, M. C. Torrijos, and R. Zerbino, "Contribution of fiber reinforcement in concrete affected by alkali–silica reaction," *Cem. Concr. Res.*, vol. 67, pp. 310–317, Jan. 2015.
[32] R. D. Tolêdo Filho, K. Scrivener, G. L. England, and K. Ghavami, "Durability of alkali-sensitive sisal and coconut fibres in cement mortar composites," *Cem. Concr. Compos.*, vol. 22, no. 2, pp. 127–143, Apr. 2000.
[33] J. Claramunt, M. Ardanuy, J. A. García-Hortal, and R. D. T. Filho, "The hornification of vegetable fibers to improve the durability of cement mortar composites," *Cem. Concr. Compos.*, vol. 33, no. 5, pp. 586–595, 2011.
[34] M. Ardanuy, J. Claramunt, J. A. García-Hortal, and M. Barra, "Fiber-matrix interactions in cement mortar composites reinforced with cellulosic fibers," *Cellulose*, vol. 18, no. 2, pp. 281–289, Apr. 2011.
[35] S. F. Santos, G. H. D. Tonoli, J. E. B. Mejia, J. Fiorelli, and H. Savastano Jr, "Non-conventional cement-based composites reinforced with vegetable fibers: A review of strategies to improve durability," *Mater. Construcción*, vol. 65, no. 317, p. e041, 2015.
[36] R. M. de Gutiérrez, L. N. Díaz, and S. Delvasto, "Effect of pozzolans on the performance of fiber-reinforced mortars," *Cem. Concr. Compos.*, vol. 27, no. 5, pp. 593–598, May 2005.
[37] L. Fernández-Carrasco, J. Claramunt, and M. Ardanuy, "Autoclaved cellulose fibre reinforced cement: Effects of silica fume," *Constr. Build. Mater.*, vol. 66, no. September, pp. 138–145, 2014.
[38] M. Khorami and E. Ganjian, "The effect of limestone powder, silica fume and fibre content on flexural behaviour of cement composite reinforced by waste Kraft pulp," *Constr. Build. Mater.*, vol. 46, pp. 142–149, 2013.
[39] M. E. A. Fidelis, R. D. Toledo Filho, F. de A. Silva, V. Mechtcherine, M. Butler, and S. Hempel, "The effect of accelerated aging on the interface of jute textile reinforced concrete," *Cem. Concr. Compos.*, vol. 74, pp. 7–15, Nov. 2016.
[40] F. Majstorović, V. Sebera, M. Mrak, S. Dolenec, M. Wolf, and L. Marrot, "Impact of metakaolin on mechanical performance of flax textile-reinforced cement-based composites," *Cem. Concr. Compos.*, vol. 126, p. 104367, Feb. 2022.
[41] F. D. Tolêdo Romildo D., K. Ghavami, G. L. England, and K. Scrivener, "Development of vegetable fibre-mortar composites of improved durability," *Cem. Concr. Compos.*, vol. 25, no. 2, pp. 185–196, Feb. 2003.
[42] J. Claramunt, H. Ventura, L. J. Fernández-Carrasco, and M. Ardanuy, "Tensile and flexural properties of cement composites reinforced with flax nonwoven fabrics," *Materials (Basel).*, vol. 10, no. 2, pp. 1–12, 2017.
[43] F. D. A. Silva, R. D. T. Filho, J. D. A. M. Filho, and E. D. M. R. Fairbairn, "Physical and mechanical properties of durable sisal fiber–cement composites," *Constr. Build. Mater.*, vol. 24, no. 5, pp. 777–785, May 2010.
[44] M. Ramirez, J. Claramunt, H. Ventura, and M. Ardanuy, "Evaluation of the mechanical performance and durability of binary blended CAC-MK/natural fiber composites," *Constr. Build. Mater.*, vol. In progres, 2019.
[45] V. da Costa Correia, S. F. Santos, and H. Savastano, "Vegetable fiber as reinforcing elements for cement based composite in housing applications – a Brazilian experience," *MATEC Web Conf.*, vol. 149, p. 01007, 2018.
[46] G. H. D. Tonoli, S. F. Santos, A. P. Joaquim, and H. Savastano, "Effect of accelerated carbonation on cementitious roofing tiles reinforced with lignocellulosic fibre," *Constr. Build. Mater.*, vol. 24, no. 2, pp. 193–201, Feb. 2010.
[47] B. Koohestani, A. K. Darban, P. Mokhtari, E. Yilmaz, and E. Darezereshki, "Comparison of different natural fiber treatments: a literature review," *Int. J. Environ. Sci. Technol. 2018 161*, vol. 16, no. 1, pp. 629–642, Jul. 2018.
[48] J. Claramunt, M. Ardanuy, and J. A. García-Hortal, "Effect of drying and rewetting cycles on the

structure and physicochemical characteristics of softwood fibres for reinforcement of cementitious composites," *Carbohydr. Polym.*, vol. 79, no. 1, pp. 200–205, 2010.
[49] "High energy performing buildings - Publications Office of the EU." [Online]. Available: https://publications.europa.eu/en/publication-detail/-/publication/d8e3702d-c782-11e8-9424-01aa75ed71a1/language-en/format-PDF/source-77709912.
[50] F. Bagheri Moghaddam, J. M. Fort Mir, I. Navarro Delgado, and E. Redondo Dominguez, "Evaluation of Thermal Comfort Performance of a Vertical Garden on a Glazed Façade and Its Effect on Building and Urban Scale, Case Study: An Office Building in Barcelona," *Sustain. 2021, Vol. 13, Page 6706*, vol. 13, no. 12, p. 6706, Jun. 2021.
[51] A. F. Abd Rashid and S. Yusoff, "A review of life cycle assessment method for building industry," *Renewable and Sustainable Energy Reviews*, vol. 45. Elsevier Ltd, pp. 244–248, 01-May-2015.
[52] L. Cândido, W. Kindlein, R. Demori, L. Carli, R. Mauler, and R. Oliveira, "The recycling cycle of materials as a design project tool," *J. Clean. Prod.*, vol. 19, no. 13, pp. 1438–1445, Sep. 2011.
[53] J. Giesekam, J. Barrett, P. Taylor, and A. Owen, "The greenhouse gas emissions and mitigation options for materials used in UK construction," *Energy Build.*, vol. 78, pp. 202–214, Aug. 2014.
[54] H. Nautiyal, V. Shree, S. Khurana, N. Kumar, and Varun, "Recycling Potential of Building Materials: A Review," Springer, Singapore, 2015, pp. 31–50.
[55] F. Colangelo, A. Forcina, I. Farina, and A. Petrillo, "Life Cycle Assessment (LCA) of Different Kinds of Concrete Containing Waste for Sustainable Construction," *Build. 2018, Vol. 8, Page 70*, vol. 8, no. 5, p. 70, May 2018.
[56] F. Colangelo, I. Farina, M. Travaglioni, C. Salzano, R. Cioffi, and A. Petrillo, "Innovative Materials in Italy for Eco-Friendly and Sustainable Buildings," *Mater. 2021, Vol. 14, Page 2048*, vol. 14, no. 8, p. 2048, Apr. 2021.
[57] CHF, "Licensed for The Fiber Year GmbH The Fiber Year 2018 World Survey on Textiles & Nonwovens," 2018.
[58] S. Spadea, I. Farina, A. Carrafiello, and F. Fraternali, "Recycled nylon fibers as cement mortar reinforcement," *Constr. Build. Mater.*, vol. 80, pp. 200–209, Apr. 2015.
[59] C. Correia, S. Francisco, H. Savastano, and V. Moacyr, "Utilization of vegetal fibers for production of reinforced cementitious materials," no. 2017, 2018.
[60] H. Savastano, P. G. Warden, and R. S. P. Coutts, "Potential of alternative fibre cements as building materials for developing areas," *Cem. Concr. Compos.*, vol. 25, no. 6, pp. 585–592, Aug. 2003.
[61] B. Ütebay, P. Çelik, and A. Çay, "Textile Wastes: Status and Perspectives," in *Waste in Textile and Leather Sectors*, IntechOpen, 2020.
[62] A. Villanueva, L. Delgado, Z. Luo, P. Eder, A. Sofia Catarino, and D. Litten, "Study on the selection of waste streams for end-of-waste assessment. Final Report."
[63] J. J. Lu and H. Hamouda, "Current status of fiber waste recycling and its future," in *Advanced Materials Research*, 2014, vol. 878, pp. 122–131.
[64] A. Briga-Sá *et al.*, "Textile waste as an alternative thermal insulation building material solution," *Constr. Build. Mater.*, vol. 38, pp. 155–160, 2013.
[65] A. Paiva, H. Varum, F. Caldeira, A. Sá, D. Nascimento, and N. Teixeira, "Textile Subwaste as a Thermal Insulation Building Material."
[66] X. Zhou, F. Zheng, H. Li, and C. Lu, "An environment-friendly thermal insulation material from cotton stalk fibers," *Energy Build.*, vol. 42, no. 7, pp. 1070–1074, Jul. 2010.
[67] Y. Lee and C. Joo, "Sound absorption properties of recycled polyester fibrous assembly absorbers," *Autex Res. J.*, vol. 3, no. 2, pp. 78–84, 2003.
[68] D. Rajput, S. S. Bhagade, S. P. Raut, R. V. Ralegaonkar, and S. A. Mandavgane, "Reuse of cotton and recycle paper mill waste as building material," *Constr. Build. Mater.*, vol. 34, pp. 470–475, Sep. 2012.

[69] F. F. Aspiras and J. R. I. Manalo, "Utilization of textile waste cuttings as building material," *J. Mater. Process. Technol.*, vol. 48, no. 1–4, pp. 379–384, Jan. 1995.
[70] K. Aghaee and M. Foroughi, "Mechanical properties of lightweight concrete partition with a core of textile waste," *Adv. Civ. Eng.*, vol. 2013, 2013.
[71] N. P. Tran, C. Gunasekara, D. W. Law, S. Houshyar, S. Setunge, and A. Cwirzen, "Comprehensive review on sustainable fiber reinforced concrete incorporating recycled textile waste," *J. Sustain. Cem. Mater.*, vol. 0, no. 0, pp. 1–22, 2021.
[72] H. Mohammadhosseini, M. M. Tahir, A. R. Mohd Sam, N. H. Abdul Shukor Lim, and M. Samadi, "Enhanced performance for aggressive environments of green concrete composites reinforced with waste carpet fibers and palm oil fuel ash," *J. Clean. Prod.*, vol. 185, pp. 252–265, Jun. 2018.
[73] "STRENGTH, MODULUS OF ELASTICITY AND SHRINKAGE BEHAVIOUR OF CONCRETE CONTAINING WASTE CARPET FIBER | International Journal of GEOMATE." [Online]. Available: https://www.geomatejournal.com/node/288. [Accessed: 31-May-2021].
[74] W. Xuan, X. Chen, G. Yang, F. Dai, and Y. Chen, "Impact behavior and microstructure of cement mortar incorporating waste carpet fibers after exposure to high temperatures," *J. Clean. Prod.*, vol. 187, pp. 222–236, Jun. 2018.
[75] H. Mohammadhosseini, A. S. M. Abdul Awal, and J. B. Mohd Yatim, "The impact resistance and mechanical properties of concrete reinforced with waste polypropylene carpet fibres," *Constr. Build. Mater.*, vol. 143, pp. 147–157, Jul. 2017.
[76] X. Wu, J. Zhou, T. Kang, F. Wang, X. Ding, and S. Wang, "Laboratory Investigation on the Shrinkage Cracking of Waste Fiber-Reinforced Recycled Aggregate Concrete.," *Mater. (Basel, Switzerland)*, vol. 12, no. 8, Apr. 2019.
[77] M. S. Meddah and M. Bencheikh, "Properties of concrete reinforced with different kinds of industrial waste fibre materials," *Constr. Build. Mater.*, vol. 23, no. 10, pp. 3196–3205, Oct. 2009.
[78] P. Sadrolodabaee, J. Claramunt, M. Ardanuy, and A. de la Fuente, "Mechanical and durability characterization of a new textile waste micro-fiber reinforced cement composite for building applications," *Case Stud. Constr. Mater.*, vol. 14, p. e00492, Jun. 2021.
[79] P. Sadrolodabaee, J. Claramunt, M. Ardanuy, and A. de la Fuente, "Characterization of a textile waste nonwoven fabric reinforced cement composite for non-structural building components," *Constr. Build. Mater.*, vol. 276, p. 122179, Mar. 2021.
[80] P. Sadrolodabaee, J. Claramunt, M. Ardanuy, and A. de la Fuente, "A Textile Waste Fiber-Reinforced Cement Composite: Comparison between Short Random Fiber and Textile Reinforcement," *Mater. 2021, Vol. 14, Page 3742*, vol. 14, no. 13, p. 3742, Jul. 2021.
[81] P. Sadrolodabaee *et al.*, "Experimental characterization of comfort performance parameters and multi-criteria sustainability assessment of recycled textile-reinforced cement facade cladding," *J. Clean. Prod.*, vol. 356, p. 131900, Jul. 2022.
[82] P. Sadrolodabaee, J. Claramunt Blanes, M. Ardanuy Raso, and A. de la Fuente Antequera, "Preliminary study on new micro textile waste fiber reinforced cement composite," *ICBBM 2021 4th Int. Conf. Bio-based Build. Mater. Barcelona, Catalunya June 16-18, 2021 Proc.*, pp. 37–42, 2021.
[83] P. Sadrolodabaee, S. M. A. Hosseini, M. Ardunay, J. Claramunt, and A. de la Fuente, "A New Sustainability Assessment Method for Façade Cladding Panels: A Case Study of Fiber/Textile Reinforced Cement Sheets," pp. 809–819, Sep. 2021.

2. CHAPTER ° II

JOURNAL PAPERS OF THE COMPENDIUM

This chapter reproduces the four published journals derived from the research work. Each paper follows its own numbering of sections, figures, equations, and references.

2.1 Journal paper I:

Mechanical and durability characterization of a new textile waste micro-fiber reinforced cement composite for building applications

Published in Case Studies in Construction Materials (Volume 14, June 2021, e00492)

Payam Sadrolodabaeea[a*] (payam.sadrolodabaee@upc.edu), Josep Claramunt[b] (josep.claramunt@upc.edu), Monica Ardanuy [c](monica.ardanuy@upc.edu), Albert de la Fuente[a] (albert.de.la.fuente@upc.edu)

a: Department of Civil and Environmental Engineering- Universitat Politècnica de Catalunya-BarcelonaTECH- Barcelona, Spain
b: Department of Agricultural Engineering- Universitat Politècnica de Catalunya-BarcelonaTECH- Barcelona, Spain
c: Department of Material Science and Engineering (CEM)-Universitat Politècnica de Catalunya-BarcelonaTECH-Barcelona, Spain
*: Corresponding author

Abstract

Fiber-reinforced mortars (FRM) are growingly used in several fields of building technology (e.g., façade panels, roofing, raised floors, and masonry structures) as building elements. One of the promising types of fiber for these composite materials can be textile waste originating from cloth wastes. The use of this sort of recycled materials and wastes as cement reinforcement within the building sector can play a relevant role in sustainability, both the environmental, economic, and social perspectives. In this paper, the design mechanical properties (flexural and compressive strengths at 7,28 and 56 days as well as toughness and stiffness) together with durability properties of cement pastes reinforced with short Textile Waste Fiber (TWF) in contents ranging from 6 to 10% by weight fraction cement was investigated. The results were compared with those obtained from Kraft Pulp pine Fiber (KPF), taken as reference. The main conclusion is the feasibility of using this type of fiber as potential reinforcement in construction materials with the optimum dosage of 8%. Although the flexural resistance and toughness of the TWF composite are lower than KPF control by almost 9%, the compressive strength and stiffness together with durability properties have proven to be enhanced with respect to the reference composite.

Keywords: cementitious materials; durability; fiber-reinforced composites; mechanical properties; sustainability; textile waste fibers

1. Introduction

Cementitious materials present the highest compressive strength to weight ratio compared to other construction materials [1]. Nonetheless, both tensile strength capacity and toughness result to be an order of magnitude less respect to the former, which thereby leads to cracking under tensile stresses caused by low service loads [2]. This lack of tensile strength capacity derives in material prone to crack and fragile in case of failure [3]. For this reason, fibers have been predominantly used in cementitious matrices aiming at enhancing the toughness, energy absorption capacity, post-cracking behavior [4–6] as well as flexural and tensile strength [7, 8].

The incorporation of fibers has also resulted in improvements respect to shrinkage [9,10] and durability according to several authors [11–13]. In this regard, the use of fibers can limit crack propagation and control the crack width, which can result in an effective reduction of the aggressive agents' ingress and the associated consequences. This is of particular interest when the use of this composite material is oriented to applications with a certain level of structural responsibility for which strength, ductility and durability requirements are demanded.

Although during the past decades various types of fibers such as asbestos [7], steel [13–15], glass [16,17] and polymeric [18–20] have been tested in brittle matrices, there have been some disadvantages

such as detrimental health effects, high cost, and specifically, substantial environmental footprint [21–23]. Likewise, based on the statistics, the construction sector is responsible for about 40% of the European Union's total final energy consumption and 36% of its total CO_2 emissions [24]. That is why significant efforts should be devoted to applying the '3Rs' concept of reducing, reusing and recycling in the building sector and material fabrication [25].

The use of more environmentally friendly materials obtained from renewable sources or secondary raw materials with sustainable recycling processes could be an interesting solution for the reduction of CO_2 emissions and energy intake, even in fiber production [26,27]. World fiber production has been steadily increasing in the past few decades, now exceeding 100 million tons per year [28]. In this sense, vegetable and cellulosic fibers have been already used as sustainable and durable [29–36] reinforcement in mortars and composites for low-performance structural applications [37–39]. Another promising and sustainable type of fiber as reinforcement for cement-based materials could be textile waste fiber.

The textile leftover is one of the predominant wastes' resources worldwide. Just in the EU, around 5.8 million tons of textiles per year are unprocessed while only 25% of these textiles are recycled by charities and industrial enterprises; the remaining goes to landfills or municipal waste incinerators [40,41]. Thus, the reuse of these textile waste cutting - including all fiber, yarn and fabric waste produced during the garment manufacturing process as well as all worn out or not fashionable clothing discarded by the users - in constructions is becoming a potential alternative due to the shortage of natural mineral resources and increasing waste disposal costs [42,43].

The production process of these shredded fibers involves low energy consumption and it is mainly mechanically with low-heat emission [44]. Textile waste (TW, hereinafter) fibers manufactured from a combination of several fibers, natural or synthetic such as cotton, wool, silk, polyester, nylon, and polypropylene is a very abundant waste. These can draw great attention as reinforcement of fragile matrices, building insulations and lightweight bricks owing to low-cost, lightweight, availability, energy-saving, and environmental preservation [45]. The production of materials reinforced with TW fibers is feasible and economically viable in regions where the raw material is abundant - almost everywhere.

According to several studies [46–50], TW fibers can be used as thermal insulation building materials. In this sense, the application of this kind of waste in external double walls resulted in increasing the thermal insulation capacity to 40% respect to the double-wall with the air cavity. The thermal conductivity and properties value of the woven and nonwoven fabrics waste were similar to other conventional insulation materials [50] (expanded polystyrene, extruded polystyrene, and mineral wool).

Fibrous structures are also good examples of sound-absorbing materials. Several authors investigated the acoustic performances of these materials. Lee et al.[51] put forward the use of recycled polyester fibers to produce sound absorbing non-woven materials. The authors indicated that by increasing the diameter, thickness, length, and content of fibers, the sound absorption coefficient of the non-woven fabric improved. In another study by Tiuc et al. [52], different non-woven fabrics containing natural and synthetic textile fibers were tested. The results proved a good sound absorption coefficient at medium and high frequencies, but a lower sound absorption coefficient at low frequencies.

In another research [53], the flammability of this composite was studied. The textile waste composite was subjected to an open flame for 30 minutes. Despite the high flammability of the TW cuttings, the composite showed no evidence of burning, thus proving a good fireproofing material.

Several authors [54–56] carried out research on the use of textile fibers to produce lightweight bricks. Results showed that with the increase of the textile waste fibers content, predominately cotton, the porosity of the cement bricks increased. A more porous structure allowed an improvement in the thermal performance and an increase in the water absorption. Experimental investigations indicated that these innovative bricks were lighter in comparison with commercial concrete bricks. Also, the insulation capacity of the former was better, i.e. the thermal conductivity coefficient was 29.3% lower respect to commercial concrete brick. In a similar study [57], textile waste fiber clay bricks tested and the results indicated that the samples containing fibers had lower water absorption than the simple clay sample.

The compatibility of fiber residues from the nonwoven textile industry with Portland cement has been studied by Monteiro et al. [58]. It was reported that the textile waste used in this investigation resulted to be incompatible with the cement setting probably due to high cotton content which disturbed cement setting reactions. So, cement did not set in a full extent as observed by temperature monitoring; this being the unique research, according to the author's knowledge, that stated this negative effect.

In order to identify the target potential applications of this material, the mechanical properties should be characterized. In this sense, the engineering design properties of TWF reinforced cement composites have not been deeply investigated yet and, consequently, its structural suitability cannot be confirmed. Hence, the main goal of this research consists in carrying out an extensive experimental program to characterize the mechanical and durability properties of a new short randomly dispersed TW fiber-reinforced cement paste meant for constructional purposes. As a result, both compressive and flexural (at pre-and post-cracking stages) strength capacities, together with the toughness and stiffness properties as well as the optimum dosage were derived from the experimental program. The results were finally compared with those obtained from reference mortar samples reinforced with kraft pulp pine fibers, these fibers being one of the most prevailing fibers in cellulose fiber-reinforced composites.

2. Experimental Procedure

2.1 Materials

2.1.1 Binder

A Portland cement Type I 52.5R supplied by Cementos Molins Industrial, S.A. (Spain) has been used for producing the mortars. Chemical composition criteria and physical/mechanical requirements according to EN 197-1:2011 and given by the supplier are reported in previous work [36].

2.1.2 Fibers

TW fibers were provided by Triturats La Canya S.A (Spain) and these consisted of 30.7% polyester and 69.3 cotton. The moisture content (expressed as relative humidity) and the water retention values were 7% and 85, respectively. The gross 75% of the weight is represented by fibers with diameters ranging from 3.6 to 32.1 μm, the rest being a mix of yarns and fabrics (see Figures 1-a,b,c).

Unbleached softwood kraft pulp (Pinus insignis) with 7.8% (over the total weight) of lignin, and an aspect ratio of 88 supplied by Smurfit Kappa Nervión, S.A. (Spain) [39] was used as the reference mortar reinforcement (Figure 1-d)

2.2 Samples preparation

The TW fiber-reinforced mortars were prepared in a laboratory mixer pan and posteriorly casted into a 20x40x160 mm mold in which a 5 MPa pressure was applied in order to eliminate the water excess. The

specimens remained 24 hrs. under the press machine and posteriorly demolded and placed in a climate chamber (20°C and 90% of RH) for 7, 28 and 56 days according to the test procedure considered in [32,59,60]. Figure 2 depicts the casting and curing procedure carried out.

The designation of the specimens (Table 1) is based on the fiber type: TW being the Textile Waste and CTR the Control Kraft Pulp. The numbers indicate the fiber dosages expressed in percentage of the cement weight (6, 8 and 10%). Samples for durability tests are designated with D (TWD8 and CTRD8). The initial and final water/cement ratios, (w/c) initial and (w/c) final, together with the initial dosage of the materials to make the fiber-reinforced mortar for 1000 cm3 are also reported in Table 1. Six specimens were cast for each sample.

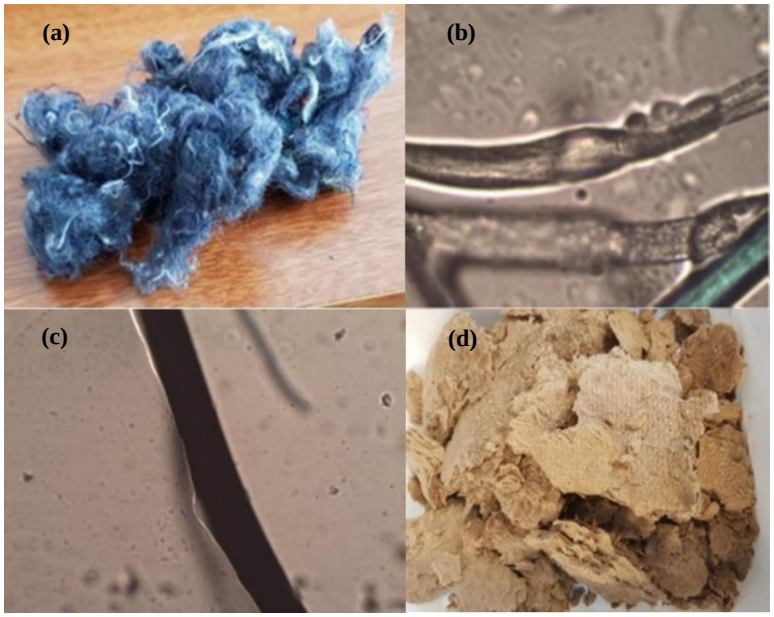

Figure 1. (a) Textile Waste Fiber (TWF); microscopic image of the TWF components: (b) cotton – magnification 40x1 and (c) polyester – magnification 40x1.25 and (d) Kraft Pulp Fiber (KPF)

The KPF was saturated before its addition to the mortar paste, in order to facilitate the dispersion. For this reason, the initial water/cement ratio of the CTR samples was higher than those of TW specimens. However, the final water/cement ratio of both composites varied between 0.35-0.50 after the elimination of excess water by compression during 24 hrs.

Table 1 – w/c of the samples and codification of the specimens

CODE		**TW6**	**TW8**	**TW10**	**TWD8**	**CTR6**	**CTR8**	**CTR10**	**CTRD8**
$(w/c)_{initial}$		0.50	0.50	0.50	0.50	1.00	1.50	1.40	1.50
$(w/c)_{final}$	**7 days**	0.42	0.44	0.44	-	0.43	0.44	0.44	-
	28 days	0.40	0.50	0.50	0.45	0.42	0.42	0.35	0.50
	56 days	0.45	0.40	0.45	-	0.45	0.39	0.35	-
Initial Cement(gr)		1600	1400	1200	1400	1600	1400	1200	1400
Initial Water(gr)		800	700	600	700	500	440	360	440
Initial Dried Fiber(gr)		96	112	120	112	96	112	120	112

Figure 2. Preparation of the samples: (a) mixing process; (b) molds filled with material; (c) compression and water excess elimination process and (d) curing conditions

2.3 Mechanical Tests

2.3.1 Flexural tensile strength and toughness

Three-point bending tests (Figure 3) on 100 mm span-length unnotched beam specimens were carried out in order to quantify the pre and post-cracking contribution of the fiber reinforcement. For this purpose, an INCOTECNIC press equipped with a load cell of 3 KN capacity based on EN 12467:2012 [61] was used. The test was controlled with a closed-loop system, the loading rate being 4 mm/min. Six specimens were tested for each sample at 7, 28 and 56 days.

The maximum flexural tensile strength (or also named Modulus of Rupture, MOR) of the composite was determined by means of Equation 1, where Pmax is the maximum load recorded, L is the span length (100 mm), and b (40 mm) and h (20 mm) are the cross-sectional width and thickness, respectively.

$$MOR = \frac{3P_{max}L}{2bh^2} \qquad (Equation\ 1)$$

The toughness index (I_G), defined as the area beneath the force-displacement curve comprised from zero to a post-failure load of 0.4 MOR was established as the reference parameter to characterize the type of failure (ductile or fragile) and the post-failure deformation capacity.

The flexural stiffness (K) was also measured from the force-displacement relationships during elastic deformation by using Equation 2 based on [61], where Δp and Δf are the variations of forces and deflections of 2 points on the elastic regime, and the rest of the parameters as defined per Equation 1.

$$K = = \frac{\Delta P . L^3}{4 \Delta f . b h^3} \qquad (Equation\ 2)$$

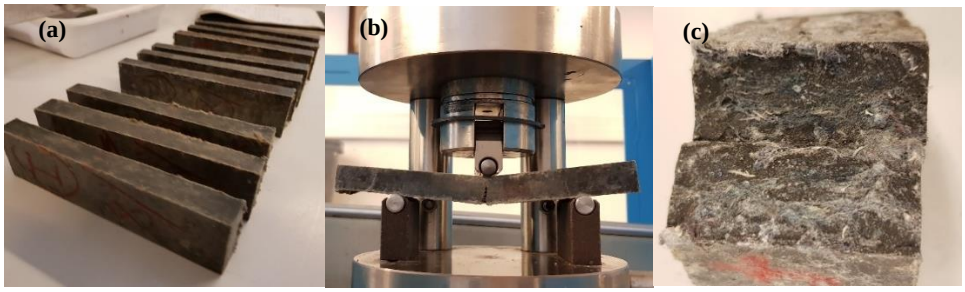

Figure 3. Flexural tests set-up: (a) 20x40x160 mm specimens; (b) flexural test configuration; (c) cross-section of a tested-to-failure specimen

2.3.2 Compressive strength test

After completion of the flexural tensile tests, the remaining halves were subjected -on a 20mm side- to compression (Figure 4a). To this end, an INCOTECNIC press equipped with a maximum load cell of 300 kN was used and the test procedure was carried out according to UNE-EN 196-1 [62] (Figure 4b).

The compressive strength is computed as $f_c = P_{max}/A$, where A is the total area of the rectangular plate placed between the loading jack and the specimen tested. Twelve specimens were tested for each sample at each age.

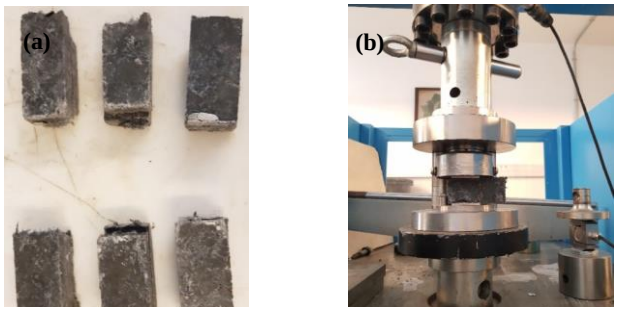

Figure 4. Compressive strength tests: (a) remaining halves of the flexural tests and (b) test configuration

2.3.3 Durability test and microscope analyses

Durability in environments where wet-dry cycles are predominant is considered one of the main problems in vegetable fibers [35,36]. In this sense, those TW specimens resulted to provide better mechanical properties subjected to a durability test. This consisted of applying 25 dry-wet cycles, after 28 days of curing in a climatic chamber, according to EN 12467. Each dry-wet cycle consisted of drying for 6 hours at 60°C and 60% of RH followed by 18 hours of immersion in water at 20°C. The climatic chambers for this process as well as the samples after accelerated aging cycles are shown in Figure 5.

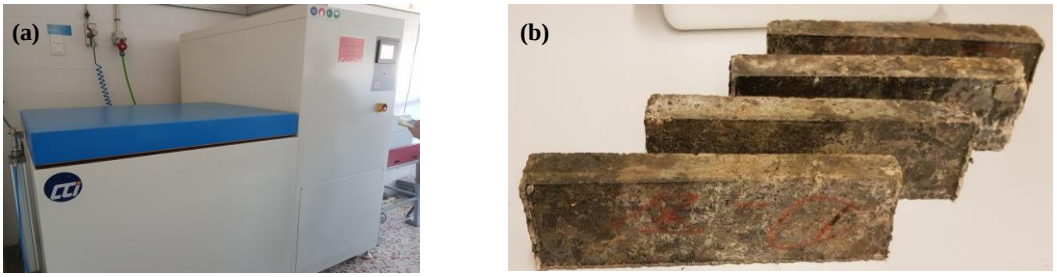

Figure 5. Durability test: (a) CCI chamber (b) Specimens after 25 cycles

Finally, the scanning electron microscope observation was carried out by using a Jeol JSM 5610 SEM device in order to analyze the fractured surface microstructure and the effects of the wet-drying cycles.

3. Results and discussions

3.1 Flexural test

In Figure 6, representative flexural stress-displacement curves derived from the bending tests are depicted. Likewise, Tables 2-3 gather the mean, minimum, maximum, and CoV of the Limit of proportionality (LOP) and the Modulus of rupture (MOR) obtained for each composite at different ages. According to the results depicted in Figure 6, the bending response consists of three stages: First, an elastic range is represented by a linear tendency until the appearance of the first crack when the LOP strength is achieved; the LOP magnitude is mainly governed by the strength of the matrix. Second, a post-cracking branch with a decreasing positive slope in which both matrix and fibers contribute to the strength of the composite and increase the toughness and ductility. Finally, a post-failure regime with a decreasing negative slope represents the pre-and failure of the composite.

Based on the LOP values of the TWF composites presented in Table 2 it can be concluded that flexural resistance to the first crack decreased averagely 10% with the addition of fibers. This was due to the reduction of the cement amounts with the increase of the number of fibers (see Table 1). In this sense, it must be remarked that the fibers barely contribute to the resistant mechanism before the occurrence of the first crack. The reduction of LOP for CTR composites was less than 2%, this indicating that kraft pulp fibers were mixed more homogeneously inside the matrix and creating fewer voids. The LOP values were higher in TWF composite respect to CTR when a 6% fiber dosage was used, while by increasing the amount of fiber to 10%, the trend was reversed. Finally, it can also be observed an increase in the LOP with the aging of the samples from 7 to 56 days by 25% for both composites due to the cement hydration and the hardening time-dependent processes.

On the other hand, the values of MOR gathered in Table 3 permit to confirm that the addition of these type of fibers provide a post-cracking flexural strength capacity ($MOR_m > LOP_m$) to the composite, this presenting, thus, a flexural-hardening response. In this regard, fibers bridge the cracks by controlling the opening and guaranteeing a stress transfer mechanism across the crack height. The results gathered in Figure 7 highlight that the MOR increased with the increase of the fiber content up to 8% for both types of fibers whilst this decreases for higher fiber amounts, independently of the composite age. This phenomenon could be caused by the technical difficulties associated with the mixing, balling effect, and compaction of these high amounts of fibers [4]. In fact, an 8% fiber dosage had the highest contribution in the post flexural

resistance,i.e., highest MOR_m/LOP_m. This result is in agreement with the finding of [63], in which the MOR of cement boards reinforced by different amounts of waste kraft pulp fiber (1–14%) was investigated and it was proved that with increasing contents up to 8%, MOR increased whilst adding fibers content superior than 8% had the opposite effect.

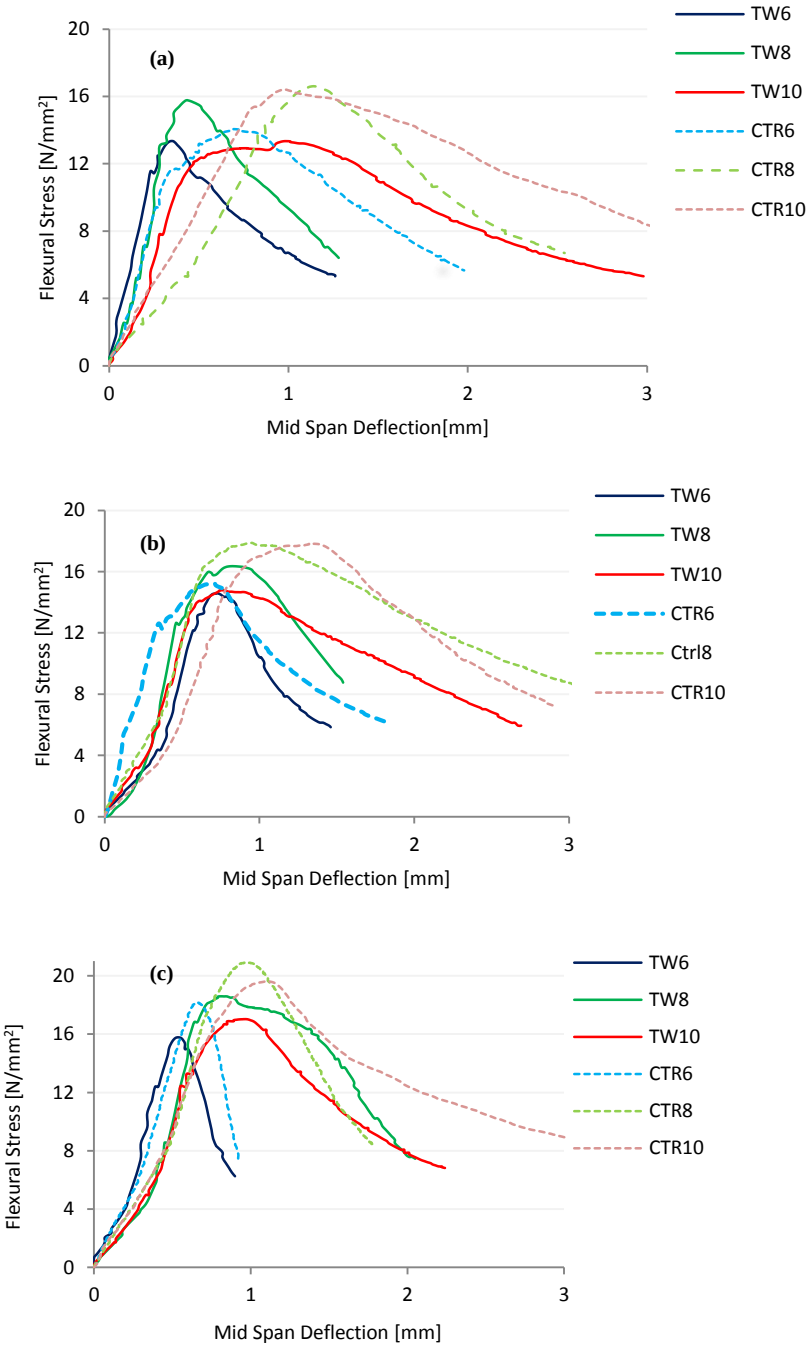

Figure 6. Representative stress – deflection relationships obtained from the flexural tests at (a) 7; (b) 28 and (c) 56 days

According to the results presented in Table 3 and Figure 7, TW6 and TW10 composites presented similar MOR while TW8 composites evidenced averagely 15, 6, and 17% higher MOR at 7, 28, and 56 days curing, respectively. Nonetheless, kraft pulp samples (CTR) presented differences in terms of MOR smaller than 5% for the different amounts considered. This could indicate that pulp fibers distribute more homogeneously for high amounts (>8%) respect to the TWF. The average MOR of the TWF composite (17.7 N/mm^2) was lower than kraft pulp control (19.8 N/mm^2) by 9% for 8% of both fibers at 56 days. Hence, an 8% fiber dosage has been considered the optimum amount for both composites in terms of MOR. It can also be noticed a slight increase of the MOR with the composite aging from 7 to 56 days, 15% (TW) and 26% (CTR).

Table 2– LOP in N/mm^2 (CoV in %) of the composites at different ages

Ages		TW6	TW8	TW10	CTR6	CTR8	CTR10
7 days	LOP_m	11.6(18)	11.1(16)	10.7(4)	11.5(3)	11.1(13)	10.6(15)
	LOp_{min}–LOP_{max}	10.0–15.0	9.3-14.0	10.5-11.1	11.0–12.0	9.0–12.3	8.1–12.1
28 days	LOp_m	12.7(12)	11.1(10)	10.7(10)	12.4(8)	11.9(14)	12.4(9)
	LOp_{min}–LOp_{max}	12.1–14.1	11.0–12.0	9.1–12.0	10.8–13.1	10.2–14.0	11.0–13.5
56 days	LOp_m	13.5(5)	14.4(6)	12.9(14)	13.3(8)	14.0(8)	15.0(12)
	LOp_{min}–LOP_{max}	12.3–14.1	12.0–15.2	11.0–15.0	12.2–14.9	13.0–15.1	12.2–17.0

Table 3– MOR in N/mm^2 (CoV in %) of the composites at different ages

Ages		TW6	TW8	TW10	CTR6	CTR8	CTR10
7 days	MOR_m	13.7(19)	15.4(8)	13.4(4)	13.7(12)	15.8(10)	15.0(25)
	MOR_{min}–MOR_{max}	11.2–17.2	13.7–17.1	12.5–14.0	10.6–15.0	13.7–18.6	9.0–18.3
	MOR_m/LOP_m	1.2	1.4	1.2	1.2	1.4	1.4
28 days	MOR_m	14.7(9)	15.6(20)	14.9(23)	14.7(18)	16.8(14)	16.5(19)
	MOR_{min}–MOR_{max}	12.8–16.5	11.7–20.2	10.1–19.1	10.5–17.4	13.0–18.9	10.5–19.6
	MOR_m/LOP_m	1.1	1.4	1.4	1.2	1.4	1.3
56 days	MOR_m	16.0(9)	17.7(8)	15.1(11)	17.6(29)	19.8(5)	18.9(30)
	MOR_{min}–MOR_{max}	14.5–18.2	18.4–20.3	14.7–19.1	11.0–21.5	19.1–21.8	11.0–22
	MOR_m/LOP_m	1.2	1.2	1.2	1.3	1.4	1.2

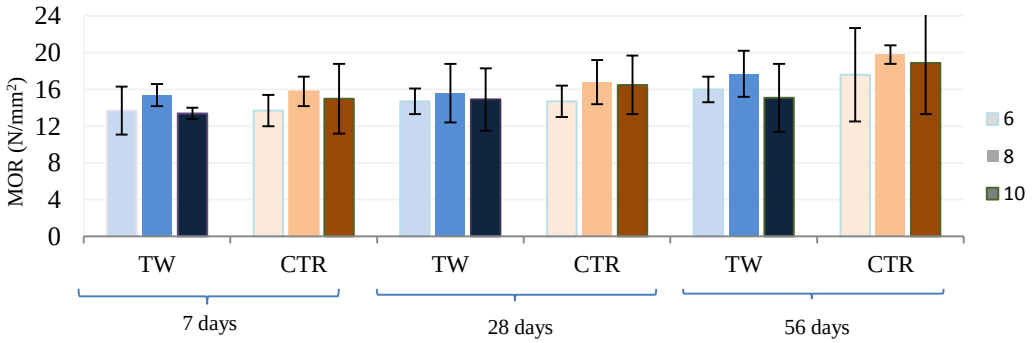

Figure 7. Results of MOR_m at different ages for the tested composites

Table 4 and Figure 8 present the toughness (I_G) of the samples tested. In this regard, the results denoted an increase of I_G with the fiber dosage, the composites with 10% of fibers performing with the higher energy absorption, with 81 and 100% higher values than 6% composites for TW and CTR respectively. The average

I_G of the CTR composites evidenced slightly greater magnitudes in comparison with those made of TWF in almost all the samples, possibly owing to the better fiber distribution in the matrix. Nonetheless, the toughness index showed for those composites with fiber amounts of 8 and 10%, all above 2 KJ/m^2, can be sufficient for low-performance structural purposes, for which deformability capacity is required. Finally, it must be highlighted that no relation between I_G and the composite age can be established.

The flexural stiffness (K) showed the opposite trend respect to the toughness since K decreases with the increase of the fiber amount, by 5% for TWF composites (see Table 5). In fact, K is mainly dependent on the matrix characteristics and as the amount of cement is reduced by fiber dosage, this parameter decreases accordingly, by following a similar trend as the LOP. Averagely, the stiffness of the TWF composites was 12% higher than those of CTR composites.

Table 4– I_G in KJ/m^2 (CoV in %) of the composites at different ages

Ages		TW6	TW8	TW10	CTR6	CTR8	CTR10
7 days	I_{Gm}	1.6(22)	2.2(32)	3.1(26)	2.0(10)	2.3(26)	3.7(11)
	I_{Gmmin}– I_{Gmax}	1.1–2.1	1.5–3.5	2.2–4.1	1.7–2.3	1.6–2.9	3.3–4.3
28 days	I_{Gm}	1.6(31)	2.1(19)	2.5(24)	1.6(25)	2.8(28)	2.9(21)
	I_{Gmmin}– I_{Gmax}	1.1–2.3	1.6–2.6	1.6–3.4	1.2–2	1.7–3.8	2.1–3.6
56 days	I_{Gm}	1.6(31)	2.7(18)	3.2(16)	1.7(29)	2.3(13)	3.6(11)
	I_{Gmmin}– I_{Gmax}	1.1–2.3	1.6–3.3	2.9–3.9	1.3–2.6	1.7–2.4	3.2–4

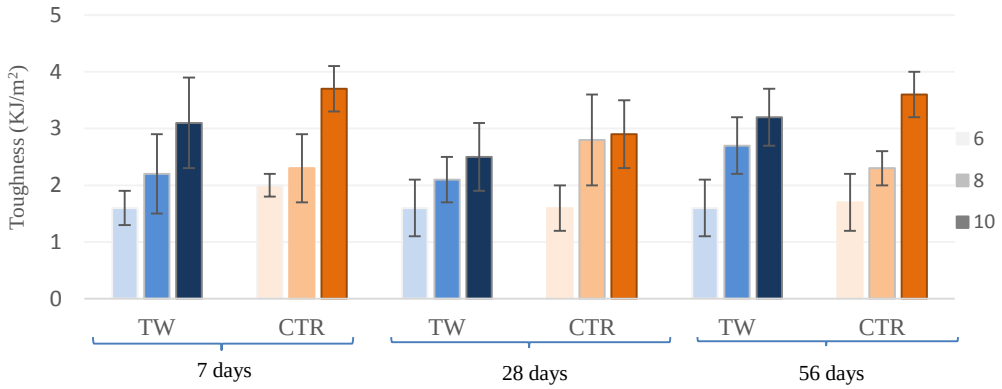

Figure 8. Results of I_{Gm} at different ages for the tested composites

Table 5– K in GPa (CoV in %) of the composites at different ages

Ages		TW6	TW8	TW10	CTR6	CTR8	CTR10
7 days	K_m	3.8(21)	3.7(24)	3.5(29)	3.4(21)	3.1(26)	3.1(29)
	K_{min}--K_{max}	2.8–5.1	2.5–4.8	1.8–4.6	2.8–4.4	2.3–4.4	2.0–4.1
28 days	K_m	4.0(19)	3.9(15)	3.7(19)	3.8(13)	3.3(9)	3.1(10)
	K_{min}--K_{max}	2.9–4.7	3.4–4.8	3.0–4.8	3.1–4.5	2.7–3.5	2.7–3.5
56 days	K_m	4.0(18)	4.0(22)	4.0(25)	3.7(29)	3.5(17)	3.1(23)
	K_{min}--K_{max}	3.2–4.8	3.1–5	2.7–4.7	1.9–4.7	3.0–4.2	2.5–4.1

3.2 Compressive test

Table 6 gathers the mean minimum, maximum, and CoV of the compressive strength (f_c), obtained for each composite, and Figure 9 depicts the results graphically.

Table 6– f_c in N/mm^2 (CoV in %) of the composites at different ages

Ages		TW6	TW8	TW10	CTR6	CTR8	CTR10
7 days	fc_m	85.8(20)	83.0(13)	43.2(31)	82.2(18)	73.7(15)	33.9(26)
	fc_{min}--fc_{max}	60.3–105.7	59.1–92.7	25.9–60.8	54.5–100.0	55.5–90.1	23.4–50.2
28 days	fc_m	112.1(20)	103.1(24)	86.7(26)	109.2(20)	79.9(28)	77.8(18)
	fc_{min}--fc_{max}	74.5–144.2	60.8–133.5	48.8–116.0	75.0–121.9	45.6–112.1	55.5–102.0
56 days	fc_m	119.1(17)	107.0(25)	88.9(29)	108.3(13)	105.4(12)	78.1(14)
	fc_{min}--fc_{max}	92.0–156.7	61.8–145.0	50.5–133.7	80.3–126.7	91.8–122.0	65.9–96.2

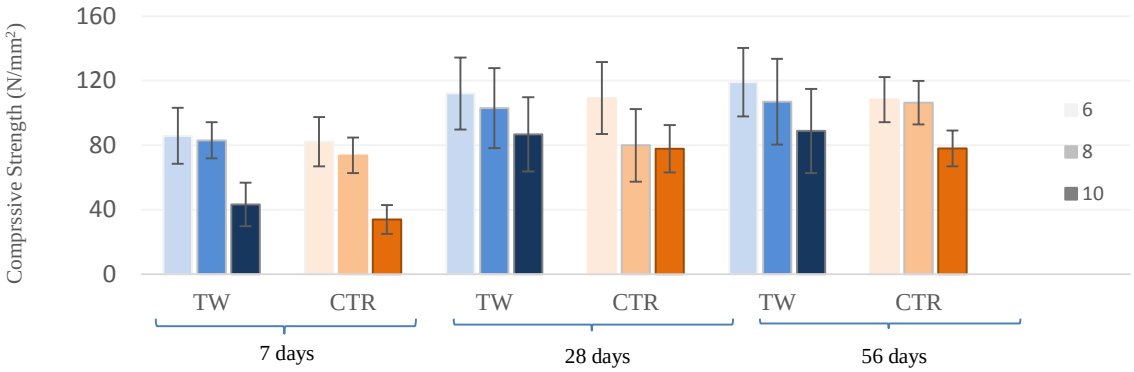

Figure 9. Results of f_c at different ages for the tested composites

In this sense, f_c decreased significantly with the increase of the fiber content, independently of the fiber type. Thus, the TWF composite with 6% of fibers had the highest values (f_{cm} from 85.8 N/mm^2 to 119.1 N/mm^2 for 7 and 56 days) while those with 10% had the lowest (f_{cm} from 43.2 N/mm^2 at 7 days to 88.9 N/mm^2 at 56 days). This decrease could be explained by the fact that increasing fiber content induces more voids which lightens and weakens the material.

Previous studies also indicated similar negative effects for cementitious materials reinforced with other natural fibers with less than 2 mm of length [10,64]. The reduction in compressive strength can also be attributed to the congestion or balling of the fibers which weakens the bond between the fibers and the matrix. Khedari et al. [65] related the reduction in compressive strength of fiber-reinforced cementitious materials to the low density of the specimens. Hence, specimens containing flexible fibers are expected to have a lower density as compared to an unreinforced specimen since these fibers induce more voids, which reduces the mass of the material [66].

It must be, however, remarked that f_c increased with the curing time and that the $f_c \geq 25$ N/mm^2 broadly accepted as the minimum required for structural applications was achieved by all the composites at any age. The results gathered in Table 6 allow stating that the TWF composites achieved an average of 12% higher f_{cm} than the CTR composites.

3.3 Durability test

Based on the previous results, a fiber dosage of 8% by weight fraction of the cement has resulted to lead to better flexural tensile strength results with also a suitable compressive strength for low/medium-performance structural applications. Therefore, the accelerated aging cycles were carried out on composites with this fiber dosage.

In Figure 10, the representative flexural stress-displacement curves derived from the flexural tests on specimens subjected to accelerated aging are depicted (D indicates specimen subjected to aging). Likewise, Table 7 gathers the mean and CoV of the LOP, MOR, I_G, K, and f_c obtained for the composited subjected to aging. As it can be noticed in Figure 10, after the accelerated aging test a drop in the reinforcing capacity of the fibers was observed, this represented by the drastic fall of the stress-deflection curve immediately after reaching the MOR.

The toughness (I_G) of the samples after the durability test decreased dramatically, dropped to 1.2 and 1.1 KJ/m^2 for TW and CTR samples, respectively (reduction of 42 and 62%). Similarly, the MOR for the aged TW composite, showed a minor reduction of 3% whilst the reduction for the CTR sample was about 20%. This deterioration effect can be justified by the following process: when the fiber-reinforced composite, mainly cellulose fibers, is subjected to various wet-dry cycles the fibers lose adherence and bond with the matrix; reprecipitation of the hydrated compounds within the void space at the fiber–cement interface and finally full mineralization occurred, this resulting in the embrittlement of the vegetable fibers [36,67].

Regarding the compressive resistance, it was reduced by 2% (TW) and 20% (CTR). Indeed, the reduction of vegetal fiber durability is caused mainly by the alkaline environment (PH ~12-13) of the cement matrix and the gradually filling of the inner cores of the vegetal fibers with the cement hydration products, this leading to the embrittlement of the fibers, and reducing their mechanical performance [37].

The elastic pre-cracking properties (LOP and K) resulted in averagely unaltered, or even higher amounts due to further cement hydration since these are mainly dependent on the matrix, which is not affected by the aging procedure. This result is in agreement with the finding of [21].

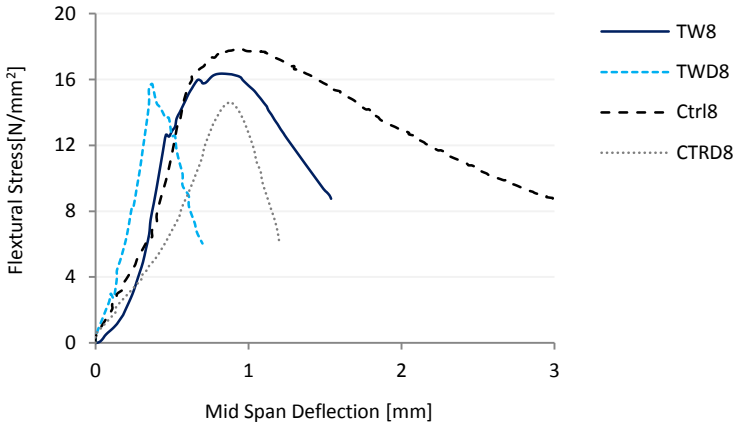

Figure 10. Representative stress – deflection relationships obtained from the flexural tests at 28 days after 25 cycles of accelerated aging for specimens with 8% of TWF and reference fiber

Table 7– Results of durability tests (CoV in %)

Samples	LOP_m (N/mm^2)	MOR_m (N/mm^2)	I_{Gm} (KJ/m^2)	K_m (GPa)	f_{cm} (N/mm^2)	MOR_m/LOP_m
TWD8	13.3(11)	15.2(10)	1.2(21)	4.0(17)	101.8(30)	1.1
CTRD8	11.9(10)	13.3(15)	1.1(17)	3.0(20)	63.5(21)	1.1

As it can be seen in Table 7, all the aged mechanical properties were higher for TWD respect to CTRD. The negative effect of aging on the flexural and compressive resistance in the TW composite was negligible, both less than 3%, while in the CTR sample both strengths were reduced by 25%. The reason for the better behavior of the TW composite could be that the TWF is constituted of vegetable fiber (cotton) together with synthetics (polyester) while the KPF is exclusively composed of vegetable fiber and, consequently, the latter is more vulnerable to the alkaline environment produced by the Portland cement.

This finding is in agreement with the results of [36], in which the mechanical properties of the cement composites reinforced with 4% Pinus Kraft Pulp (KP) was compared with those reinforced by 4% cotton linter (CL) in both normal and aging conditions. Based on that study, the reduction of MOR after accelerated aging was 23 and 17% for KP and CL respectively. Regarding the IG, the deterioration was more significant, 70% (KP) and 23% (CL). Moreover, the compressive resistance loss was about 24 and 11% for KP and CL samples, respectively. Thus, the detrimental effect of accelerated aging could be more significant on Kraft Pulp, followed by cotton linter and Textile Waste fiber.

3.4 SEM observations

In Figure 11, micrographs of the fracture surfaces of TW and CTR composite exposed to normal aging and accelerated are depicted while Figure 12 focuses on the micrographs regarding the fiber surfaces.

The TWF and KPF were averagely longer in the composite cured in the normal condition respect to accelerate aging. This occurred since the fiber pull-out mechanism was predominant in fiber-cement interactions in unaged samples, this generating considerable frictional energy losses, which contribute to toughness. For example, Figure 11a depicts a break section of sample TW28 where it can be noticed a large set of fibers protruding from the cement matrix. In this group of fibers, including synthetic (fine) and natural (thick) fibers, the surface of the fiber is smooth and has no particles attached to the surface. Moreover, almost none of the fibers have been broken. This is an indication that fibers detached from the matrix by following a pull-out mechanism.

On the other hand, in Figure 11-b it can be observed that the fibers in the composites exposed to dry-wet cycles had generally shorter lengths since most of the fibers detached due to rupture, which reduces the toughness. Therefore, it can be stated that the damage induced by the durability test led to an increase in the number of fibers failing due to rupture and consequently, to a decrease in fibers presenting pull-out.

As it is shown in Figure 12a to Figure 12d, the vegetable fibers including the kraft pulp and cotton fibers were cracked and wrinkled after accelerated aging respect to those polyester-based due to the alkali attack. The kraft pulp, with some pits on its surface, could favor the precipitation of hydration products of the cement in the lumen of the fibers and, consequently, facilitate the degradation of the fibers in the cementitious matrix. Thus, the permeability of the kraft pulp and cotton fibers facilitated the degradation and the loss of resistance [36]. The precipitation of the calcium hydroxide onto the fibers due to the dry-wet cycles follows this mechanism [35]: a) loss of fiber adherence and the appearance of void spaces at the fiber-matrix interface in the first dry cycle since the transverse section of the vegetable fibers shrunk due to the loss of water; b) the water dissolves the hydration compounds of the cement in the subsequent wet cycle. The vegetable fibers absorb this dissolution of calcium hydroxide and thus swell; c) water is lost by evaporation in the second dry cycle, and the calcium hydroxide precipitates on the surface and in the lumen of the fibers.

On the other hand, Figure 12f shows the synthetic fiber accumulated with some hydrated cement products without any significant crack or damage. This might be an objective explanation regarding the better mechanical performance of the TW composite after accelerated aging.

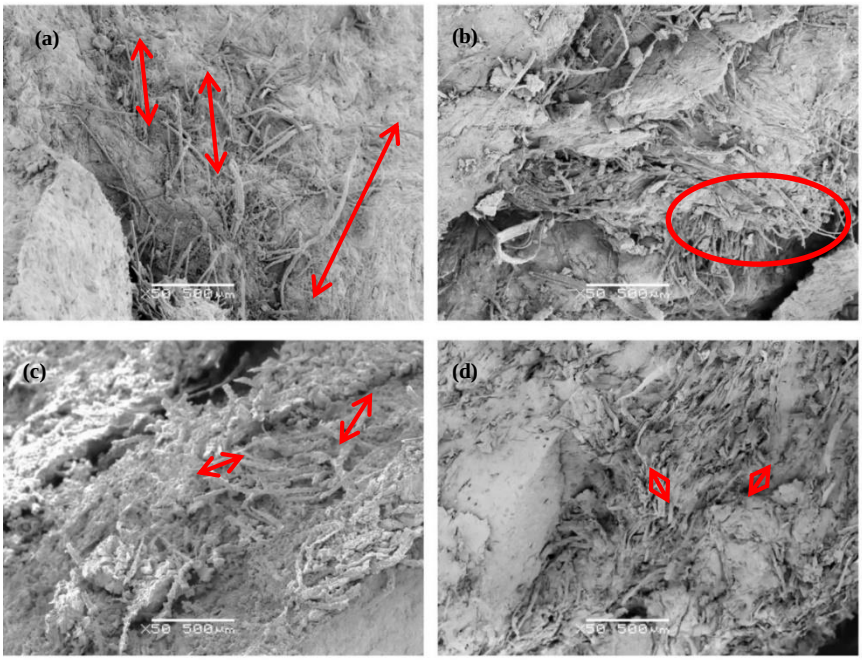

Figure 11. SEM micrographs of the fracture surfaces of the Composites: (a) TW28; (b) TWD; (c) CTR28; (d) CTRD

4. Conclusions

The objective of this research was to verify both the mechanical and durability properties of short random textile waste fiber (TWF) as a potential reinforcement for cement composites oriented to building components with low structural responsibility (ex., aesthetic façade panels, cladding,). These recycled fibers are constituted of cotton and polyester from the garment and textile waste industries. The use of these plate composites for producing building components can valorize this waste while reducing the impact of construction.

Three different mixtures considering 6 to 10% of TWFs were investigated within the context of an extensive experimental program. Flexural and compressive tests were carried out after 7, 28, and 56 days. Moreover, tests simulating accelerated aging conditions and SEM observations were included to assess the mechanical suitability of this material in terms of durability. The same tests were performed for reference samples with kraft pulp pine (CTR). The following conclusions were derived from the results:

- The results showed that the control sample had higher bending resistance and toughness index on average, almost by 9% respect to the TWF composite. However, both composites showed post-cracking performance and improvement in energy absorption suitable for the targeted building components, mainly non-structural ones. On the other hand, the compressive strength and flexural stiffness of the TW composite were averagely 12% higher respect to the CTR sample.

- Compressive and flexural maximum strengths were observed for those composites with 8% of the TWF. The flexural stiffness was found to be maximum for composites with 6% of the TWF while the maximum toughness was obtained when 10% of this TWF is used. Based on the standard mechanical

requirements for non-structural building components, 8% of the TWF resulted in the optimum fiber dosage.

- TWF and reference composites were exposed to accelerated aging conditions. The results for the TWF composites proved a better mechanical performance (at least 10%) respect to the reference samples. The SEM observation results confirmed that this TWF was barely affected by the Portlandite contained in the cement.

After these promising results, the possibility of producing nonwoven textile fabric composites from this short textile waste fiber is under investigation since it is expected that the post cracking performance and energy absorption can be further enhanced and the range of the applications widened thereof.

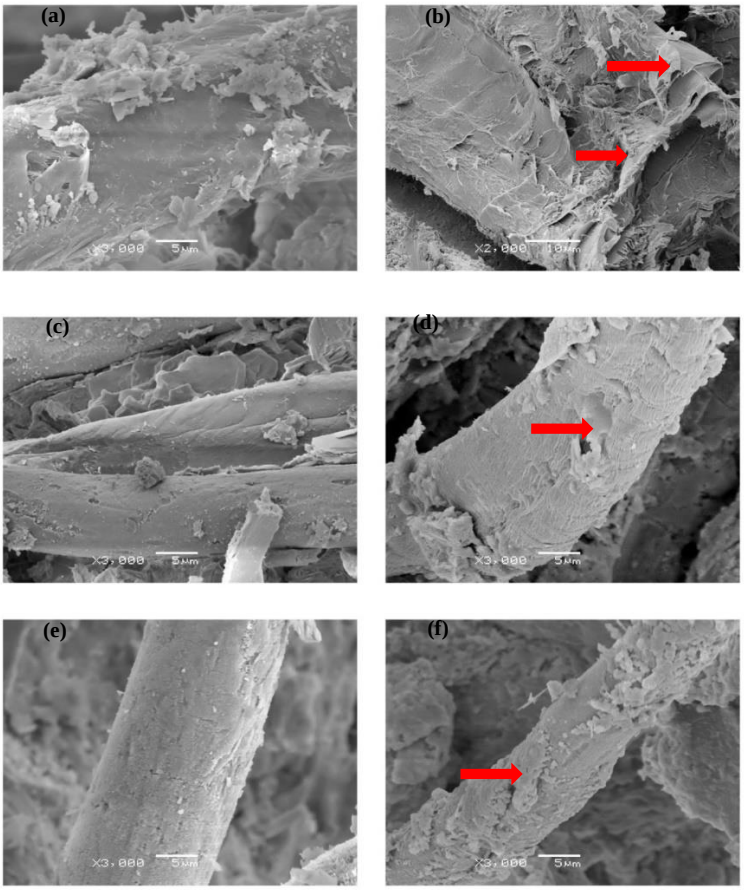

Figure 12. SEM micrographs of the fibers surfaces:(a) Kraft Pulp; (b) Kraft Pulp-Durability; (c) Cotton;(d) Cotton-Durability; (e) Synthetic (f) Synthetic-Durability

Acknowledgments

The authors wish to express their gratitude to the Ministerio de Ciencia e Innovación of Spain for the economic support in the scope of the project SAES (BIA2016-78742-C2-1-R) and RECYBUILDMAT (PID2019-108067RB-I00).

References

[1] B. Mobasher, Mechanics of fiber and textile reinforced cement composites, CRC Press, 2012. https://www.crcpress.com/Mechanics-of-

Fiber-and-Textile-Reinforced-Cement-Composites/Mobasher/p/book/9781439806609 (accessed April 4, 2019).

[2] O.S. Abiola, Natural fibre cement composites, Elsevier Ltd, 2016. https://doi.org/10.1016/B978-0-08-100411-1.00008-X.

[3] E. Erdogmus, Use of Fiber-Reinforced Cements in Masonry Construction and Structural Rehabilitation, Fibers. 3 (2015) 41–63. https://doi.org/10.3390/fib3010041.

[4] M. Ardanuy, J. Claramunt, R.D. Toledo Filho, Cellulosic fiber reinforced cement-based composites: A review of recent research, Constr. Build. Mater. 79 (2015) 115–128. https://doi.org/10.1016/j.conbuildmat.2015.01.035.

[5] F. Pacheco-Torgal, S. Jalali, Cementitious building materials reinforced with vegetable fibres: A review, Constr. Build. Mater. 25 (2011) 575–581. https://doi.org/10.1016/j.conbuildmat.2010.07.024.

[6] J.O. Lerch, H.L. Bester, A.S. Van Rooyen, R. Combrinck, W.I. de Villiers, W.P. Boshoff, The effect of mixing on the performance of macro synthetic fibre reinforced concrete, Cem. Concr. Res. 103 (2018) 130–139. https://doi.org/10.1016/j.cemconres.2017.10.010.

[7] A.M. Brandt, Fibre reinforced cement-based (FRC) composites after over 40 years of development in building and civil engineering, Compos. Struct. 86 (2008) 3–9. https://doi.org/10.1016/j.compstruct.2008.03.006.

[8] Y. Jia, R. Zhao, P. Liao, F. Li, Y. Yuan, S. Zhou, Experimental study on mix proportion of fiber reinforced cementitious composites, 020002 (2017).

[9] R.D. Toledo Filho, K. Ghavami, M.A. Sanjuán, G.L. England, Free, restrained and drying shrinkage of cement mortar composites reinforced with vegetable fibres, Cem. Concr. Compos. 27 (2005) 537–546. https://doi.org/10.1016/j.cemconcomp.2004.09.005.

[10] E. Booya, K. Gorospe, H. Ghaednia, S. Das, Free and restrained plastic shrinkage of cementitious materials made of engineered kraft pulp fibres, Constr. Build. Mater. 212 (2019) 236–246. https://doi.org/10.1016/J.CONBUILDMAT.2019.03.296.

[11] A.M. Brandt, Cement-Based Composites, CRC Press, 2005. https://doi.org/10.1201/9781482265866.

[12] P.J.M. Mehta, P.K.; Montiero, Concrete Microstructure, Properties, and Materials, 3rd ed.; M, 2006.

[13] L. Feo, F. Ascione, R. Penna, D. Lau, M. Lamberti, An experimental investigation on freezing and thawing durability of high performance fiber reinforced concrete (HPFRC), Compos. Struct. 234 (2020). https://doi.org/10.1016/j.compstruct.2019.111673.

[14] M.I. Khan, M.A. Al-Osta, S. Ahmad, M.K. Rahman, Seismic behavior of beam-column joints strengthened with ultra-high performance fiber reinforced concrete, Compos. Struct. 200 (2018) 103–119. https://doi.org/10.1016/j.compstruct.2018.05.080.

[15] J.A. Ortiz, A. de la Fuente, F. Mena Sebastia, I. Segura, A. Aguado, Steel-fibre-reinforced self-compacting concrete with 100% recycled mixed aggregates suitable for structural applications, Constr. Build. Mater. 156 (2017) 230–241. https://doi.org/10.1016/j.conbuildmat.2017.08.188.

[16] G. Promis, T.Q. Bach, A. Gabor, P. Hamelin, Failure behavior of E-glass fiber- and fabric-reinforced IPC composites under tension and compression loading, Mater. Struct. Constr. 47 (2014) 631–645. https://doi.org/10.1617/s11527-013-0085-6.

[17] I. Colombo, M. Colombo, A. Magri, G. Zani, M. Di Prisco, Textile reinforced mortar at high temperatures, Appl. Mech. Mater. 82 (2011) 202–207. https://doi.org/10.4028/www.scientific.net/AMM.82.202.

[18] Y. Wang, S. Backer, V.C. Li, An experimental study of synthetic fibre reinforced cementitious composites, J. Mater. Sci. 22 (1987) 4281–4291. https://doi.org/10.1007/BF01132019.

[19] J. Wang, Q. Dai, R. Si, S. Guo, Mechanical , durability , and microstructural properties of macro synthetic polypropylene (PP) fi ber-reinforced rubber concrete, 234 (2019).

[20] J. Wang, Q. Dai, R. Si, S. Guo, Investigation of properties and performances of Polyvinyl Alcohol (PVA) fiber-reinforced rubber concrete, 193 (2018) 631–642.

[21] J. Claramunt, L.J. Fernández-Carrasco, H. Ventura, M. Ardanuy, Natural fiber nonwoven reinforced cement composites as sustainableClaramunt, J., Fernández-Carrasco, L. J., Ventura, H., & Ardanuy, M. (2016). Natural fiber nonwoven reinforced cement composites as sustainable materials for building envelopes. Constructio, Constr. Build. Mater. 115 (2016) 230–239. https://doi.org/10.1016/j.conbuildmat.2016.04.044.

[22] A.J. Majumdar, R.W. Nurse, Glass fibre reinforced cement, Mater. Sci. Eng. 15 (1974) 107–127. https://doi.org/10.1016/0025-5416(74)90043-3.

[23] J. Wei, C. Meyer, Improving degradation resistance of sisal fiber in concrete through fiber surface treatment, Appl. Surf. Sci. 289 (2014) 511–523. https://doi.org/10.1016/j.apsusc.2013.11.024.

[24] High energy performing buildings - Publications Office of the EU, (n.d.). https://publications.europa.eu/en/publication-detail/-/publication/d8e3702d-c782-11e8-9424-01aa75ed71a1/language-en/format-PDF/source-77709912.

[25] L. Cândido, W. Kindlein, R. Demori, L. Carli, R. Mauler, R. Oliveira, The recycling cycle of materials as a design project tool, J. Clean. Prod. 19 (2011) 1438–1445. https://doi.org/10.1016/J.JCLEPRO.2011.04.017.

[26] J. Giesekam, J. Barrett, P. Taylor, A. Owen, The greenhouse gas emissions and mitigation options for materials used in UK construction, Energy Build. 78 (2014) 202–214. https://doi.org/10.1016/J.ENBUILD.2014.04.035.

[27] H. Nautiyal, V. Shree, S. Khurana, N. Kumar, Varun, Recycling Potential of Building Materials: A Review, in: Springer, Singapore, 2015: pp. 31–50. https://doi.org/10.1007/978-981-287-643-0_2.

[28] CHF, Licensed for The Fiber Year GmbH The Fiber Year 2018 World Survey on Textiles & Nonwovens, 2018. www.thefiberyear.com (accessed April 18, 2019).

[29] J. Claramunt, L. Fernandez-carrasco, Mechanical Performance of Flax Nonwoven-Calcium Aluminate Cement Composites, 1 (n.d.). https://doi.org/10.1007/978-94-024-1194-2.

[30] S.F. Santos, G.H.D. Tonoli, J.E.B. Mejia, J. Fiorelli, H. Savastano Jr, Non-conventional cement-based composites reinforced with vegetable fibers: A review of strategies to improve durability, Mater. Construcción. 65 (2015) e041. https://doi.org/10.3989/mc.2015.05514.

[31] F. de A. Silva, B. Mobasher, R.D.T. Filho, Cracking mechanisms in durable sisal fiber reinforced cement composites, Cem. Concr. Compos. 31 (2009) 721–730. https://doi.org/10.1016/j.cemconcomp.2009.07.004.

[32] L. Fernández-Carrasco, J. Claramunt, M. Ardanuy, Autoclaved cellulose fibre reinforced cement: Effects of silica fume, Constr. Build. Mater. 66 (2014) 138–145. https://doi.org/10.1016/j.conbuildmat.2014.05.050.

[33] R.M. de Gutiérrez, L.N. Díaz, S. Delvasto, Effect of pozzolans on the performance of fiber-reinforced mortars, Cem. Concr. Compos. 27 (2005) 593–598. https://doi.org/10.1016/J.CEMCONCOMP.2004.09.010.

[34] V. da Costa Correia, S.F. Santos, H. Savastano, Vegetable fiber as reinforcing elements for cement based composite in housing applications – a Brazilian experience, MATEC Web Conf. 149 (2018) 01007. https://doi.org/10.1051/matecconf/201814901007.

[35] M. Ardanuy, J. Claramunt, J.A. García-Hortal, M. Barra, Fiber-matrix interactions in cement mortar composites reinforced with cellulosic fibers, Cellulose. 18 (2011) 281–289. https://doi.org/10.1007/s10570-011-9493-3.

[36] J. Claramunt, M. Ardanuy, J.A. García-Hortal, R.D.T. Filho, The hornification of vegetable fibers to improve the durability of cement mortar composites, Cem. Concr. Compos. 33 (2011) 586–595. https://doi.org/10.1016/j.cemconcomp.2011.03.003.

[37] C. Correia, S. Francisco, H. Savastano, V. Moacyr, Utilization of vegetal fibers for production of reinforced cementitious materials, (2018).

[38] L. Mercedes, L. Gil, E. Bernat-maso, Mechanical performance of vegetal fabric reinforced cementitious matrix (FRCM) composites, Constr. Build. Mater. 175 (2018) 161–173. https://doi.org/10.1016/j.conbuildmat.2018.04.171.

[39] J. Claramunt, M. Ardanuy, J.A. García-Hortal, Effect of drying and rewetting cycles on the structure and physicochemical characteristics of softwood fibres for reinforcement of cementitious composites, Carbohydr. Polym. 79 (2010) 200–205. https://doi.org/10.1016/j.carbpol.2009.07.057.

[40] A. Villanueva, L. Delgado, Z. Luo, P. Eder, A. Sofia Catarino, D. Litten, Study on the selection of waste streams for end-of-waste assessment. Final Report, (n.d.). https://doi.org/10.2791/41968.

[41] J.M. Hawley, Textile recycling: A systems perspective, Recycl. Text. (2006). http://krex.k-state.edu/dspace/handle/2097/595 (accessed April 17, 2019).

[42] H. Song, W. Baek, S. Lee, S.H. Hong, Materials Processing Technology, Milling. 48 (1997) 4–9. https://doi.org/10.1039/c3nr33619k.

[43] K. Slater, E. Textile Institute (Manchester, Environmental impact of textiles : production, processes and protection, CRC Press, 2003.

[44] Triturats la Canya S.A. – Reciclatge tèxtil, (n.d.). http://trituratslacanya.com/en/main/ (accessed April 15, 2019).

[45] C. Rubino, S. Liuzzi, F. Martellotta, P. Stefanizzi, Modelling , Measurement and Control B Textile wastes in building sector : A review, 87 (2018) 172–179.

[46] A. Briga-Sá, D. Nascimento, N. Teixeira, J. Pinto, F. Caldeira, H. Varum, A. Paiva, Textile waste as an alternative thermal insulation building material solution, Constr. Build. Mater. 38 (2013) 155–160. https://doi.org/10.1016/j.conbuildmat.2012.08.037.

[47] X. Zhou, F. Zheng, H. Li, C. Lu, An environment-friendly thermal insulation material from cotton stalk fibers, Energy Build. 42 (2010) 1070–1074. https://doi.org/10.1016/J.ENBUILD.2010.01.020.

[48] A. Korjenic, V. Petránek, J. Zach, J. Hroudová, Development and performance evaluation of natural thermal-insulation materials composed of renewable resources, Energy Build. 43 (2011) 2518–2523. https://doi.org/10.1016/J.ENBUILD.2011.06.012.

[49] M. El Wazna, M. El Fatihi, A. El Bouari, O. Cherkaoui, Thermo physical characterization of sustainable insulation materials made from textile waste, J. Build. Eng. 12 (2017) 196–201. https://doi.org/10.1016/J.JOBE.2017.06.008.

[50] A. Paiva, H. Varum, F. Caldeira, A. Sá, D. Nascimento, N. Teixeira, Textile Subwaste as a Thermal Insulation Building Material, n.d. http://www.ipcbee.com/vol26/15-ICPSD2011-P2001.pdf (accessed April 18, 2019).

[51] Y. Lee, C. Joo, Sound absorption properties of recycled polyester fibrous assembly absorbers, Autex Res. J. 3 (2003) 78–84. http://www.autexrj.org/No2-2003/0047.pdf (accessed April 18, 2019).

[52] A.-E. Tiuc, H. Vermeşan, T. Gabor, O. Vasile, Improved Sound Absorption Properties of Polyurethane Foam Mixed with Textile Waste, Energy Procedia. 85 (2016) 559–565. https://doi.org/10.1016/J.EGYPRO.2015.12.245.

[53] F.F. Aspiras, J.R.I. Manalo, Utilization of textile waste cuttings as building material, J. Mater. Process. Technol. 48 (1995) 379–384. https://doi.org/10.1016/0924-0136(94)01672-N.

[54] D. Rajput, S.S. Bhagade, S.P. Raut, R.V. Ralegaonkar, S.A. Mandavgane, Reuse of cotton and recycle paper mill waste as building material, Constr. Build. Mater. 34 (2012) 470–475. https://doi.org/10.1016/J.CONBUILDMAT.2012.02.035.

[55] H. Binici, R. Gemci, O. Aksogan, H. Kaplan, Insulation properties of bricks made with cotton and textile ash wastes, Int. J. Mater. Res. 101 (2010) 894–899. https://doi.org/10.3139/146.110348.

[56] H. Binici, O. Aksogan, Engineering properties of insulation material made with cotton waste and fly ash, J. Mater. Cycles Waste Manag. 17 (2015) 157–162. https://doi.org/10.1007/s10163-013-0218-6.

[57] S.K. Agrawal, R.K. Watile, P. V Mohata, S.C. Makwana, UTILIZATION OF TEXTILE APPAREL WASTE IN CLAY BRICK, IJARET, n.d. www.iaeme.com/ijaret.asp (accessed April 18, 2019).

[58] H. Monteiro, F. Caldeira, J. Pinto, H. Varum, Recycling Textile Residues Into Cement Composites, Environ. Eng. Manag. J. 17 (2018) 1863–1868.

[59] J. Claramunt, H. Ventura, L.J. Fernández-carrasco, M. Ardanuy, Tensile and Flexural Properties of Cement Composites Reinforced with Flax Nonwoven Fabrics, Materials (Basel). (2017) 1–12. https://doi.org/10.3390/ma10020215.

[60] J.E.M. Ballesteros, S.F. Santos, G. Mármol, H. Savastano, J. Fiorelli, Evaluation of cellulosic pulps treated by hornification as reinforcement of cementitious composites, Constr. Build. Mater. 100 (2015) 83–90. https://doi.org/10.1016/j.conbuildmat.2015.09.044.

[61] BS EN 494-12, Fibre-cement flat sheets - Product specification and test methods, Br. Stand. Inst. (2012) 60.

[62] UNE-EN 196-1: 2018 Cement test methods. Part 1: Stop ..., (n.d.). https://www.une.org/encuentra-tu-norma/busca-tu-norma/norma?c=N0060675 (accessed September 25, 2020).

[63] M. Khorami, E. Ganjian, The effect of limestone powder, silica fume and fibre content on flexural behaviour of cement composite reinforced by waste Kraft pulp, Constr. Build. Mater. 46 (2013) 142–149. https://doi.org/10.1016/j.conbuildmat.2013.03.099.

[64] E. Booya, H. Ghaednia, S. Das, H. Pande, Durability of cementitious materials reinforced with various Kraft pulp fibers, Constr. Build. Mater. 191 (2018) 1191–1200. https://doi.org/10.1016/j.conbuildmat.2018.10.139.

[65] J. Khedari, B. Suttisonk, N. Pratinthong, J. Hirunlabh, New lightweight composite construction materials with low thermal conductivity, Cem. Concr. Compos. 23 (2001) 65–70. https://doi.org/10.1016/S0958-9465(00)00072-X.

[66] M. Bentchikou, A. Guidoum, K. Scrivener, K. Silhadi, S. Hanini, Effect of recycled cellulose fibres on the properties of lightweight cement composite matrix, Constr. Build. Mater. 34 (2012) 451–456. https://doi.org/10.1016/j.conbuildmat.2012.02.097.

[67] G.H.D. Tonoli, A.P. Joaquim, M.A. Arsne, K. Bilba, H. Savastano, Performance and durability of cement based composites reinforced with refined sisal pulp, Mater. Manuf. Process. 22 (2007) 149–156. https://doi.org/10.1080/10426910601062065.

2.2 Journal paper II:
Characterization of a textile waste nonwoven fabric-reinforced cement composite for non-structural building components

Published in Construction and Building Materials (Volume 276, 22 March 2021, 122179)

Payam Sadrolodabaee[a*] (payam.sadrolodabaee@upc.edu), Josep Claramunt[b] (josep.claramunt@upc.edu), Monica Ardanuy [c] (monica.ardanuy@upc.edu), Albert de la Fuente[a] (albert.de.la.fuente@upc.edu)

a: Department of Civil and Environmental Engineering- Universitat Politècnica de Catalunya-BarcelonaTECH- Barcelona, Spain
b: Department of Agricultural Engineering- Universitat Politècnica de Catalunya-BarcelonaTECH- Barcelona, Spain
c: Department of Material Science and Engineering (CEM)-Universitat Politècnica de Catalunya-BarcelonaTECH-Barcelona, Spain
*: Corresponding author

Abstract

Large amounts of nonrenewable resources are depleted by the construction industry in addition to the generation of million tons of mineral waste and carbon dioxide gas every year. For the sake of a more sustainable consumption pattern of building materials, as well as for reducing the waste flux to landfills, the use of recycled materials and wastes should be researched and motivated. In this sense, textile waste (TW) nonwoven fabric from residues of the garments and textile industries is investigated as internal reinforcement for cement-based matrices to enhance ductility and cracking control. To this end, an extensive experimental program was carried out to characterize both the mechanical and durability properties of the composite. The results were compared with those obtained from flax nonwoven fabric, taken as a reference (FNH and FH composites). All the composites showed a remarkable improvement in terms of toughness and post-cracking stress-bearing capacity, six being the optimum number of TW reinforcing layers. Through the analysis of the results obtained, the feasibility of using TW composite as a potential construction material in non-structural applications was confirmed. The extension to structural applications of low-medium responsibility is still required further research; nonetheless, the results are promising in this respect.

Keywords: Cementitious materials; Durability; Fiber-reinforced composites; Mechanical properties; Sustainability; Textile reinforced mortars; Textile waste nonwoven fabric

1. Introduction

It is already known that the incorporation of certain types of fibers into the cementitious materials improves several characteristics of the materials, among others: toughness, energy absorption capacity, and post-cracking residual strength [1]–[4]. Furthermore, reduction of shrinkage potential [5], [6], crack width control and enhancement of durability have also been reported [7], [8]. During the past decades, various types of short fibers such as asbestos, steel, glass and polymeric have been tested as reinforcement of cement-based matrices [3], [9]. However, there have been some disadvantages related to the use of those fibers such as detrimental health effects (asbestos), high costs (steel and polymeric) and, particularly, remarkable environmental footprint [10], [11].

Based on the statistics, in the EU the building sector accounts for 35–40% of the final total energy consumption and 25–40% of the associated carbon dioxide emission [12]. That is why significant efforts have been devoted to applying the '3Rs' concept of reducing, reusing, and recycling in the building sector including material fabrication [13]. Thus, reusing and recycling the leftover materials with sustainable processes in material fabrication (ex., in fiber production) can mitigate the waste and environmental impacts [14], [15]. World fiber production has been steadily increasing in the past few decades, now exceeding 100 million tons per year [16].

Vegetable or cellulosic fibers [1], [17], [18], together with short textile waste fibers [19] have been recently used as sustainable reinforcement for mortars and composites oriented to low-performance structural applications.

The textile industry produces textile wastes from the primary stages of garment production (pre-consumer waste such as fiber, yarn, and fabric) to the end of its useful life (post-consumer waste: discarded clothes) [20], [21]. Thus, the reuse of this textile waste in construction is becoming interesting and convenient due to the shortage of natural mineral resources and increasing waste disposal costs [22], [23].

Waste fibers to produce building thermal insulations were explored in previous researches [24], [25], sound-absorbing materials [26], [27] and lightweight bricks [28], [29] owing to low-cost, lightweight, availability, energy-saving, and environmental preservation [30]. Moreover, in [19], short fibers from textile clothing wastes composed of cotton/polyester mixtures were used as reinforcement for brittle cement-based materials.

However, using short randomly distributed fibers can bring some limitations in terms of strength and specifically toughness due to the short length and the maximum quantity mixable [31]. Thereby, longer fibers in the form of strands as well as the woven and nonwoven fabrics, although representing a more difficult production procedure, have become an interesting alternative for reinforcing cement-based matrices. Owing to the higher fiber length and more contact with the cement paste, the formation of multiple micro-cracking can lead to an improvement of the tensile mechanical properties [32]–[35].

In this regard, there is already some research available regarding the cementitious mortars reinforced with long fibers including sisal strands [31], [33]–[35], and woven fabrics including alkali resistance glass fabrics [37]–[43]. However, there is still scarce, and only incipient, research on the nonwoven fabric [31], [44], [45] as reinforcement for mortars. Nonetheless, all those confirmed that textile reinforced cementitious (TRC) composites oriented to thin, lightweight and sustainable structures have improved tensile and flexural performances as well as strain hardening behavior even when the reinforcing yarns have a low modulus of elasticity.

It must be also remarked, some mechanical parameters that govern the internal mechanism and behavior of the TRC such as the load-transfer length, textile/matrix interface stress distribution and the final crack spacing were already studied [41], [46], [47]. In fact, when a crack occurs, the strain of the textile reaches its maximum value at the crack position since the textile resists the tensile stress that the matrix releases while the strain at the latter decreases. Starting from the crack, the matrix strain increases gradually until it becomes equal to the strain in the textile reinforcement, i.e, away from the crack position the textile transmitted a portion of this load to the matrix. The length for which the strain of the matrix increases until stabilization was considered the load-transfer length. The load-transfer length was potentially related to the reinforcement ratio and decreased with an increase in this ratio, which implies that the spacing between the cracks decreases.

In view of the abovementioned, the mechanical performance and durability of cement boards reinforced with Textile Waste (TW, hereinafter) nonwovens fabric were investigated within this research aiming at identifying the potential applications of this material (ex, architectural façades or raised floors). As a result, flexural (at pre-and post-cracking stages) strength capacities, together with the toughness and stiffness properties as well as the optimum layers of fabric were derived from an extensive experimental program carried out. The results were finally compared with two other types of nonwoven composites (FNH and FH) made from flax fabric. FNH refers to the unmodified flax composite while physical treatment was carried out on FH composite to reach higher dimensional stability in addition to improving the fiber-matrix

interface and durability of cementitious materials [48]. The results of this experimental program were analyzed and treated from a design perspective since the focus of this material is put on potential low-medium responsibility structural applications.

2. Experimental Procedure

2.1 Materials

2.1.1 Binder

A Portland cement Type I 52.5R supplied by Cementos Molins Industrial, S.A. (Spain) was used for producing the mortars. Chemical composition criteria and physical/mechanical requirements according to EN 197-1:2011 and given by (MOLINS, 2016) are reported in Table 1.

2.1.2 Fibers

Textile Waste (TW) short fibers used for making the nonwoven fabric were provided by Triturats La Canya S.A (Spain) which consisted of around 31% polyester and 69% cotton. Producing fabric from 100% TW failed as those were too short. For this reason, longer flax fibers (F, hereinafter) with an average length of 60 mm provided by Institut Wlokien Naturalnych (Poland) were mixed with the TW fibers (see Figure 1). Moreover, in the reference composites, only long flax fibers were used.

Table 1– Chemical composition and physical and mechanical properties for cement Type I 52.5R

Content	Typical values	EN 197-1:2011
Clinker (%)	98	min95 - max100
Minor component (%)	2	min0 - max5
Loss of Calcination (%)	2.5	max 5
Sulfate, SO3 (%)	3.4	max 4
Chlorides, Cl- (%)	0.04	max 0.1
Insoluble residue (%)	0.7	max 5
Blaine specific surface (cm^2/g)	4600	-
Expansion of Le Chatelier (mm)	0.5	max 10
Initial setting time (min)	110	min 45
Final setting time (min)	170	max 720
1-day compressive strength (N/mm2)	27	-
2-days compressive strength (N/mm2)	40	min 30
7-days compressive strength (N/mm2)	52	-
28- days compressive strength (N/mm2)	61	min 52.5

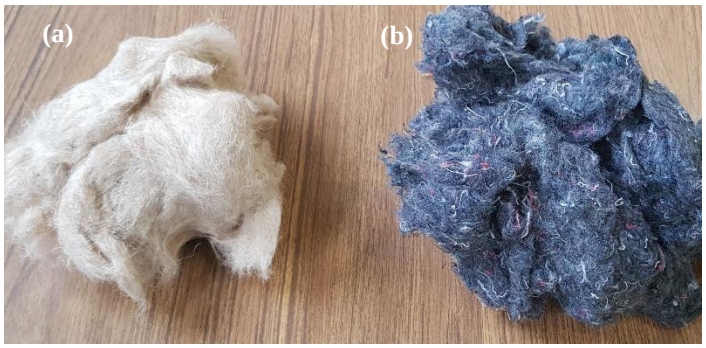

Figure 1. (a) Long Flax Fiber (F); (b) Short Textile Waste Fiber (TW)

2.1.3 Nonwoven fabric preparation

Taking into account the characteristics of the raw material used and the previous works carried out to optimize the nonwovens [31], [49], the mats must have thicknesses less than 2 mm and areal weights between 150 and 275 gr / m^2. Accordingly, different tests were performed to optimize the procedure. Thus, Textile Waste nonwoven fabric samples were prepared on card clothing and needle-punching machines. Firstly, 52 gr TW short fibers with 28 gr long flax fibers, were opened in 3 layers and carded to form a thin web which was laid by the cross-laying method to form batts (see Figure 2). These batts, each constituted of 65%TW and 35%F fiber, were consolidated on the needle-punching machine to form the nonwoven mats (see Figure 3). The machine parameters to prepare these fiber mats were determined in previous research [31], [49]. The process of manufacturing the Flax nonwoven fabric, almost similar to the TW, was described in the same research. To briefly describe, the nonwoven flax fabric samples were prepared on a pilot plant, double needle-punching machine DILO OUG-II-6, equipped with universal card clothing, cross-lapper, batt feeder, and needle-punching loom. After opening and carding the flax fibers to form the batts, consolidation on the needle-punching machine was done to form the nonwoven mats.

As the alkalinity of the cement matrix and the volumetric instability of the fibers are the main causes of the resistance loss in vegetable fiber-reinforced composite [50], [51], some of the flax nonwoven fabrics were subjected to physical treatment. The treatment called hornification produces an irreversible effect on cellulosic fibers when exposed to drying and rewetting cycles. It could have an important impact on the fiber-matrix adherence, resistance, and durability of cementitious mortar composites [52], [53]. The hornification of the flax nonwoven mats was achieved by four drying and rewetting cycles, drying in an oven with air recirculation at 60C for 7 h and rewetting by soaking overnight.

The physical properties of the nonwoven mats used in the composite laminates show in Table 2. FNH has the highest areal weight and density which can induce a weak infiltration of the cement particles into the porous structure of the nonwoven fabrics [31]. On the other hand, TW nonwoven fabric with the lowest areal weight and thickness could prepare more homogeneous composites, with a good matrix infiltration through the fabric.

Figure 2. Carding process: (a) opening the fibers in 3 layers; (b) carding; (c) final batts

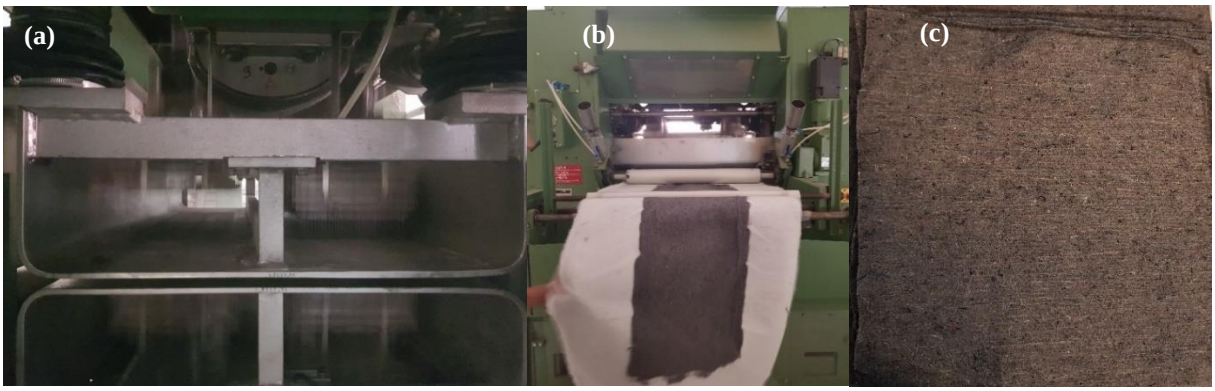

Figure 3. Needle punching process: (a) needling; (b) after needling process; (c) final mats of TW

Table 2 – Physical properties of the Nonwoven Fabrics

Nonwoven Fabrics	**Thickness (mm)**	**Mass (gr)**	**Areal Weight (gr/m^2)**	**Fiber Density ($gr/m^2.mm$)**
TW: 65% short TW+ 35% long F (60 mm, non-treated)	0.75	14	155	207
FNH: 100% long F fibers (60 mm, non-hornified)	0.95	24	266	280
FH: 100% long F fibers (60 mm, hornified)	0.95	16	177	186

2.2 Composite preparation

For the composite preparation, the methodology used was to apply the reinforcement by taking special care of the wetting of the nonwoven with the matrix. The pure cement paste without any aggregate was chosen as even with very fine aggregates, the mortar penetration into the flax nonwoven could be unsatisfactory [54]. Moreover, based on the previous study, superplasticizers resulted in insufficiently efficient in improving penetration to the vegetable fabrics [55]. Thus, in order to have a suitable penetration of the paste into the fabrics, and thereby, have a required interaction between the cement and the nonwoven mats, the initial water/cement ratio for preparing the paste was established as 1.0. However, the treatment of dewatering including the elimination of the excess of water by vacuuming and compressing the mold for 24 hrs. was done on the composites. The process of making the composite was carried out in a mold with internal dimensions of 300 × 300 mm × 10 mm which was specially designed to apply homogeneous pressure (3.5 MPa). Laminates of 3 to 7 nonwoven layers impregnated with the cement paste placed cross-oriented were produced. The plates with a thickness of 6-11 mm were cured for 28 days at ambient temperature (20 ºC) in a humidity chamber (approximately 95% of relative humidity). From each plate, 6 specimens were machined. Figure 4 depicts the casting and curing procedure carried out on TW laminates.

The designation of the specimens (Tables 3-5) is based on the number of laminates and layers. Samples for durability tests are designated with D. The final water/cement ratios (final water was calculated after weighing the amount of water eliminated by the dewatering treatment) together with some other parameters related to the laminate plates are also reported in the aforementioned tables. The (w/c) final and the thickness of the plates were affected by the efficiency of the vacuuming process. As the mass of the FNH mat was higher than the others, the approximate fiber dosage by weight fraction cement of this plate was the highest, followed by FH.

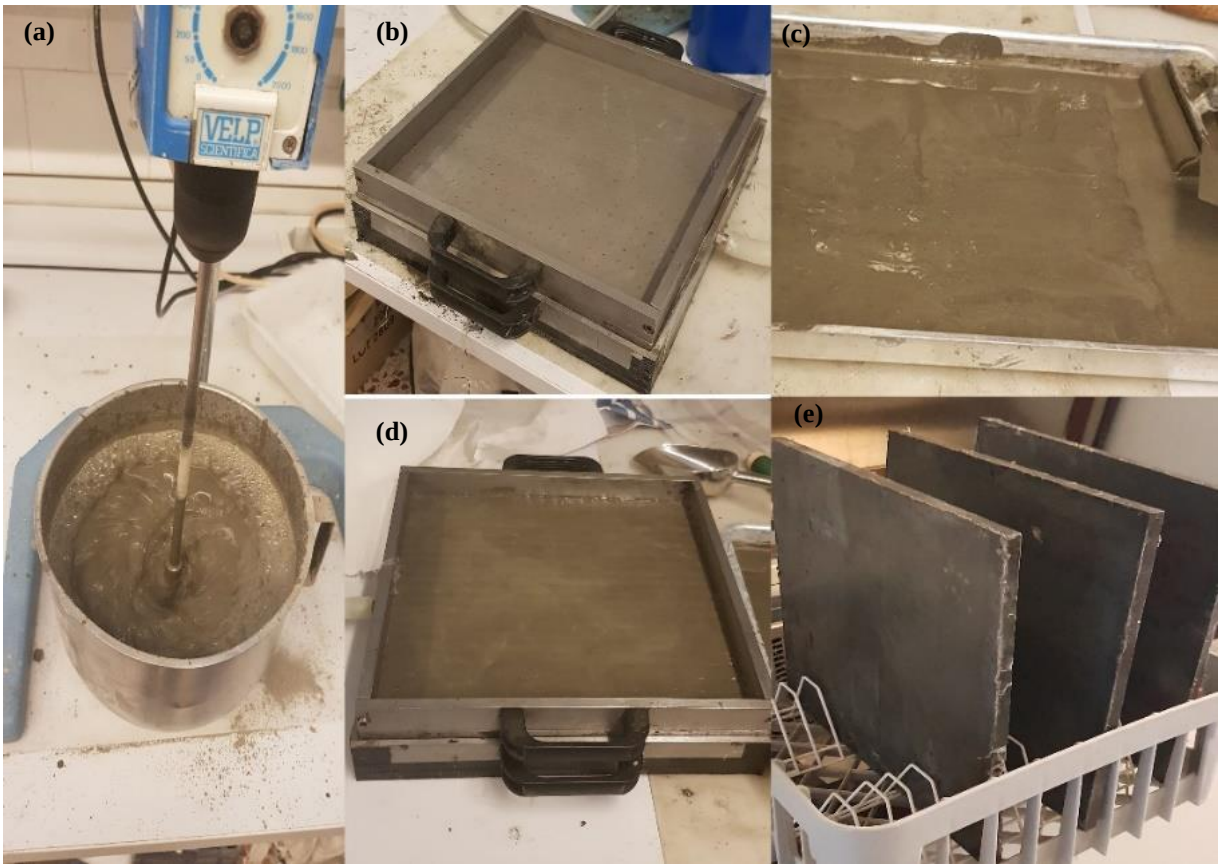

Figure 4. Preparation of the TW composite sample: (a) preparation the paste; (b)especial mold; (c) impregnation of the nonwoven with the paste (d) molds filled with laminated composites; (e) Curing condition of the final plates

Table 3 – Physical properties of the Textile Waste fabric composites

	No. Layers	**3L**	**4L**	**5L**	**6L**	**7L**	**3LD**	**4LD**	**5LD**	**6LD**
TW	**$(w/c)_{final}$**	0.40	0.40	0.40	0.40	0.45	0.50	0.40	0.40	0.40
	Cement final -gr	1350	1500	1530	1550	1600	1082	1256	1287	1474
	No. Specimens	6	6	6	6	6	6	12	12	12
	Fibre Weight Fraction	3.1	3.7	4.9	5.4	6.1	5.1	5.5	5.4	5.7
	Fibre Volume Fraction	9.3	11.1	14.7	16.2	18.3	15.3	16.5	16.2	17.1
	Plate Thickness-mm	6.5	8.5	9.2	10.0	10.2	6.9	8.2	8.5	10.0
	Mat Thickness-mm	2.2	3.0	3.7	4.5	5.2	2.2	3.0	3.7	4.5
	Mortar Thickness-mm	4.3	5.5	5.5	5.5	4.8	4.7	5.2	5.4	5.5

Table 4 – Physical properties of the Flax Non-Hornified fabric composites

	No. Layers	3L	4L	5L	6L	7L	3LD	4LD	5LD	6LD
FNH	$(w/c)_{final}$	0.40	0.45	0.45	0.45	0.45	0.40	0.50	0. 45	0.45
	Cement final -gr	812	887	1025	1117	1158	758	1045	1144	1285
	No. Specimens	6	6	6	6	6	6	6	6	6
	FibreWeight Fraction	8.8	10.8	11.7	12.9	14.5	9.5	9.1	10.4	11.2
	Fibre Volume Fraction	26.4	32.4	35.1	38.7	43.5	28.5	27.3	31.2	33.6
	Plate Thickness-mm	6.5	7.5	8.8	9.8	10.0	6.5	8.0	9.0	10.0
	Mat Thickness-mm	2.8	3.8	4.7	5.7	6.6	2.8	3.8	4.7	5.7
	Mortar Thickness-mm	3.7	3.7	4.1	4.1	3.4	3.7	4.2	4.3	4.3

Table 5 – Physical properties of the Flax Hornified fabric composites

	No. Layers	3L	4L	5L	6L	7L	3LD	4LD	5LD	6LD
FH	$(w/c)_{final}$	0.35	0.35	0.40	0.35	0.40	0.50	0.50	0.45	0.50
	Cement final -gr	792	842	877	1037	1100	742	851	1148	1262
	No. Specimens	6	6	6	6	6	6	6	6	6
	FibreWeight Fraction	6.0	7.6	9.1	9.2	10.1	6.4	7.5	7.0	7.6
	Fibre Volume Fraction	18.0	22.8	27.3	27.6	30.3	19.2	22.5	21.0	22.8
	Plate Thickness-mm	6.0	6.7	7.0	9.5	9.7	6.0	6.5	8.0	9.7
	Mat Thickness-mm	2.8	3.8	4.7	5.7	6.6	2.8	3.8	4.7	5.7
	Mortar Thickness-mm	3.2	2.9	2.3	3.8	3.1	3.2	2.7	3.3	4.0

2.3 Mechanical Tests

2.3.1 Tensile rupture load of the nonwoven mats

From each nonwoven mat, 20 specimens were cured at standard 20±2 ºC temperature and relative humidity of 65±2% prior to testing. Tensile tests based on UNE-EN ISO 13934-1 were performed to determine the rupture load capacity of the nonwovens as shown in Figure 5. The tests were done in a Textueometer TA.XT machine with a load cell of 0.5 KN using a displacement rate of 100 mm/min.

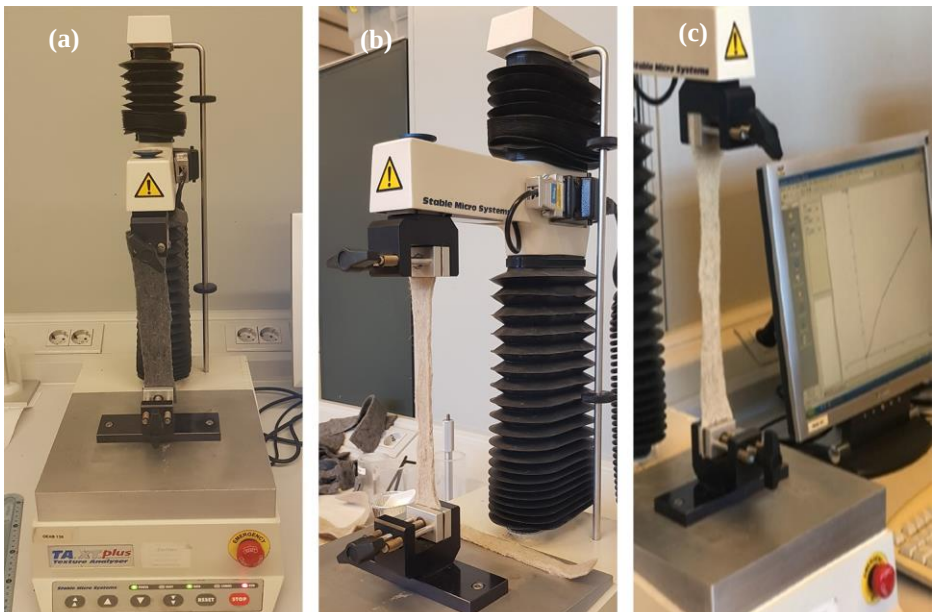

Figure 5. Tensile test on the nonwoven fabric: (a) mat TW; (b) mat FNH; (c) mat FH

2.3.2 Flexural tensile strength and toughness of the composites

The mechanical properties of the composites were determined under a four-point bending test configuration (Figure 6) following the RILEM TFR1 and TFR 4 [56]. An Incotecnic press equipped with a maximum load cell of 3 kN at a crosshead speed of 20 mm/min was used. The specimens were tested with a major span (L) of 270 mm.

The maximum flexural tensile strength (or also named Modulus of Rupture, MOR) of the composites was determined through Equation 1, where P_{max} is the maximum load recorded, L is the span length (270 mm), *b* and *h* are the cross-sectional width, and thickness, respectively.

$$MOR = \frac{P_{max}L}{bh^2} \qquad (Equation\ 1)$$

The toughness index (I_G), established as the reference parameter to characterize the type of failure (ductile or fragile). This is defined as the area beneath the force-displacement curve derived from the flexural test and comprised from zero to a post-failure load of 40% of MOR or the deformation value corresponding to 10% of the span- whichever occurs first. In the current test, the limitation of 10% of the displacement value (27 mm) occurred first and this point was considered for the calculation of the toughness index.

The elastic flexural stiffness or Modulus of Elasticity of the pre-cracked zone (E_1), was also measured from the force-displacement relationships by using Equation 2, where Δp and Δf are the variations of forces and deflections of two points on the elastic regime, and the rest of parameters as defined per Equation 1. Moreover, the flexural stiffness of the post-cracking zone (E_3) was calculated also through Equation 2.

$$E = \frac{23\Delta P.L^3}{108\Delta f.bh^3} \qquad (Equation\ 2)$$

Figure 6. Flexural tests set-up: (a) specimens; (b) flexural test configuration-initial of the test; (c) flexural test configuration-end of the test; (d) Cross-sections of tested-to-failure specimens

2.3.3 Durability test

Durability against wet-dry cycles is considered a challenge in cement-based composites reinforced with vegetable fibers [50], [57]. In this regard, to confirm the durability of the nonwoven fabrics within the mortar matrix, plates were subjected to accelerated aging. This consisted of subjecting the plates to 25 dry-wet cycles, after 28 curing days in a climatic chamber, according to the EN 12467 [58]. Each dry-wet cycle consists of drying for 6 hours at 60°C and 60% of RH followed by 18 hours of immersion in water at 20°C. Repeated wetting-drying cycles simulated some natural weathering conditions and could estimate roughly and preliminary the durability of the TRC. It must be emphasized, however, that it has already been proved that the majority of strength and toughness loss occurs within the first two to five cycles [59]. Climatic chambers for this process as well as the samples after accelerated aging cycles are shown in Figure 7.

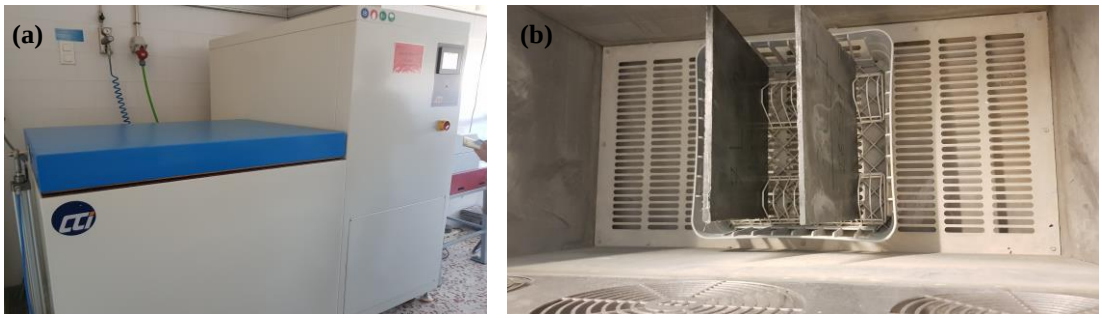

Figure 7. Durability test: (a) CCI chamber (b) aged specimens

2.4 Microscopy analyses

The scanning and backscattered electron microscope (SEM and BSEM) observations using JEOL JSM 5610 and JEOL JSM 7001F devices, equipped with an energy dispersive X-ray spectrometer (EDS) for EDS analysis, were carried out on the TW composites in order to analyze the microstructural properties. The hydration reactions of the specimens were frozen by immersion in isopropyl alcohol. Samples were kept under vacuum conditions until the analysis which is focused on the fractured surface microstructure, the effects of the wet-drying cycles, and the fiber-matrix interface. Before BSEM analysis, the specimens were encapsulated in an epoxy resin and polished.

3. Results and Discussions

3.1 Nonwoven mats' tensile rupture load

Table 6 shows the results of the tensile test of the nonwoven mats. The maximum load was normalized by the weight of each specimen. The mean maximum failure force of the FNH fabric is more than two times higher than the TW nonwoven. The reason for such a lower value in TW could be that short and recycled fibers made up of cotton and polyester are the main component of the TW nonwoven [19] while the homogenous long flax fibers made the FNH.

On the other hand, the hornification treatment on the flax fabrics increased the maximum failure force of FH by 50%. The hornification process was reported to create a greater number of hydrogen bridge bonds inside the fibers that cause shrinkage of the fibers and therefore, a higher density of the individual fiber [50]. Generally, it is expected that the hornificated fibers will have higher values of stiffness and tensile strength as a consequence of the formation of a more close-packed crystalline[52]. During the hornification process, the fibrils inside the fibers are in contact after drying and the cellulose polysaccharide chains are grouped firmly together with water removal, causing the binding of microfibrils as a flat strip. This all ends in the irreversible loss of water retention capacity of the fibers and the collapse of the vegetable fiber with slightly changing strength properties[60]. As will be explained more in Section 3.3, the reduction of the water retention capacity of the vegetable fibers may have beneficial effects when incorporated as a reinforcement for cement matrices, since these fibers have greater dimensional stability, providing better adhesion between fiber-matrix and reducing the formation of precipitated hydroxide calcium on the surface and lumen of the fibers, resulting in a reduction in the degradation of cellulose in the cement matrix [50].

Table 6. Maximum tensile rupture load (per weight) of the nonwoven mats (CoV in %)

CODE	TW	FNH	FH
Tensile Force (N/gr)	2.0 (19%)	5.1 (26%)	7.9 (24%)

3.2 Flexural test on unaged composites

In Figure 8, the representative flexural stress-displacement curves of each composite according to the different layers, derived from the flexural tests, are depicted. Likewise, Table 7 gathers the mean and CoV of the Limit of proportionality (LOP) and the Modulus of rupture (MOR) obtained for each composite at 28 days. The characteristic values (associated with 95% of confidence) were also calculated (LOP_k and MOR_k) since these statistical values are accepted in the commonly used structural design safety formats. A normal distribution of both LOP and MOR was assumed.

Results depicted in Figure 8 confirm that 5-7 nonwoven fabrics layers contribute to increasing both the flexural resistance and the ductility of the composites in comparison to those with a less number of layers. This mechanical performance is required (at different levels and magnitudes) for construction applications of fiber-reinforced composites. However, it must be highlighted that all the composites showed post-failure behavior under flexural configuration with a high capacity for deformation due to the formation of multiple cracking. The cracking phases of most specimens could be divided into three distinct branches: (1) Linearly ascending branch (the pre-cracking zone), the external load is mainly undertaken by the cement matrix while internal micro-cracking is occurring until a visible crack in the cement matrix is formed. The flexural stiffness of the first stage is mainly influenced by the mechanical properties of the matrix and is hardly influenced by those of the textile reinforcement [46]. (2) The transition zone along which both load fluctuation and multiple cracking formations occur. Right after the cracking onset, a load drop followed by load recovery is recorded in all the specimens. In the crack propagation zone, the matrix is subjected to the compression stresses on the upper part of the specimen (above the neutral axis position) and the textile reinforcement guarantees the equilibrium of the internal forces (bending moment) by resisting tensile stresses. Under these conditions, the stress transfer mechanism is achieved by the reinforcement-matrix adhesion in the zones between cracks. If there was insufficient matrix-reinforcement adhesion, the onset of cracking would trigger a brittle failure of the composite in flexure. On the contrary, as it happened in all the tests carried out, the adhesion was sufficient to allow full interaction between the matrix and the textile reinforcement and a ductile response of the composite with the occurrence of multiple cracking, this proving the mechanical compatibility between both materials. (3) Another ascending branch (the post-cracking zone), with the lowest slope due to the degradation of the composites' stiffness owing to matrix damage, the fabric reinforcement bridging the cracks and bearing the loads. No further new crack occurs in this zone and only the cracks widen. Finally, a failure happens due to the rupture or debonding of the fibers followed by further widening of the cracks and, eventually, forming the main crack that leads to the collapse.

It is also to be remarked that the mechanical contribution of the TW layers permits to generate of a uniformly distributed multi-cracking pattern with crack width inferior to 0.10 mm (see Figure 9). The pattern with more and thinner cracks (like TW6L and TW7L) showed less noticeable peaks at the crack formation area since good chemical adhesion between fiber-matrix has been attributed to bending behavior with multiple thinner and closer cracks [61]. On the other hand, most three and four-layer composites like TW3L, have larger and more separated post crack teeth and peaks (see Figure 8) probably because when one of the layers breaks, the next layer is much closer to the neutral axis and has less ability to prevent deformation. Since a deeper crack leads to a higher stress loss, the bending curves reveal more pronounced

and separated peaks in this case[62]. Moreover, composites with greater reinforcement ratio (see Tables 3-5) presented lower load transfer length and consequently higher density of cracks respect to those with lower reinforcement ratio [46].

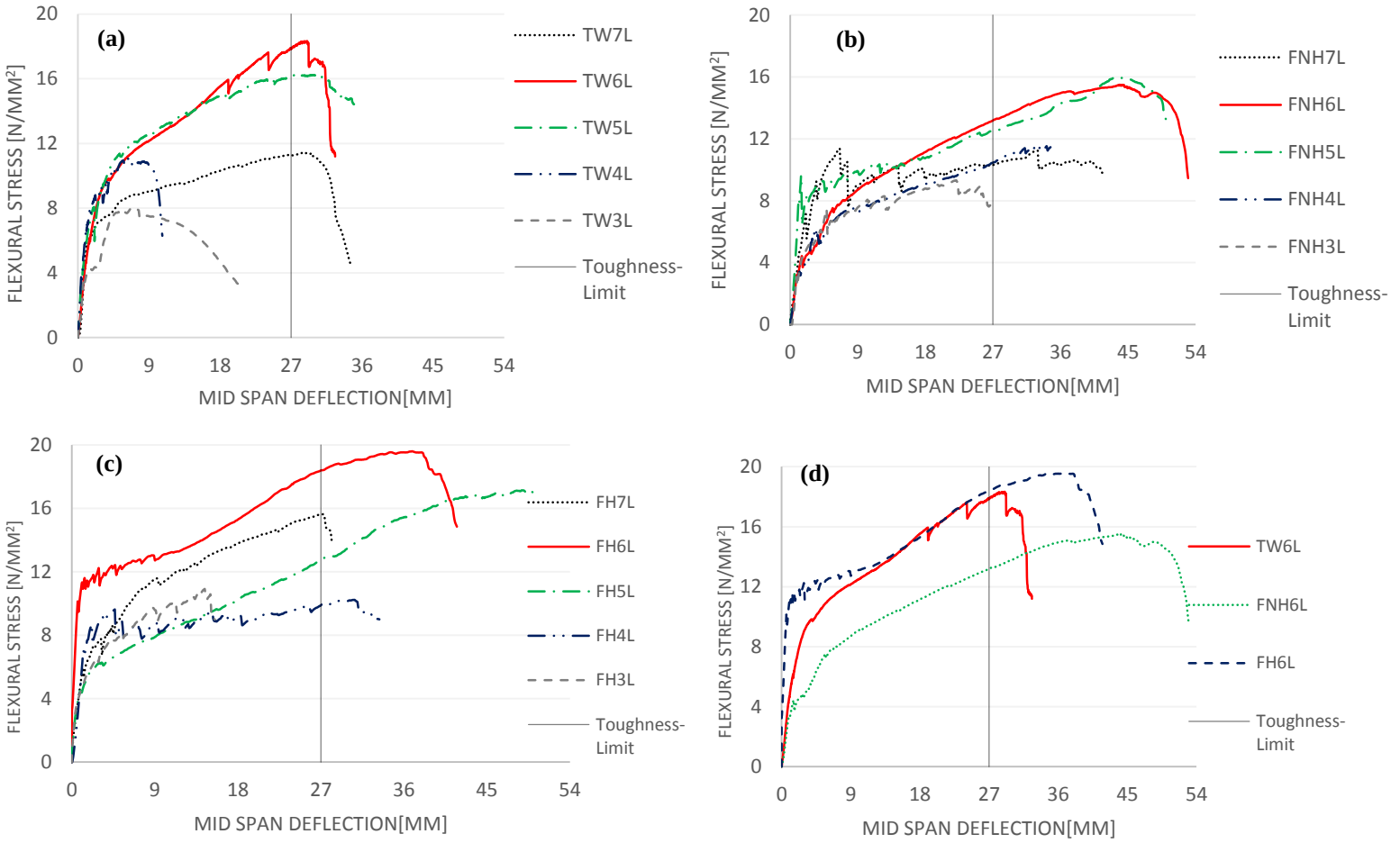

Figure 8. Experimental flexural stress – deflection relationships obtained at 28 days for nonwoven composites: (a) TW; (b) FNH; (c) FH; (d) six-layers composites

From the structural point of view, this crack pattern is beneficial as the deflections and rotation can be reduced under the service loads. For high loads, close to the failure of the material, the mechanical capacity is governed by one to two major cracks in which the damage is concentrated.

According to the results presented in Table 7 and Figure 10, the LOP is rather independent of the number of layers and the observed variations can be attributed to the scatter related to the material (mainly due to the cement-based matrix, which controls the first crack resistance) and the test. It should be mentioned that the range of variation of LOPm for FNH composites comprised values from 3.6 N/mm^2 (FNH3L) to 5.4 N/mm^2 (FNH5L), while the TW composites showed more stable values of LOP_m, these ranging from 4.1 N/mm^2 (TW5L) to 4.6 N/mm^2 (TW6L). This allows concluding that the textile layers have an ineffective contribution to the flexural strength capacity throughout the pre-cracking stage and if any, the scatter observed does not permit to take this contribution into account from the design perspective since the LOPk values obtained for FNH composites, decrease with the number of layers. The same pattern was

observed for the FH composites respect to the number of layers; nevertheless, an average 2.0 N/mm^2 increase of LOPm was detected respect to those for TW and FNH composites. This effective increase might be due to the treatment that the fibers underwent that could cause a reduction of the porosity and, hence, less water absorption. This non-absorbed water was therefore available for cement hydration which could increase the mechanical strength of the matrix. Moreover, the average final w/c ratio of the FH composite was less than the two other kinds which, in turn, can cause a higher strength of LOP.

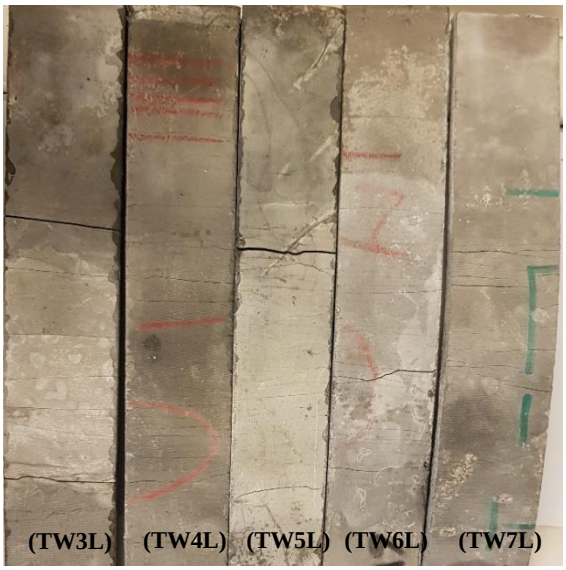

Figure 9. Crack pattern of the TW composites after testing.

Table 7– LOP and MOR of all the nonwoven composites at 28 days

CODE	LOP			MOR			MOR_m/LOP_m
	LOP_m (N/mm^2)	CoV_{LOP} (%)	LOP_k (N/mm^2)	MOR_m (N/mm^2)	CoV_{MOR} (%)	MOR_k (N/mm^2)	
TW3L	4.1	29	2.2	8.1	14	6.2	2
TW4L	4.5	24	2.7	12.4	14	9.6	2.8
TW5L	4.1	24	2.5	13.9	13	10.9	3.4
TW6L	4.6	19	3.2	15.5	12	12.4	3.4
TW7L	4.2	12	3.4	12.1	12	9.7	2.8
FNH3L	3.6	13	2.8	10.0	9	8.5	2.8
FNH4L	4.8	18	3.4	12.4	12	10.0	2.6
FNH5L	5.4	17	3.9	15.6	17	11.3	2.9
FNH6L	4.3	23	2.7	15.7	6	14.2	3.7
FNH7L	4.1	22	2.6	12.5	14	9.6	3.0
FH3L	5.7	15	4.3	11.4	14	8.8	2
FH4L	6.7	25	4.0	12.7	19	8.7	1.9
FH5L	6.6	20	4.4	16.4	9	14.0	2.5
FH6L	7.6	5	7.0	19.8	6	17.9	2.6
FH7L	5.7	19	3.9	16.8	12	13.5	2.9

On the other hand, the MOR values presented in Table 7 permit to confirm that the addition of layers guaranteed a residual flexural strength capacity, this leading to a flexural-hardening response of the composite ($MOR_m/LOP_m > 1.0$, see Table 7). In this regard, the cracking activated the effective contribution of the fiber layers, which controlled the crack opening by bearing tensile stresses across the cracks. It must be remarked that the reinforcement provided by the fiber layers led to a ductile response, necessary in structures made of brittle matrices in case of a pre-failure situation (ex., for evacuating and/or for stresses redistribution in case of redundant structures). Likewise, the relationships MORm - nº layers shown in Figure 11 for the different composites allow stating that the optimum number of layers ranged from 5 to 6. In this regard, the results confirm that more than 6 layers led to a decrease in the bearing capacity since the high amount of fabric and the insufficient impregnation of these layers caused an agglomeration effect and, as consequence, a reduction of both bonding and anchorage capacity between the matrix and the fiber. In fact, averagely in the 7 layers laminates, the mat thickness and (w/c) final were higher than the corresponding 6 layers (see Table 3-5) which causes the unbalanced relationship between the amount of matrix and fiber. Thus, the matrix strength reduced, as observed in the LOP values, which would reduce the mechanical performance in the transition zone. It must be also remarked that the efficiency of fibers close to the neutral axis (or within the compressive zone) is limited (or inexistent) and this phenomenon can be more noticeable as the number of fabric layers increases to more than 6.

As can be seen in Figure 11 and Table 7, FH composites had higher values of MOR in all the 3-7 layers respect to FNH and TW. The most value of MOR of all samples related to the FH6L with 19.8 MPa which is almost 25% higher than TW6L and FNH6L.This higher post-cracking flexural strength capacity of FH is mainly owing to the higher values of LOP since the fiber reinforcement contribution (MOR_m/LOP_m) of FH is not higher than the two other kinds of composites. Furthermore, it should be mentioned that the hornificated fibers had higher dimensional stability and thus higher fiber–matrix adherence which cause improvement in mechanical performance [52]. However, as shown in Figure 8-d, the TW6L proved to be comparable and almost the same post flexural behavior respect to those with Flax fibers both in flexural strength capacity and energy absorption, thereby it could be a suitable replacement for these.

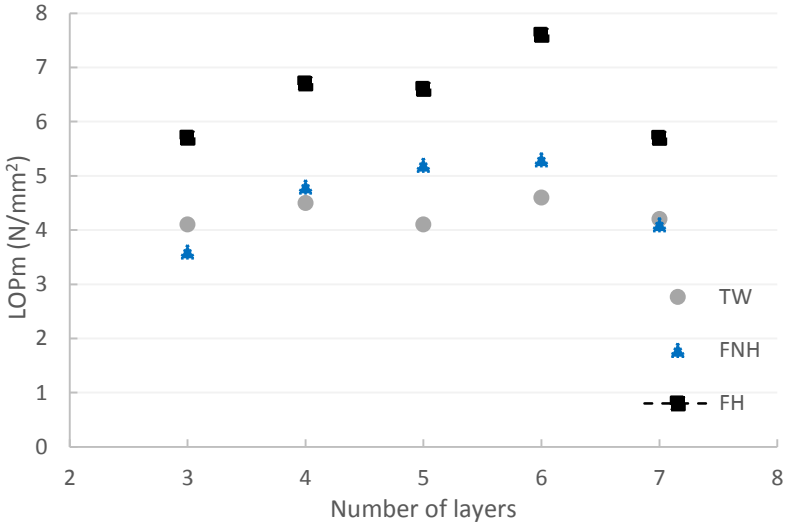

Figure 10. LOP_m – nº layers at 28 days for the tested samples

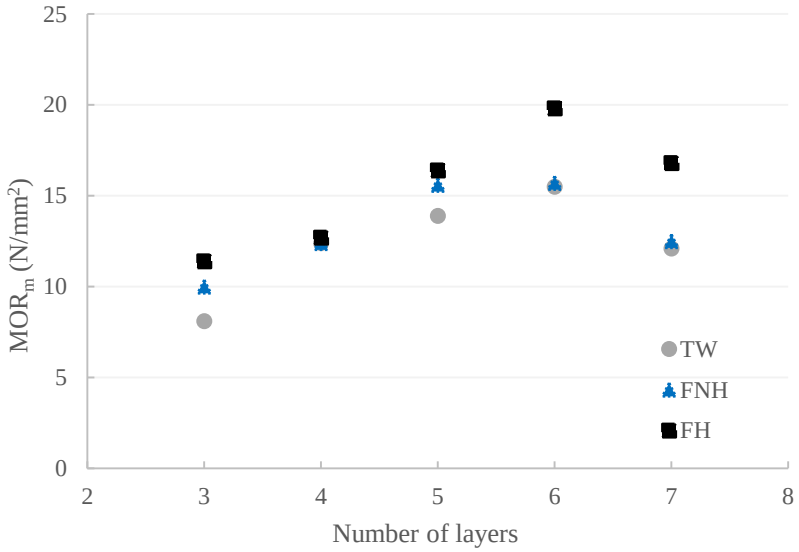

Figure 11. MOR$_m$ – nº layers at 28 days for the tested composites

Table 8 presents the values of toughness (I_G) as a reference parameter for assessing the ductility and energy absorption of the composites. The relationship I_{Gm} - nº layers is depicted in Figure 12. The results highlight that IGm follows similar tendency respect to that obtained for MORm (Figure 11), that is, it was found that IGm reached a maximum for an optimum nº of layers 6. The toughness index was almost the same for all three kinds of reinforcement mats up to 5 layer laminates, nevertheless, the FH sample showed higher values by 25% with increasing the layers to 6 and 7. This higher energy absorption could be due to the better penetration of the matrix to FH fabrics, FH has a lower density than the two other types of fabrics-see Table 2, which can promote a well-balanced interaction between fiber-matrix together with better fiber debonding and pull-out. Furthermore, a large ductility was guaranteed by the small crack spacing which reduced for higher reinforcement layers [39]. As can be seen in Figure 9, the crack distance decreased for higher reinforcement ratios, compared to the crack distance of 3-4 layers to 5-7 layers in TW composites.

Finally, the flexural stiffness of the pre-cracked zone (E_1) and post-cracked zone (E_3), see Table 8, were also computed from the flexural stress–midspan deflection curves (Figure 8) as a reference parameter to quantify the deformability in the linear stages. Building elements to be produced with these composites shall not crack under service conditions and both deflections and rotations be limited according to the application and the requirements imposed by the designer. For that purpose, E_1 plays an important role as a deformation control mechanical parameter. In Figure 13 the relation E_1 – nº of layers is presented, from which it can be noticed that the reinforcement is not a governing factor ($E_{3m}/E_{1m} \leq 0.05$ in all cases) as the matrix did not crack at this stage and, therefore, the fibers do not effectively contribute. Moreover, E_1 is rather independent of the number of layers and almost follows the same trend as LOP since both parameters are mainly dependent on the matrix characteristics.

On the other hand, E_3 is governed by the stiffness of the fabrics as the matrix was cracked in this regime, and only fibers bearing the tensile stresses. In Figure 14 the relation E_{3m} – nº of layers is presented, from which it can be noticed that the reinforcement ratio is a governing factor. Moreover, it must be noticed that the increase of E_{3m} for the FH and FNH composites is linear with the number of layers and both with a similar slope (similar efficiency of the reinforcement); contrarily, the TW composites presented lower magnitudes of E_{3m} whilst the increase of E_{3m} is superior (higher slope) respect to the FH and FNH composites provided that the nº of layers is equal or inferior to six.

Table 8– I_G and E (CoV in %) of all the nonwoven composites at 28 days

CODE	I_{Gm} (KJ/m^2)	E_{1m} (GPa)	E_{3m} (GPa)
TW3L	3.9(28)	8.7(17)	0.13(27)
TW4L	7.0(24)	10.7(14)	0.25(13)
TW5L	8.5(7)	7.8(26)	0.38(24)
TW6L	9.7(12)	11.3(21)	0.41(9)
TW7L	9.4(8)	10.6(21)	0.30(7)
FNH3L	4.6(8)	6.8(17)	0.37(18)
FNH4L	6.2(11)	9.5(11)	0.39(10)
FNH5L	8.7(14)	11.0(16)	0.40(16)
FNH6L	9.2(3)	7.3(12)	0.43(12)
FNH7L	7.6(18)	7.6(9)	0.43(22)
FH3L	4.7(17)	10.3(21)	0.39(20)
FH4L	6.8(20)	11.0(18)	0.40(18)
FH5L	8.2(9)	10.5(16)	0.46(12)
FH6L	12.0(10)	11.4(14)	0.47(10)
FH7L	10.8(12)	9.2(18)	0.48(6)

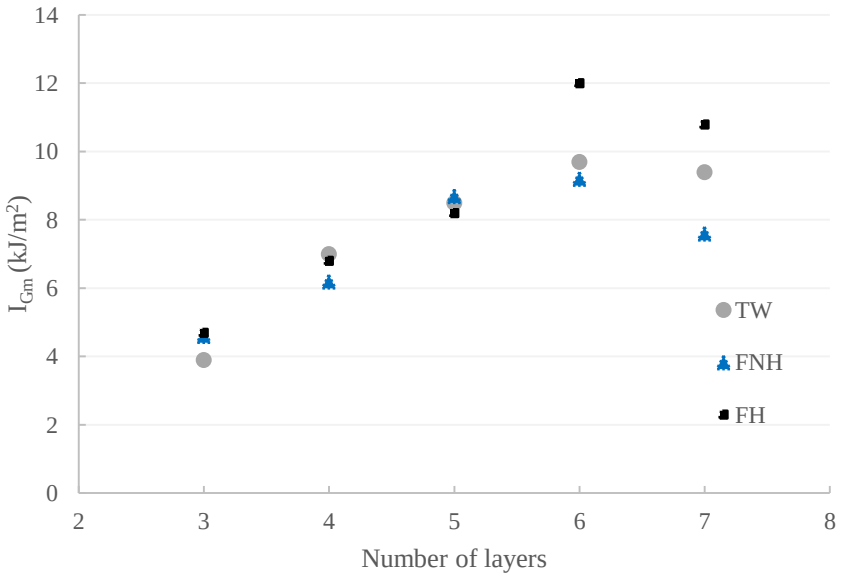

Figure 12. Results of I_{Gm} at 28 days for the tested Nonwowen composites

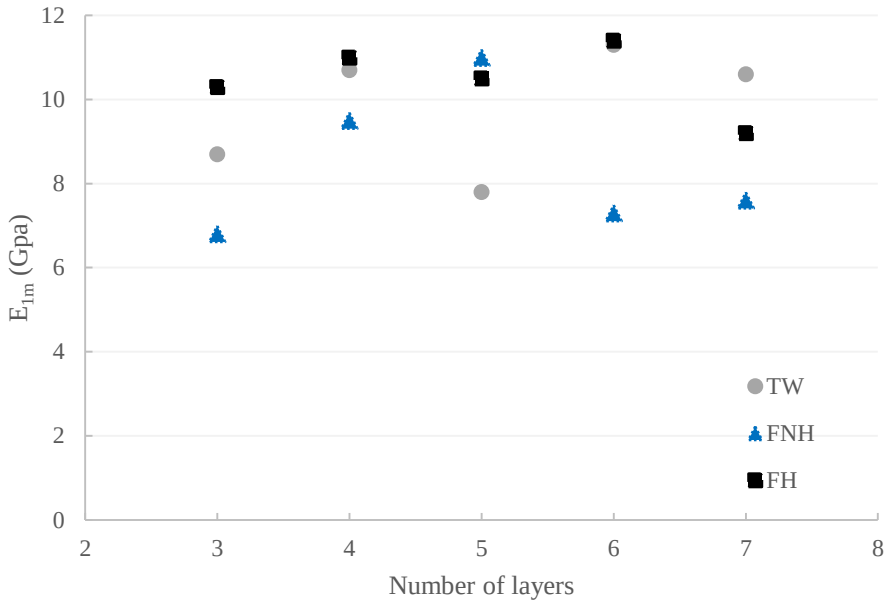

Figure 13. Results of E_{1m} at 28 days for the tested Nonwoven composites

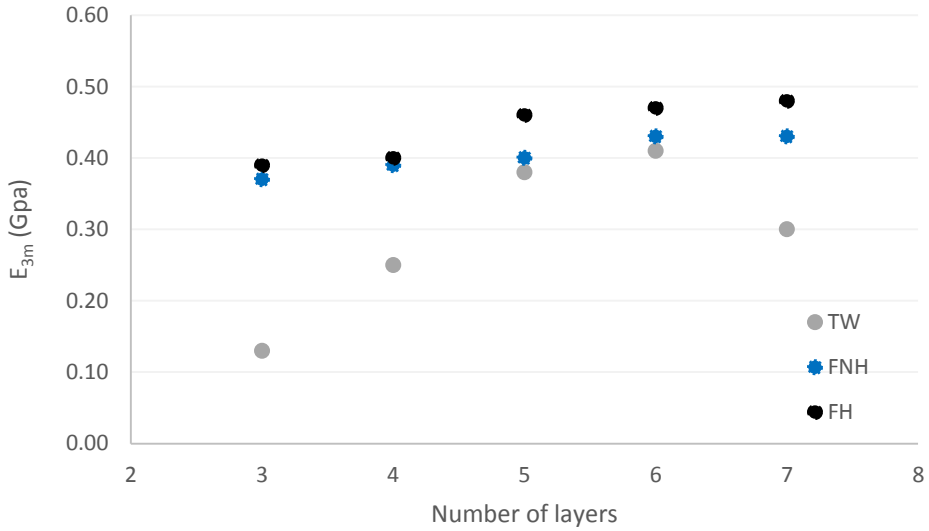

Figure 14. Results of E_{3m} at 28 days for the tested Nonwoven composites

Overall in the unaged samples, the composites prepared with FH fiber mats had superior mechanical properties, followed by the TW and FNH. This finding is in agreement with the research of [50], which proved that the composites reinforced with the micro hornificated fibers had a flexural strength of between 8% (kraft pulp) and 16% (cotton linters) higher than the composites prepared with the untreated fibers. Similarly, the fracture energy was between 20% (kraft pulp) and 5% (cotton linters) higher in the composites prepared with the hornificated fibers. Also in another research [54], for the same number of layers of fabric reinforcement, the composites prepared with the water treated nonwoven fabrics presented

a considerably higher flexural strength and fracture energy, by 36%, than the corresponding ones prepared with the untreated fabrics.

3.3 Flexural tests on aged composites

As the optimum layers of fabric reinforcement in unaged conditions proved to be six, the durability test was done on 3-6 layers of laminates. In Figure 15, the representative stress-displacement curves derived from the flexural tests on specimens subjected to accelerated aging are depicted (D indicates specimens subjected to aging). Likewise, Table 9 gathers the mean and CoV of the MOR*, I_G*, LOP*, E_1*, and E_3* obtained for the composited subjected to aging. Moreover, Figures 16-17 showed the relationship between ξ and the number of layers for the LOP, MOR, and I_G, where the factor ξ is a relative increment of the property after the aging process respects its unaged value (ex., (MOR* - MOR)/MOR).

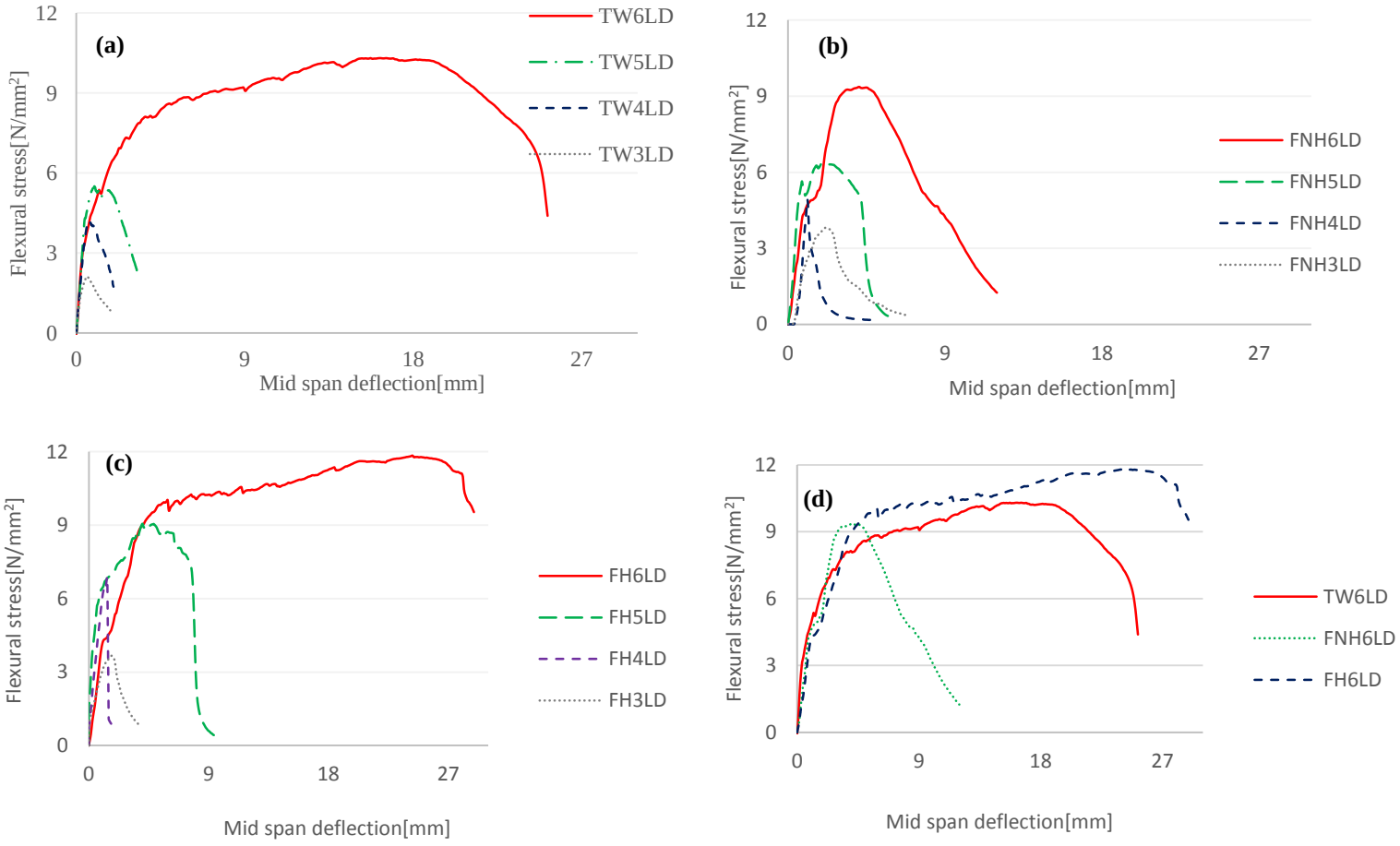

Figure 15. . Experimental flexural stress – deflection relationships obtained at 28 days for nonwoven aged composites: (a) TWD; (b) FNHD; (c) FHD ; (d) six-layers composites

The results presented in Figure 15 and Table 9 allow confirming that the accelerated aging procedure carried out led affected the mechanical response of the composites respect to those unaged (Figure 8 and Table 7). The post-cracking mechanical properties are remarkably affected by aging. As can be seen in

Figure 15, most of the curves after the ascending elastic zone experienced the strain-softening branch without a noticeable post-cracking regime. As can be seen in Figure 15-d, only the 6 layers reinforcement of TW and FH composites demonstrated strain hardening with multiple cracking behaviors though the slope of these zones (E_3*) was lower than the corresponding unaged ones (E_3) by almost 62% pointed to a loss of the fibers' stiffness due to the degradation.

As expected, there was a loss of resistance in the composites after aging. The relationship ξ – nº layers for MOR presented in Figure 16 confirms that this property seems to be affected almost to the same extent independently of the textile reinforcement type, the reduction being of about 70% for reinforcing 3 layers and 40% for 6 layers. Hence, as the number of layers increases, the impact of aging in relative terms appears to be reduced. This might be since the aging effect could not affect the most internal reinforcing layers. As a result, the six layers of nonwoven textile reinforcement led to the best post-cracking mechanical performance after the aging process, independently of the material type and treatment of the reinforcement. In this regard, it is remarkable the superior performance of TW6LD and FH6LD with MOR_m* above 10.0 N/mm^2.

The main issue of durability is the sharp reduction of the toughness and energy absorption of the composites. This problem is associated with an increase in fiber rupture and a decrease in fiber pull-out due to a combination of the weakening of the fibers by alkali attack, fiber mineralization due to the migration of hydration products to lumens, and space and volume variation due to the high water absorption of fibers [1]. As shown in Figure 17, this property followed roughly the same reduction trend as MOR, that is, the loss of the toughness decreased by the number of layers, from 95% for 3 layers to 35% for 6 layers. Based on the results of Table 9, it was found that I_{Gm}* reached a maximum for an optimum nº of 6 layers in all kinds of composites. Nonetheless, FH6LD and TW6LD showed significantly better energy absorption behavior than FNH6LD, more than fourfold. The reason for the better performance of TW could be that in this composite the synthetic fiber would not degrade as much as cellulosic ones. A similar result was already observed in a comparison between the aged short TW composite with the cellulose kraft pulp. On the other hand, as a consequence of the lower water retention value of the hornificated fibers, a reduction in the formation of incrustations of calcium hydroxide on the surface and lumen of the fibers and consequently a reduction in the degradation of the cellulose happened [63]. The result is in compliance with [50], which compared the aged flax hornified and nonhornified composites. As reported in [59], hornification treatment improves the durability of the natural fiber in the cement matrix. The formation of bonds inside the fiber reduces the volumetric variation due to moisture changes. Under these conditions, the stresses between the fiber and the matrix during the dry-wet cycles are reduced which resulted in maintaining the adhesion between the fiber-matrix for a higher number of cycles. Besides [64], the reduction of water absorption and retention capacity decreases the reprecipitation of calcium hydroxide inside the fibers produced during aging cycles.

The elastic pre-cracking properties (LOP and E1) resulted in averagely unaltered since these are mainly dependent on the matrix, which is not affected by this aging procedure. The relationship ξ – nº layers depicted in Figure 16 for LOP confirms that the variation of ξ is primarily due to both material and test scatter as a net effect of the aging cannot be clearly observed. Likewise, an average increase of 8.0% of E1m for the aged specimens (Table 9) respect to those unaged (Table 8) was measured. This stiffening can be caused by the embrittlement of the matrix and a possible greater hydration reaction of the matrix after the aging, which would not be significant in terms of this being considered an enhancement of the structural performance. A similar trend, unaltered or even higher amounts, for LOP and E_1 after the aging of the cement composites was observed in other research [10][19].

Finally, it must be highlighted as the ratio MOR_m/LOP_m of the aged specimens is superior to 1.00 in all cases, therefore, the ductility requirement is still fulfilled. In this regard, TW6L proved to perform with the best mechanical response after the accelerated aging and, therefore, this composite could be a proper alternative to FNH6L and, even, to FH6L.

Table 9– Results of durability tests on aged-composites (CoV in %)

CODE	**LOP_m*** (N/mm^2)	E_{1m}* (GPa)	E_{3m}* (GPa)	**MOR_m*** (N/mm^2)	**I_{Gm}*** (kJ/m^2)	**MOR_m*/LOP_m*** **[-]**
TW3LD	2.3(34)	7.2(29)	-	2.5(44)	0.11(45)	1.09
TW4LD	4.3(30)	11.2(17)	-	4.8(31)	0.21(45)	1.12
TW5LD	4.2(26)	11.4(12)	-	4.9(36)	0.54(37)	1.17
TW6LD	5.1(31)	12.0(5)	0.16(24)	10.0(27)	6.8(33)	1.96
FNH3LD	3.7(13)	9.5(16)	-	3.8(12)	0.15(26)	1.03
FNH4LD	4.5(31)	10.5(14)	-	4.7(27)	0.16(25)	1.04
FNH5LD	5.5(20)	11.6(13)	-	6.0(16)	0.68(27)	1.09
FNH6LD	5.2(11)	10.0(14)	-	7.8(24)	1.6(43)	1.50
FH3LD	3.0(16)	8.3(37)	-	3.8(21)	0.13(46)	1.27
FH4LD	5.2(30)	9.0(18)	-	5.4(29)	0.13(38)	1.04
FH5LD	6.8(7)	10.5(23)	-	9.3(20)	3.2(46)	1.37
FH6LD	7.0(12)	10.7(23)	0.14(12)	11.6(16)	7.3(39)	1.66

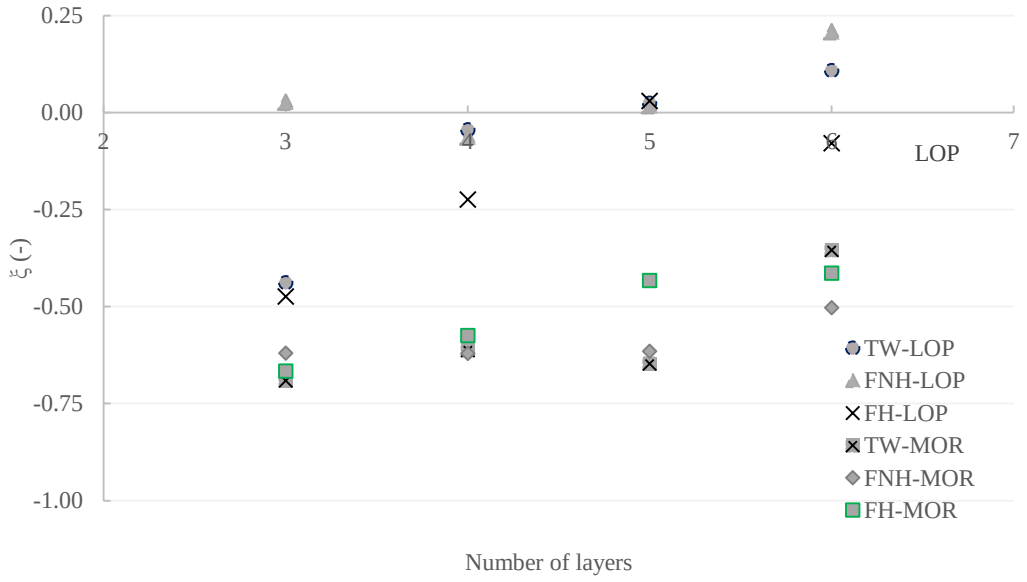

Figure 16. Relationship ξ – number of layers for the LOP and MOR

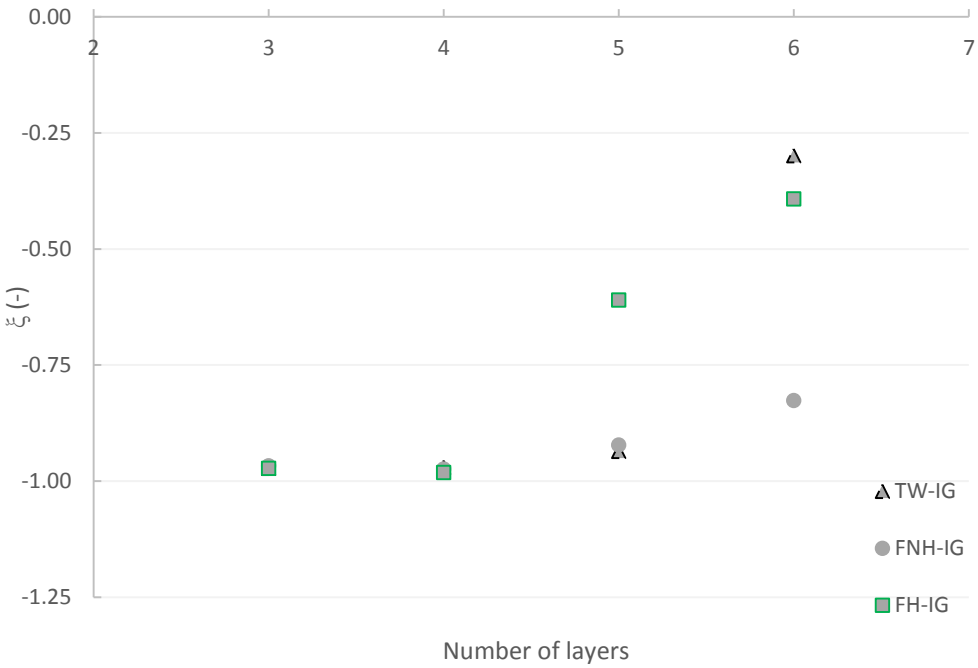

Figure 17. Relationship ξ – number of layers for the I_G

3.4 SEM-BSEM observations

Based on the previous results, a complementary characterization of the morphology of the samples by SEM-BSEM was made. To analyze the results in more depth, this study was limited to TW3L and TW6L composites in both aged and unaged conditions.

Figure 18 identifies the different zones of the TW3L matrix and the chemical composition by EDS. As can be seen, the unhydrated cement phases, the lighter areas, are including C_3A (SP_1), C_2S, or C_3S (SP_2). Spectrum 4 is CSH products while $Ca(OH)_2$ and amorphous zones dominate in spectrum 3, large neutral gray particles. Finally, there are also very dark ellipsoidal spots that correspond to the fibers embedded in the matrix. The cracks that are observed may be due to the drying and polishing of the sample to make possible the BSEM observation or due to accelerated aging treatment in the aged samples.

Figure 19 shows the microimages from BSEM observation, in which, the matrix area located between two layers of nonwoven fabrics was depicted. As can be seen in the unaged condition (Figures 19-a and b) the matrix of the TW3L had more unhydrated particles rather than the matrix of TW6L justified the higher LOP of TW6L. Similarly, larger anhydrous cement particles were observed in TW3LD rather than TW6LD (Figures 19-c and d). Moreover, the fibers especially the vegetable ones (marked with a red arrow) were more damaged and cracked in TW3LD rather than TW6LD probably because the aging effect could not affect significantly the most internal reinforcing layers. Generally, the synthetic fiber (marked with a green arrow) showed better adhesion and behavior respect to natural one when subjected to aging. The cellulosic fiber had more internal holes and cracks due to hydrophilic behavior. Similarly in another research [45] regarding the accelerated aging of cellulosic fibers, it was observed that the kraft pulp, with some pits on its surface, could favor the precipitation of hydration products of the cement in the lumen of the fibers and, consequently, facilitate the degradation of the fibers.

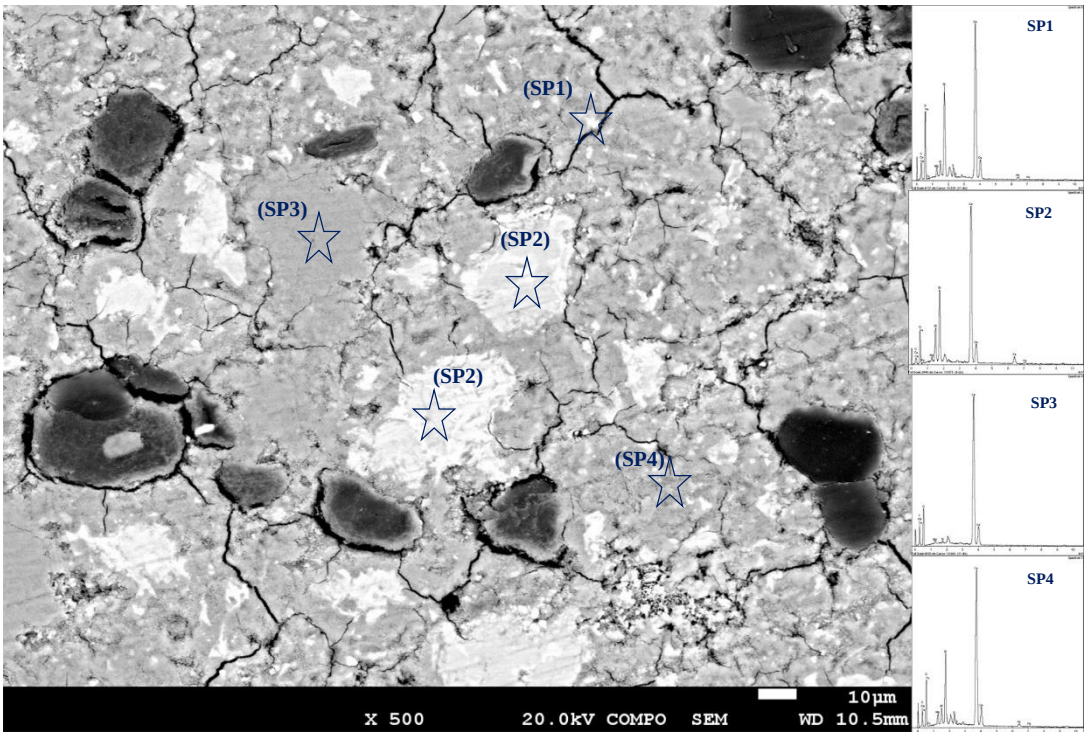

Figure 18. BSE-SEM micrograph showing the areas for EDS analysis of TW3L matrix

Figure 20, focuses on the micrographs regarding the fracture surfaces of TW obtained from SEM while Figure 21 shows the micrographs regarding the fiber surfaces. The breakdown of the matrix into pieces was observed in almost all samples which can generate energy absorption. The unaged composites (Figure 20-a and b) together with TW6LD (Figure 20-d) had longer fibers respect to the TW3LD. This happened because the fiber pull-out mechanism was predominant in fiber-cement interactions in these samples, generating considerable fractional energy losses, which contribute to high toughness. For instance in TW6L and TW6LD, it is seen how a large set of fibers protrudes from the cement matrix. In this group of fibers, synthetic fiber (finer one) and natural fiber (thicker one) can be distinguished. The surface of the fiber is smooth and has no particles attached to its surface. Moreover, none of the fibers have been broken which causes to withstand more tensile stress. This is an indication that the fibers had detached from the matrix producing a type of break called "pull out."

On the other hand, in most of the composites after wet-dry cycles, like TW3LD, the fibers had shorter lengths since the fiber rupture mechanism mostly occurred which mitigated the desirable toughness characteristics, see Figure 20-c. In other words, as proved for long unidirectional sisal fibers by [32], the aging process due to the fiber mineralization results in reducing the tensile strength of fibers and decreasing the fiber pullout ligament followed by a fracture. This mineralization process is a result of the migration of hydration products, mainly $Ca(OH)_2$, to the fiber structure. So generally, the durability test is associated with an increase in fiber fracture and a decrease in fiber pull-out and among the TW composites, only TW6LD showed good behavior after aging.

As shown in Figure 21, the vegetable fibers including flax and cotton were cracked and wrinkled more significantly after accelerated aging, due to the alkali attack, respect to the polyester one. Figure 21-c shows

the synthetic fiber accumulated with some hydrated cement products without any significant crack or damage. This is in agreement with the finding of [11] which declares that because of the low corrosion resistance of lignin and hemicelluloses that exist in the middle lamellae of cellulose fibers, in a high alkali environment of cement matrix vegetable fibers gradually degrade and lose the reinforcing capacity in a later stage of service life. So that is why after wet-dry cycles, the TW composite reinforced with both vegetable and synthetic fibers, had better behavior respect to FNH composite, only reinforced with flax fibers.

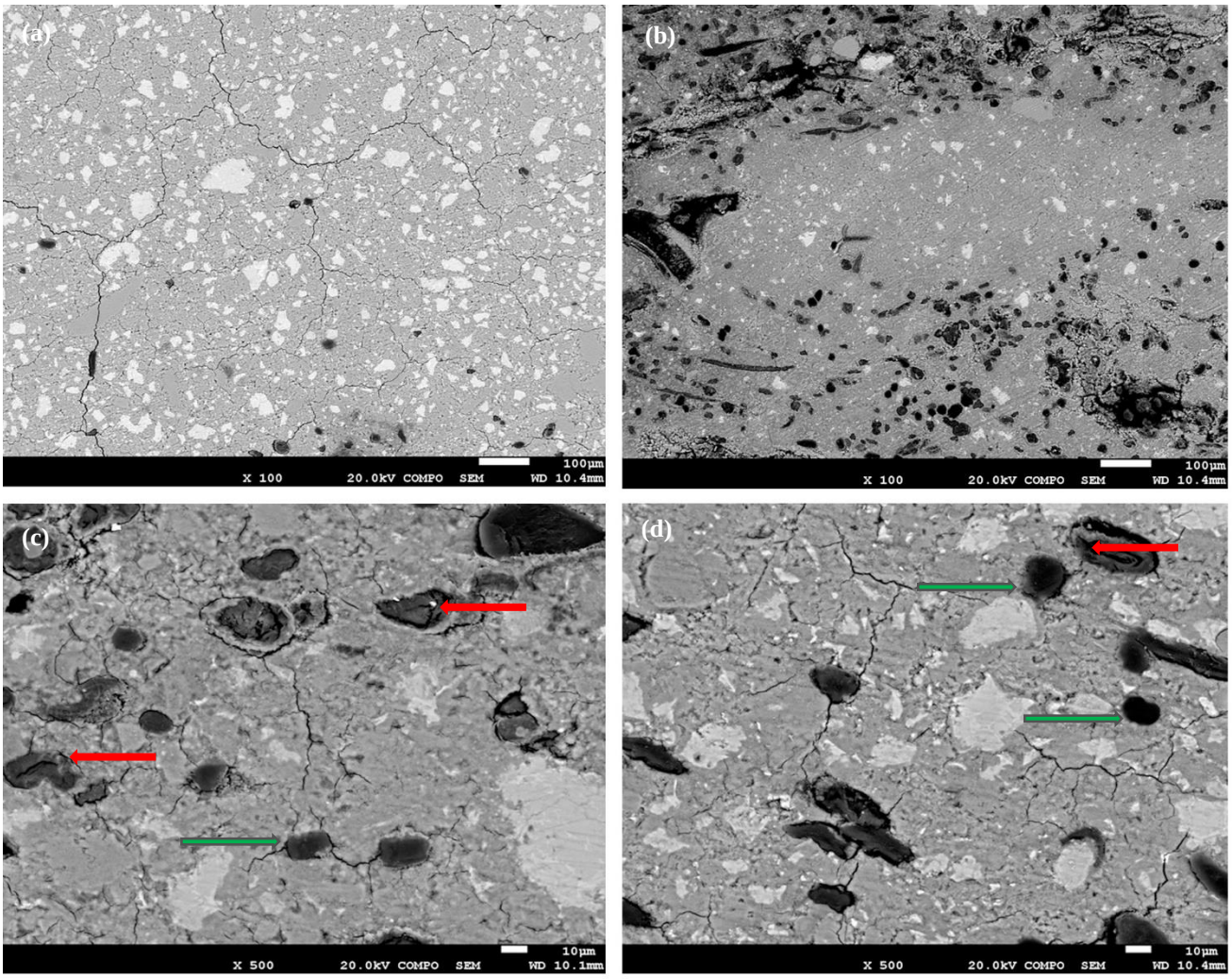

Figure 19. BSEM micrographs of the TW composites: (a) TW3L (b) TW6L (c) TW3LD (d) TW6LD

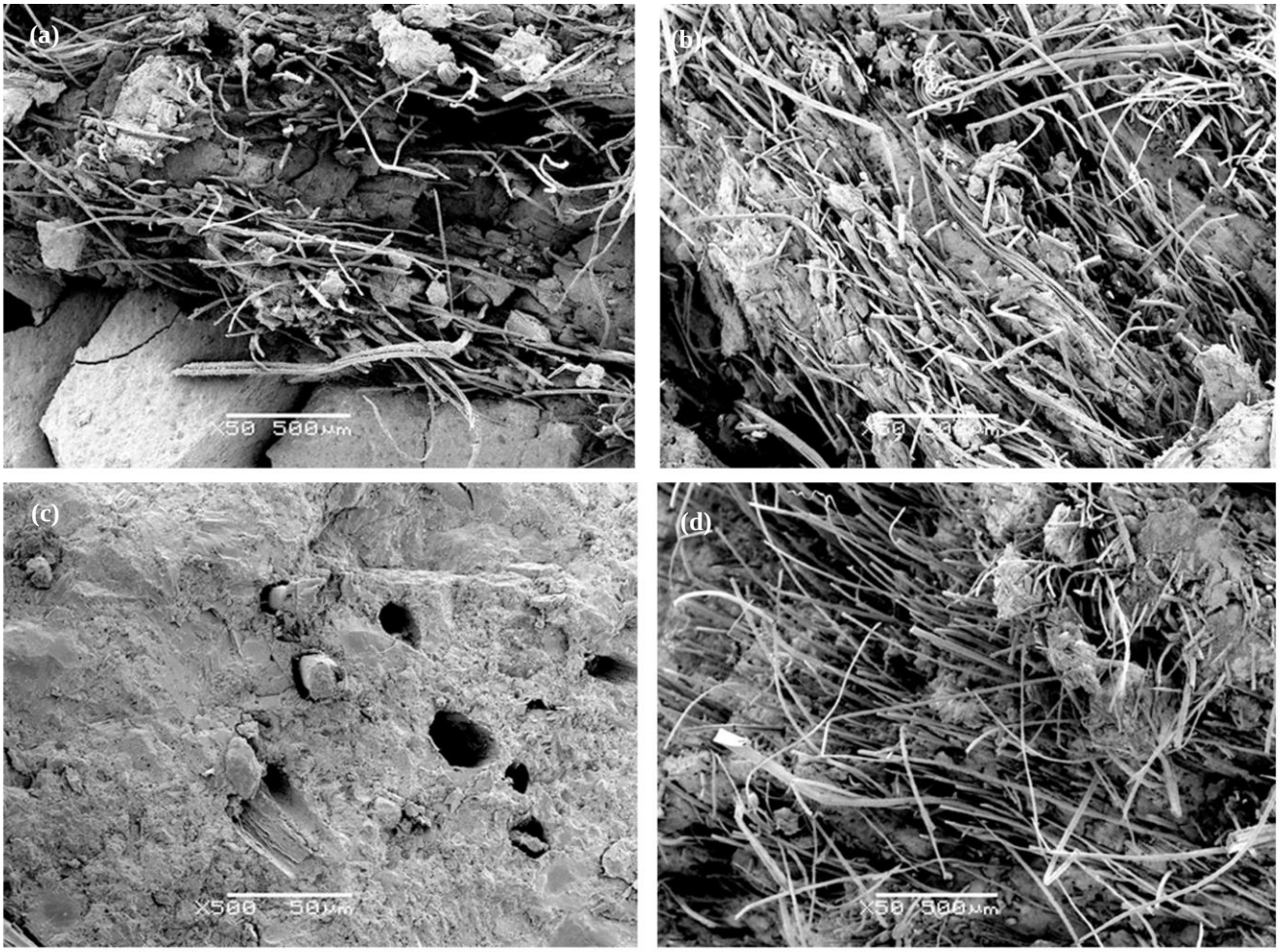

Figure 20. SEM micrographs of the fracture surfaces of the TW composites: (a) TW3L (b) TW6L (c) TW3LD (d) TW6LD

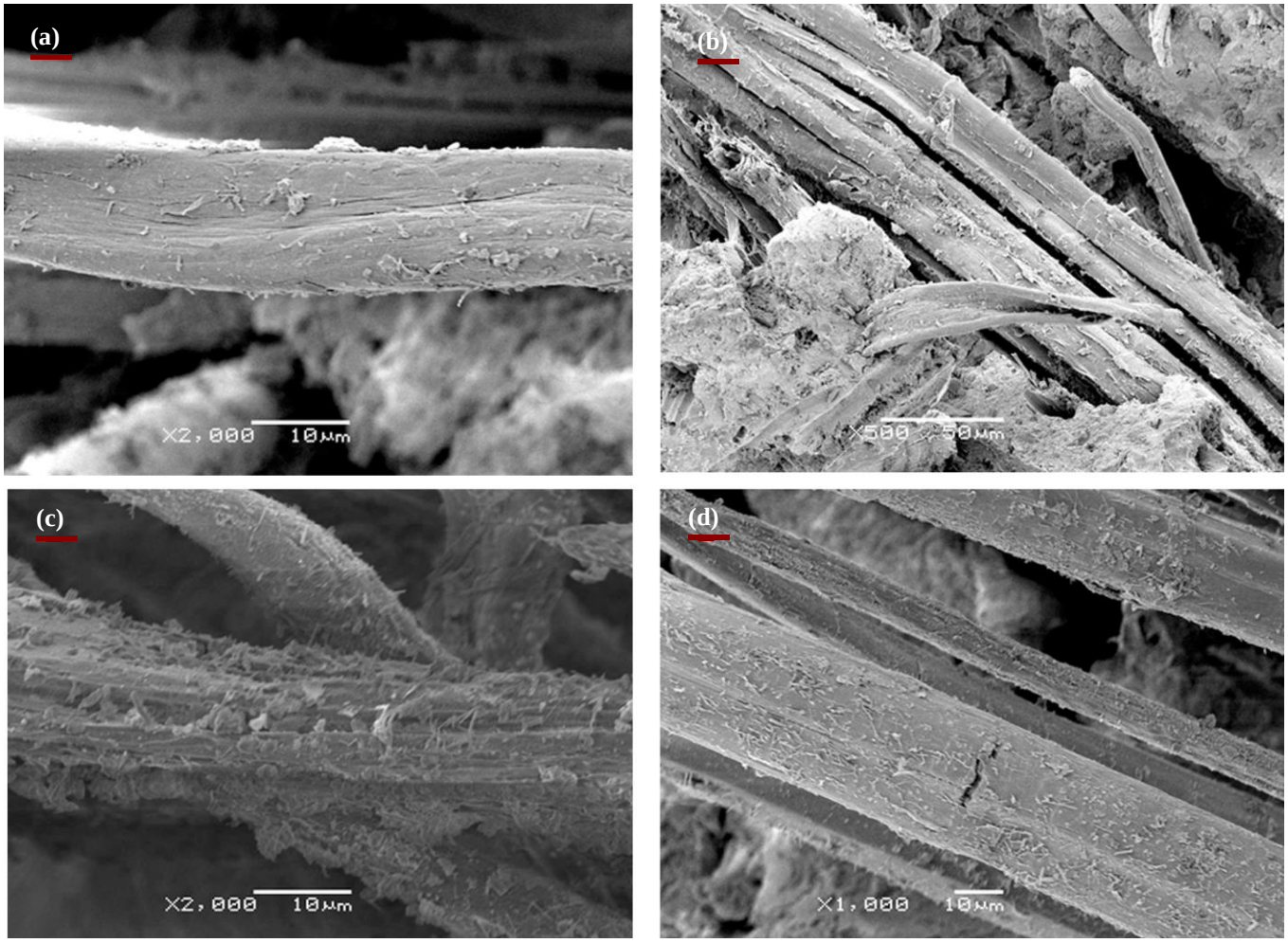

Figure 21. SEM micrographs of the fiber surfaces of the TW composites: (a) TW3L (b) TW6L (c) TW3LD (d) TW6LD

4. Conclusions

The main objective of this research was to verify both mechanical and durability properties of the textile waste (TW) nonwoven fabric as reinforcement for cement composites. This material is constituted of recycled short fibers from garment-textile waste. The use of these composites for producing building components can valorize this waste while reducing the impact of construction on natural resources.

The design-oriented flexural properties of a cement-based matrix reinforced with 3 to 7 reinforcement layers of TW laminates were investigated within the context of an extensive experimental program. Flexural tests were carried out after 28 days to characterize the pre-and post-cracking response of these composites. Additionally, tests simulating accelerated aging conditions in addition to SEM and BSEM observations were included to assess the suitability of this material in terms of durability and to provide a preliminary quantification of the post-cracking flexural capacity after inducing damage by means of accelerated aging. The same

tests were performed for reference samples with flax nonwoven fabric (FNH). Some of the fabrics of the reference samples were previously undergone the physical treatment of hornification (FH).

The following conclusions were derived from the results:

- Flexural tests' results on unaged specimens confirmed that all composites achieved a post cracking response with the formation of multiple cracking, being requirements to be fulfilled in terms of structural applicability of these composites. Likewise, the results evidenced a clear relationship between the number of reinforcing layers and the post-cracking mechanical properties characterized by an optimum performance when the number of layers ranged from 5 to 6.
- Post-cracking mechanical properties of specimens subjected to an accelerated aging process were found to be remarkably affected. As a preliminary proposal in terms of design, it is proposed to reduce by a factor of 4.0 the short-term value of MOR so that the degradation due to aging during service conditions can be taken into consideration. This, however, must be further investigated by carrying out an extensive experimental program on accelerating aging. It must also be added that those composites reinforced with six layers proved to lead to better mechanical performance after the accelerated aging, especially FH6L and TW6L.
- SEM and BSEM observations confirmed that the accelerated aging process is associated with an increase in fiber fracture and a decrease in fiber pull-out, especially in vegetable fibers, due to the alkali attack. TW composite had better behavior respect to FNH composite since the former was reinforced with both vegetable and synthetic fibers, while the latter was only reinforced with untreated flax fibers.

Finally, these preliminary characterization results of TW composites allow confirming the potentiality of this material in non-structural applications for building components as an alternative to FH composites, although the formers presented less mechanical capacity. Nevertheless, from the sustainability point of view, TW reinforcement is a valorized material produced from waste. Both aspects –suitability as construction material and sustainability assessment of TW composites– as well as improving the matrix with pozzolanic materials to reduce the porosity are topics being researched within the context of the Ph.D. thesis of the first author of this paper.

Acknowledgments

The authors express their gratitude to the Spanish Ministry of Economy, Industry, and Competitiveness for the financial support received under the scope of the projects RECYBUILDMAT (PID2019-108067RB-I00) and CREEF (PID2019-108978RB-C32).

References

[1] M. Ardanuy, J. Claramunt, and R. D. Toledo Filho, "Cellulosic fiber reinforced cement-based composites: A review of recent research," Constr. Build. Mater., vol. 79, pp. 115–128, 2015.

[2] J. O. Lerch, H. L. Bester, A. S. Van Rooyen, R. Combrinck, W. I. de Villiers, and W. P. Boshoff, "The effect of mixing on the performance of macro synthetic fibre reinforced concrete," Cem. Concr. Res., vol. 103, no. May, pp. 130–139, 2018.

[3] A. M. Brandt, "Fibre reinforced cement-based (FRC) composites after over 40 years of development in building and civil engineering," Compos. Struct., vol. 86, no. 1–3, pp. 3–9, 2008.

[4] Y. Jia, R. Zhao, P. Liao, F. Li, Y. Yuan, and S. Zhou, "Experimental study on mix proportion of fiber reinforced cementitious composites," vol. 020002, 2017.

[5] E. Booya, K. Gorospe, H. Ghaednia, and S. Das, “Free and restrained plastic shrinkage of cementitious materials made of engineered kraft pulp fibres,” Constr. Build. Mater., vol. 212, pp. 236–246, Jul. 2019.

[6] R. D. Toledo Filho, K. Ghavami, M. A. Sanjuán, and G. L. England, “Free, restrained and drying shrinkage of cement mortar composites reinforced with vegetable fibres,” Cem. Concr. Compos., vol. 27, no. 5, pp. 537–546, 2005.

[7] P. J. M. Mehta, P.K.; Montiero, Concrete Microstructure, Properties, and Materials, 3rd ed.; M. 2006.

[8] A. M. Brandt, Cement-Based Composites. CRC Press, 2005.

[9] Y. Wang, S. Backer, and V. C. Li, “An experimental study of synthetic fibre reinforced cementitious composites,” J. Mater. Sci., vol. 22, no. 12, pp. 4281–4291, 1987.

[10] J. Claramunt, L. J. Fernández-Carrasco, H. Ventura, and M. Ardanuy, “Natural fiber nonwoven reinforced cement composites as sustainableClaramunt, J., Fernández-Carrasco, L. J., Ventura, H., & Ardanuy, M. (2016). Natural fiber nonwoven reinforced cement composites as sustainable materials for building envelopes. Constructio,” Constr. Build. Mater., vol. 115, pp. 230–239, 2016.

[11] J. Wei and C. Meyer, “Improving degradation resistance of sisal fiber in concrete through fiber surface treatment,” Appl. Surf. Sci., vol. 289, pp. 511–523, 2014.

[12] “High energy performing buildings - Publications Office of the EU.” [Online]. Available: https://publications.europa.eu/en/publication-detail/-/publication/d8e3702d-c782-11e8-9424-01aa75ed71a1/language-en/format-PDF/source-77709912.

[13] L. Cândido, W. Kindlein, R. Demori, L. Carli, R. Mauler, and R. Oliveira, “The recycling cycle of materials as a design project tool,” J. Clean. Prod., vol. 19, no. 13, pp. 1438–1445, Sep. 2011.

[14] J. Giesekam, J. Barrett, P. Taylor, and A. Owen, “The greenhouse gas emissions and mitigation options for materials used in UK construction,” Energy Build., vol. 78, pp. 202–214, Aug. 2014.

[15] H. Nautiyal, V. Shree, S. Khurana, N. Kumar, and Varun, “Recycling Potential of Building Materials: A Review,” Springer, Singapore, 2015, pp. 31–50.

[16] CHF, “Licensed for The Fiber Year GmbH The Fiber Year 2018 World Survey on Textiles & Nonwovens,” 2018.

[17] C. Correia, S. Francisco, H. Savastano, and V. Moacyr, “Utilization of vegetal fibers for production of reinforced cementitious materials,” no. 2017, 2018.

[18] L. Mercedes, L. Gil, and E. Bernat-maso, “Mechanical performance of vegetal fabric reinforced cementitious matrix (FRCM) composites,” Constr. Build. Mater., vol. 175, pp. 161–173, 2018.

[19] P. Sadrolodabaee, J. Claramunt, M. Ardanuy, and A. de la Fuente, “Mechanical and durability characterization of a new textile waste micro-fiber reinforced cement composite for building applications,” Case Stud. Constr. Mater., vol. 14, p. e00492, Jun. 2021.

[20] A. Villanueva, L. Delgado, Z. Luo, P. Eder, A. Sofia Catarino, and D. Litten, “Study on the selection of waste streams for end-of-waste assessment. Final Report.”

[21] J. M. Hawley, “Textile recycling: A systems perspective,” Recycl. Text., 2006.

[22] H. Song, W. Baek, S. Lee, and S. H. Hong, “Materials Processing Technology,” Milling, vol. 48, pp. 4–9, 1997.

[23] K. Slater and E. Textile Institute (Manchester, Environmental impact of textiles : production, processes and protection. CRC Press, 2003.

[24] A. Briga-Sá et al., "Textile waste as an alternative thermal insulation building material solution," Constr. Build. Mater., vol. 38, pp. 155–160, 2013.

[25] A. Paiva, H. Varum, F. Caldeira, A. Sá, D. Nascimento, and N. Teixeira, "Textile Subwaste as a Thermal Insulation Building Material."

[26] Y. Lee and C. Joo, "Sound absorption properties of recycled polyester fibrous assembly absorbers," Autex Res. J., vol. 3, no. 2, pp. 78–84, 2003.

[27] A.-E. Tiuc, H. Vermeşan, T. Gabor, and O. Vasile, "Improved Sound Absorption Properties of Polyurethane Foam Mixed with Textile Waste," Energy Procedia, vol. 85, pp. 559–565, Jan. 2016.

[28] D. Rajput, S. S. Bhagade, S. P. Raut, R. V. Ralegaonkar, and S. A. Mandavgane, "Reuse of cotton and recycle paper mill waste as building material," Constr. Build. Mater., vol. 34, pp. 470–475, Sep. 2012.

[29] H. Binici and O. Aksogan, "Engineering properties of insulation material made with cotton waste and fly ash," J. Mater. Cycles Waste Manag., vol. 17, no. 1, pp. 157–162, Jan. 2015.

[30] C. Rubino, S. Liuzzi, F. Martellotta, and P. Stefanizzi, "Modelling , Measurement and Control B Textile wastes in building sector : A review," vol. 87, no. 3, pp. 172–179, 2018.

[31] J. Claramunt, H. Ventura, L. J. Fernández-carrasco, and M. Ardanuy, "Tensile and Flexural Properties of Cement Composites Reinforced with Flax Nonwoven Fabrics," Materials (Basel)., pp. 1–12, 2017.

[32] F. de A. Silva, B. Mobasher, and R. D. T. Filho, "Cracking mechanisms in durable sisal fiber reinforced cement composites," Cem. Concr. Compos., vol. 31, no. 10, pp. 721–730, 2009.

[33] M. E. A. Fidelis, F. de Andrade Silva, and R. D. Toledo Filho, "The Influence of Fiber Treatment on the Mechanical Behavior of Jute Textile Reinforced Concrete," Key Eng. Mater., vol. 600, pp. 469–474, Mar. 2014.

[34] R. D. Toledo Filho, F. de A. Silva, E. M. R. Fairbairn, and J. de A. M. Filho, "Durability of compression molded sisal fiber reinforced mortar laminates," Constr. Build. Mater., vol. 23, no. 6, pp. 2409–2420, Jun. 2009.

[35] F. de Andrade Silva, B. Mobasher, and R. D. T. Filho, "Fatigue behavior of sisal fiber reinforced cement composites," Mater. Sci. Eng. A, vol. 527, no. 21–22, pp. 5507–5513, Aug. 2010.

[36] F. de A. Silva, D. Zhu, B. Mobasher, C. Soranakom, and R. D. Toledo Filho, "High speed tensile behavior of sisal fiber cement composites," Mater. Sci. Eng. A, vol. 527, no. 3, pp. 544–552, Jan. 2010.

[37] M. C. Rampini, G. Zani, M. Colombo, and M. Prisco, "applied sciences Mechanical Behaviour of TRC Composites : Experimental and Analytical Approaches," 2019.

[38] I. Colombo, M. Colombo, A. Magri, G. Zani, and M. Di Prisco, "Textile reinforced mortar at high temperatures," Appl. Mech. Mater., vol. 82, no. July, pp. 202–207, 2011.

[39] C. Paper, I. G. Colombo, M. Colombo, A. Magri, and G. Zani, "Tensile Behavior of Textile : Influence of Multilayer Reinforcement Tensile behaviour of Textile : influence of multilayer reinforcement," no. May 2014, 2011.

[40] G. Zani, M. Colombo, and M. Di Prisco, "High performance cementitious composites for

sustainable roofing panels," Proc. 10th fib Int. PhD Symp. Civ. Eng., no. February 2015, pp. 333–338, 2014.

[41] M. Saidi and A. Gabor, "Experimental measurement of load-transfer length in textile-reinforced cementitious matrix composites using distributed optical fibres," Eur. J. Environ. Civ. Eng., vol. 0, no. 0, pp. 1–19, 2020.

[42] G. Promis, T. Q. Bach, A. Gabor, and P. Hamelin, "Failure behavior of E-glass fiber- and fabric-reinforced IPC composites under tension and compression loading," Mater. Struct. Constr., vol. 47, no. 4, pp. 631–645, 2014.

[43] O. Homoro, X. H. Vu, and E. Ferrier, "Experimental and analytical study of the thermo-mechanical behaviour of textile-reinforced concrete (TRC) at elevated temperatures: Role of discontinuous short glass fibres," Constr. Build. Mater., vol. 190, pp. 645–663, 2018.

[44] M. Ramirez, J. Claramunt, H. Ventura, and M. Ardanuy, "Evaluation of the mechanical performance and durability of binary blended CAC-MK/natural fiber composites," Constr. Build. Mater., vol. In progres, 2019.

[45] L. Gonzalez-Lopez, J. Claramunt, Y. Lo Hsieh, H. Ventura, and M. Ardanuy, "Surface modification of flax nonwovens for the development of sustainable, high performance, and durable calcium aluminate cement composites," Compos. Part B Eng., vol. 191, no. February, 2020.

[46] M. Saidi and A. Gabor, "Iterative analytical modelling of the global behaviour of textile-reinforced cementitious matrix composites subjected to tensile loading," Constr. Build. Mater., vol. 263, p. 120130, 2020.

[47] C. Caggegi, E. Lanoye, K. Djama, A. Bassil, and A. Gabor, "Tensile behaviour of a basalt TRM strengthening system: Influence of mortar and reinforcing textile ratios," Compos. Part B Eng., vol. 130, pp. 90–102, 2017.

[48] S. R. Ferreira, F. de A. Silva, P. R. L. Lima, and R. D. Toledo Filho, "Effect of hornification on the structure, tensile behavior and fiber matrix bond of sisal, jute and curauá fiber cement based composite systems," Constr. Build. Mater., vol. 139, pp. 551–561, 2017.

[49] H. Ventura, M. Ardanuy, X. Capdevila, F. Cano, and J. A. Tornero, "Effects of needling parameters on some structural and physico-mechanical properties of needle-punched nonwovens," J. Text. Inst., vol. 105, no. 10, pp. 1065–1075, 2014.

[50] J. Claramunt, M. Ardanuy, J. A. García-Hortal, and R. D. T. Filho, "The hornification of vegetable fibers to improve the durability of cement mortar composites," Cem. Concr. Compos., vol. 33, no. 5, pp. 586–595, 2011.

[51] F. D. Tolêdo Romildo D., K. Ghavami, G. L. England, and K. Scrivener, "Development of vegetable fibre-mortar composites of improved durability," Cem. Concr. Compos., vol. 25, no. 2, pp. 185–196, Feb. 2003.

[52] J. Claramunt, M. Ardanuy, and J. A. García-Hortal, "Effect of drying and rewetting cycles on the structure and physicochemical characteristics of softwood fibres for reinforcement of cementitious composites," Carbohydr. Polym., vol. 79, no. 1, pp. 200–205, 2010.

[53] K. Zhao, S. Xue, P. Zhang, Y. Tian, and P. Li, "Application of natural plant fibers in cement-based composites and the influence on mechanical properties and mass transport," Materials (Basel)., vol. 12, no. 21, 2019.

[54] J. Claramunt, H. Ventura, L. J. Fernández-Carrasco, and M. Ardanuy, "Tensile and flexural properties of cement composites reinforced with flax nonwoven fabrics," Materials (Basel)., vol. 10, no. 2, pp. 1–12, 2017.

[55] J. Claramunt, H. Ventura, and M. Ardanuy, "Rheology of CAC-based cement pastes and the relationship to penetrability through nonwoven fabric reinforcements," Cem. Concr. Compos., vol. 94, no. February, pp. 85–93, 2018.

[56] "RILEM - Publications." [Online]. Available: https://www.rilem.net/publication/publication/4?id_papier=4003. [Accessed: 04-Sep-2020].

[57] M. Ardanuy, J. Claramunt, J. A. García-Hortal, and M. Barra, "Fiber-matrix interactions in cement mortar composites reinforced with cellulosic fibers," Cellulose, vol. 18, no. 2, pp. 281–289, Apr. 2011.

[58] BS EN 494-12, "Fibre-cement flat sheets - Product specification and test methods," Br. Stand. Inst., p. 60, 2012.

[59] B. J. Mohr, H. Nanko, and K. E. Kurtis, "Durability of kraft pulp fiber-cement composites to wet/dry cycling," Cem. Concr. Compos., vol. 27, no. 4, pp. 435–448, 2005.

[60] J. E. M. Ballesteros, S. F. Santos, G. Mármol, H. Savastano, and J. Fiorelli, "Evaluation of cellulosic pulps treated by hornification as reinforcement of cementitious composites," Constr. Build. Mater., vol. 100, pp. 83–90, 2015.

[61] G. Fischer, "FIBER-REINFORCED CEMENT COMPOSITES BY THEIR TENSILE STRESS-STRAIN BEHAVIOR AND QUANTIFICATION OF CRACK FORMATION," no. September, pp. 331–338, 2004.

[62] O. A. Cevallos and R. S. Olivito, "Composites : Part B Effects of fabric parameters on the tensile behaviour of sustainable cementitious composites," Compos. PART B, vol. 69, pp. 256–266, 2015.

[63] S. F. Santos, G. H. D. Tonoli, J. E. B. Mejia, J. Fiorelli, and H. Savastano Jr, "Non-conventional cement-based composites reinforced with vegetable fibers: A review of strategies to improve durability," Mater. Construcción, vol. 65, no. 317, p. e041, 2015.

[64] B. J. Mohr, J. J. Biernacki, and K. E. Kurtis, "Microstructural and chemical effects of wet/dry cycling on pulp fiber-cement composites," Cem. Concr. Res., vol. 36, no. 7, pp. 1240–1251, 2006.

2.3 Journal paper III:
A TextileWaste Fiber-Reinforced Cement Composite: Comparison between Short Random Fiber and Textile Reinforcement

Published in materials (2021, 14(13), 3742)

Payam Sadrolodabaee[a*] (payam.sadrolodabaee@upc.edu), Josep Claramunt[b] (josep.claramunt@upc.edu), Monica Ardanuy [c] (monica.ardanuy@upc.edu), Albert de la Fuente[a] (albert.de.la.fuente@upc.edu)

a: Department of Civil and Environmental Engineering- Universitat Politècnica de Catalunya-BarcelonaTECH- Barcelona, Spain
b: Department of Agricultural Engineering- Universitat Politècnica de Catalunya-BarcelonaTECH- Barcelona, Spain
c: Department of Material Science and Engineering (CEM)-Universitat Politècnica de Catalunya-BarcelonaTECH-Barcelona, Spain
*: Corresponding author

Abstract

Currently, millions of tons of textile waste from the garment and textile industries are being generated worldwide each year. As a promising option in terms of sustainability, textile waste fibers could be used as internal reinforcement of cement-based composites by enhancing ductility and decreasing crack propagation. To this end, two extensive experimental programs were carried out, involving the use of either a fraction of short random fibers at 6–10% by weight or nonwoven fabrics in 3–7 laminate layers in the textile waste-reinforcement of cement and the mechanical and durability properties of the resulting composites were characterized. Flexural resistance in pre-and post-crack, toughness, and stiffness of the resulting composites were assessed in addition to unrestrained drying shrinkage testing. In this study, the results obtained from those programs were analyzed and compared to identify the optimal composite and potential applications. Based on the results of experimental analysis, the feasibility of using this textile waste composite as a potential construction material in nonstructural concrete structures such as façade cladding, raised floor, or pavement was confirmed. The optimal composite was proven to be the one reinforced with 6 layers of nonwoven fabric, a flexural strength of 15.5 MPa, and toughness of 9.7 KJ/m^2.

Keywords: cementitious materials; fiber-reinforced composites; mechanical properties; recycled fibers; sustainability; textile waste

1. Introduction

The building sector is one of the major consumers of natural resources and one of the biggest waste producers worldwide. Data indicate that the construction and building sector consumes almost 40% of all the raw materials extracted worldwide and is responsible for around 40% of all the global greenhouse gas emissions in addition to the generation of around 35% of all global waste [1,2]. Therefore, the gradual replacement of the traditional linear economy model with a circular material flow approach focused on reusing and re-cycling is necessary to ensure a sustainable future [3].

The building sector is increasingly interested in innovative sustainable solutions, i.e., materials obtained from recycling and reusing processes so that CO_2 emissions and energy intake can be reduced [4]. In this regard, fiber- and textile-reinforced mortars (FRM and TRM, hereinafter) have generated great interest among both the scientific and construction sectors. These composite materials may be composed of various materials for reinforcement—short fibers [5], long fibers [6], and textiles including woven [7] or nonwoven fabrics [8]—within a cementitious matrix, which can be in the form of cement paste, lime binder, mortar, or concrete. The primary role of reinforcement is to bridge cracks as well as to enhance the toughness, energy absorption capacity, and post-cracking behavior of cementitious matrices [5,9].

World fiber production, including steel, glass, and polymers, has been steadily increasing in the past few decades and has garnered increasing interest with the use of sustainable fibers produced from

renewable, biodegradable, waste, recycled, available, and low-cost resources becoming a focal point. In this sense, vegetable and cellulosic fibers have already been used as reinforcement in cementitious materials for low- to medium-performance structural applications [5], [10–13]. Textile waste fiber could be another sustainable alternative for reinforcement in cementitious composites.

The global production of textiles amounts to over 110 million tons annually, which makes textile production one of the biggest industries that affect global environmental pollution through greenhouse gas emissions, depletion of natural resources, and the generation of huge amounts of waste [3]. Textile leftovers can be categorized as pre-or post-consumer waste, where the former includes all fiber, yarn, and fabric waste produced during garment manufacturing while the latter refers to worn-out clothing discarded by users [14]. In Europe and America, more than 10 million tons of discarded textile products are disposed of in landfills [15], and the estimation for China is double this amount, which implies serious environmental and economic issues. Nevertheless, the rate of textile waste recycling is rather low at less than 20%; 95% of this waste material has recyclability potential [16]. The use of textile waste (TW, hereinafter) in cementitious composites as an alternative material for reinforcement is therefore a promising option for reusing this waste.

TW fibers can be made of natural or human-made fibers including cotton, silk, flax, polypropylene, nylon, and polyester, all of which have a lower elastic modulus than the matrix. According to several studies [17–22], TW fibers from polyester and nonwoven fabrics can be used as thermal and sound insulating elements. Moreover, lightweight bricks, cement blocks, and concrete partitions containing TW fiber, namely cotton, are already being produced [23–26]. In addition, textile effluent sludge is being reused in non-load-bearing concrete blocks [27].

Regarding the mechanical properties of TW fiber-reinforced concrete, some studies have investigated concrete reinforced with nylon or polypropylene fibers recycled from carpets [28]. In the literature, the engineering of concrete has, in most cases, enhanced properties such as tensile and flexural strength whilst others such as compressive strength, workability, and elastic modulus have declined [29–33]. The inclusion of recycled textile fibers was observed to influence the mechanical performance of concrete through a bridging action against crack propagation and redistribution of the porous matrix structure toward a more uniform structure [28, 34]. Nonetheless, the use of a high dosage of waste fibers leads to an agglomeration effect which, in turn, causes the formation of voids and entrapped air, thereby diminishing the concrete properties [35].

Furthermore, the effect of textile waste cuttings from garments on the mechanical properties of polymer concrete was investigated in [36]. The results showed that the addition of TW fibers, with lengths between 2 and 6 cm, eliminates the brittleness of unrein-forced polymer concrete, thereby leading to smoother failure, although no considerable enhancement in flexural and compressive resistance was observed.

It is widely believed that the incorporation of fibers can improve the shrinkage behavior of cementitious materials. Shrinkage cracks of restrained cementitious materials can be a problem in terms of aesthetics and durability since water, chlorides, and other harmful minerals could enter those cracks, causing early deterioration and damage. Thus, controlling shrinkage cracks is of paramount importance for improving the service life and for minimizing repair costs [37]. The majority of available research on the addition of vegetable or synthetic fibers suggests that they have a favorable effect on minimizing the plastic and autogenous shrinkage of cement composites [37–40].

However, the drying shrinkage of a fiber-reinforced cement-based composite has scarcely been reported, and the results are inconclusive. Toledo et al. [40] and Silva et al. [41] investigated the drying shrinkage of a matrix consisting of fine aggregate and supplementary cementitious materials reinforced with short and long sisal fibers. The conclusion was that the shrinkage increased with respect to the reference sample as the addition of vegetable fibers increased matrix porosity, thereby contributing to higher drying shrinkage of the composite. In other studies [42–44], it was reported that the addition of low contents of pulp and cellulose fiber could reduce drying shrinkage and thereby mitigate related cracking in the concrete. Moreover, Wang et al. [45] and Mohammadhosseini et al. [46] concluded that the inclusion of recycled polypropylene carpet fibers in concrete reduced the drying shrinkage of the control by up to 30% due to the interruption of moisture transfer from the internal microstructure of the cementitious matrix to the external environment.

According to our literature review, the mechanical properties of cement-based composites reinforced with short TW from garment resources of cotton and polyester have not been comprehensively investigated. Furthermore, research on nonwoven fabric in cementitious mortars as reinforcement remains scarce [8, 12,47] whilst the majority of studies cover other different woven textile forms including glass, carbon, and vegetal fabrics [48–57] as well as long fibers including sisal strands [58–60]. Nonetheless, all studies have concluded that TRMs with thin and lightweight composites have enhanced flexural, tensile, and strain-hardening behaviors.

In view of the abovementioned, two experimental programs were carried out to evaluate the properties of engineered TW-reinforced cement composites. One involved the use of a fraction of short randomly dispersed TW fiber in contents ranging from 6% to 10% by weight in cement [61], while the other was focused on textile lamination of nonwoven fabrics, ranging from 3 to 7 layers of this fiber [62]. The goal of this scientific contribution is to analyze and compare the results obtained from these experimental programs—including flexural resistance in pre-and post-crack, toughness, stiffness, durability, and shrinkage—to identify the most suitable composite for potential application in building construction.

2. Materials and Methods

2.1 Materials

A Portland cement type I 52.5R, with physical and chemical properties reported in [62] and supplied by Cementos Molins Industrial, S.A. (Spain), was used to produce the pastes in all samples.

TW short fibers from the waste of clothes were provided by Triturats La Canya S.A. (Spain) and consisted of almost 31% polyester and 69% cotton, two prevailing types of fiber in the global market. As reported in [61], the water retention value and the moisture content of the fiber were 85% and 7%, respectively. Furthermore, the majority of these short fibers have a diameter ranging from 3.6 to 32.1 µm, while the rest is a mix of yarns and fabrics.

As the production of nonwoven fabric from 100% TW fiber failed, those that were too short, longer flax fibers (F, hereinafter) with an average length of 60 mm, provided by Institut Wlokien Naturalnych (Poland), were mixed with TW fibers. Each TW nonwoven fabric (see Figure 1), with dimensions of 0.75 mm × 300 mm × 300 mm and an areal weight of 155 gr/m^2, was composed of 65% TW and 35% F fibers. Thus, the TW nonwoven fabric consisted of almost 80% vegetable fibers (35% Flax and 45% cotton) and 20% synthetic fiber. The production of nonwoven fabric including card clothing and needle-punching has been described in depth in [62]. Furthermore, the maximum tensile rupture load (per weight) of the TW nonwoven mats was reported as 2.0 N/gr.

Figure 1. (a) flax fiber; (b) textile waste fiber; (c) final nonwoven fabric.

2.2 Sample preparation

The FRM, a mortar reinforced with short TW fiber, was prepared in a laboratory mix-er pan and cast into a 20 mm × 40 mm × 160 mm mold in which 5 MPa pressure was applied for 24 hours to eliminate excess water. The TRM, a mortar reinforced with nonwoven textile, was prepared as plates of nonwoven layers impregnated with the cement paste placed cross-oriented in a mold with internal dimensions of 10 mm × 300 mm × 300 mm that underwent a homogeneous pressure of 3.3 MPa. The dewatering process for TRM plates includes vacuuming as well as compressing the mold for 24 hours. All samples of FRM and TRM were cured for 28 days at ambient temperature (20 °C) in a humidity chamber (approximately 95% of relative humidity). Figure 2 depicts the process of preparation and casting of both composites.

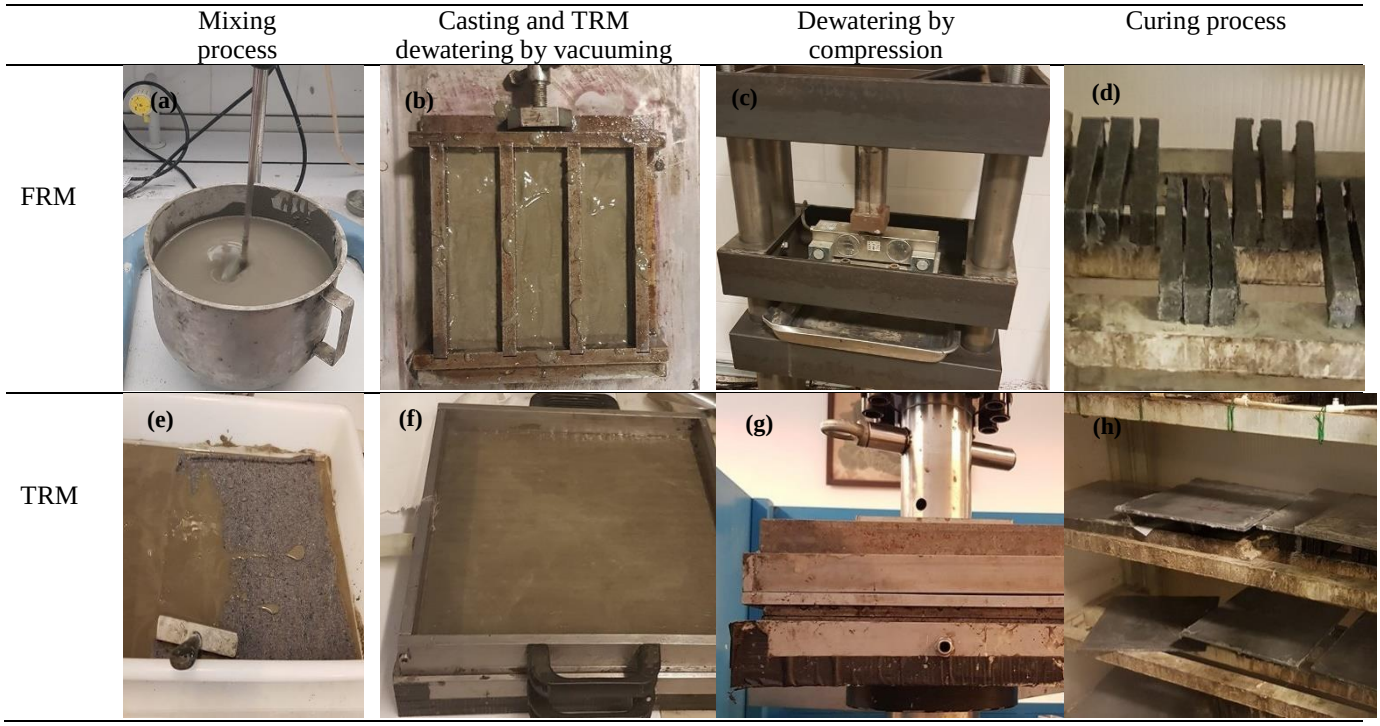

Figure 2. Preparation of the samples: (a) mixing process; (b) FRM casting; (c) dewatering of the FRM; (d) curing condition of the FRM; (e) impregnation of the nonwoven fabric with the paste; (f) TRM casting and vacuuming; (g) dewatering of the TRM; and (h) curing condition of the TRM plates.

The designation of the specimens (Table 1) is based on the fiber dosage of the cement weight for FRM, (6%, 8%, and 10%) and the number of reinforcement layers for TRM (3–7). The samples used for durability tests are those whose code ends in D. The final water/cement ratios (the final amount of water was calculated after weighing the amount of water eliminated by the dewatering treatment) together with the dosage of the materials—for FRM, it is related to making the mortar for 1000 cm^3—are also reported in Table 1. The initial water/cement ratio for preparing the paste was established as 1.0 and 0.5 for TRM and FRM, respectively. Six specimens were cast for each code of FRM, while from each plate of TRM, six specimens were machined.

Table 1. Physical properties of the composites.

	CODE	$(w/c)_{final}$	Cement [gr]	Fiber [gr]	Fiber weight fraction (%)	Thickness [mm]	Mortar/Fabric thickness	No. of specimens
	TW6	0.40	1600	96	6	20	-	6
FRM	**TW8**	0.50	1400	112	8	20	-	6
	TW10	0.50	1200	120	10	20	-	6
	TW8D	0.45	1400	112	8	20	-	6
	TW3L	0.40	1350	42	3.1	6.5	1.95	6
	TW4L	0.40	1500	56	3.7	8.5	1.83	6
TRM	**TW5L**	0.40	1530	70	4.9	9.2	1.48	6
	TW6L	0.40	1550	84	5.4	10.0	1.22	6
	TW7L	0.45	1600	98	6.1	10.2	0.92	6
	TW6LD	0.40	1474	84	5.7	10.0	1.22	12

2.3 Flexural tensile strength test and toughness

Three-point (3P) flexural tests based on EN 12467:2012 [63] (Figure 3a-c) using an INCOTECNIC press machine equipped with a load cell of 3 KN capacity and a loading rate of 4 mm/min on 100 mm span-length FRM specimens were carried out to identify the extent of the fiber's contribution to bridging cracks. On the other hand, the mechanical properties of the TRM composites were determined under a four-point (4P) bending test configuration (Figure 3d-f) following RILEM TFR1 and TFR 4 [64]. An Incotecnic press equipped with a maximum load cell of 3 KN with a crosshead speed of 20 mm/min with a major span (L) of 270 mm was used.

The maximum flexural tensile strengths (also named modulus of rupture, MOR) of the FRM and TRM composites were determined using Equations (1) and (2), respectively, where Pmax is the maximum load recorded, L is the span length, and b and h are the cross-sectional width and thickness, respectively.

$$MOR_{3P} = \frac{3P_{max}L}{2bh^2} \quad (1)$$

$$MOR_{4P} = \frac{P_{max}L}{bh^2} \quad (2)$$

The toughness index (I_G) was established as the reference parameter to characterize the type of failure (ductile or brittle) and the post-cracking deformation capacity. This parameter, based on the previously mentioned RILEM documents, is defined as the area beneath the force-displacement curve derived from the flexural test and values range from 0 to 0.4 MOR or the deformation value corresponding to 10% of the span, depending on which occurs first. For FRM samples, the limitation of 40% MOR dominated, while

for the TRM composites, the limitation of 10% of the displacement value (27 mm) occurred first. This method has previously been used in other studies [5, 12, 47, 62].

The flexural stiffness or modulus of elasticity in the pre-cracked zone (K) was also measured from the force-displacement relationships within the elastic regime using Equations (3) and (4) for FRM and TRM, respectively. In these equations, Δp and Δf are the variations in forces and deflections of two points on the linear-elastic state, and the rest of the parameters were already defined.

$$K_{3P} = \frac{\Delta P.\, L^3}{4\Delta f.\, bh^3} \quad (3)$$

$$K_{4P} = \frac{23\Delta P.\, L^3}{108\Delta f.\, bh^3} \quad (4)$$

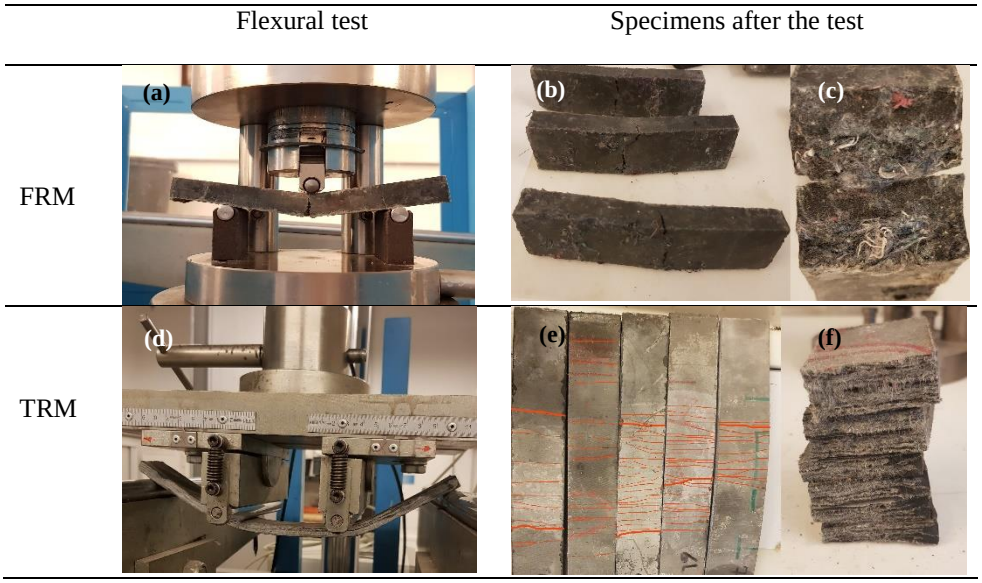

Figure 3. Flexural tests setup: (a) FRM three-point bending test; (b) cracks of FRM specimens; (c) cross-section of FRM specimens; (d) TRM four-point bending test; (e) cracks of TRM specimens; and (f) cross-section of TRM specimens.

2.4 Durability test and microscope analyses

Among the different durability tests, resistance against dry–wet cycles is considered a challenge for cement-based composites reinforced with vegetable fibers [62,63]. As the short TW fiber and the fabric form consisted of vegetable fiber, cotton, and flax, the durability of the composite subjected to accelerated aging was investigated. To this end, those composites provided better unaged mechanical properties subjected to 25 dry-wet cycles after 28 days of curing. Each dry–wet cycle consists of drying for 6 hours at 60 °C and 60% of RH followed by 18 hours of immersion in water at 20 °C according to EN 12467:2012. In fact, repeated wetting–drying cycles simulated natural weathering conditions and could allow for a rough estimate of the durability of the composites.

To analyze the fractured surface microstructure and the effects of the wetting–drying cycles, the observations were made from scanning electron microscope images.

2.5 Drying Shrinkage test

In this study, the free drying shrinkages of the reference sample— cement paste only, without any fiber— and the FRM and TRM samples were measured using a digital micrometer to monitor the change in length at room temperature (see Figure 4). The shrinkage measurement started after 28 days of curing until reaching the maximum value. The shrinkage in microstrain was computed using Equation (5), where ΔL_{sh} is the contraction of the length and L0 is the initial length of the specimen.

$$\varepsilon_{sh} = \frac{\Delta L_{sh}}{L_0} \times 10^6 \quad (5)$$

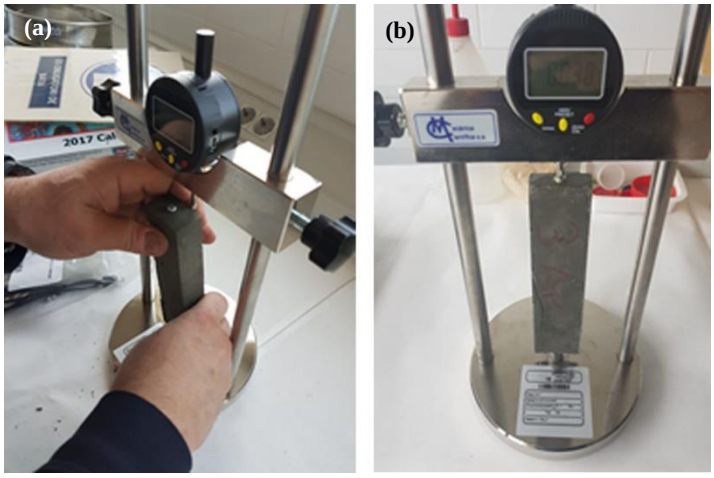

Figure 4. Shrinkage test: (a) shrinkage test setup; (b) monitoring the change in length.

3. Results and Discussions

3.1 Flexural test on unaged composites

On the one hand, the results depicted in Figure 5a suggest that TRM specimens show significantly greater post-failure energy absorption capacities under flexure with respect to FRM specimens due to the multiple cracking patterns generated in the former. The bending response of TRM specimens could be divided into four distinct branches: (1) A linearly ascending branch, in which the external load is mainly borne by the cement matrix until a visible crack in the cement matrix is formed when the LOP (limit of proportionality) for strength is reached. (2) Crack propagation occurs along with multiple cracking formations. In this transition zone, the matrix contributes to the composite's strength in non-cracked zones (tension stiffening) whilst the reinforcement's contribution dominates in the cracked zones. In the zones between cracks, the stress transfer mechanism is guaranteed by the reinforcement–matrix adhesion. (3) In another ascending branch (post-cracking), with the lowest slope due to degradation of the composites' stiffness, the fabric reinforcement bridges the cracks and bears the loads. No further new cracks occur in this zone, and the cracks grow only in width. (4) Finally, a failure occurs due to rupture or debonding of the fibers followed by further widening of the cracks, and, eventually, failure occurs due to the concentration of damage in a single crack.

On the other hand, the FRM specimens (Figures 5a,b) showed rather brittle responses once cracking began. In this regard, the bending response of FRM specimens could be divided into three distinct branches: (1) an elastic range for the pre-cracking zone, as observed in TRM; (2) a post-cracking regime with a reduced number of cracks (1–2) leading to a significantly smaller deformation capacity with respect to TRM; and (3) pre-and post-failure branches comprising less than 2 mm of deflection (from the cracking onset) and, hence, limiting both the ductility and energy absorption capacity and being insufficient for the majority of structural building applications.

According to the results presented in Table 2, the LOP of TRM samples was proven to be independent of the number of layers, while for the FRM composites, it can be concluded that crack flexural resistance decreased slightly with the addition of fiber. Thus, the FRM composite with 6% fiber had the highest LOP due to the lower w/c ratio and higher matrix volume (see Table 1). It must be remarked that the fibers in both types of composites slightly contribute to the flexural resistance throughout the pre-cracking stage given that the modulus of elasticity of the fibers is significantly lower (at least 10 times) than that of the matrix; however, the magnitude of the LOP is mainly governed by the strength of the matrix in each composite. Finally, it seems that the different distributions of the reinforcement—a homogenous fiber in FRM but a textile laminate in TRM—cause different stress distributions in the matrix, which, in turn, leads to higher LOP values for FRMs. Furthermore, it should be mentioned that the higher amount of vegetable fibers in the TRM samples can increase matrix porosity, which results in lower LOPs. Nonetheless, these partial conclusions regarding the magnitude of the LOP require more analysis and experimental evidence for confirmation.

On the other hand, the MOR values of TRM allow us to confirm that the addition of layers guaranteed a residual (post-cracking) flexural strength capacity, leading to a flexural hardening response of the composite ($MOR_m/LOP_m > 2.0$, see Table 2). Furthermore, the results suggest that the optimal number of layers might range from 5 to 6. A drop in the bearing capacity of the 7-layer laminate could be due to insufficient impregnation of the increased number of layers as well as ineffective layers above the neutral axis. In fact, fiber agglomeration due to a large amount of fabrics could weaken the interfacial transition zone within the matrix, making this area vulnerable to tension stresses, as reported in [67]. Furthermore, the use of 7-layer laminate with lower mortar/fabric thickness and higher $(w/c)_{final}$ (see Table 1) results in an unbalanced relationship between the amount of matrix and fabric which, in turn, reduces the LOP and the mechanical performance in the transition zone. It should be mentioned that laminates with 5–6 layers had the highest contribution to post flexural resistance and highest MOR_m/LOP_m.

Likewise, the addition of short TW fibers provides a post-cracking flexural strength capacity (MORm/LOPm > 1.0) to the FRM composite. In this sense, fibers can bridge the cracks by controlling the opening and by ensuring a stress transfer mechanism across the crack height. The results highlight that the TW6 and TW10 composites presented similar MORs while the TW8 composites presented a 6% higher MOR at 28 days of curing (see Figure 6). Hence, MOR increased with an increase in the fiber content by up to 8% but decreased for greater fiber amounts due to the technical difficulties associated with mixing, the balling effect, and compaction [5]. Similar results have been reported by Khorami et al. [68], in which the MOR of FRM reinforced by different amounts of waste kraft pulp fiber (1–14%) was investigated, for which it was shown that 8% fiber had the highest bending resistance. Nevertheless, although this material shows signs of post-cracking strength, its ductility and energy absorption capacity are limited and, hence only nonstructural applications can be considered for this material.

Regarding toughness (I_{Gm}), this parameter follows a similar tendency in TRM with respect to that obtained for MOR_m, i.e., it was found that I_{Gm} reached a maximum for an optimal number of 6 layers, with 148% higher values than TW3L. However, in FRM, the results presented an increase in I_{Gm} with fiber

dosage, with TW10 having the higher energy absorption (56% higher values than TW6). As shown in Figure 7, the toughness index of all TRM composites had a greater value than that of the FRM due to the formation of multiple cracking; for instance, TW6L had more than four times greater energy absorption than TW8. Hence, the previous statement regarding the potential structural and nonstructural applicability of both materials is further reinforced by these results.

Finally, and only as a reference, the flexural stiffness of the pre-cracked zone (K_m) was computed to quantify the deformability in the linear stages. The K parameter remained almost constant for the FRM samples, decreasing by only 5% with the increase in fiber content, while in TRM composites, this parameter is rather independent of the number of layers and follows the same trend as LOP. The reinforcement in a nonwoven fabric form was proven to have a higher stiffness with respect to the short fibers as K was more than twofold greater in TRM samples.

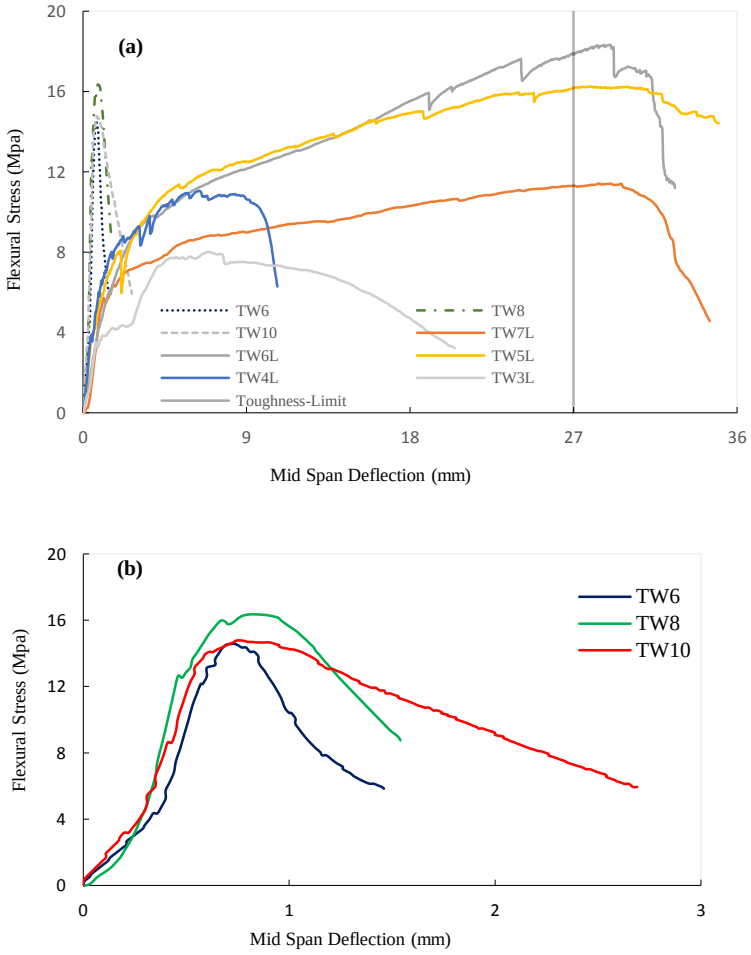

Figure 5. Representative flexural stress: deflection relationships obtained at 28 days for (a) all samples and (b) FRM samples.

Table 2. Results of all of the TW composites at 28 days (CoV in %).

	CODE	LOP_m [N/mm2]	MOR_m [N/mm2]	I_{Gm} [KJ/m2]	K_m [GPa]	MOR_m/LOP_m
TRM	TW3L	4.1 (29)	8.1 (14)	3.9 (28)	8.7 (17)	2.0
	TW4L	4.5 (24)	12.4 (14)	7.0 (24)	10.7 (14)	2.8
	TW5L	4.1 (24)	13.9 (13)	8.5 (7)	7.8 (26)	3.4
	TW6L	4.6 (19)	15.5 (12)	9.7 (12)	11.3 (21)	3.4
	TW7L	4.2 (12)	12.1 (12)	9.4 (8)	10.6 (21)	2.8
FRM	TW6	12.7 (12)	14.7 (9)	1.6 (31)	4.0 (19)	1.1
	TW8	11.1 (10)	15.6 (20)	2.1 (19)	3.9 (15)	1.4
	TW10	10.7 (10)	14.9 (23)	2.5 (24)	3.7 (19)	1.4

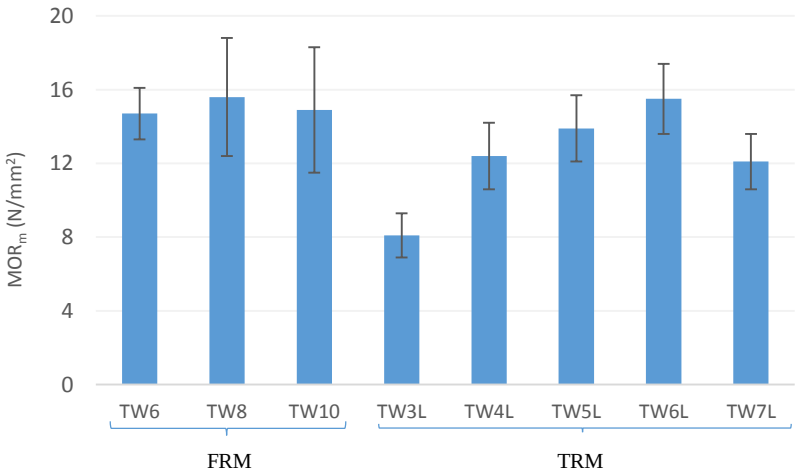

Figure 6. Results of MORm for the tested

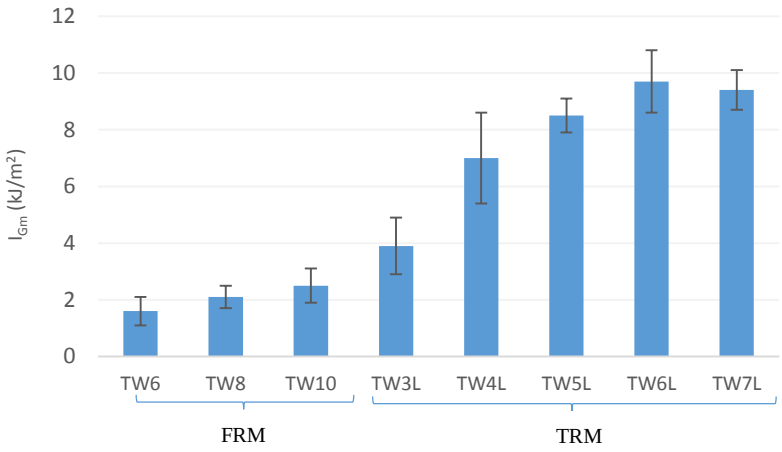

Figure 7. Results of IGm for the tested composites.

Overall, in the unaged samples, TW8 and TW6L had superior mechanical properties among FRMs and TRMs, respectively. Consequently, the accelerated aging cycles were carried out on these composites to identify and quantify the damage and strength degradation of both FRM and TRM composites.

3.2 Flexural test on aged composites

The results presented in Figure 8 and Table 3 allow us to confirm that the accelerated aging procedure negatively affected the post-cracking mechanical properties of the composites compared to those that are unaged. As expected, there was a loss of bending resistance in the composites after aging. In the textile laminate, the reduction of MOR* was about 35% (from 15.5 to 10 MPa), while this reduction was only 3% (from 15.6 to 15.2 MPa) for short reinforcement. Likewise, the reduction in the reinforcement contribution was 21% and 42% for FRM and TRM, respectively, though the TW6LD still had a higher reinforcement contribution. It should be also mentioned that the TW short fibers were only made of cotton and polyester while TW fabric also contained flax. Thus, the amount of synthetic fiber—which is more durable than vegetable-based fibers—in short reinforcement exceeded that of fabric fibers. When the fiber-reinforced composite was subjected to various wet-dry cycles the fibers, mainly those based on vegetable fibers, lost adherence to the matrix due to reprecipitation of the hydrated compounds within the void space at the fiber–cement interface. Finally, full mineralization occurred, resulting in embrittlement of the vegetable fibers [65].

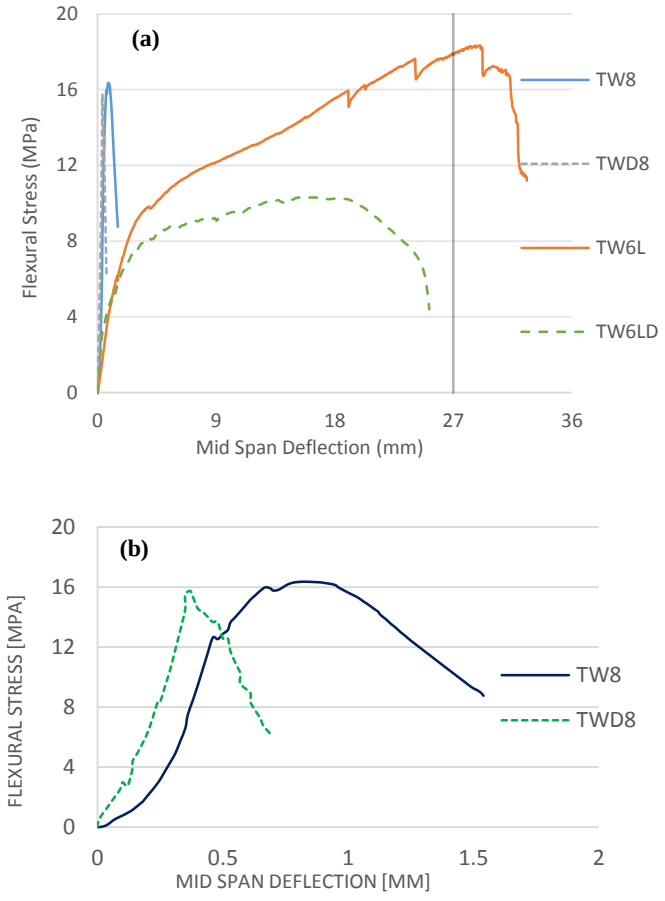

Figure 8. Representative flexural stress: deflection relationships obtained for aged samples for (a) all samples and (b) the FRM samples.

Table 3. Test results on the aged composites (CoV in %).

Samples	LOPm* [N/mm^2]	MORm* [N/mm^2]	IGm* [KJ/m^2]	Km* [GPa]	MORm*/LOPm*
TW8D (FRM)	13.3 (11)	15.2 (10)	1.2 (21)	4.0 (17)	1.10
TW6LD (TRM)	5.1 (31)	10.0 (27)	6.8 (33)	12.0 (5)	1.96

The reduction in toughness and energy absorption is considered one of the key matters of durability. This issue is related to an increase in fiber rupture and a decrease in fiber pull-out strength due to a combination of the weakening of the fibers by an alkali attack, fiber mineralization, and volume variation due to the high water absorption of fibers. In this regard, the FRM and TRM samples experienced 42% and 30% I_{Gm}* reductions, respectively. Nonetheless, due to the longer fiber length and more contact with the cement paste, the TRM sample could still develop a flexural hardening response with multiple cracking though the slope of this zone was less than the corresponding unaged ones, demonstrating the loss in fiber stiffness due to degradation.

Finally, the elastic pre-cracking properties (LOP* and K*) presented averagely unaltered or even higher values due to further cement hydration as these are mainly dependent on the matrix, which is slightly affected by the aging procedure. Similar results have been reported by Claramunt et al. [69].

3.3 SEM observations

The loss of mechanical properties of the aged composites, mainly in absorbed energy and toughness, occurred due to the loss of adhesion and degradation of the vegetable fiber, as already explained. Both phenomena are more critical in the FRM than in the TRM due to the different distributions of the fibers. In the microimages of Figure 9 comparing the samples TW8 (Figure 9a) and TW8D (Figure 9b), the length of the fibers in the former are seen to be somewhat longer than those of the latter since most of the fibers in the aged samples were cut near the surface due to rupture. Therefore, the longer fibers generate more energy loss than the shorter ones through the pull-out mechanism of the fiber–cement interactions. Moreover, in Figure 9c,d, you can see the differences between the fibers plucked from the unaged samples and the split fibers, indicated with a yellow circle, from the aged samples. Therefore, the wet-dry cycles induced the damage, leading to an increase in the number of fibers failing due to rupture, thereby decreasing the fiber's pull-out.

Nonetheless, regarding the TRM samples (see Figure 9e,f), the difference between the aged and unaged composite was insignificant since even after the accelerated aging, although properties are lost, a certain reinforcement effect is still maintained, which prevents breakage of the sample due to brittleness (see Figure 8a). Furthermore, longer fibers and the protrusion of a large set of fibers from the cement matrix were evident in TRM images with respect to FRM images. In fact, the fibers were dispersed randomly but homogeneously in the section of FRMs, while in the TRMs, the fibers were grouped in layers parallel to the surface, where a higher reinforcement density was obtained, which allowed for greater mechanical properties, mainly better energy absorption and toughness, of this type of composite.

In general, fibers in the unaged composites had clean surfaces whilst those in the aged composites appeared rougher and surrounded by precipitation products. In Figure 10a depicting the fibers from the broken section of unaged conditions, a set of synthetic fibers (S) can be observed that are clearly distinguished by their almost cylindrical shape, with some extrusion marks as indicated by a yellow circle. A vegetable fiber (V) is also distinguished by being more oblong due to its more irregular and hollow section. After the accelerated aging procedure, Figure 10b, we observed that the synthetic fiber (S) seems to have greater durability since the surface does not appear to have been affected and only some cement

hydration products appear. By contrast, in the vegetable fiber (V), some type of damage with superficial cracks appears, indicated by green arrows. Figure 10c shows the surface roughness caused by the accelerated aging treatment in detail.

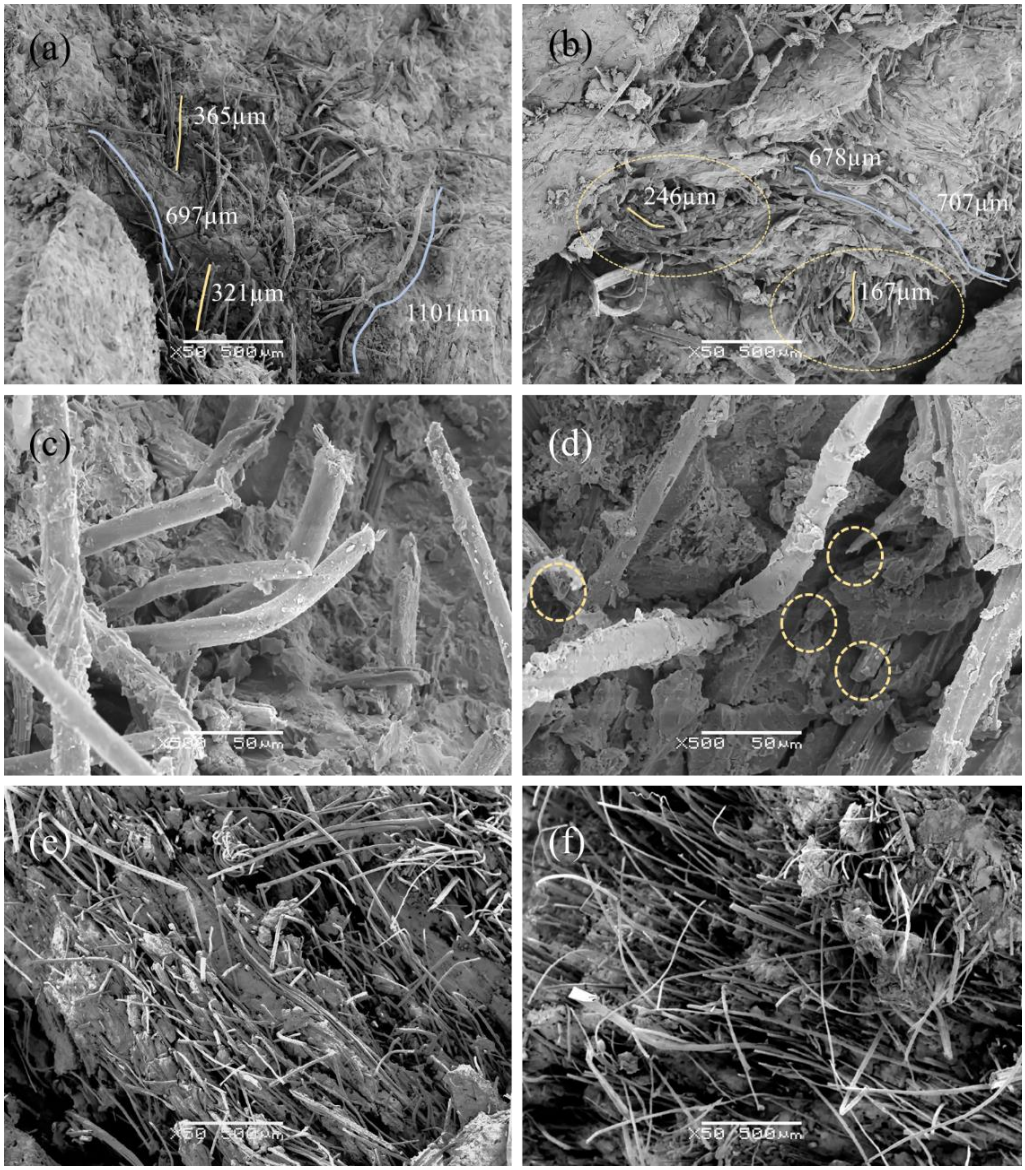

Figure 9. SEM micrographs of the fracture surfaces of the composites: (a) TW8; (b) TW8D; (c) TW8; (d) TW8D; (e) TW6L; and (f) TW6LD.

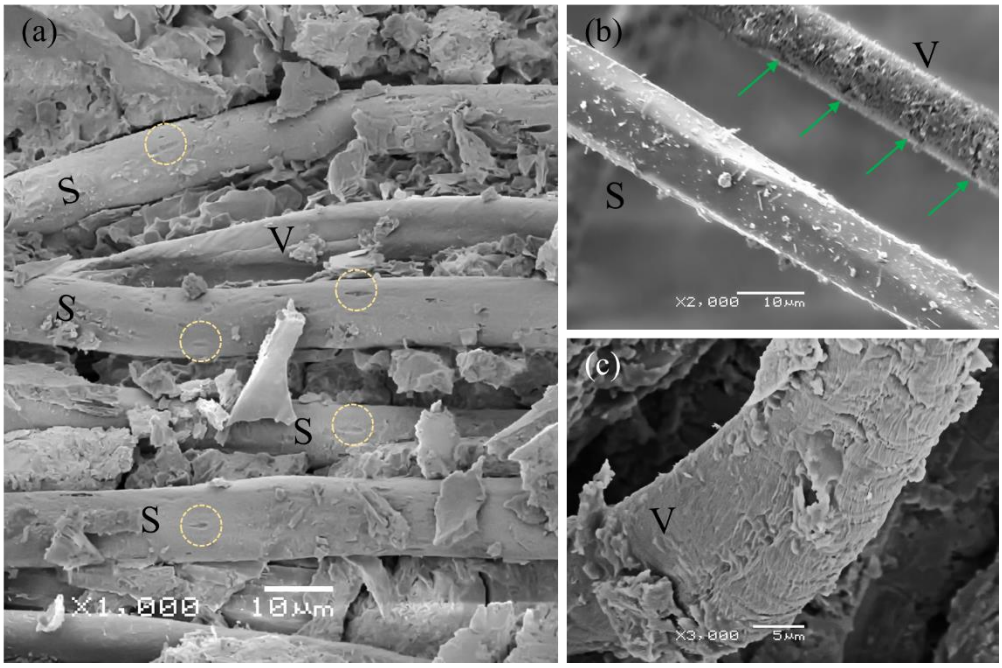

Figure 10. SEM micrographs of the fiber surfaces: (a) fibers from the broken section of unaged samples; (b,c) fibers from the broken section of aged samples.

3.4 Shrinkage

As can be seen in Table 4, the reference sample had the highest shrinkage strain. In general, hardened cement paste undergoes high drying shrinkage with respect to concrete or mortar as the changes in the volume of the latter are largely restrained by the rigidity of the aggregates [70]. In both types of reinforced composites, the incorporation of fibers leads to a decrease in the amount of shrinkage. For instance, TW8 and TW6L could reduce the shrinkage of the paste by 44% and 30%, respectively. It seems the higher percentage of vegetable fibers in textile reinforcement with respect to the short random reinforcement (almost 10%) causes an increase in the matrix porosity, which leads to a higher drying shrinkage due to the higher water absorption.

Table 4. Results for shrinkage strain of tested samples.

Samples	Reference	TW6	TW8	TW10	TW3L	TW6L
Shrinkage (Microstrain)	2560	1490	1420	1370	2550	1870
Time (Days)	160	56	56	56	84	84

4. Conclusions

The objective of this paper was to compare the mechanical performance of two types of cement composites reinforced by two forms of textile waste, either short random fibers or nonwoven fabrics. To identify potential applications of the resulting materials, the mechanical and durability properties of both FRM, composites with three different dosages of short fibers (6–10%), and TRM, laminates with 3–7 layers,

were characterized. The following conclusions were derived from the results and may be limited to the scope of the current study:

- The pre-cracking flexural performance of both unaged 6-layer nonwoven TRM and FRM with 8% of fibers are comparable. However, the post-cracking flexural performance and especially the energy absorption capacity of the former are significantly superior (by four times) with respect to the latter. The results suggest that randomly distributed short fibers from textile waste have limitations in terms of mechanical performance due to the limited cracking capacity and maximum mixable amount of these fibers.

- Both composites were subjected to an accelerated aging process that primarily affected the energy absorption of the materials. Nonetheless, the toughness and the stiffness of the aged TRM were greater (three times) than the FRM. The SEM observations confirmed that accelerated aging is associated with an increase in fiber fracture and a decrease in fiber pull-out, especially in vegetable fibers, due to the alkali attack. Nonetheless, modifying the matrix with pozzolanic materials such as silica fume could improve the durability of this composite.

Finally, the results for the 6-layer TRM panel as the most prominent TW composite—showing a flexural strength of 15.5 MPa and a toughness of 9.7 KJ/m^2—demonstrate that the application of this type of waste is technically feasible and could be potentially used for reinforcement of nonstructural constructs (e.g., façade panels, roofing, raised floors, and masonry structures). The application of the 6-layer TRM panel as a façade cladding is currently under investigation due to its potential benefits in terms of sustainability (cost and environmental and social impacts).

We highlight that these results and conclusions are preliminary and incipient since the experimental program is in its early stages. The increase in the statistical population of the experimental results is expected to shed more light on and reinforce some of the preliminary conclusions stated herein.

Author Contributions: Conceptualization: Josep Claramunt, Mònica Ardanuy, and Albert de la Fuente; methodology: Payam Sadrolodabaee and Josep Claramunt; validation: Josep Claramunt, Mònica Ardanuy, and Albert de la Fuente; formal analysis: Payam Sadrolodabaee and Josep Claramunt; investigation: Payam Sadrolodabaee, Josep Claramunt, and Mònica Ardanuy; data curation: Josep Claramunt and Albert de la Fuente; writing—original draft preparation, Payam Sadrolodabaee; writing—review and editing, Josep Claramunt, Mònica Ardanuy, and Albert de la Fuente; visualization: Payam Sadrolodabaee.; supervision, Josep Claramunt and Albert de la Fuente; funding acquisition: Josep Claramunt, Mònica Ardanuy, and Albert de la Fuente. All authors have read and agreed to the published version of the manuscript.

Funding: This research was funded by the Spanish Ministry of Economy, Industry, and Competitiveness, RECYBUILDMAT (PID2019-108067RB-I00), and CREEF (PID2019-108978RB-C32).

Institutional Review Board Statement: Not applicable.

Informed Consent Statement: Not applicable.

Data Availability Statement: The data presented in this study are available upon request from the corresponding author.

Conflicts of Interest: The authors declare no conflicts of interest.

References

[1] D. Kvočka et al., “Life cycle assessment of prefabricated geopolymeric façade cladding panels made from large fractions of recycled construction and demolition waste,” Materials (Basel)., vol.

13, no. 18, 2020.

[2] A. F. Abd Rashid and S. Yusoff, "A review of life cycle assessment method for building industry," Renewable and Sustainable Energy Reviews, vol. 45. Elsevier Ltd, pp. 244–248, 01-May-2015.

[3] B. Ütebay, P. Çelik, and A. Çay, "Textile Wastes: Status and Perspectives," in Waste in Textile and Leather Sectors, IntechOpen, 2020.

[4] H. Nautiyal, V. Shree, S. Khurana, N. Kumar, and Varun, "Recycling Potential of Building Materials: A Review," Springer, Singapore, 2015, pp. 31–50.

[5] M. Ardanuy, J. Claramunt, and R. D. Toledo Filho, "Cellulosic fiber reinforced cement-based composites: A review of recent research," Constr. Build. Mater., vol. 79, pp. 115–128, 2015.

[6] F. de A. Silva, B. Mobasher, and R. D. T. Filho, "Cracking mechanisms in durable sisal fiber reinforced cement composites," Cem. Concr. Compos., vol. 31, no. 10, pp. 721–730, 2009.

[7] B. Torres, S. Ivorra, F. Javier Baeza, L. Estevan, and B. Varona, "Textile reinforced mortars (TRM) for repairing and retrofitting masonry walls subjected to in-plane cyclic loads. An experimental approach," Eng. Struct., vol. 231, no. November 2020, 2021.

[8] L. Gonzalez-Lopez, J. Claramunt, Y. Lo Hsieh, H. Ventura, and M. Ardanuy, "Surface modification of flax nonwovens for the development of sustainable, high performance, and durable calcium aluminate cement composites," Compos. Part B Eng., vol. 191, no. February, 2020.

[9] F. Pacheco-Torgal and S. Jalali, "Cementitious building materials reinforced with vegetable fibres: A review," Constr. Build. Mater., vol. 25, no. 2, pp. 575–581, 2011.

[10] G. Ferrara, C. Caggegi, E. Martinelli, and A. Gabor, "Shear capacity of masonry walls externally strengthened using Flax-TRM composite systems: experimental tests and comparative assessment," Constr. Build. Mater., vol. 261, 2020.

[11] C. Correia, S. Francisco, H. Savastano, and V. Moacyr, "Utilization of vegetal fibers for production of reinforced cementitious materials," no. 2017, 2018.

[12] M. Ramirez, J. Claramunt, H. Ventura, and M. Ardanuy, "Evaluation of the mechanical performance and durability of binary blended CAC-MK/natural fiber composites," Constr. Build. Mater., vol. In progres, 2019.

[13] L. Mercedes, L. Gil, and E. Bernat-maso, "Mechanical performance of vegetal fabric reinforced cementitious matrix (FRCM) composites," Constr. Build. Mater., vol. 175, pp. 161–173, 2018.

[14] A. Villanueva, L. Delgado, Z. Luo, P. Eder, A. Sofia Catarino, and D. Litten, "Study on the selection of waste streams for end-of-waste assessment. Final Report."

[15] J. J. Lu and H. Hamouda, "Current status of fiber waste recycling and its future," in Advanced Materials Research, 2014, vol. 878, pp. 122–131.

[16] "The limitations of textile recycling - recovery." [Online]. Available: https://www.recovery-worldwide.com/en/artikel/the-limitations-of-textile-recycling_3411757.html. [Accessed: 15-Jan-2021].

[17] A. Briga-Sá et al., "Textile waste as an alternative thermal insulation building material solution," Constr. Build. Mater., vol. 38, pp. 155–160, 2013.

[18] X. Zhou, F. Zheng, H. Li, and C. Lu, "An environment-friendly thermal insulation material from cotton stalk fibers," Energy Build., vol. 42, no. 7, pp. 1070–1074, Jul. 2010.

[19] M. El Wazna, M. El Fatihi, A. El Bouari, and O. Cherkaoui, "Thermo physical characterization of sustainable insulation materials made from textile waste," J. Build. Eng., vol. 12, pp. 196–201, Jul. 2017.

[20] A. Paiva, H. Varum, F. Caldeira, A. Sá, D. Nascimento, and N. Teixeira, "Textile Subwaste as a Thermal Insulation Building Material."

[21] Y. Lee and C. Joo, "Sound absorption properties of recycled polyester fibrous assembly absorbers," Autex Res. J., vol. 3, no. 2, pp. 78–84, 2003.

[22] A.-E. Tiuc, H. Vermeşan, T. Gabor, and O. Vasile, "Improved Sound Absorption Properties of Polyurethane Foam Mixed with Textile Waste," Energy Procedia, vol. 85, pp. 559–565, Jan. 2016.

[23] D. Rajput, S. S. Bhagade, S. P. Raut, R. V. Ralegaonkar, and S. A. Mandavgane, "Reuse of cotton and recycle paper mill waste as building material," Constr. Build. Mater., vol. 34, pp. 470–475, Sep. 2012.

[24] H. Binici, R. Gemci, O. Aksogan, and H. Kaplan, "Insulation properties of bricks made with cotton and textile ash wastes," Int. J. Mater. Res., vol. 101, no. 7, pp. 894–899, Jul. 2010.

[25] F. F. Aspiras and J. R. I. Manalo, "Utilization of textile waste cuttings as building material," J. Mater. Process. Technol., vol. 48, no. 1–4, pp. 379–384, Jan. 1995.

[26] K. Aghaee and M. Foroughi, "Mechanical properties of lightweight concrete partition with a core of textile waste," Adv. Civ. Eng., vol. 2013, 2013.

[27] B. J. Zhan and C. S. Poon, "Study on feasibility of reutilizing textile effluent sludge for producing concrete blocks," J. Clean. Prod., vol. 101, pp. 174–179, Aug. 2015.

[28] N. P. Tran, C. Gunasekara, D. W. Law, S. Houshyar, S. Setunge, and A. Cwirzen, "Comprehensive review on sustainable fiber reinforced concrete incorporating recycled textile waste," J. Sustain. Cem. Mater., vol. 0, no. 0, pp. 1–22, 2021.

[29] H. Mohammadhosseini, M. M. Tahir, A. R. Mohd Sam, N. H. Abdul Shukor Lim, and M. Samadi, "Enhanced performance for aggressive environments of green concrete composites reinforced with waste carpet fibers and palm oil fuel ash," J. Clean. Prod., vol. 185, pp. 252–265, Jun. 2018.

[30] "STRENGTH, MODULUS OF ELASTICITY AND SHRINKAGE BEHAVIOUR OF CONCRETE CONTAINING WASTE CARPET FIBER | International Journal of GEOMATE." [Online]. Available: https://www.geomatejournal.com/node/288. [Accessed: 31-May-2021].

[31] W. Xuan, X. Chen, G. Yang, F. Dai, and Y. Chen, "Impact behavior and microstructure of cement mortar incorporating waste carpet fibers after exposure to high temperatures," J. Clean. Prod., vol. 187, pp. 222–236, Jun. 2018.

[32] H. Mohammadhosseini, A. S. M. Abdul Awal, and J. B. Mohd Yatim, "The impact resistance and mechanical properties of concrete reinforced with waste polypropylene carpet fibres," Constr. Build. Mater., vol. 143, pp. 147–157, Jul. 2017.

[33] Y. Wang, H. C. Wu, and V. C. Li, "Concrete Reinforcement with Recycled Fibers," J. Mater. Civ. Eng., vol. 12, no. 4, pp. 314–319, Nov. 2000.

[34] X. Wu, J. Zhou, T. Kang, F. Wang, X. Ding, and S. Wang, "Laboratory investigation on the shrinkage cracking of waste fiber-reinforced recycled aggregate concrete," Materials (Basel)., vol. 12, no. 8, 2019.

[35] M. S. Meddah and M. Bencheikh, "Properties of concrete reinforced with different kinds of

industrial waste fibre materials," Constr. Build. Mater., vol. 23, no. 10, pp. 3196–3205, Oct. 2009.

[36] J. M. L. dos Reis, "Effect of textile waste on the mechanical properties of polymer concrete," Mater. Res., vol. 12, no. 1, pp. 63–67, 2009.

[37] E. Booya, K. Gorospe, H. Ghaednia, and S. Das, "Free and restrained plastic shrinkage of cementitious materials made of engineered kraft pulp fibres," Constr. Build. Mater., vol. 212, pp. 236–246, Jul. 2019.

[38] P. Soroushian and S. Ravanbakhsh, "Control of plastic shrinkage cracking with specialty cellulose fibers," ACI Mater. J., vol. 95, no. 4, pp. 429–435, Jul. 1998.

[39] P. Jongvisuttisun and K. E. Kurtis, "The role of hardwood pulp fibers in mitigation of early-age cracking," Cem. Concr. Compos., vol. 57, pp. 84–93, Mar. 2015.

[40] R. D. Toledo Filho, K. Ghavami, M. A. Sanjuán, and G. L. England, "Free, restrained and drying shrinkage of cement mortar composites reinforced with vegetable fibres," Cem. Concr. Compos., vol. 27, no. 5, pp. 537–546, 2005.

[41] F. D. A. Silva, R. D. T. Filho, J. D. A. M. Filho, and E. D. M. R. Fairbairn, "Physical and mechanical properties of durable sisal fiber–cement composites," Constr. Build. Mater., vol. 24, no. 5, pp. 777–785, May 2010.

[42] E. Booya, K. Gorospe, A. Adesina, and S. Das, "PERMEABILITY CHARACTERISTICS OF CEMENTITIOUS MATERIALS REINFORCED WITH KRAFT PULP FIBRES," pp. 1–7, 2019.

[43] E. Booya, H. Ghaednia, S. Das, and H. Pande, "Durability of cementitious materials reinforced with various Kraft pulp fibers," Constr. Build. Mater., vol. 191, pp. 1191–1200, Dec. 2018.

[44] S. Kawashima and S. P. Shah, "Early-age autogenous and drying shrinkage behavior of cellulose fiber-reinforced cementitious materials," Cem. Concr. Compos., vol. 33, no. 2, pp. 201–208, 2011.

[45] Y. Wang, A. H. Zureick, B. S. Cho, and D. E. Scott, "Properties of fibre reinforced concrete using recycled fibres from carpet industrial waste," J. Mater. Sci., vol. 29, no. 16, pp. 4191–4199, Jan. 1994.

[46] H. Mohammadhosseini, R. Alyousef, N. H. Abdul Shukor Lim, M. M. Tahir, H. Alabduljabbar, and A. M. Mohamed, "Creep and drying shrinkage performance of concrete composite comprising waste polypropylene carpet fibres and palm oil fuel ash," J. Build. Eng., vol. 30, p. 101250, Jul. 2020.

[47] J. Claramunt, H. Ventura, L. J. Fernández-carrasco, and M. Ardanuy, "Tensile and Flexural Properties of Cement Composites Reinforced with Flax Nonwoven Fabrics," Materials (Basel)., pp. 1–12, 2017.

[48] M. C. Rampini, G. Zani, M. Colombo, and M. Prisco, "applied sciences Mechanical Behaviour of TRC Composites : Experimental and Analytical Approaches," 2019.

[49] I. Colombo, M. Colombo, A. Magri, G. Zani, and M. Di Prisco, "Textile reinforced mortar at high temperatures," Appl. Mech. Mater., vol. 82, no. July, pp. 202–207, 2011.

[50] C. Paper, I. G. Colombo, M. Colombo, A. Magri, and G. Zani, "Tensile Behavior of Textile : Influence of Multilayer Reinforcement Tensile behaviour of Textile : influence of multilayer reinforcement," no. May 2014, 2011.

[51] G. Zani, M. Colombo, and M. Di Prisco, "High performance cementitious composites for sustainable roofing panels," Proc. 10th fib Int. PhD Symp. Civ. Eng., no. February 2015, pp. 333–

338, 2014.

[52] M. Saidi and A. Gabor, "Experimental measurement of load-transfer length in textile-reinforced cementitious matrix composites using distributed optical fibres," Eur. J. Environ. Civ. Eng., vol. 0, no. 0, pp. 1–19, 2020.

[53] L. Mercedes, E. Bernat-Maso, and L. Gil, "In-plane cyclic loading of masonry walls strengthened by vegetal-fabric-reinforced cementitious matrix (FRCM) composites," Eng. Struct., vol. 221, p. 111097, Oct. 2020.

[54] G. Ferrara, "Mechanical Behaviour and Durability of Flax Textiles to Be Used as Reinforcement in TRMs," Springer, Cham, 2021, pp. 47–73.

[55] G. Ferrara, M. Pepe, E. Martinelli, and R. D. Tolêdo Filho, "Tensile behavior of flax textile reinforced lime-mortar: Influence of reinforcement amount and textile impregnation," Cem. Concr. Compos., vol. 119, p. 103984, May 2021.

[56] M. E. A. Fidelis, R. D. Toledo Filho, F. de A. Silva, V. Mechtcherine, M. Butler, and S. Hempel, "The effect of accelerated aging on the interface of jute textile reinforced concrete," Cem. Concr. Compos., vol. 74, pp. 7–15, Nov. 2016.

[57] C. Caggegi, E. Lanoye, K. Djama, A. Bassil, and A. Gabor, "Tensile behaviour of a basalt TRM strengthening system: Influence of mortar and reinforcing textile ratios," Compos. Part B Eng., vol. 130, pp. 90–102, 2017.

[58] R. D. Toledo Filho, F. de A. Silva, E. M. R. Fairbairn, and J. de A. M. Filho, "Durability of compression molded sisal fiber reinforced mortar laminates," Constr. Build. Mater., vol. 23, no. 6, pp. 2409–2420, Jun. 2009.

[59] F. de Andrade Silva, B. Mobasher, and R. D. T. Filho, "Fatigue behavior of sisal fiber reinforced cement composites," Mater. Sci. Eng. A, vol. 527, no. 21–22, pp. 5507–5513, Aug. 2010.

[60] F. de A. Silva, D. Zhu, B. Mobasher, C. Soranakom, and R. D. Toledo Filho, "High speed tensile behavior of sisal fiber cement composites," Mater. Sci. Eng. A, vol. 527, no. 3, pp. 544–552, Jan. 2010.

[61] P. Sadrolodabaee, J. Claramunt, M. Ardanuy, and A. de la Fuente, "Mechanical and durability characterization of a new textile waste micro-fiber reinforced cement composite for building applications," Case Stud. Constr. Mater., vol. 14, p. e00492, Jun. 2021.

[62] P. Sadrolodabaee, J. Claramunt, M. Ardanuy, and A. de la Fuente, "Characterization of a textile waste nonwoven fabric reinforced cement composite for non-structural building components," Constr. Build. Mater., vol. 276, p. 122179, Mar. 2021.

[63] BS EN 494-12, "Fibre-cement flat sheets - Product specification and test methods," Br. Stand. Inst., p. 60, 2012.

[64] "RILEM - Publications." [Online]. Available: https://www.rilem.net/publication/publication/4?id_papier=4003. [Accessed: 04-Sep-2020].

[65] J. Claramunt, M. Ardanuy, J. A. García-Hortal, and R. D. T. Filho, "The hornification of vegetable fibers to improve the durability of cement mortar composites," Cem. Concr. Compos., vol. 33, no. 5, pp. 586–595, 2011.

[66] M. Ardanuy, J. Claramunt, J. A. García-Hortal, and M. Barra, "Fiber-matrix interactions in cement mortar composites reinforced with cellulosic fibers," Cellulose, vol. 18, no. 2, pp. 281–289, Apr. 2011.

[67] S. A. Zareei, F. Ameri, N. Bahrami, P. Shoaei, H. R. Musaeei, and F. Nurian, "Green high strength concrete containing recycled waste ceramic aggregates and waste carpet fibers: Mechanical, durability, and microstructural properties," J. Build. Eng., vol. 26, p. 100914, Nov. 2019.

[68] M. Khorami and E. Ganjian, "The effect of limestone powder, silica fume and fibre content on flexural behaviour of cement composite reinforced by waste Kraft pulp," Constr. Build. Mater., vol. 46, pp. 142–149, 2013.

[69] J. Claramunt, L. Fernández-Carrasco, H. Ventura, and M. Ardanuy, "Natural fiber nonwoven reinforced cement composites as sustainable materials for building envelopes," Constr. Build. Mater., vol. 115, pp. 230–239, 2016.

[70] J. Zhang and V. Li, "Influences of Fibers on Drying Shrinkage of Fiber-Reinforced Cementitious I NFLUENCES OF F IBERS ON D RYING S HRINKAGE OF F IBER -R EINFORCED C EMENTITIOUS C OMPOSITE," vol. 9399, no. February 2015, 2001.

2.4 Journal paper IV:

Experimental Characterization of Comfort Performance Parameters and Multi-Criteria Sustainability Assessment of Recycled Textile-Reinforced Cement Facade Cladding

Published in Journal of Cleaner Production 356 (2022) 131900

Payam Sadrolodabaee[a] (payam.sadrolodabaee@upc.edu), S.M.Amin Hosseini [b] (amin@resumetec.com), Josep Claramunt[c] (josep.claramunt@upc.edu), Mònica Ardanuy[d](monica.ardanuy@upc.edu), Laia Haurie[e](laia.haurie@upc.edu), Ana M. Lacasta[e](ana.maria.lacasta@upc.edu), and Albert de la Fuente[a] *(albert.de.la.fuente@upc.edu)

a: Department of Civil and Environmental Engineering- Polytechnic University of Catalonia (UPC) - Barcelona, Spain.
b: RESUME TECH- Barcelona, Spain
c: Department of Agri-Food Engineering and Biotechnology - Polytechnic University of Catalonia (UPC) - Barcelona, Spain.
d: Department of Materials Science and Engineering - Polytechnic University of Catalonia (UPC) - Barcelona, Spain.
e: Department of Building Construction and Architecture - Polytechnic University of Catalonia (UPC) - Barcelona, Spain.

*: Corresponding author

Abstract

Within the building construction sector, fiber cement boards have attracted interest as facade cladding materials in the last ten years, especially those that incorporate –for reinforcing purposes– natural and/or recycled synthetic fibers (i.e, from the textile industry). So far, the design-governing parameters of facade cladding panels have been mechanical strength, durability, constructability, aesthetics, insulation capacity, and fire resistance. From the sustainability perspective, the impact of the facade on the economic and energy efficiency performance is most often the parameter that leads the decision-making process. Within this context, the quantification of the sustainability performance of the facade –accounting for economic, environmental, and social indicators– is unfrequently carried out in design and project phases, this being attributed to the lack of methodologies that allow considering and quantifying some relevant indicators representative of the facade sustainability performance. As consequence, decisions made based on solely economic and on some of the environmental indicators might lead to solutions with lower sustainability performance than that required (or expected). Recycled textile waste fabric-reinforced cement board as a facade-cladding material for building envelopes is the focus of this research. In order to characterize the fire resistance, and thermal and acoustic insulation –as relevant serviceability parameters– of this material, an experimental program was carried out. Likewise, the sustainability performance of this facade cladding is assessed through a method based on the *Integrated Value Model for Sustainability Assessment* (MIVES). This multi-criteria decision-making (MCDM) model relies on the value function concept and the multi-disciplinary participation of experts to identify and quantify the relevant indicators of the facade sustainability performance and the relative importance of indicators and requirements. The MIVES-based model generated for this research can be straightforwardly used for assessing the sustainability performance of facade-cladding techniques made of any material and for any type of building (and location). The application of the MIVES model led to the sustainability index of this new material for facade cladding ranging from 0.68–0.71 (/1.00) for different weighting scenarios.

Keywords: Fiber cement sheets, Fire behavior, MIVES, Multi-criteria decision making, Sustainable criteria, Textile waste fiber, Thermal and acoustic behavior

1. Introduction

The construction sector adversely affects the environment during phases that comprise material manufacture, site building, usage phase, and demounting/demolition (Pons and Wadel, 2011). According to statistics, the construction industry accounts for approximately 35% of CO_2 emissions, 40% of total energy consumption, and 45% of generated waste in the EU (High energy performing buildings -

Publications Office of the EU; Gálvez-Martos et al., 2018; Lazar and Chithra, 2020). Thus, although significant efforts are being carried out, research and innovations are still required to improve the sustainability performance of buildings in all phases. In this sense, there is a wide array of development strategies and materials that can be utilized in different elements of buildings.

Facades, as one of the main parts of buildings, play a key role in improving energy efficiency through protecting the interior space against adverse environmental effects, such as climate change, noise, or pollution (Gilani et al., 2019; Hartkopf et al., 2012). In this regard, a construction solution known as double-skin facade systems is increasingly being used in both new and renovated buildings (Densley Tingley et al., 2015). In this facade system, the exterior lightweight cladding panel and the outdoor side of the external wall are divided by an air cavity or insulation layer, typically constructed by perforated steel studs. The presence of an external discontinuous protective enclosure permits air ventilation while preventing direct sunlight heating, thereby providing energy-saving benefits in terms of heating and cooling loads (Claramunt et al., 2016).

The external cladding material should fulfill both the engineering and architectural requirements such as strength-to-weight ratio, durability, serviceability, and aesthetics while guaranteeing an acceptable level of sustainability performance. Conventional materials for facade cladding include natural stones and ceramics, as well as aluminum and wood composites. Although these materials are predominantly used for facade construction due to their competitive costs and availability, there are some drawbacks. On the one hand, the formers are known to present limited flexibility against imposed deformations (i.e., due to variation of temperature and movements of the building) and elevated weights that lead to costly connections and mounting operations. On the other hand, the latter group suffers from durability aspects and less competitive costs when compared with the formers (Claramunt et al., 2016). Furthermore, regarding sustainability, marble and aluminum panels are recognized for being scarcely environment-friendly materials due to the high environmental burden involved with the extraction and processing of the raw materials (Kvočka et al., 2020). As a result, a new generation of composite panels for facade cladding known as fiber-reinforced cement (FRC) sheets, which were believed to be more eco-friendly than aluminum or steel (Nguyen et al., 2020), stated to be researched and promoted.

Over the previous decade, steel, glass, and polymers have been considered as predominant materials for fibers oriented to reinforcing cement-based matrices (Brandt, 2008; Gong et al., 2020; Jia et al., 2017; Lei et al., 2021; Wang et al., 1987). However, there are some shortcomings associated with the use of these fibers, these being high cost, and specifically, substantial environmental footprint (Ardanuy et al., 2015). Therefore, natural (i.e., cellulose) fibers (Batista dos Santos et al., 2021; Claramunt et al., 2017a; Rakhsh Mahpour et al., 2022), as well as recycled fibers (Brazão Farinha et al., 2021; Halvaei, 2021; Rahman et al., 2022; Yina et al., 2016), have gained significant attention in recent years as sustainable reinforcements in cement composites for construction applications.

Sustainability assessment in the construction industry plays a pivotal role in moving toward buildings that have less negative economic, environmental, and social impacts (Balali and Valipour, 2020; Pons et al., 2016). The construction industry and the built environment are involved in several targets and objectives of the Sustainable Development Goals (SDGs) assigned by the United Nations, namely in the 9th and 11th SDGs (United Nations Sustainable Development Action, 2015). In building and civil engineering fields, there are a variety of databases, tools, and methods to evaluate sustainability performance, namely Green Star, BREEAM, LEED, and LCA, among others (Cabeza et al., 2014; Colangelo et al., 2021; Sørensen and Wenzel, 2014). However, most of the existing assessment approaches merely consider environmental performance, thus, leading to a non-comprehensive evaluation (Akadiri et al., 2013; Ding, 2008). Tools and

methods that include other sustainability requirements, such as economic, social, technical, and functional have been recently developed (Ali and Al Nsairat, 2009; Salzer et al., 2016).

In addition, sustainability assessment of building elements such as slabs, columns, pavements, and facades should be investigated further since this kind of assessment could contribute significantly to the selection of sustainable materials in the early design stages of construction projects (John et al., 2005; Mohammadi et al., 2022). Based on the literature review, a few studies have evaluated the environmental sustainability of facade-cladding panels through life cycle assessment (LCA), such as geopolymers or ceramic facade panels (Han et al., 2015; Kvočka et al., 2020), concrete panels (Hay and Ostertag, 2018), green facades (Ottelé et al., 2011), and curtain walls (Kim, 2011).

This study aims to develop a novel model for evaluating the sustainability index (SI) of facade-cladding panels by analyzing multiple requirements based on MIVES. This multi-criteria decision making (MCDM) method, enables an objective assessment and quantification of indicators governing the sustainability performance (economic, environmental, social, and even technical) through the value function concept (Alarcon et al., 2010; Gilani et al., 2017). MIVES has already been successfully used in other fields, such as post-disaster housing management (Hosseini et al., 2021, 2018; S M Amin Hosseini et al., 2016; S. M. Amin Hosseini et al., 2016); active architectural learning (Pons et al., 2019); school edifices (Pons and Aguado, 2012); Spanish code of concrete structures (del Caño et al., 2012), and infrastructure (de la Fuente et al., 2016). Moreover, the initial and conceptual of this model for facade panels was reported by the authors in the recent contribution (Sadrolodabaee et al., 2021e).

To this end, the MIVES-based model for facade-cladding sustainability performance assessment was applied to the textile waste fiber reinforced-cement (TWFRC) panel as a potential alternative in residential buildings in Barcelona, Spain. The remainder of this paper is laid out as follows: Section 2 presents a review of TWFRC boards, including their mechanical characteristics. Section 3 presents the details of the experimental programs carried out within the context of this research to characterize the thermal, acoustic, and fire-resistant properties of this material. In Section 4 the MIVES-based model developed for the sustainability assessment of facade claddings is thoroughly explained. Section 5 is devoted to covering the results and discussion. This is finally, followed by a summary of conclusions.

2. TWFRC board

Proper waste materials management can be beneficial to the recycling and building industries, especially in terms of lower environmental impacts (Perugini et al., 2005). However, recycling and reusing rates are quite low since there is still skepticism about the quality of recycled materials. Thus, new research should be conducted using recycled materials to overcome these uncertainties (Li et al., 2022). The textile leftover, including pre-consumer and post-consumer waste, is one of the predominant waste resources worldwide, (Giesekam et al., 2014; Nautiyal et al., 2015).

In our previous studies, cement composites reinforced with recycled textile waste (TW) fibers from discarded fashion clothes, in both short random fibers and fabric form, were developed (Sadrolodabaee et al., 2021a, 2021b, 2021c). Those studies proved that a composite made of Portland cement paste as a matrix, reinforced with six layers of TW nonwoven fabric (TW6L, hereinafter), had the most efficient mechanical characteristics to be used as a thin and lightweight cement board. This cement board was successful in improving the flexural strength, energy absorption, durability, and crack resistance by exhibiting multiple cracking behaviors with deflection hardening.

Figure 1a shows a TW nonwoven fabric reinforcement and Figure 1b shows an uncoated TW cement board without any pigments. This prefabricated panel had a square-size of 300 mm and a surface mass of

approximately 16 kg/m^2 which is often lighter than comparable products constructed of concrete or natural stone. The mechanical properties of this type of cement composite obtained from our previous study (Sadrolodabaee et al., 2021d) are summarized in Table 1. The configuration of the flexural test was shown in Figure 1c,d, while Figure 1e demonstrates the experimental flexural stress–deflection relationships obtained from a four-point flexural test in both unaged and aged conditions. Unaged samples were tested after the 28 curing days whilst the aged ones were tested after 28 curing days plus 25 wet/dry accelerating aging cycles as a durability test.

To comprehensively assess the SI of this cement board based on the defined model design (section 4), more experimental properties were needed; thus, new tests were carried out on TW6L to assess the thermal, acoustic, and fire behaviors.

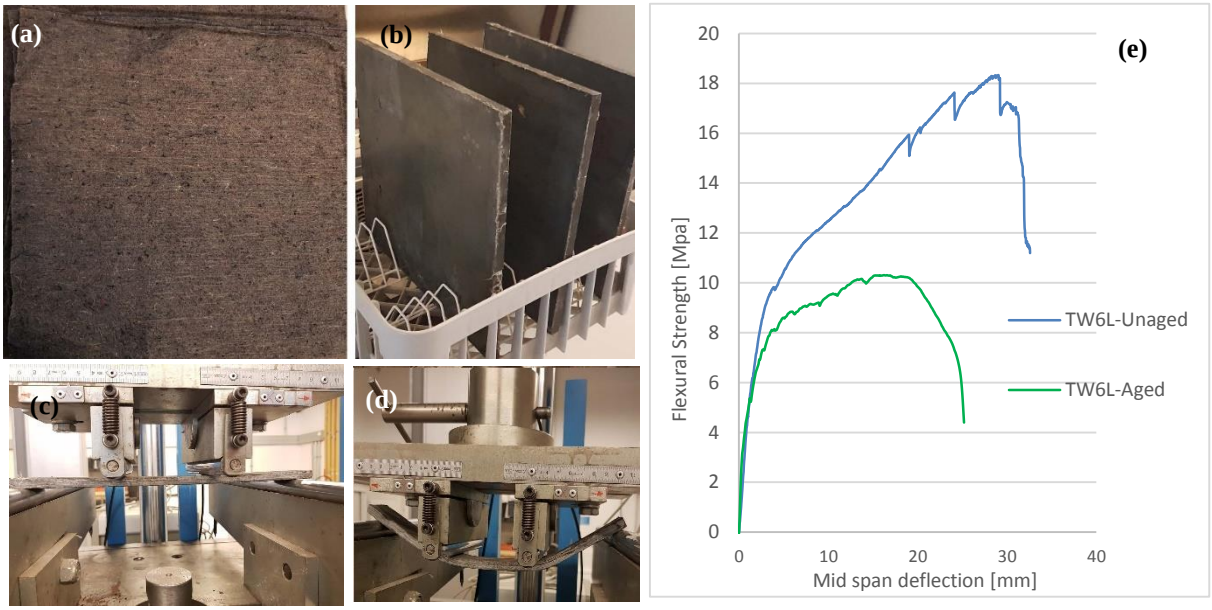

Figure 1. TW cement composites: a) TW fabric; b) TW cement boards; c) initial of the flexural test on the machined specimen; d) end of the flexural test; e) representative flexural stress – deflection relationships; According to Sadrolodabaee et al., 2021d

Table 1. Mechanical characteristics of TW6L cement board composite obtained from four-point flexural test.; According to Sadrolodabaee et al., 2021d

Parameters	Unaged sample	Aged sample
Modulus of rupture [MPa]	15.5	10
Toughness index [kJ/m^2]	9.7	6.8
Flexural stiffness of the pre-cracked zone [GPa]	11.3	12
Flexural stiffness of the post-cracking zone [GPa]	0.41	0.16

3. New experimental procedures

3.1 Materials and sample preparation

The cement paste was made with Portland cement Type I 52.5R, UNE-EN 197-1:2011, provided by Cementos Molins Industrial, S.A. (Spain). TW nonwoven fabric as an internal reinforcement is made up of

roughly 80% vegetable fibers (45% cotton and 35% Flax) together with 20% polyester fiber produced through card clothing and needle-punching process as explained in detail in (Sadrolodabaee et al., 2021d). This fabric, roughly 1 mm thick and weighed 155 g/m^2, had a tensile rupture force of 2.0 N/g.

The composite production technique, including vacuuming and compression treatments, was described in detail in previous studies by the authors (Sadrolodabaee et al., 2021d, 2021c). Briefly, TW6L was made with 6 layers of nonwoven TW fabrics saturated in matrix paste and stacked as a laminate in a vacuum-treated drilled-bed mold. The sample was then pressed at 3.3 MPa and cured for 28 days at >90% RH and 20 ± 1 ° C, resulting in a laminate plate with a thickness of roughly 10 mm. The control sample (CTR) without any fiber was produced with dewatering treatment as well. From each plate, specimens of different sizes were machined to carryout out the thermal, acoustic, and fire tests. Table 2 shows the mix proportions and the properties of the two samples.

Table 2. *Mix proportions* of the samples

Sample	$(w/c)_{initial}$	$(w/c)_{final}$	Cement (gr)	Water (gr)	Fiber weight fraction	Density [kg/m^3]
TW6L	1	0.45	1500	1500	5.4	1600
CTR	1	0.50	2000	2000	0	1900

3.2 Thermal test

The thermal conductivity coefficient (λ) was determined by using a Quickline-30 Electronic Thermal Properties Analyser, based on ASTM D5930 standard, with a surface probe (Figure 2a). Such equipment is based on the analysis of the transient temperature response of the material to heat flow variations induced by electrical heating using a resistor heater having direct thermal contact with the surface of the sample. The same method has been already used in some other studies to calculate λ (Gonzalez-Lopez et al., 2021). Two opposite surfaces of each sample, TW6L and CTR plates (300 mm × 300 mm × 10 mm) were tested, each surface two times. When the samples were in thermal equilibrium with the surrounding environment, the heat flow has been generated by applying heat impulse.

3.3 Acoustic test

Cylindrical specimens of diameter and height of 50 and 10 mm, respectively, were used to assess the acoustic characteristics of the samples, namely the sound absorption coefficient (α), as shown in Figure 2b. Measurements were carried out in an impedance tube in accordance with EN ISO 10534- 2, as described in detail in (Novais et al., 2020). Briefly, the approach is based on measurements of the transfer function between two microphones. The sample was inserted at one end of the tube whilst the sound source was attached to the other end. Two microphones monitored the acoustic pressures of the tube near the sample. The source created a random signal from which the complex acoustic transfer function for frequencies between 500-3150 Hz was calculated. Three samples of TW6L with six runs and one sample of CTR with two runs were tested.

3.4 Fire tests

3.4.1 Epiradiator test

The samples were subjected to a fire reaction test using an epiradiator, according to standard UNE 23725-90, to assess the effect of the inclusion of TW fibers on the composites' fire resistance (Figure 2c). Specimens of 70 × 70 mm2 were put on a metallic grid 3 cm below a 500 W heating source, implying a heat flux of 3 W/cm2 for 5 mins. The time of the first ignition, flame persistence time, and sample weight loss were determined. Two specimens of TW6L and two specimens of the CTR were tested.

3.4.2 Small-scale fire resistance test

The impact of high temperatures (up to 950 °C) on the characteristics of the plaques was studied by Hobersal JM3-15 oven, as shown in Figure 2d. Samples of 100 × 100 mm^2 were placed on the oven door with one of the faces exposed to an ISO 834-1:1999 temperature-time curve. Attaching k-type thermocouples to the sample's external face allowed the temperatures to be measured during the test.

3.4.3 Post-fire mechanical behavior

The mechanical behavior of the samples after exposure to the small-scale fire test (exposure up to 950 °C) was evaluated using a three-point flexural test with a cross-head speed of 6 mm/min, as illustrated in Figure 2e. The dimensions of the tested specimens were 100 × 50 mm^2, and the distance between the supports was fixed at 70 mm. The following mechanical parameters were obtained through the same procedure as described in the literature (Claramunt et al., 2017b): the limit of proportionality (LOP) as the breaking flexural stress of the matrix (first crack strength), the modulus of rupture (MOR) as the maximum flexural stress of the composite, toughness index (I_G) as specific fracture energy through the area under the force-displacement curve, and elastic flexural stiffness of the pre-cracked zone (E) between 60% and 80% of the LOP.

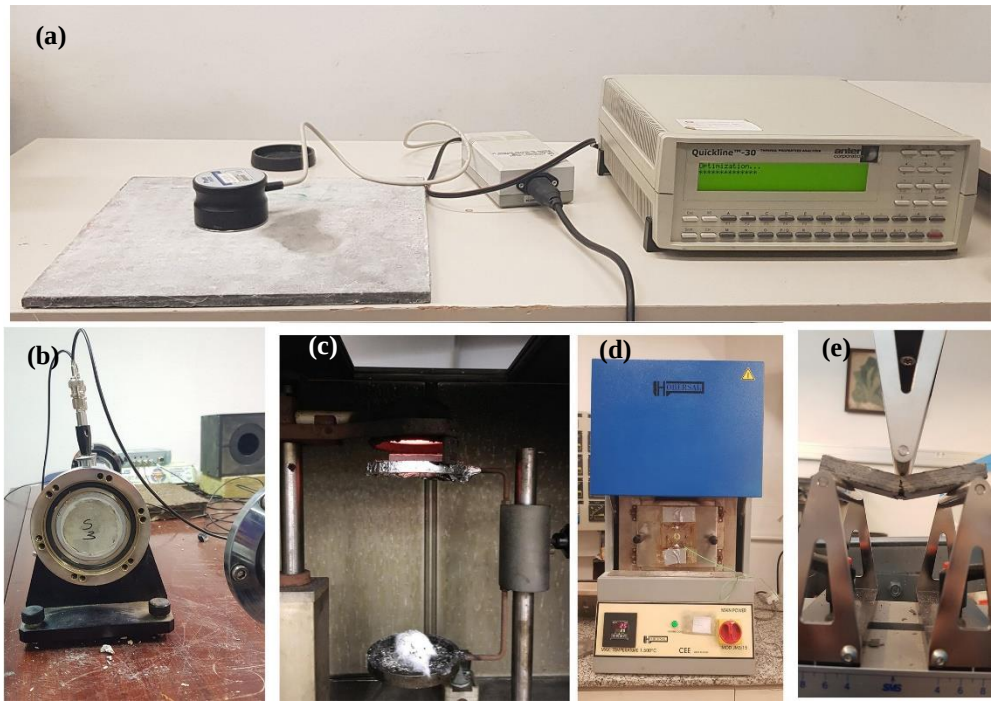

Figure 2 . Experimental setup*: a) thermal test; b) acoustic test; c) epiradiator test; d) oven for small-scale fire resistance test ; e) three-point flexural tests setup*

4. Model design

The general methodology of the MIVES was described in detail in previous studies (Hosseini et al., 2021, 2018; S M Amin Hosseini et al., 2016; S. M. Amin Hosseini et al., 2016). Briefly, the MIVES method includes a particular holistic discriminatory tree of requirements, assigning of weights for each index, value function concept to attain specific and global satisfaction, and expert seminars using the analytic hierarchy process (AHP) to define the previous components. In the following, the aforementioned steps of MIVES are designed and oriented for facade-cladding panels in order to analyze the SI for the TWFRC board as a real case.

4.1 Requirements tree

The requirements tree, a unique hierarchical diagram showing the main properties of the products, is organized at three levels: indicators, criteria, and requirements. This requirements tree is fixed a priori and filtered according to the preferences of the stakeholders, as identified through seminars with experts and an extensive literature review.

The preliminary requirement tree for facade-cladding panels was reported by the authors in (Sadrolodabaee et al., 2021e). However, the final filtered one for this case study is shown in Figure 3. As can be seen, the requirements (R) were considered in three main aspects: economic, environmental, and social. These requirements were further divided into seven criteria (C) and ten indicators (I). The functional unit in analyzing the indicators considered a 1-m^2 area of the facade cladding panel, where applicable. In the following, each index and the boundaries considered in the estimation of each indicator's value are discussed. Generally, the values of indicators were estimated based on the various methods, including experimental test results; various databases mainly the BEDEC from the Technological Institute of Catalonia (ITeC) (BEDEC, 2020), as well as the Inventory of Carbon and Energy (ICE) (Hammond and Jones, 2011); Environmental Product Declaration (EPD) of materials; and seminars with experts. Table 3 shows the data source used in the calculation of each indicator.

Economic requirement (R_1) represents the whole expenditure required to implement the facade cladding for the estimated life cycle, with *Cost* (C_1) serving as the only criterion. *Environmental requirement* (R_2) considers the overall environmental impact of the life cycles of the panels through *Global warming potential* (C_2), *Resource consumption* (C_3), *and Waste management* (C_4) criteria. Finally, *Social sustainability requirement* (R_3), with the aim of improving the quality of human life and the health of the users (Shen et al., 2010) embraces three criteria: *Comfort* (C_5), *Safety* (C_6), and *Urban landscape* (C_7).

C_1 encompassed two indicators: *Construction cost* (I_1) and *Maintenance cost* (I_2) of the external cladding panel. The former, assessed by considering roughly 40 composites and cladding panels of various materials, comprises material manufacture, shipping, installation, and labor costs. However, only the most relevant and homogenous data were collected, for instance, copper and bronze claddings were not considered, as their values would be much higher than those of the other conventional claddings. The online BEDEC database was implemented for this purpose. The latter predicts the cost of cleaning, repairing, and replacing the panel over its expected service life of 50 years. I_2 was estimated as approximately 10% of I_1 yearly (Brunsdon, 2018).

Carbon dioxide equivalent (kg CO_2-eq) is a common unit of measurement for *Global warming potential* (Yina et al., 2016). Thus, C_2 was represented by the indicator of *CO_2-eq emissions* (I_3) quantifying the amount of CO_2-eq emissions (carbon footprint) for each cladding panel during the production and construction phases. The reference databases used for measuring C_2 were the BEDEC and the ICE. According to Kvočka et al. (2020), the manufacturing and construction stages contribute the most to the environmental footprint of prefabricated panels, thus just these two stages were considered in the estimation of environmental indicators.

C_3 was designed to measure the consumption of natural resources by means of two indicators: *Energy consumption* (I_4) and *Material consumption* (I_5). The former quantified the amount of energy used during the production and construction stages (embodied carbon) by employing BEDEC and ICE databases. Energy consumption during the demolition phase was reported to be negligible, less than 3% (Pons and Aguado, 2012), with respect to the previous phases, thus, it was ignored. The other indicator considered the

amount of raw materials and water consumed in the manufacturing stage through BEDEC, EPD of materials, and the experimental reports available in the literature.

C_4 was evaluated by the indicator of *Recyclability* (I_6) to estimate the amount of waste and recycled materials consumed during the fabrication process or the amount that could be recycled after demolition or end-of-life. I_6 was rated qualitatively on a measurable scale of 0–20 through seminars with multidisciplinary experts as well as literature reviews. Fifteen experts (6 civil engineers, 6 architects, and 3 building engineers), mainly from UPC, gave their opinions on the mentioned scale and the final value was the average of those proposed values.

C_5 comprised two indicators: *Acoustic* (I_7) and *Thermal performances* (I_8). I_7 considered the rate of α of the material by calculating the noise reduction coefficient (NRC) while I_8 was used to assess the thermal conductivity of cladding panels. The thermal performance of facade systems could significantly reduce the annual energy demand (Monge-Barrio and Sánchez-Ostiz, 2015).

C_6 was used to evaluate the safety and security levels of the occupants and included the indicator *Fire vulnerability* (I_9), which assessed the post-fire residual resistance in MPa through a flexural strength test.

C_7 included *the aesthetic* indicator (I_{10}) and qualitatively assessed the appearance and visual quality of the facade cladding. I_{10} was rated on a measurable scale of 0–10 through seminars with fifteen multidisciplinary engineers/architects, mainly from UPC.

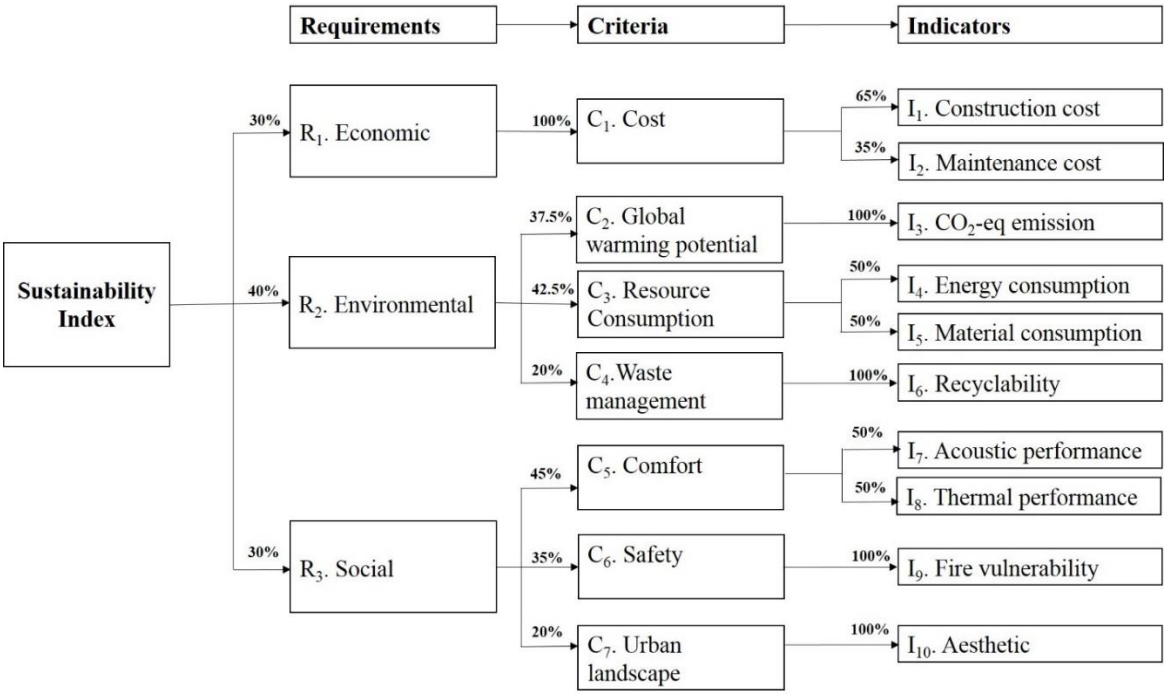

Figure 3. Requirements tree for facade cladding panels

It should be emphasized that the indicators were identified and determined based on an extensive literature review (see Table 3). Furthermore, although the indicator categorizations were mentioned above,

these indicators could have been allocated to other requirement groups simultaneously concerning their impact. In other words, there could be many interactions among the indicators; however, according to the concept of the MIVES method (Gilani et al., 2017), each indicator is normally considered according to its main impacts in order to prevent the double-counting effect in the assessment. That is the reason why technical sustainability (to construct a durable and reliable structure) was not considered separately, as its indicators, such as strength-to-weight ratio or durability, could be covered and overlapped by the economic indicators. Moreover, the ultimate identification and filtration of the indicators are influenced by the function and location of the building. The above-mentioned indicators were fixed and filtered for residential buildings in Barcelona. Nonetheless, for a similar building in another region or a building with different functionalities, the final indicators could be different. For instance, earthquake vulnerability could be considered as a final indicator for earthquake-prone countries, however, due to the region's low seismicity, this indicator could be ignored in Barcelona.

Table 3. Summary of data sources used.

Indicators	Sources
I_1	BEDEC database (BEDEC, 2020)
I_2	BEDEC database (BEDEC, 2020); Scientific publications : (Brunsdon, 2018)
I_3	BEDEC (BEDEC, 2020) and ICE (Hammond and Jones, 2011) databases; Scientific publications : (Claramunt et al., 2016; Malabi Eberhardt et al., 2021; Ricciardi et al., 2014)
I_4	BEDEC (BEDEC, 2020) and ICE databases (Hammond and Jones, 2011); Scientific publications : (Ricciardi et al., 2014)
I_5	BEDEC database (BEDEC, 2020); EPD of materials; Experimental test
I_6	Seminars with experts; Scientific publications : (Addis, 2012; Alarcon et al., 2010; Li et al., 2022; Souza et al., 2021)
I_7	Experimental test results; Scientific publications : (António, 2011; Novais et al., 2021; Quintaliani et al., 2022; Ricciardi et al., 2014; Rubino et al., 2018.; Tie et al., 2020)
I_8	Experimental test results; Scientific publications : (Asadi et al., 2018; Bagheri Moghaddam et al., 2021; Borri et al., 2016; Buratti et al., 2016; Gonzalez-Lopez et al., 2021; Quintaliani et al., 2022; Rubino et al., 2018)
I_9	Experimental test results; Scientific publications : (British Standards Institution., 2018; Gonzalez-Lopez et al., 2021; Kolaitis et al., 2016; Nguyen et al., 2020)
I_{10}	Seminars with experts

4.2 Assigning weights to parameters

To identify the relative importance of each parameter in addition to prioritizing the indices, weights should be assigned to each branch of the requirements. The weights of the tree were assigned qualitatively based on the knowledge of fifteen professors/experts, mainly from the architecture and civil engineering faculties of the UPC, via their involvement in a seminar on the AHP method (Cartelle Barros et al., 2015; Saaty, 1990). The final filtered proposed weight of each index is the average of those proposed by the experts after eliminating the outliers.

4.3 Establishing value functions for each parameter

After estimating the value of each indicator based on its specific unit (see X_i in Table 6), the value function concept needs to be implemented in the indicators' values to normalize the indicators' units and transform the results into non-dimensional values. This dimensionless value (ranging from 0.0 to 1.0, the minimum and maximum degrees of sustainability satisfaction) intends to indirectly measure the satisfaction grade of the stakeholders and users leading to minimizing subjectivity in assessments.

Allocating value function to the indicators was explained in-depth in (Aguado et al., 2012; Alarcon et al., 2010; Gilani et al., 2019; Hosseini et al., 2020). Briefly, the function's tendency (increasing or decreasing) should be specified initially. An increasing (In) function indicates that an increase in the measurement unit caused an increase in satisfaction whilst a decreasing (D) one was used when an increase in the measurement variable decreased the decision maker's satisfaction. Secondly, the points (X_{min} and X_{max}) that produced the lowest and highest level of satisfaction for each indicator should be defined according to existing rules and regulations, experience gained from previous projects, and values obtained by various alternatives (see Table 3). These points would be the *x*-axis boundaries with satisfaction values of 0.0 (X_{min}) and 1.0 (X_{max}) that were connected by one of the suggested shapes for the value function's type: concave, convex, linear, and S-shaped. A concave-shaped (C_v) function was used if satisfaction increased swiftly or decreased marginally whilst a convex (C_x) one was more appropriate on the contrary case to the former. If the satisfaction increased/decreased continuously, a linear (L) function was employed while an S-shaped (S) one was more suitable when the satisfaction tendency contained a combination of C_v and C_x (see Figure 4). Finally, the mathematical expression of the value function was applied through Equation 1 to obtain each indicator value satisfaction, V_i. Equation 2 was applied to achieve factor B for Equation 1, which would allow homogenization of the indicators' values ($V_i(x_i)$) between 0.0 and 1.0.

$$V_i = A + B \cdot \left[1 - e^{-k_i \cdot \left(\frac{|X_i - X_{min}|}{c_i}\right)^{p_i}}\right] \qquad \text{(Equation 1)}$$

$$B = \left[1 - e^{k_i \cdot \left(\frac{|X_{max} - X_{min}|}{c_i}\right)^{p_i}}\right]^{-1} \qquad \text{(Equation 2)}$$

Where

V_i: the indicator's satisfaction value;
A: response value of X_{min} (usually A = 0);
B: factor that keep the function in the range (0.0, 1.0);
X_i: an indicator that generates the value, V_i;
X_{min}: point with the lowest satisfaction;
X_{max}: point with the highest satisfaction;
P_i: shape factor
($P < 1$ means the curve is concave; $P > 1$ means it is convex or S-shaped; $P = 1$ means it is linear);
C_i: factor that is used for the inflection point in curves with $P_i > 1$.
K_i: factor that describes the response value to C_i;

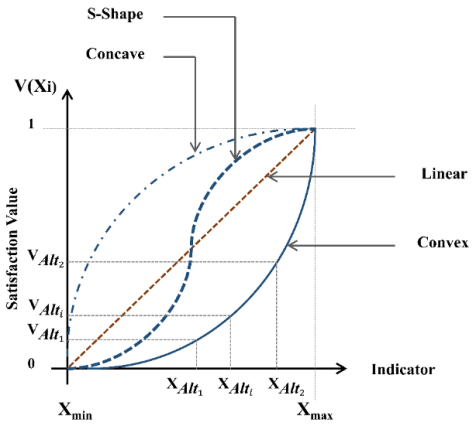

Figure 4. Value function shapes: a) all shapes; b) value function shape of indicator I_1

4.4 Assessing sustainability index (SI)

Equation 3 was applied to each level of the requirement tree to calculate the SI of each alternative. In addition to determining the total SI, this method enabled the calculation of economic, social, and environmental satisfaction indices separately.

$$SI = \sum \lambda i \cdot V_i(x_i) \quad \text{(Equation 3)}$$

Where $V_i(x_i)$ and λ_i are the value function of each index and the associated weight, respectively.

5. Results and Discussion

5.1 Thermal test

As shown in Table 4, the control sample, without any fiber, had 40% higher thermal conductivity than the TW6L plate, proving that the incorporation of TW fibers improved the thermal behavior of the material. Thus, the indicator I8 for the TW cement plate and control plate were chosen, 0.83 W/mK and 1.17 W/mK, respectively.

This result was in line with the study of (Gonzalez-Lopez et al., 2021), in which the thermal conductivity of two-overlapped cement plates, composed of calcium aluminate cement (CAC) and different percentages of metakaolin reinforced with flax fiber, was evaluated with the same method. Based on that study, the thermal conductivity of the cement composite varied between 0.650 and 0.840. Further, other studies (Khedari et al., 2001; Lertwattanaruk and Suntijitto, 2015) similarly proved that the addition of vegetal and natural fibers to the cement-based materials could enhance the thermal performance with respect to the control sample by 40-80 %, depending on the fiber type and volume. Increasing the fiber quantity in the material, generally, leads to higher porosity which, in turn, may decrease the thermal conductivity, thereby better thermal insulation (Quintaliani et al., 2022).

Table 4. Values of thermal conductivity of the analyzed samples

Sample	Thermal Conductivity [W/(m·°K)]
TW6L	0.83
CTR	1.17

5.2 Acoustic test

The sound absorption coefficient (α) of the TW6L and CTR specimens across the frequency range of 500–3150 Hz is shown in Figure 5. The maximum α for the CTR sample was 0.17 at a frequency of approximately 2270 Hz, whereas for the composite, which incorporated the TW fiber, this increased to 0.26 at 1530 Hz. Thus, the fiber improved the acoustic behavior by up to 50%. This result was consistent with the study of Quintaliani et al. (2022), in which the addition of various waste vegetal fibers by 10% weight, could increase the absorption coefficient by 42-60% in cementitious materials.

For the indicator I_7, the NRC, which was the average value of α at specific frequencies (500, 1000, and 2000 Hz) was calculated. The values of this parameter for the TW6L and CTR specimens were approximately 0.2 and 0.12, respectively. The values of α and NRC theoretically ranged from 0 to 1; however, for most of the relevant cladding panels, the NRC ranged from 0 to 0.5 (Tie et al., 2020). However, the acoustic performance of TW6L was relatively low, and one solution to increase this parameter was to increase the thickness of the layer, which could increase α, as reported in (Novais et al., 2021). Furthermore, the sound absorption of cement-based materials can be increased by adding porous structures into the

materials by various means, such as integrating lightweight aggregates or generating voids with the use of foam in cellular concrete (Tie et al., 2020). In general, the creation of pore structures in cementitious materials decreases the density, which, in turn, improves α and NRC. Nonetheless, TW fibers in the present study could only marginally increase the porosity and reduce the density of the cement plate, as the production of this type of plate is accompanied by vacuuming and compressing, which reduce the voids and porosity.

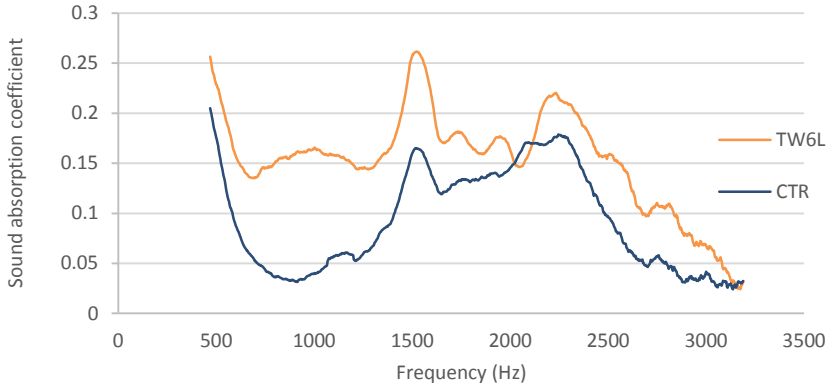

Figure 5. Sound absorption coefficient spectra of the measured samples

5.3 Fire test

5.3.1 Epiradiator test

The TW6L specimens did not display any ignition, flames, or smoke during the epiradiator test after attaining a temperature of 420 °C for 5 minutes. This suggests that the fibers did not contribute to the appearance of flames. Figures 6a,b show images of the faces unexposed and exposed to the radiation, respectively, for TW6L. As can be seen, the studied sample had some surface cracks but no major material detachment. TW6L lost approximately 15.6% of its weight due to the dehydration and the transformation of various hydrated cement components into oxides, with a corresponding volume reduction. The lack of chipped pieces on the surface of the samples indicates a remaining bridging effect of the fiber reinforcement. As reported in (Gonzalez-Lopez et al., 2021), the vegetable fibers were discovered to retain their reinforcing capacity up to 450 °C, beyond which disintegration increased. Thus, the capability of this material to preserve its integrity could be attributed to the fiber reinforcement's bridging effect, which caused no material loss by spalling. On the other hand, the control cement plate after 5 min of exposure to 420 °C showed no flame or smoke. However, owing to the loss of fiber and brittleness, it broke after the appearance of the cracks (Figure 6c).

5.3.2 Small-scale fire resistance test

As can be seen in Figures 7a,b, the TW6L sample developed superficial, fine, and uniformly distributed cracks, which were more prevalent on the heat source-facing face; this face may have reached up to 950 °C, compared to the face exposed to room temperature, which hardly reached 850 °C (Figure 8). The cracks were caused by water loss as a result of sample drying; however, the integrity of the composite was maintained even when subjected to temperatures more than 800 °C for approximately 100 min. The CTR sample showed a cracking pattern with more separated, thicker, and deeper cracks, which ended in chipped pieces and spalling owing to a lack of fibers (Figure 7c). Thus, as reported by Nguyen et al. (2020); Zhang et al. (2018), the addition of fibers could mitigate the explosive spalling of the inorganic binder matrix at elevated temperatures by releasing gradually the accumulated vapor pressure. As can be seen in Figure 8,

as the CTR plate had a higher heat transfer coefficient, the non-exposed face of this plate has a higher temperature than TW6L. For instance, when the exposed faces had a temperature of approximately 800 ºC at 40 min, the unexposed faces of TW6L and CTR samples had temperatures of approximately 400 and 600 ºC, respectively. In other words, the incorporation of TW induced a thermal delay of roughly 20 min because the unexposed face of the CTR specimen reached 600 ºC after approximately 40 min, while the unexposed face of the TW board reached this temperature at approximately 60 min.

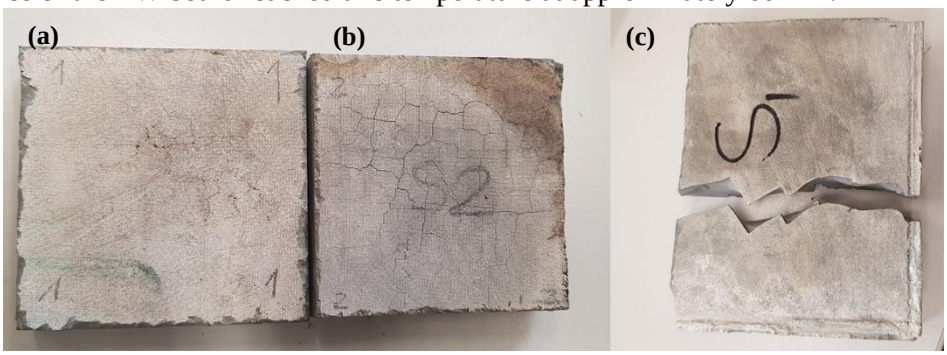

Figure 6. Epiradiator test: a) TW6L surface not exposed to the heat source ; b) TW6L surface exposed to the heat source after 5 min; c) CTR after exposure

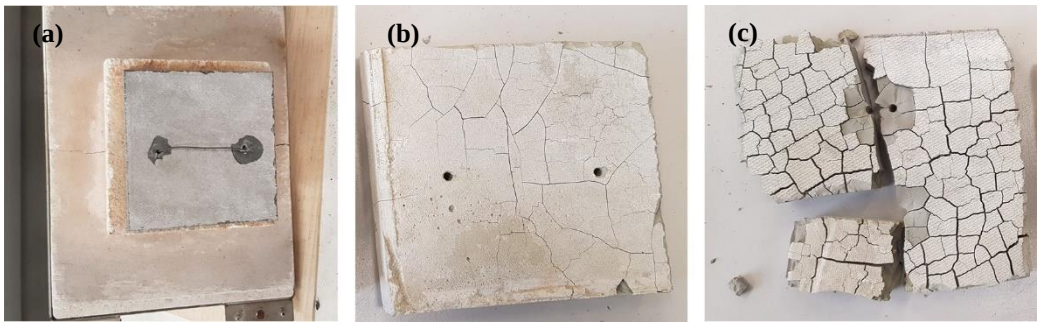

Figure 7. Small-scale fire resistance tests: a) specimen before the test ; b) heat-exposed face of TW6L specimen after the test; c) heat-exposed face of CTR plate after the test

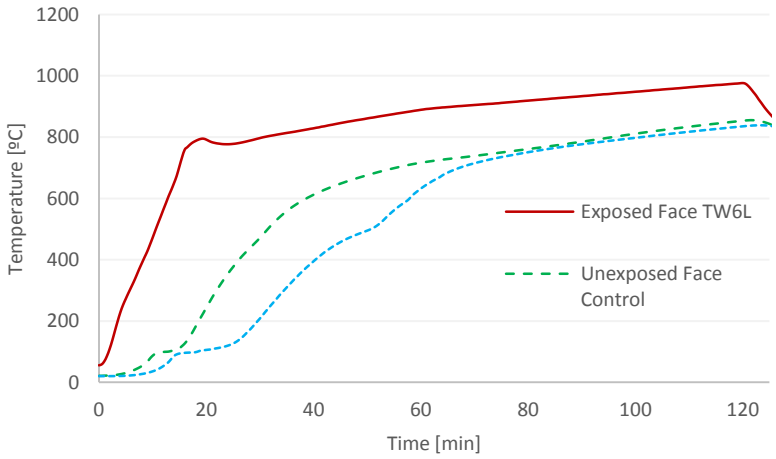

Figure 8. Temperature evolution of the surfaces in the small-scale fire resistance test based on ISO 834

5.3.3 Post-fire mechanical behavior

Figure 9 depicts the representative flexural stress-displacement curves of the tested samples, and Table 5 summarizes the mechanical parameters. For the composite not exposed to high temperatures (TW6L), the reinforcing effect of the fibers allowed a relatively high deformation capacity, which led to an increase in toughness and post-cracking flexural strength (MORm/LOPm > 1.0). Nonetheless, after exposing the composite to 950 °C (TW6L-Fire), the bending behavior changed with respect to the former sample. In this case, the fibers mostly lost their effectiveness and the material became relatively brittle, that is, the effect of the reinforcement was negligible (MORm ≈ LOPm). Therefore, the toughness decreased considerably as it depended mainly on the fiber pull-out mechanism. The cement matrix degraded as well owing to the high temperature; the LOP_m and E_m decreased dramatically from 11.4 to 0.85 MPa and from 1.50 to 0.28 GPa, respectively.

As for the non-exposed cement plate sample, i.e., CTR, the fracture type was brittle, as there was no fiber for bridging the cracks. After the exposure to fire (CTR-Fire), the sample still exhibited brittle behavior but with less flexural resistance. However, among the samples exposed to fire, the plate reinforced with the fibers showed better mechanical properties than those without the reinforcement. As shown in Table 5, TW6L-Fire had a higher MOR (almost six times) and I_G (almost 2 times) compared to CTR-Fire. The MOR of TW6L-Fire, 0.9 MPa, was chosen as the value of indicator I_9. This result was in line with (Gonzalez-Lopez et al., 2021), in which the flexural strength after exposure to fire test was measured for the cement plates consisting of CAC and different percentages of metakaolin reinforced with flax fibers. Based on that study, the MOR varied between 0.0 and 1.7.

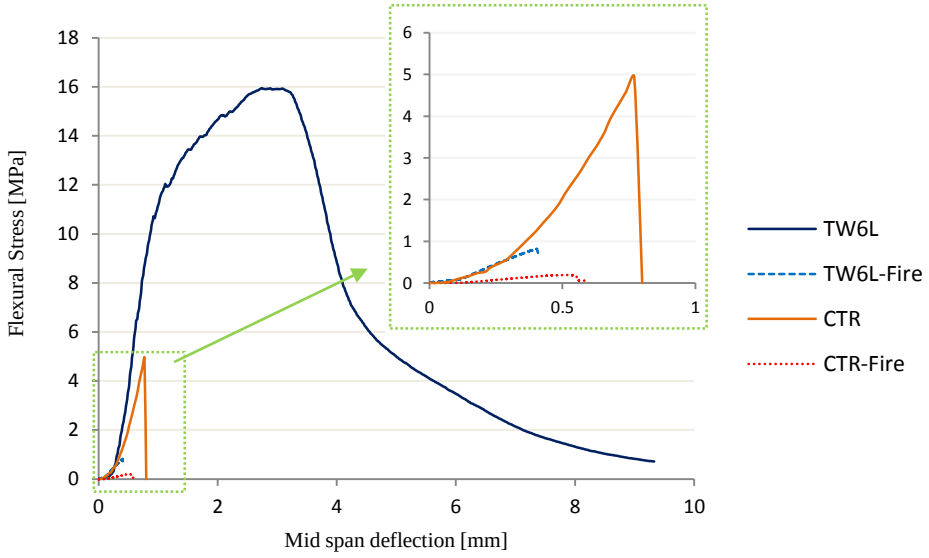

Figure 9. Representative flexural stress: deflection relationships obtained from the three-point flexural test

Table 5. Mechanical properties obtained from the three-point flexural test (CoV in %)

Code	**LOP_m** [N/mm^2]	**MOR_m** [N/mm^2]	**I_{Gm}** [kJ/m^2]	**E_m** [GPa]	**$(W/c)_{final}$**	**No. of Specimens**
TW6L	11.40 (7)	16.20 (10)	4.70 (16)	1.50 (17)	0.45	6
TW6L-Fire	0.85(24)	0.90 (22)	0.04 (19)	0.28 (14)	0.45	6
CTR	5.60 (24)	5.60 (17)	0.20 (30)	0.40 (19)	0.55	6
CTR-Fire	0.15 (19)	0.15 (29)	0.02 (10)	0.03 (20)	0.55	6

5.4 Sustainability index

Table 6 gathers all the indicators and the associated constitutive parameters for TW cement boards in order to reach the satisfaction value for each indicator (V_I). As can be seen, there were five indicators with decreasing convex shapes (I_1–I_5: DC_X), three ones with increasing concaved shapes (I_6, I_7, I_9: InC_V), only one with decreasing S-shaped (I_8:DS), and another one with an increasing linear function (I_{10}:InL). Moreover, as already explained, X_{min} and X_{max} were assigned based on the literature review (Table 3), and X_i values were calculated specifically for the case study of this research, the TW cement board. $X_{7\text{-}9}$ were measured according to the new experiments carried out in this study. Figure 10 shows the function shape of I_1, as an example, and the estimation of its satisfaction value (V_1) from the cost value of the TW cement board (X_1). As the satisfaction value of I_1 decreased rapidly with increasing cost, a convex shape was chosen.

Table 6. Parameters and coefficients for each indicator value function for TW panel

Indicators	Function Shape	Units	X_{min}	X_{max}	C	P	K	X_i
I_1	DC_X	€/m²	20.5	183.0	200.0	1.8	0.3	51.4
I_2	DC_x	€/m²	125.0	915.0	2000.0	1.8	0.3	257.0
I_3	DC_X	Kg/m²	6.1	60.0	22.0	1.5	0.4	19.0
I_4	DC_X	MJ/m²	92.6	350.8	250.0	1.5	0.4	171.0
I_5	DC_X	Kg/m²	11.0	80.0	50.0	1.5	0.4	33.0
I_6	InC_V	points	0.0	20.0	30.0	0.9	1.0	15.0
I_7	InC_V	points	0.0	0.5	0.3	1.1	0.9	0.2
I_8	DS	W/m K	0.1	6.0	4.0	0.35	4.5	0.83
I_9	InC_V	MPa	0.0	2.0	2.0	0.8	0.8	0.90
I_{10}	InL	points	0.0	10.0	10.0	1.0	45.0	5.5

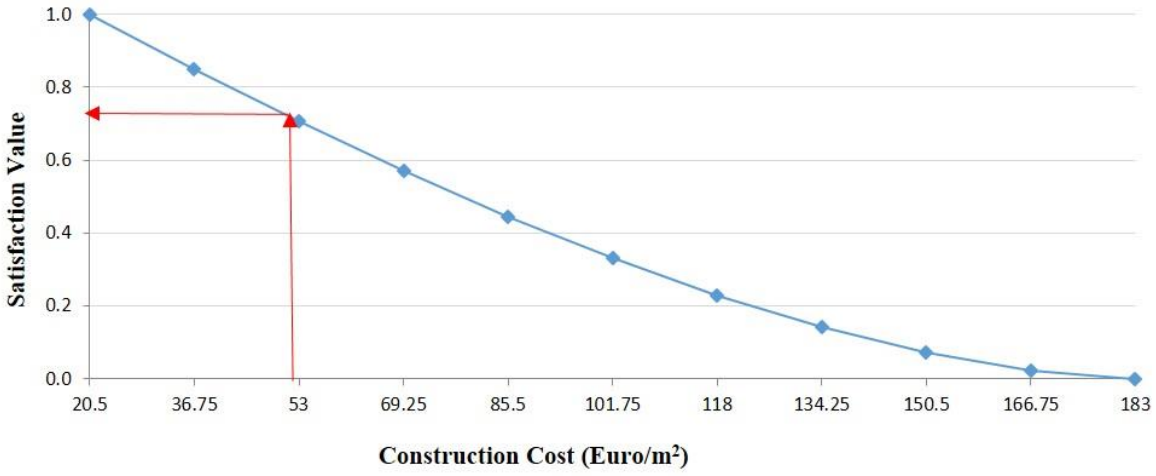

Figure 10. Value function shape of indicator I_1 for TW panel

The final proposed weights (percentage) of the indices was shown in Figure 3. As can be seen, experts believed that *Environmental requirement*, with a weight of 40%, was more important than *Economic* and *Social requirements*, each with a weight of 30%, when selecting sustainable facade materials. This ranking is in line with the study of Mohammadi et al. (2022) in which environmental sustainability gained more points than the other aspects. Regarding the criteria, C_1 had 100% as it is the only criterion of R_1. C_3 gained

the highest point among the environmental criteria, 42.5%, as it is composed of two important indicators. C_2 and C_4, each embracing only one indicator, had 37.5% and 20% respectively. Among the social criteria, C_5 was the most important one, with 45% weight, followed by C_6 and C_7, 35% and 20% respectively. Four indicators (I_3, I_6, I_9, I_{10}) were assigned 100% weight since there is only one indicator for each associated criterion. The indicators' weights of the *Cost* criterion were 65% and 35% for I_1 and I_2, respectively, showing the greater importance of the former. I_4 and I_5, as well as I_7 and I_8, weighted 50% as it was believed to have the same importance for C_3 and C_5, respectively.

The satisfaction values of each indicator, criterion, and requirement for the TW plate are shown in Figure 11. As can be seen, all the parameters yielded satisfaction values above 50%, which was promising for this type of cladding panel. However, two of the indicators and one of the criteria had values higher than 75% (the target value) and showed very high sustainability levels. The indicator I_8 had the highest value of satisfaction (85%), while the indicators I_{10} and I_7 had the lowest value (55%). The SI of this material based on the proposed weight (Figure 3) was calculated as 70%, which was only 5% less than the target value. All three requirements demonstrated an acceptable satisfaction value (> 65%), which showed that this cladding panel could satisfy all aspects of sustainability.

In terms of R_1, both indicators of construction and maintenance costs (I_1 and I_2) showed the same satisfaction value, near 75%, which was an acceptable range for the stakeholders.

R_2 attained almost the same value as R_1, i.e., 71%. Among these criteria, C_2 and C_4 had values higher than 70%. As to I_3, CO_2 emission of this material was considerably lower than that of other materials typically used for this application, such as aluminum composites, ceramics or stone, as was reported in (Claramunt et al., 2016). However, this value could be improved by partial substitution of the Portland cement matrix with pozzolanic industrial by-products such as silica fume, metakaolin, or fly ash because the production of the cement involved an emission of 5%–8% of all the CO_2 generated worldwide. I_6 had a high value as the fibers in the production of the TW board were mainly from recycled materials. Moreover, the cement board after demolition can be recycled as an aggregate in concrete or pavements. However, criterion C_3 with related indicators, I_4 and I_5 showed an average sustainability level with a satisfaction value of 64%. Using a more environmentally friendly source of energy, such as generating electricity by solar panels, could improve I_4 (Kvočka et al., 2020).

R_3 reached the lowest satisfaction value among all the requirements (65%). C_5 almost reached the target level as previously reported TW fibers and fabrics proved to be proper acoustic and thermal insulation materials (Briga-Sá et al., 2013; Lee and Joo, 2003; Zhou et al., 2010). However, there are some strategies to improve the acoustic performance of this material, as discussed in Section 5.2. In addition, it is even possible to improve further the thermal performance of the panels by adding phase change materials (PCMs). With regard to I_9, the resistance to fire was acceptable, as already reported for this type of fabric (Lee and Joo, 2003). The counterpart lightweight prefabricated composite panel made up of fiber-reinforced polymer (FRP) was reported to have unsatisfactory fire performance by causing several critical issues in the event of fire such as rapid spreading or releasing smoke and toxic gases (Nguyen et al., 2020). As for I_{10}, it should be improved by taking some measures, including production panels with a larger size, and coloring or coating the panels.

The satisfaction values of indices for the CTR plate were gathered in Table 7 as a comparison with the TW6L cement board. The SI of this material based on the proposed weight (Figure 3) was calculated as 46%, 24% less than TW6L. R_1 dropped to 52% as the construction cost (I_1) of CTR was higher due to the more cement amount used. Moreover, I_2 decreased as this panel was brittle, thus, repairing and replacing were more frequent during the service life. In terms of R_2, C_2 and C_3 decreased as more amount of cement

lead to more amount of CO_2 emission and more energy consumption in the production of the material. In addition, C_4 dropped to 47% as no waste materials were used in the manufacturing phase. R_3 reached the lowest satisfaction value among all the requirements (40%) for CTR. C_5 and C_6 decreased by 19% and 46%, respectively, as was already explained in previous sections based on the experimental results. C_7 was the only parameter that remained constant since the appearance of the plate was not changed by omitting the fibers. Thus, incorporating textile waste fabric into the cement board not only improved the mechanical characteristics, but also developed the sustainability aspects including economic, environmental, and social.

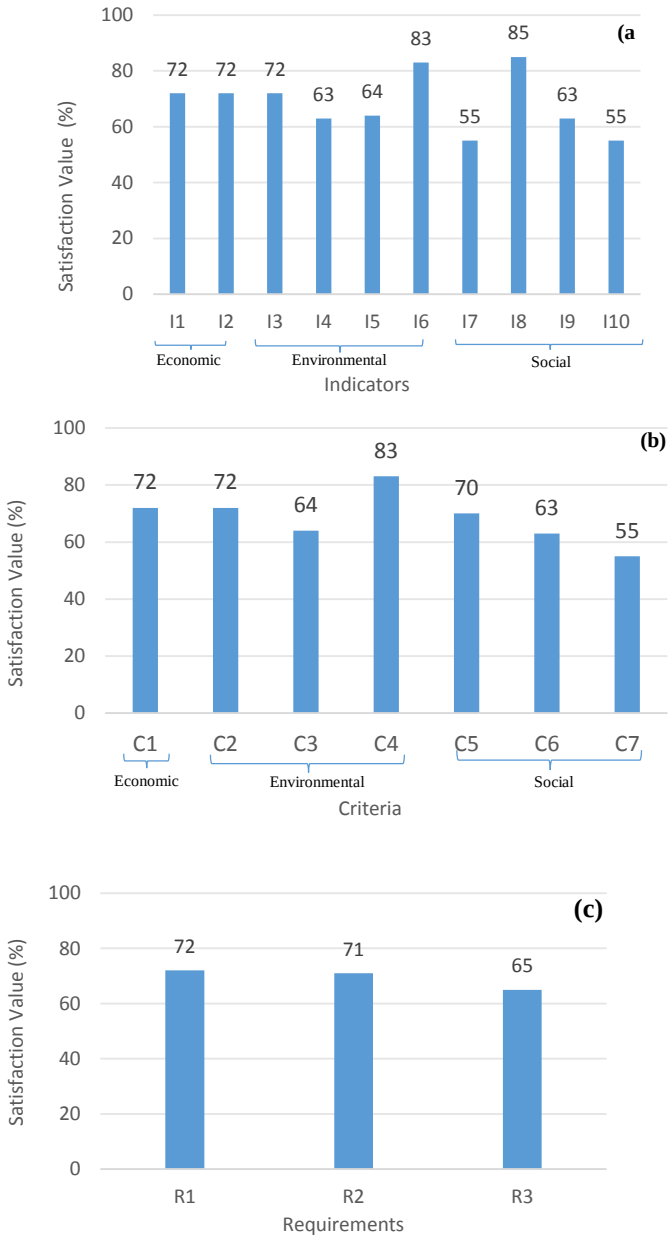

Figure 11. Satisfaction values of TW cement board : a) indicators; b) criteria; c) requirements

Table 7. Satisfaction values of all indices for the CTR and TW cement plates based on the proposed weights

Indices	Satisfaction Value of CTR	Satisfaction Value of TW
I_1	0.55	0.72
I_2	0.47	0.72
I_3	0.46	0.72
I_4	0.50	0.63
I_5	0.45	0.64
I_6	0.47	0.83
I_7	0.35	0.55
I_8	0.67	0.85
I_9	0.17	0.63
I_{10}	0.55	0.55
C_1	0.52	0.72
C_2	0.46	0.72
C_3	0.48	0.64
C_4	0.47	0.83
C_5	0.51	0.70
C_6	0.17	0.63
C_7	0.55	0.55
R_1	0.52	0.72
R_2	0.47	0.71
R_3	0.40	0.65
SI	0.46	0.70

Besides the final filtered weights allocated to the requirements for estimating the SIs of panels (30%, 40%, and 30% for *Economic*, *Environmental*, and *Social*, respectively), other possible weighting scenarios, according to the proposals by experts or those considered as outliers, were analyzed to recognize the requirements that governed the sustainability performance. This type of sensitivity analysis, a reliable validation tool in decision-making problems (Balali and Valipour, 2020), was carried out by considering 15 scenarios. As can be seen in Figure 12, the SIs did not change dramatically for the TW panel (< 5% in the range of 0.68–0.71) by changing the weights of the requirements since three requirements had satisfaction values in the same range; social requirements had a lower value of only 5%. Thus, when the weight of the social requirements reached a maximum value (70%), the SI had the lowest value (0.68). However, the economic and environmental requirements had the same importance and effect, that is, the SI value of the TW panel for the final suitable weight, the highlighted point (30Ec/40En/30S), was equal to 40Ec/30En/30S. This shows that for various stakeholders (private or public clients) and industry representatives with different viewpoints on sustainability, thereby different weighting scenarios according to the requirements, this material could maintain its acceptable SI.

Regarding the sensitivity analysis of the CTR panel, the SIs followed the same trend as the TW panel, i.e, no significant change was observed (about 7% in the range of 0.43-0.50). The lowest SI was obtained when the social requirements reached the highest point (70%) as this requirement had the lowest satisfaction value, 0.4. On the other hand, the highest SI obtained for the weight scenario included the highest economic and lowest social weights (70% and 10%, respectively).

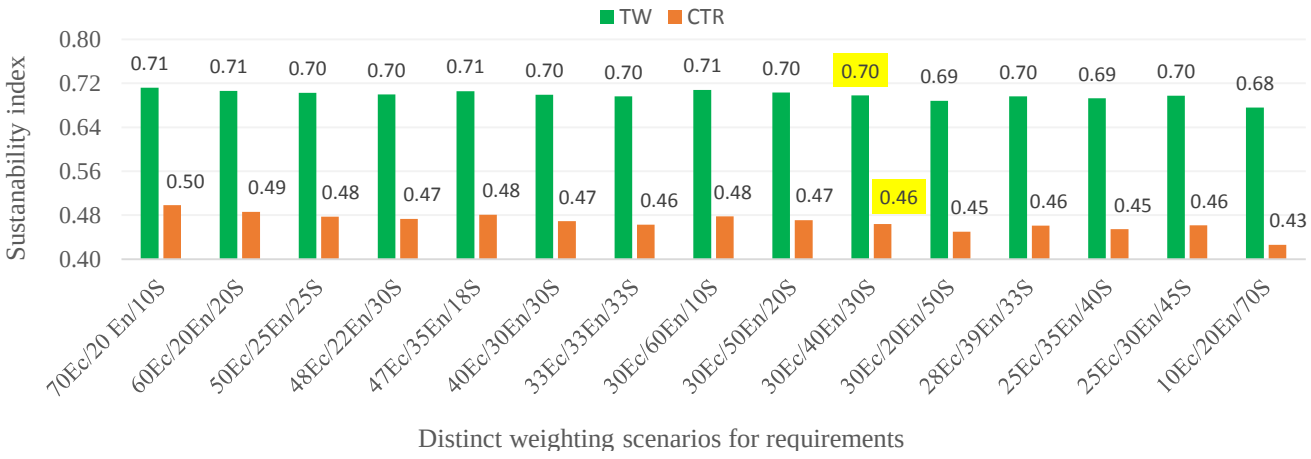

Figure 12. SIs generated by the model for TW and CTR panels based on several weighting scenarios. (Note: Ec, En and S refers to Economic, Environmnetal and Socail requirements, respectively)

6. Conclusions and perspectives

Sustainability performance assessment is complex and unfree of uncertainties related to the quantification and treatment of the indicators. This research presented a MIVES-based multi-objective approach for assessing the sustainability index (including economic., environmental. and social aspects) of facade panels. The approach was applied to new textile waste (TW) cement boards. Furthermore, an experimental program oriented to the characterization of the thermal, acoustic, and fire resistance of this material was performed within the context of this research, and the results were included in the sustainability assessment model. To this end, the sustainability sensitive indicators were identified through

extensive literature review and multi-disciplinary seminars. The relative importance (weights) of the indicators were established by means of the analytic hierarchy process with the experts' seminars. After estimating the indicators' performances for each material, and taking into account the value (satisfaction) functions defined and the weights' set, the sustainability index (ranging from 0.0 to 1.0) for each material alternative was computed.

Based on the analysis of the obtained results, the following conclusions can be drawn:

- The fire, thermal, and acoustic performance characterization revealed that the new material is compatible with external facade panels. Fire resistance was evaluated through epiradiator and small-scale fire testing. The TW samples proved not to be inflammable and maintained integrity above 950 °C. The post-fire flexural residual resistance of the TW cement board was almost six times higher than that of the control plate without any fiber. Moreover, the incorporation of TW fiber could improve the thermal and acoustic performance of the plate by 40% with respect to the benchmark.

- All the three requirements of sustainability (economic, environmental and social) resulted to perform equivalently (ranging from 0.65 to 0.72) for the TW cement board.

- The sustainability index of the prefabricated TWFRC facade-cladding panels for different weighting scenarios was in an acceptable range of 0.68–0.71, particularly for the optimum proposed weight was 0.7 (24% higher than the control plate).

- Although the general result was promising, for these new panels to achieve higher sustainability performance, some measures should be implemented: (1) to improve the aesthetic and external appearance by coating or coloring the panels and (2) to optimize the cement consumption through partial substitution by pozzolanic by-products or organic PCM paraffin waxes. However, any modification could affect other indicators, especially those related to economic performance.

Thus, based on this proposed model, designers and decision-makers may compare the sustainability index of various building materials to achieve the optimal facade cladding panels. MIVES, unlike other methods that overemphasize the environmental impacts, makes it feasible to analyze and prioritize material and construction alternatives while taking into account the three key pillars of sustainability and reducing the sources of subjectivity in the decision-making process.

It should be noted that in the present research study, this sustainability assessment was implemented on only two types of cement boards in a specific location, Barcelona. The weights proposed by the experts involved in the seminars could be adapted to reflect the perceptions and local preferences. Other study cases should be performed with the MIVES-based approach proposed in order to confirm whether the conclusions and outcomes exposed herein could be generalized and extrapolated.

Declaration of Competing Interest

The authors declare that they have no known competing financial interests or personal relationships that could have appeared to influence the work reported in this paper.

Acknowledgments

The authors express their gratitude to the Spanish Ministry of Economy, Industry, and Competitiveness for the financial support received under the scope of the projects CREEF (PID2019-108978RB-C32) and RECYBUILDMAT (PID2019-108067RB-I00).

References

Addis, B., 2012. Building with reclaimed components and materials: a design handbook for reuse and recycling.

Aguado, A., Caño, A. del, de la Cruz, M.P., Gómez, D., Josa, A., 2012. Sustainability Assessment of Concrete Structures within the Spanish Structural Concrete Code. J. Constr. Eng. Manag. 138, 268–276. https://doi.org/10.1061/(ASCE)CO.1943-7862.0000419

Akadiri, P.O., Olomolaiye, P.O., Chinyio, E.A., 2013. Multi-criteria evaluation model for the selection of sustainable materials for building projects. Autom. Constr. 30, 113–125. https://doi.org/10.1016/J.AUTCON.2012.10.004

Alarcon, B., Aguado, A., Manga, R., Josa, A., Alarcon, B., Aguado, A., Manga, R., Josa, A., 2010. A Value Function for Assessing Sustainability: Application to Industrial Buildings. Sustainability 3, 35–50. https://doi.org/10.3390/su3010035

Ali, H.H., Al Nsairat, S.F., 2009. Developing a green building assessment tool for developing countries – Case of Jordan. Build. Environ. 44, 1053–1064. https://doi.org/10.1016/J.BUILDENV.2008.07.015

António, J., 2011. Acoustic behaviour of fibrous materials, in: Fibrous and Composite Materials for Civil Engineering Applications. Elsevier, pp. 306–324. https://doi.org/10.1533/9780857095583.3.306

Ardanuy, M., Claramunt, J., Toledo Filho, R.D., 2015. Cellulosic fiber reinforced cement-based composites: A review of recent research. Constr. Build. Mater. 79, 115–128. https://doi.org/10.1016/j.conbuildmat.2015.01.035

Asadi, I., Shafigh, P., Abu Hassan, Z.F. Bin, Mahyuddin, N.B., 2018. Thermal conductivity of concrete – A review. J. Build. Eng. 20, 81–93. https://doi.org/10.1016/J.JOBE.2018.07.002

Bagheri Moghaddam, F., Fort Mir, J.M., Navarro Delgado, I., Redondo Dominguez, E., 2021. Evaluation of Thermal Comfort Performance of a Vertical Garden on a Glazed Façade and Its Effect on Building and Urban Scale, Case Study: An Office Building in Barcelona. Sustain. 2021, Vol. 13, Page 6706 13, 6706. https://doi.org/10.3390/SU13126706

Balali, A., Valipour, A., 2020. Identification and selection of building façade's smart materials according to sustainable development goals. Sustain. Mater. Technol. 26, e00213. https://doi.org/10.1016/J.SUSMAT.2020.E00213

Batista dos Santos, G.Z., Passos de Oliveira, D., de Almeida Melo Filho, J., Marques da Silva, N., 2021. Sustainable geopolymer composite reinforced with sisal fiber: Durability to wetting and drying cycles. J. Build. Eng. 43, 102568. https://doi.org/10.1016/J.JOBE.2021.102568

Borri, A., Corradi, M., Sisti, R., Buratti, C., Belloni, E., Moretti, E., 2016. Masonry wall panels retrofitted with thermal-insulating GFRP-reinforced jacketing. Mater. Struct. Constr. 49, 3957–3968. https://doi.org/10.1617/S11527-015-0766-4/FIGURES/9

Brandt, A.M., 2008. Fibre reinforced cement-based (FRC) composites after over 40 years of development in building and civil engineering. Compos. Struct. 86, 3–9. https://doi.org/10.1016/j.compstruct.2008.03.006

Brazão Farinha, C., de Brito, J., Veiga, R., 2021. Incorporation of high contents of textile, acrylic and glass waste fibres in cement-based mortars. Influence on mortars' fresh, mechanical and deformability behaviour. Constr. Build. Mater. 303. https://doi.org/10.1016/J.CONBUILDMAT.2021.124424

Briga-Sá, A., Nascimento, D., Teixeira, N., Pinto, J., Caldeira, F., Varum, H., Paiva, A., 2013. Textile waste as an alternative thermal insulation building material solution. Constr. Build. Mater. 38, 155–160. https://doi.org/10.1016/j.conbuildmat.2012.08.037

British Standards Institution., 2018. BS EN 13501-1:2018 Fire classification of construction products and building elements. Part 1 : classification using data from reaction to fire tests [WWW Document]. URL https://bsol-bsigroup-com.ezproxy.is.ed.ac.uk (accessed 11.8.20).

Brunsdon, B.N., 2018. Cladding costs over a lifetime. Build 163Better Build. 2017–2018.

Buratti, C., Belloni, E., Lunghi, L., Borri, A., Castori, G., Corradi, M., 2016. Mechanical characterization and thermal conductivity measurements using of a new "small hot-box" apparatus: innovative insulating reinforced coatings analysis. J. Build. Eng. 7, 63–70. https://doi.org/10.1016/J.JOBE.2016.05.005

Cabeza, L.F., Rincón, L., Vilariño, V., Pérez, G., Castell, A., 2014. Life cycle assessment (LCA) and life cycle energy analysis (LCEA) of buildings and the building sector: A review. Renew. Sustain. Energy Rev. 29, 394–416. https://doi.org/10.1016/J.RSER.2013.08.037

Cartelle Barros, J.J., Lara Coira, M., de la Cruz López, M.P., del Caño Gochi, A., 2015. Assessing the global sustainability of different electricity generation systems. Energy 89, 473–489. https://doi.org/10.1016/j.energy.2015.05.110

Cities - United Nations Sustainable Development Action 2015 [WWW Document], n.d. URL https://www.un.org/sustainabledevelopment/cities/#tab-2267862e52845f3d178 (accessed 3.15.22).

Claramunt, J., Fernández-Carrasco, L.J., Ventura, H., Ardanuy, M., 2016. Natural fiber nonwoven reinforced cement composites as sustainableClaramunt, J., Fernández-Carrasco, L. J., Ventura, H., & Ardanuy, M. (2016). Natural fiber nonwoven reinforced cement composites as sustainable materials for building envelopes. Constructio. Constr. Build. Mater. 115, 230–239. https://doi.org/10.1016/j.conbuildmat.2016.04.044

Claramunt, J., Ventura, H., Fernández-carrasco, L.J., Ardanuy, M., 2017a. Tensile and Flexural Properties of Cement Composites Reinforced with Flax Nonwoven Fabrics. Materials (Basel). 1–12. https://doi.org/10.3390/ma10020215

Claramunt, J., Ventura, H., Fernández-Carrasco, L.J., Ardanuy, M., 2017b. Tensile and flexural properties of cement composites reinforced with flax nonwoven fabrics. Materials (Basel). 10, 1–12. https://doi.org/10.3390/ma10020215

Colangelo, F., Farina, I., Travaglioni, M., Salzano, C., Cioffi, R., Petrillo, A., 2021. Eco-efficient industrial waste recycling for the manufacturing of fibre reinforced innovative geopolymer mortars: Integrated waste management and green product development through LCA. J. Clean. Prod. 312, 127777. https://doi.org/10.1016/J.JCLEPRO.2021.127777

De La Fuente, A., Pons, O., Josa, A., Aguado, A., 2016. Multi-criteria decision making in the sustainability assessment of sewerage pipe systems. J. Clean. Prod. 112, 4762–4770. https://doi.org/10.1016/j.jclepro.2015.07.002

Del Caño, A., Gómez, D., De La Cruz, M.P., 2012. Uncertainty analysis in the sustainable design of concrete structures: A probabilistic method. Constr. Build. Mater. 37, 865–873. https://doi.org/10.1016/j.conbuildmat.2012.04.020

Densley Tingley, D., Hathway, A., Davison, B., 2015. An environmental impact comparison of external wall insulation types. Build. Environ. 85, 182–189. https://doi.org/10.1016/J.BUILDENV.2014.11.021

Ding, G.K.C., 2008. Sustainable construction-The role of environmental assessment tools. J. Environ. Manage. 86, 451–464. https://doi.org/10.1016/j.jenvman.2006.12.025

Gálvez-Martos, J.L., Styles, D., Schoenberger, H., Zeschmar-Lahl, B., 2018. Construction and demolition waste best management practice in Europe. Resour. Conserv. Recycl. 136, 166–178. https://doi.org/10.1016/j.resconrec.2018.04.016

Giesekam, J., Barrett, J., Taylor, P., Owen, A., 2014. The greenhouse gas emissions and mitigation options for materials used in UK construction. Energy Build. 78, 202–214. https://doi.org/10.1016/J.ENBUILD.2014.04.035

Gilani, G., Blanco, A., Fuente, A.D. La, 2017. A New Sustainability Assessment Approach Based on Stakeholder's Satisfaction for Building Façades, in: Energy Procedia. Elsevier Ltd, pp. 50–58. https://doi.org/10.1016/j.egypro.2017.05.006

Gilani, G., Pons, O., de la Fuente, A., 2019. Towards the Façades of the Future: A New Sustainability Assessment Approach. IOP Conf. Ser. Earth Environ. Sci. 290, 012075. https://doi.org/10.1088/1755-1315/290/1/012075

Gong, T., Ahmed, A.H., Curosu, I., Mechtcherine, V., 2020. Tensile behavior of hybrid fiber reinforced composites made of strain-hardening cement-based composites (SHCC) and carbon textile. Constr. Build. Mater. 262, 120913. https://doi.org/10.1016/J.CONBUILDMAT.2020.120913

Gonzalez-Lopez, L., Claramunt, J., Haurie, L., Ventura, H., Ardanuy, M., 2021. Study of the fire and thermal behaviour of façade panels made of natural fibre-reinforced cement-based composites. Constr. Build. Mater. 302, 124195. https://doi.org/10.1016/J.CONBUILDMAT.2021.124195

Halvaei, M., 2021. Fibers and textiles reinforced cementitious composites. Eng. Polym. Fibrous Mater. 73–92. https://doi.org/10.1016/B978-0-12-824381-7.00001-9

Hammond, G., Jones, C., 2011. Inventory of carbon & energy Version 2.0 (ICE V2.0)-Department of Mechanical Engineering, University of Bath, Bath, UK.

Han, B., Wang, R., Yao, L., Liu, H., Wang, Z., 2015. Life cycle assessment of ceramic façade material and its comparative analysis with three other common façade materials. J. Clean. Prod. 99, 86–93. https://doi.org/10.1016/j.jclepro.2015.03.032

Hartkopf, V., Aziz, A., Loftness, V., 2012. Facades facade and Enclosures, Building building for Sustainability, in: Encyclopedia of Sustainability Science and Technology. Springer New York, pp. 3675–3705. https://doi.org/10.1007/978-1-4419-0851-3_873

Hay, R., Ostertag, C.P., 2018. Life cycle assessment (LCA) of double-skin façade (DSF) system with fiber-reinforced concrete for sustainable and energy-efficient buildings in the tropics. Build. Environ. 142, 327–341. https://doi.org/10.1016/J.BUILDENV.2018.06.024

High energy performing buildings - Publications Office of the EU [WWW Document], n.d. URL https://publications.europa.eu/en/publication-detail/-/publication/d8e3702d-c782-11e8-9424-01aa75ed71a1/language-en/format-PDF/source-77709912

Hosseini, S M Amin, De, A., Pons, O., 2016. Multi-criteria decision-making method for assessing the sustainability of post-disaster temporary housing units technologies : A case study in Bam , 2003 20, 38–51.

Hosseini, S. M. Amin, de la Fuente, A., Pons, O., 2016. Multicriteria Decision-Making Method for Sustainable Site Location of Post-Disaster Temporary Housing in Urban Areas. J. Constr. Eng. Manag. 142, 04016036. https://doi.org/10.1061/(ASCE)CO.1943-7862.0001137

Hosseini, S.M.A., Farahzadi, L., Pons, O., 2021. Assessing the sustainability index of different post-disaster temporary housing unit configuration types. J. Build. Eng. 42, 102806. https://doi.org/10.1016/J.JOBE.2021.102806

Hosseini, S.M.A., Pons, O., de la Fuente, A., 2018. A combination of the Knapsack algorithm and MIVES for choosing optimal temporary housing site locations: A case study in Tehran. Int. J. Disaster Risk Reduct. 27, 265–277. https://doi.org/10.1016/j.ijdrr.2017.10.013

Hosseini, S.M.A., Yazdani, R., Fuente, A. de la, 2020. Multi-objective interior design optimization method based on sustainability concepts for post-disaster temporary housing units. Build. Environ. 173, 106742. https://doi.org/10.1016/j.buildenv.2020.106742

ITeC - Institute of Construction Technology of Catalonia [WWW Document], 2020. . BEDEC. URL https://itec.cat/ (accessed 11.8.20).

Jia, Y., Zhao, R., Liao, P., Li, F., Yuan, Y., Zhou, S., 2017. Experimental study on mix proportion of fiber reinforced cementitious composites 020002.

John, G., Clements-Croome, D., Jeronimidis, G., 2005. Sustainable building solutions: a review of lessons from the natural world. Build. Environ. 40, 319–328. https://doi.org/10.1016/J.BUILDENV.2004.05.011

Khedari, J., Suttisonk, B., Pratinthong, N., Hirunlabh, J., 2001. New lightweight composite construction materials with low thermal conductivity. Cem. Concr. Compos. 23, 65–70. https://doi.org/10.1016/S0958-9465(00)00072-X

Kim, K.H., 2011. A comparative life cycle assessment of a transparent composite façade system and a glass curtain wall system. Energy Build. 43, 3436–3445. https://doi.org/10.1016/j.enbuild.2011.09.006

Kolaitis, D.I., Asimakopoulou, E.K., Founti, M.A., 2016. A FULL-SCALE FIRE TEST TO INVESTIGATE THE FIRE BEHAVIOUR OF THE "VENTILATED FAÇADE" SYSTEM.

Kvočka, D., Lešek, A., Knez, F., Ducman, V., Panizza, M., Tsoutis, C., Bernardi, A., 2020. Life cycle assessment of prefabricated geopolymeric façade cladding panels made from large fractions of recycled construction and demolition waste. Materials (Basel). 13. https://doi.org/10.3390/MA13183931

Lazar, N., Chithra, K., 2020. A comprehensive literature review on development of Building Sustainability Assessment Systems. J. Build. Eng. 32, 101450. https://doi.org/10.1016/J.JOBE.2020.101450

Lee, Y., Joo, C., 2003. Sound absorption properties of recycled polyester fibrous assembly absorbers. Autex Res. J. 3, 78–84.

Lei, D.Y., Guo, L.P., Li, Y., Zheng, Z., Liu, J.P., Li, S.C., Wang, P.G., Li, C.C., Mechtcherine, V., Li, Z.H., Zeng, D.Z., Zhong, B.M., 2021. The investigating on mechanical properties of ultra-high strength and ultra-high ductility cementitious composites (UHS-UHDCC). J. Build. Eng. 43, 102486. https://doi.org/10.1016/J.JOBE.2021.102486

Lertwattanaruk, P., Suntijitto, A., 2015. Properties of natural fiber cement materials containing coconut coir and oil palm fibers for residential building applications. Constr. Build. Mater. 94, 664–669. https://doi.org/10.1016/J.CONBUILDMAT.2015.07.154

Li, X., Qin, D., Hu, Y., Ahmad, W., Ahmad, A., Aslam, F., Joyklad, P., 2022. A systematic review of waste materials in cement-based composites for construction applications. J. Build. Eng. 45, 103447. https://doi.org/10.1016/J.JOBE.2021.103447

Malabi Eberhardt, L.C., Rønholt, J., Birkved, M., Birgisdottir, H., 2021. Circular Economy potential within the building stock - Mapping the embodied greenhouse gas emissions of four Danish examples. J. Build. Eng. 33, 101845. https://doi.org/10.1016/J.JOBE.2020.101845

Mohammadi, P., Ramezanianpour, A.M., Erfani, A., 2022. Identifying and Prioritizing Criteria for Selecting Sustainable Façade Materials of High-Rise Buildings. Constr. Res. Congr. 2022 583–593. https://doi.org/10.1061/9780784483978.060

Monge-Barrio, A., Sánchez-Ostiz, A., 2015. Energy efficiency and thermal behaviour of attached sunspaces, in the residential architecture in Spain. Summer Conditions. Energy Build. 108, 244–256. https://doi.org/10.1016/j.enbuild.2015.09.037

Nautiyal, H., Shree, V., Khurana, S., Kumar, N., Varun, 2015. Recycling Potential of Building Materials: A Review. Springer, Singapore, pp. 31–50. https://doi.org/10.1007/978-981-287-643-0_2

Nguyen, K.T.Q., Navaratnam, S., Mendis, P., Zhang, K., Barnett, J., Wang, H., 2020. Fire safety of composites in prefabricated buildings: From fibre reinforced polymer to textile reinforced concrete. Compos. Part B Eng. 187, 107815. https://doi.org/10.1016/J.COMPOSITESB.2020.107815

Novais, R.M., Carvalheiras, J., Senff, L., Lacasta, A.M., Cantalapiedra, I.R., Giro-Paloma, J., Seabra, M.P., Labrincha, J.A., 2020. Multifunctional cork – alkali-activated fly ash composites: A sustainable material to enhance buildings' energy and acoustic performance. Energy Build. 210, 109739. https://doi.org/10.1016/J.ENBUILD.2019.109739

Novais, R.M., Senff, L., Carvalheiras, J., Lacasta, A.M., Cantalapiedra, I.R., Labrincha, J.A., 2021. Simple and effective route to tailor the thermal, acoustic and hygrothermal properties of cork-containing waste derived inorganic polymer composites. J. Build. Eng. 42, 102501. https://doi.org/10.1016/J.JOBE.2021.102501

Ottelé, M., Perini, K., Fraaij, A.L.A., Haas, E.M., Raiteri, R., 2011. Comparative life cycle analysis for green façades and living wall systems. Energy Build. 43, 3419–3429. https://doi.org/10.1016/j.enbuild.2011.09.010

Perugini, F., Mastellone, M.L., Arena, U., 2005. A life cycle assessment of mechanical and feedstock recycling options for management of plastic packaging wastes. Environ. Prog. 24, 137–154. https://doi.org/10.1002/EP.10078

Pons, O., Aguado, A., 2012. Integrated value model for sustainable assessment applied to technologies used to build schools in Catalonia, Spain. Build. Environ. 53, 49–58. https://doi.org/10.1016/j.buildenv.2012.01.007

Pons, O., Franquesa, J., Hosseini, S.M.A., 2019. Integrated Value Model to Assess the Sustainability of Active Learning Activities and Strategies in Architecture Lectures for Large Groups. Sustainability 11, 2917. https://doi.org/10.3390/su11102917

Pons, O., Fuente, A. De, Aguado, A., Star, G., 2016. The Use of MIVES as a Sustainability Assessment MCDM Method for Architecture and Civil Engineering Applications. https://doi.org/10.3390/su8050460

Pons, O., Wadel, G., 2011. Environmental impacts of prefabricated school buildings in Catalonia. Habitat Int. 35, 553–563. https://doi.org/10.1016/J.HABITATINT.2011.03.005

Quintaliani, C., Merli, F., Fiorini, C.V., Corradi, M., Speranzini, E., Buratti, C., 2022. Vegetal Fiber Additives in Mortars: Experimental Characterization of Thermal and Acoustic Properties. Sustain. 2022, Vol. 14, Page 1260 14, 1260. https://doi.org/10.3390/SU14031260

Rahman, S.S., Siddiqua, S., Cherian, C., 2022. Sustainable applications of textile waste fiber in the construction and geotechnical industries: A retrospect. Clean. Eng. Technol. 6, 100420. https://doi.org/10.1016/J.CLET.2022.100420

Rakhsh Mahpour, A., Ardanuy, M., Ventura, H., Rosell, J.R., Claramunt, J., 2022. Rheology, Mechanical Performance and Penetrability through Flax Nonwoven Fabrics of Lime Pastes. Constr. Technol. Archit. 1, 480–490. https://doi.org/10.4028/WWW.SCIENTIFIC.NET/CTA.1.480

Ricciardi, P., Belloni, E., Cotana, F., 2014. Innovative panels with recycled materials: Thermal and acoustic performance and Life Cycle Assessment. Appl. Energy 134, 150–162. https://doi.org/10.1016/J.APENERGY.2014.07.112

Rubino, C., Liuzzi, S., Martellotta, F., Stefanizzi, P., n.d. Textile wastes in building sector: A review. https://doi.org/10.18280/mmc_b.870309

Saaty, T.L., 1990. How to make a decision: The analytic hierarchy process. Eur. J. Oper. Res. 48, 9–26. https://doi.org/10.1016/0377-2217(90)90057-I

Sadrolodabaee, P., Claramunt Blanes, J., Ardanuy Raso, M., Fuente Antequera, A. de la, 2021a. Preliminary study on new micro textile waste fiber reinforced cement composite. ICBBM 2021 4th Int. Conf. Bio-based Build. Mater. Barcelona, Catalunya June 16-18, 2021 Proc. 37–42.

Sadrolodabaee, P., Claramunt, J., Ardanuy, M., de la Fuente, A., 2021b. Mechanical and durability characterization of a new textile waste micro-fiber reinforced cement composite for building applications. Case Stud. Constr. Mater. 14, e00492. https://doi.org/10.1016/j.cscm.2021.e00492

Sadrolodabaee, P., Claramunt, J., Ardanuy, M., de la Fuente, A., 2021c. A Textile Waste Fiber-Reinforced Cement Composite: Comparison between Short Random Fiber and Textile Reinforcement. Mater. 2021, Vol. 14, Page 3742 14, 3742. https://doi.org/10.3390/MA14133742

Sadrolodabaee, P., Claramunt, J., Ardanuy, M., Fuente, A. de la, 2021d. Characterization of a textile waste nonwoven fabric reinforced cement composite for non-structural building components. Constr. Build. Mater. 276, 122179. https://doi.org/10.1016/j.conbuildmat.2020.122179

Sadrolodabaee, P., Hosseini, S.M.A., Ardunay, M., Claramunt, J., Fuente, A. de la, 2021e. A New Sustainability Assessment Method for Façade Cladding Panels: A Case Study of Fiber/Textile Reinforced Cement Sheets 809–819. https://doi.org/10.1007/978-3-030-83719-8_69

Salzer, C., Wallbaum, H., Lopez, L.F., Kouyoumji, J.L., 2016. Sustainability of social housing in Asia: A holistic multi-perspective development process for bamboo-based construction in the Philippines. Sustain. 8. https://doi.org/10.3390/su8020151

Schneider, M., Romer, M., Tschudin, M., Bolio, H., 2011. Sustainable cement production-present and future. Cem. Concr. Res. https://doi.org/10.1016/j.cemconres.2011.03.019

Shen, L.Y., Hao, J.L., Wing, V., Tam, Y., Yao, H., Shen, L., Hao, J.L., Tam, V.W., Yao, H., 2010. A checklist for assessing sustainability performance of construction projects PERFORMANCE OF CONSTRUCTION PROJECTS 3730.

Sørensen, B.L., Wenzel, H., 2014. Life cycle assessment of alternative bedpans – a case of comparing disposable and reusable devices. J. Clean. Prod. 83, 70–79. https://doi.org/10.1016/J.JCLEPRO.2014.07.022

Souza, A.B., Ferreira, H.S., Vilela, A.P., Viana, Q.S., Mendes, J.F., Mendes, R.F., 2021. Study on the feasibility of using agricultural waste in the production of concrete blocks. J. Build. Eng. 42, 102491. https://doi.org/10.1016/J.JOBE.2021.102491

Tie, T.S., Mo, K.H., Putra, A., Loo, S.C., Alengaram, U.J., Ling, T.C., 2020. Sound absorption performance of modified concrete: A review. J. Build. Eng. 30, 101219. https://doi.org/10.1016/J.JOBE.2020.101219

Villar-Cociña, E., Rodier, L., Savastano, H., Lefrán, M., Rojas, M.F., 2020. A Comparative Study on the Pozzolanic Activity Between Bamboo Leaves Ash and Silica Fume: Kinetic Parameters. Waste and Biomass Valorization 11, 1627–1634. https://doi.org/10.1007/s12649-018-00556-y

Wang, Y., Backer, S., Li, V.C., 1987. An experimental study of synthetic fibre reinforced cementitious composites. J. Mater. Sci. 22, 4281–4291. https://doi.org/10.1007/BF01132019

Yina, S., Tuladhar, R., Sheehan, M., Combe, M., Collister, T., 2016. A life cycle assessment of recycled polypropylene fibre in concrete footpaths. J. Clean. Prod. 112, 2231–2242. https://doi.org/10.1016/J.JCLEPRO.2015.09.073

Zhang, D., Dasari, A., Tan, K.H., 2018. On the mechanism of prevention of explosive spalling in ultra-high performance concrete with polymer fibers. Cem. Concr. Res. 113, 169–177. https://doi.org/10.1016/J.CEMCONRES.2018.08.012

Zhou, X., Zheng, F., Li, H., Lu, C., 2010. An environment-friendly thermal insulation material from cotton stalk fibers. Energy Build. 42, 1070–1074. https://doi.org/10.1016/J.ENBUILD.2010.01.020

3. CHAPTER ° III

RESEARCH CONTRIBUTIONS

This chapter reproduces the two published research contributions for conferences derived from the research work. Each paper follows its own numbering of sections, figures, equations, and references.

3.1 Research contribution I:
Preliminary study on new micro textile waste fiber reinforced cement composite

Published and Presented in ICBBM 2021: 4th International Conference on Bio-based Building Materials: Barcelona, Catalunya: June 16-18, 2021: proceedings

P.Sadrolodabaee [1], J.Claramunt [2], M.Ardanuy [3], A. de la Fuente[1]*
1: Department of Civil and Environmental Engineering- Universitat Politècnica de Catalunya-BarcelonaTECH-Barcelona, Spain
2: Department of Agricultural Engineering- Universitat Politècnica de Catalunya-BarcelonaTECH- Barcelona, Spain
3: Department of Material Science and Engineering (CEM)-Universitat Politècnica de Catalunya-BarcelonaTECH-Barcelona, Spain
**Corresponding author; payam.sadrolodabaee@upc.edu*

Abstract
Large amounts of nonrenewable resources are depleted by the construction industry in addition to the generation of million tons of mineral waste and carbon dioxide gas every year. For the sake of a more sustainable consumption pattern of building materials, as well as for reducing the waste flux to landfills, the use of recycled materials and wastes should be researched and motivated. One of the promising wastes is textile waste from residues of the garments and textile industries. The recycling and reusing of textile waste would be beneficial for reducing CO_2 emissions and energy intake. In this sense, there are already some studies regarding the thermal behavior of this type of material, however, the engineering design properties of textile waste fiber reinforced cement composites to identify the proper application have not been deeply investigated. Hence, the objective of this study was to evaluate the potentiality of using textile waste fiber as reinforcement in the cement paste. To this end, the composites with three different treatments were made and the optimum treatment was chosen based on the flexural test. The result is the feasibility of using this kind of fiber as reinforcement of mortar elements with dewatering treatment.

Keywords:
cementitious materials; fiber-reinforced composites; mechanical properties; recycled fibers; sustainability; textile waste.

1. INTRODUCTION
The construction and building sector is one of the biggest consumers of natural resources in the world and consequently, one of the biggest waste producers worldwide [1]. Based on the statistics, this sector consumes 25% of virgin wood, 17% of freshwater, and 40% of all raw materials (e.g., stone, gravel and sand) extracted worldwide, and is responsible for around 40% of all global greenhouse gas emissions in addition to the generation of around 35% of all global waste [2],[3]. That is why it is necessary to implement reduce, reuse, and recycle concepts (3Rs) as well as development in waste management policy in all aspects of the construction sector including material fabrication.

The use of more sustainable materials obtained from renewable sources or secondary raw materials with recycling and reusing processes could be an interesting solution for the reduction of CO_2 emissions and energy intake [4]. Fiber-reinforced mortars are among the materials which have attained great interest in several fields of building technology (e.g., façade panels, roofing, raised floors, and masonry structures). These composite materials can be constituted of various kinds of fibers - steel, glass, and polymeric - together with a cementitious matrix which can be in the form of cement paste, lime binder, mortar, or

concrete. The main role of the fiber is to bridge the cracks as well as enhancing the toughness, energy absorption capacity and post-cracking behavior of the cementitious matrices [5]–[7].

World fiber production has been steadily increasing in the past few decades, now exceeding 100 million tons per year [8]. Thus, the incorporation of more sustainable fibers produced from renewable, biodegradable, recycled, available and low-cost resources could be profitable. In this sense, vegetable and cellulosic fibers have been already used as sustainable reinforcement in mortars and composites for low to medium-performance structural applications [5], [6], [9], [10]. Another promising and sustainable type of fiber as reinforcement for cement-based materials could be textile waste fiber.

The textile leftover - including all fiber, yarn and fabric waste produced during the garment manufacturing in addition to worn out clothing discarded by the users - is one of the main waste resources worldwide. Nevertheless, only 25% of these textiles are recycled and the rest goes to landfills which resulted in rising waste disposal costs [11],[12]. Thus, reusing and recycling of these textile waste cutting in material production can reduce this cost as well as preserving the natural mineral resources.

Since there is still a lack of confidence in the quality of recycled materials, the recycling rate is relatively low. Therefore, new research projects with innovative solutions by implanting recycled materials should be carried out in order to overcome these uncertainties. In this sense, the goal of this research consists of carrying out an experimental program to characterize the mechanical properties of a new short randomly dispersed textile waste fiber-reinforced cement paste meant for construction purposes. To this end, after identifying the initial physical and chemical properties of the textile waste fiber, the reinforced composites with three different treatments were made and the optimum treatment was chosen based on the flexural strength capacities.

2. EXPERIMENTAL PROCEDURE

2.1 Materials

Binder

A Portland cement Type I 52.5R supplied by Cementos Molins Industrial, S.A. (Spain) has been used for producing the mortars. Chemical composition criteria and physical/mechanical requirements according to EN 197-1:2011 and given by (MOLINS, 2016) are reported in Tab. 1.

Fibers

Textile Waste (TW, hereinafter) fibers used for reinforcing the mortars were provided by Triturats La Canya S.A (Spain) and these consisted of 30.7% polyester and 69.3% cotton. In order to reach this composition, several samples of fibers were tested based on the UNE 40-110-94, in which sulfuric acid was used to dissolve the cotton, so the amount of polyester was remained and estimated. Moreover, the moisture content (expressed as relative humidity) and the water retention values were calculated which resulted in 7 and 85%, respectively. The gross 75% of the total weight of the analyzed TW is represented by fibers with diameters ranging from 3.6 to 32.1 μm, the rest being a mix of yarns and fabrics (see Fig. 1).

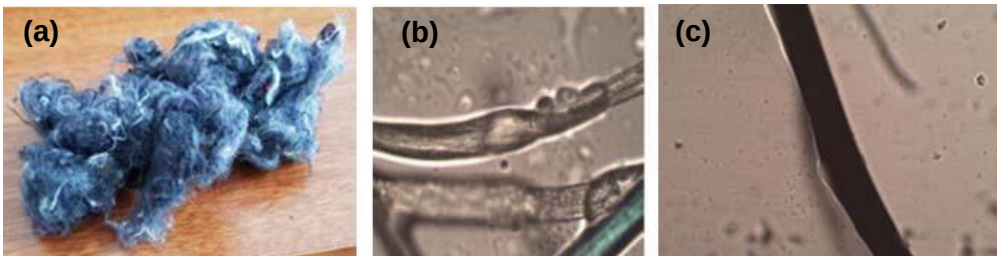

Fig. 1: (a) Textile Waste Fiber (TWF); microscopic image of the TWF components: (b) cotton – magnification 40x1 and (c) polyester – magnification 40x1.25

Tab. 1: Chemical composition and physical and mechanical properties for cement Type I 52.5R supplied by Cementos Molins and requirements according to EN 197-1:2011

Content	Typical values	EN 197-1:2011
Clinker (%)	98	min95 - max100
Minor component (%)	2	min0 - max5
Loss of Calcination (%)	2.5	max 5
Sulfate, SO3 (%)	3.4	max 4
Chlorides, Cl- (%)	0.04	max 0.1
Insoluble residue (%)	0.7	max 5
Blaine specific surface (cm^2/g)	4600	-
Expansion of Le Chatelier (mm)	0.5	max 10
Initial setting time (min)	110	min 45
Final setting time (min)	170	max 720
1-day compressive strength (N/mm^2)	27	-
2-days compressive strength (N/mm^2)	40	min 30
7-days compressive strength (N/mm^2)	52	-
28- days compressive strength (N/mm^2)	61	min 52.5

2.2 Samples preparation

In order to reach the best treatment for the composite, three different samples by different methods were produced. The first sample (NT: Non-Treatment) was made with virgin and intact TW fibers without any treatment, neither on the fibers nor on the composite. The second one (CT: Compression Treatment) was made also with the intact fibers, however after the mortar was cast, the mould underwent the dewatering procedure, including compression of 4 Mpa for 24 h to eliminate the excess water. The third sample (CFT: Compression and Fiber Treatment) produced with treated fibers underwent the dewatering process as well. The fiber treatment consisted of cleaning by means of degreasing soap and water in addition to sieving with the aim of eliminating the yarns and too short fibers, which resulted in more homogeneous fiber with diameters between 0.25 to 1.0 mm. Finally, the reference sample (REF) without any fibers was produced while fine sand substituted the fibers with the same volume. The REF sample also underwent the press machine for the dewatering process.

All the mentioned samples were prepared in a laboratory mixer pan and posteriorly cast into a 5×10×70 mm mold. After remaining 24 h under the press machine for dewatering, except NT, posteriorly demolded and placed in a climate chamber (20°C and 90% of RH) for 7 days. Fig. 2 depicts the casting and curing procedure carried out.

The designation of the specimens (Tab. 2) is based on the treatment used: NT being the Non-Treatment sample, CT refers to Compression Treatment, CFT the Compression and Fiber Treatment while REF is the Reference sample without fiber. The fiber amount was set to 6% of cement weight. The initial and final water/cement ratios, $(w/c)_{initial}$ and $(w/c)_{final}$, together with the initial dosage of the materials to make the fiber-reinforced mortar for 20 cm3 are also reported in Tab. 2. The final water was calculated after weighing the amount of water eliminated by the dewatering treatment.

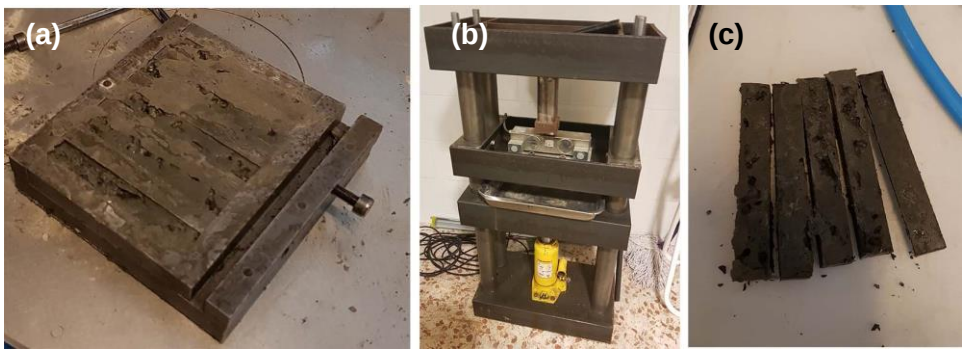

Fig. 2: Preparation of the samples: (a) molds filled with material;(b) compression and water excess elimination process and (c) demolded specimens

Tab. 2: w/c of the samples and codification of the specimens

CODE	**NT** (NonTreatment)	**CT** (Compression Treatment)	**CFT** (Compression and Fiber Treatment)	**REF** (Reference)
$(w/c)_{initial}$	0.50	0.50	0.50	0.50
$(w/c)_{final}$	0.50	0.40	0.40	0.40
Initial cement (g)	50	50	50	50
Initial fiber (g)	3	3	3	0
Fine sand (g)	0	0	0	7
No. specimens	5	5	7	3

2.3 Flexural tensile strength and toughness test

Three-point flexural tests based on EN 12467:2012 (Fig. 3), by using a Textueometer TA.XT machine equipped with a load cell of 0.5 KN capacity on 50 mm span-length unnotched beam specimens, was carried out in order to identify the extent of the fiber contribution to bridge the cracks. The test was controlled with a closed-loop system and the loading rates of 6 mm/min.

The maximum flexural tensile strength (or also named Modulus of Rupture, MOR) of the composite was determined by means of Eq. 1, where Pmax is the maximum load recorded, L is the span length, and b and h are the cross-sectional width and thickness, respectively. The toughness index (I_G), defined as the area beneath the force-displacement relationship derived from the flexural test and comprised from zero to a post-failure load of 0.4.MOR was established as the reference parameter to characterize the type of failure (ductile or fragile) and the post-failure deformation capacity. The flexural stiffness or modulus of elasticity in the pre-cracked zone (K) was also measured from the force-displacement relationships during elastic deformation by using Eq. 2, where Δp and Δf are the variations of forces and deflections of two points on the elastic regime, and the rest of the parameters as defined per Eq. 1.

$$MOR = \frac{3P_{\max}L}{2bh^2} \quad (1)$$

$$K = \frac{\Delta p..L^3}{4\Delta f.bh^3} \quad (2)$$

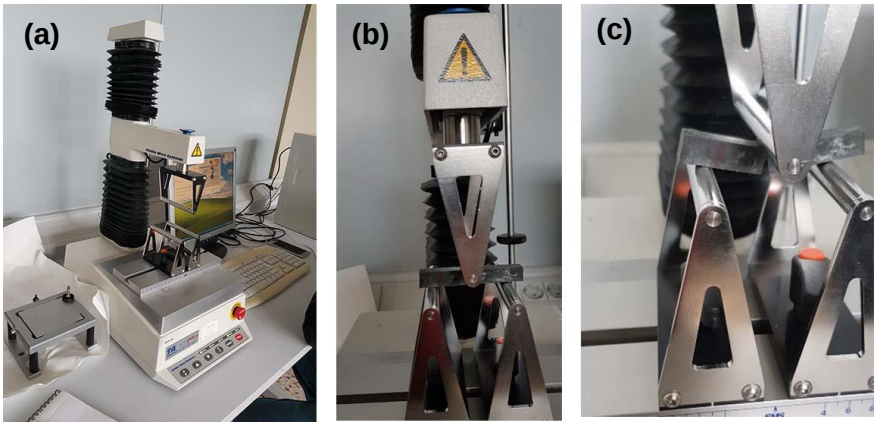

Fig. 3: Flexural tests set-up: (a) test machine; (b) flexural test configuration; (c) broken specimen

3. RESULTS AND DISCUSSIONS

In Fig. 4, the representative flexural stress-displacement curves derived from the flexural tests are depicted. Likewise, Tab. 3 gathers the mean and CoV of the Limit of proportionality (LOP), the Modulus of rupture (MOR), flexural toughness (I_G), and stiffness (k) obtained for each sample. As can be seen in Fig. 4, the bending response of all samples, except REF, consists of three stages: First, an elastic range represented by a linear tendency until the appearance of the first crack when the LOP strength is achieved. Second, a short post-cracking branch with a decreasing positive slope in which both matrix and fibers contribute to the strength of the composite and increase the toughness and ductility. Finally, a post-failure regime with a decreasing negative slope represents the pre-and failure of the composite. However, the REF sample without any fiber missed the second stage which can prove that short textile waste fibers contribute to increasing the post-failure ductility and toughness of the mortar. In this regard, the highest toughness index belongs to the CT sample followed by NT and CFT, however, the REF sample shows a brittle behavior with an 85% lower toughness magnitude with respect to CT (see Tab. 3).

The LOP values presented in Tab. 3 lead to conclude that the average flexural resistance to the first crack was reduced with the addition of 6% fibers. The reason could be that this parameter mainly depends on the mortar matrix properties and the amount of mortar decreased by adding fibers (see Tab. 2). Hence, the REF sample without any fibers proved the highest value while the NT with the highest (w/c) final, due to the non-dewatering process, had the lowest LOP. Among CT and CFT samples, the one with the virgin fiber proved a better resistance probably due to the better distribution into the matrix. The flexural stiffness modulus followed the same trend as LOP since this parameter depends mainly on the matrix characteristics as well.

On the other hand, the values of MOR gathered in Tab. 3 and Fig. 5 permit to confirm that the addition of intact TW fibers provides a post-cracking flexural strength capacity (MOR_m /LOP_m>1) to the CT and NT composite, this presenting a flexural-hardening response. Once the cracking occurs, fibers bridge the cracks by controlling the opening and guaranteeing a stress transfer mechanism across the crack which is the main role of fiber as reinforcement. However, the two other samples were deprived of this benefit due to non-homogenous distribution and absence of fiber, for CFT and REF respectively.

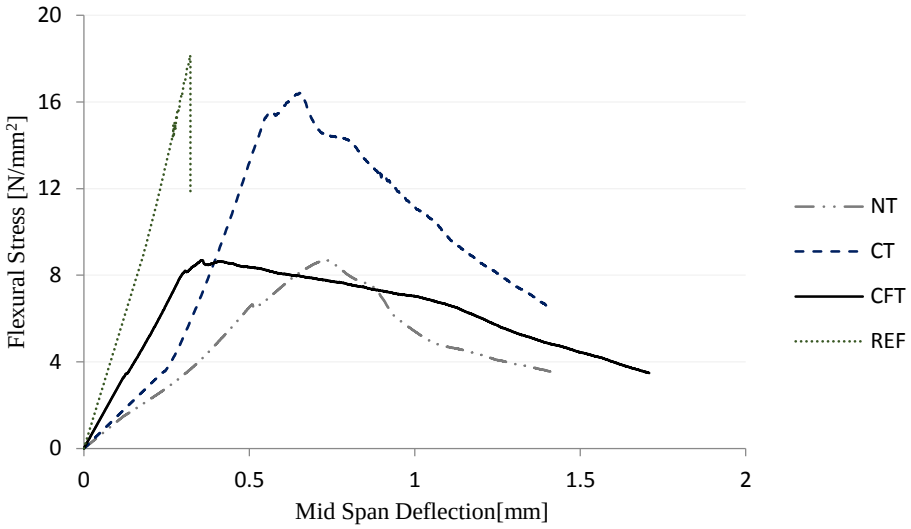

Fig. 4: Representative stress – deflection relationships obtained from the flexural tests at 7days

Table 3– Results of flexural tests (CoV in %)

CODE	LOP_m (N/mm^2)	MOR_m (N/mm^2)	I_{Gm} (KJ/m^2)	K_m (GPa)	MOR_m/LOP_m
NT	6.2(4)	7.8(14)	0.9(20)	0.9(11)	1.2
CT	12.5(17)	15.5(21)	1.4(20)	3.1(16)	1.2
CFT	9.0(12)	9.2(17)	0.9(26)	2.1(28)	1.0
REF	18.0(3)	18.0(4)	0.2(5)	6.2(8)	1.0

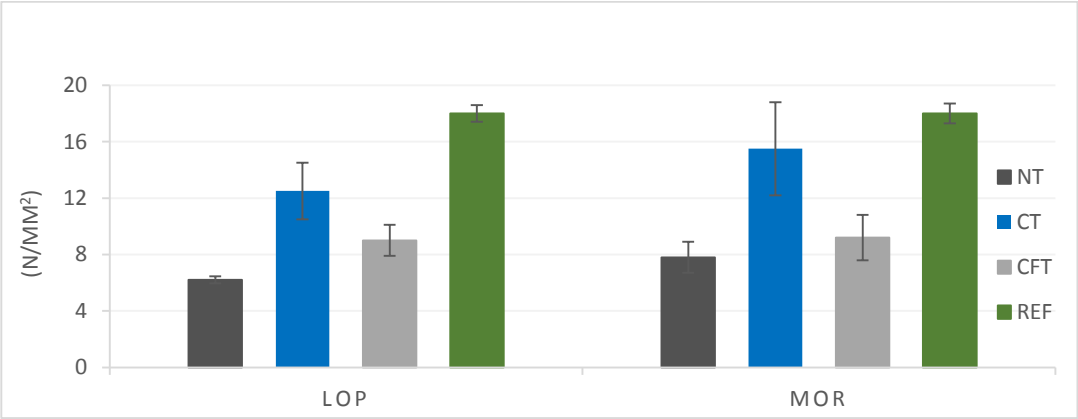

Fig. 5: Results of LOPm and MORm for the tested samples

4. CONCLUSIONS

The objective of this research was to verify the possibility of using short fibers from cloth waste as reinforcement for cement composites. In order to identify the target potential structural/nonstructural applications of this material, the mechanical properties should be characterized. These recycled fibers are constituted of cotton and polyester from the garment and textile waste industries. The use of these composites in building sectors can valorize this waste while reducing the harmful impact of construction on the environment.

To aim this purpose, three different samples with various treatments were made from this fiber and the flexural test was carried out after 7 days. The same test was performed for the reference sample without any fiber. The following conclusions were derived from the results:

- The results showed that the best treatment among the three methods for making the composite would be using the intact short TW fibers with the dewatering compression process (CT). This treatment increases the flexural tensile strength and toughness, up to 75 and 55% respectively, in comparison to the other methods.
- Although the reference sample had a little higher bending resistance than the CT sample, the toughness, and energy absorption of the former is one-seventh with respect to the latter which shows a very brittle behavior, not suitable as building components.

After this promising result in improving the toughness and energy absorption of the cement matrix, the mechanical characteristics (including flexural and compressive strengths at 7, 28, and 56 days as well as toughness and stiffness) together with durability properties- exposure to accelerated aging- of cement paste reinforced with various content of 6 to 10% randomly short Textile Waste Fiber has been currently investigated and the results are being analyzed. Moreover, the possibility of producing nonwoven textile fabric composites from this short textile waste fiber is under investigation since it is expected that the post cracking performance and energy absorption can be further enhanced and the range of the applications widened thereof. Both aspects of the potential applications and sustainability assessment of TW composites are being researched within the context of the Ph.D. thesis of the first author of this paper.

ACKNOWLEDGMENTS

This work was supported by the Spanish Government, Ministerio de Ciencia e Innovación [grant number PID2019-108067RB-I00].

REFERENCES

[1] D. Kvočka et al., “Life cycle assessment of prefabricated geopolymeric façade cladding panels made from large fractions of recycled construction and demolition waste,” Materials (Basel)., vol. 13, no. 18, 2020.

[2] A. F. Abd Rashid and S. Yusoff, “A review of life cycle assessment method for building industry,” Renewable and Sustainable Energy Reviews, vol. 45. Elsevier Ltd, pp. 244–248, 01-May-2015.

[3] A. Di Maria, J. Eyckmans, and K. Van Acker, “Downcycling versus recycling of construction and demolition waste: Combining LCA and LCC to support sustainable policy making,” Waste Manag., vol. 75, pp. 3–21, May 2018.

[4] H. Nautiyal, V. Shree, S. Khurana, N. Kumar, and Varun, “Recycling Potential of Building Materials: A Review,” Springer, Singapore, 2015, pp. 31–50.

[5] M. Ardanuy, J. Claramunt, and R. D. Toledo Filho, “Cellulosic fiber reinforced cement-based composites: A review of recent research,” Constr. Build. Mater., vol. 79, pp. 115–128, 2015.

[6] F. Pacheco-Torgal and S. Jalali, “Cementitious building materials reinforced with vegetable fibres: A review,” Constr. Build. Mater., vol. 25, no. 2, pp. 575–581, 2011.

[7] J. O. Lerch, H. L. Bester, A. S. Van Rooyen, R. Combrinck, W. I. de Villiers, and W. P. Boshoff, "The effect of mixing on the performance of macro synthetic fibre reinforced concrete," Cem. Concr. Res., vol. 103, no. May, pp. 130–139, 2018.

[8] CHF, "Licensed for The Fiber Year GmbH The Fiber Year 2018 World Survey on Textiles & Nonwovens," 2018.

[9] C. Correia, S. Francisco, H. Savastano, and V. Moacyr, "Utilization of vegetal fibers for production of reinforced cementitious materials," no. 2017, 2018.

[10] L. Mercedes, L. Gil, and E. Bernat-maso, "Mechanical performance of vegetal fabric reinforced cementitious matrix (FRCM) composites," Constr. Build. Mater., vol. 175, pp. 161–173, 2018.

[11] A. Villanueva, L. Delgado, Z. Luo, P. Eder, A. Sofia Catarino, and D. Litten, "Study on the selection of waste streams for end-of-waste assessment. Final Report."

[12] H. Song, W. Baek, S. Lee, and S. H. Hong, "Materials Processing Technology," Milling, vol. 48, pp. 4–9, 1997.

3.2 Research contribution II:
A New Sustainability Assessment Method for Façade Cladding Panels: A Case Study of Fiber/Textile Reinforced Cement Sheets

Published and Presented in RILEM-fib International Symposium on Fibre Reinforced Concrete (BEFIB 2021: Fibre Reinforced Concrete: Improvements and Innovations II pp 809-819)

Payam Sadrolodabaee [(1)] *, S.M. Amin Hosseini [(2)], Monica Ardunay[(1)], Josep Claramunt [(1)], and Albert de la Fuente [(1)]

[(1)] Polytechnic University of Catalonia - BarcelonaTECH, Barcelona, Spain.

[(2)] RESUME TECH, Barcelona, Spain.

* Corresponding author: payam.sadrolodabaee@upc.edu

ABSTRACT

As the building sector is one of the leading responsible for energy consumption and CO_2 emissions, criteria of sustainability, availability, and recyclability should be considered for developing materials even in the envelopes. Façade, as the first element against the undesirable external impact, may contribute to building sustainability by reducing the amount of energy consumption and providing indoor environment quality for the inhabitants. The envelope excluding its aesthetic function should fulfill certain requirements such as strength, flexibility, ductility, lightness, thermal and acoustical insulation, durability, and sustainability. Fiber/Textile cement sheets as an interesting architectural material attract great interest during the last decade, especially those reinforced with more sustainable fibers like vegetables or textile wastes. In this sense, this paper presents a novel model to evaluate the sustainability index of the façade cladding panel, especially the fiber/textile cement board. To this end, a new model for assessing objectively the façade cladding sustainability was designed and developed based on MIVES according to the value function concept and seminars of experts.

KEYWORDS: Cladding panels; Fiber cement boards; MIVES; Recycled fibers; Sustainability.

1. Introduction

Sustainable construction is considered as a way to contribute to sustainable development by protecting the environment. The building sector causes some negative effects on the environment during various phases including materials production, construction on the site, the usage phase and the demolition or end of life [1]. In this sense, based on the statistics, the construction sector is responsible for about 36% of the European Union's total CO_2 emissions, 40% of its final energy consumption and approximately 46% of the total waste [2]. That is why innovations to improve the energy efficiency of the buildings as well as developing more environmentally-friendly materials are then of practical importance.

The building enclosure is one of the dominant parts of each building that plays a pivotal role in sustainability and energy efficiency [3]. Currently, "Ventilated Façade", a double-wall construction comprising an external cladding panel and the outdoor side of the external wall, is among the most used constructive solutions for building envelopes. This system has continuity between the thermic and impermeable envelopes, avoiding thermal bridges and consequently avoiding the energy loss and the presence of water vapor condensations [4], [5].

The outer cladding material should satisfy both the architectural and engineering properties to meet the desired needs. Ceramics and natural stones, in addition to wood and aluminum composites, are among the conventional materials used for cladding facades. The former group usually has excessive weight and high stiffness, which limits their size and necessitates a complex supporting structure. Furthermore, the partial breaking of this heavy material which can lead to objects falling on public roads can impose a serious

risk for pedestrians. The latter group is more flexible and lightweight but less durable, has a lower hardness, and is more expensive compared to the former [5]. For these reasons the new generation of composite panels, fiber/textile reinforced cement boards (FRC/TRC boards), has been developed for building envelopes.

During the past decades, the incorporation of various types of fibers such as asbestos, steel, glass and polymeric into cement-based materials was proved to enhance the performance in terms of ductility, tensile or flexural strength, toughness, fatigue strength, impact resistance and energy absorption capacity of matrices [6]–[10]. However, some limitations such as harmful health impacts, expenses, and environmental pollution [11] make researchers discover more sustainable fibers. Vegetable and cellulosic together with textile waste fibers have recently attracted great interest as a suitable reinforcement in mortars and composites for low-performance structural applications [12]–[17]. Vegetable fibers as available and biodegradable, along with textile waste as recycled and inexpensive fibers, could allow the development of more sustainable construction materials.

Most of the existing sustainability assessment methods and tools in the building sector only consider the environmental aspect, thus leading to a non-comprehensive sustainability assessment of buildings [18]. The tools and methods which include more than one sustainability requirement, adding economic, social, or even technical and functional to environmental requirements, have recently increased [19]. Furthermore, there is scarce research on the sustainability assessment of independent building elements or structures. Regarding the facade cladding panels, a limited number of studies have employed life cycle assessment to evaluate the only environmental performance [20], [21].

In this regard, the objective of this conference paper is to present a new sustainability assessment model for analyzing the sustainability index (SI) of the cladding façade panels by evaluating more than one requirement based on MIVES (from the Spanish Integrated Value Model for the Sustainability Assessment). MIVES is a new comprehensive and integrated Multi-Criteria Decision Making (MCDM) method capable of assessing viable solutions for sustainability while considering economic, environmental, social and even technical requirements [22]. This new sustainability model for the façade cladding panel would be applied to a new Textile Reinforced Mortar (TRM) panel to consider the potentiality of this new board as a sustainable cladding material in a residential building in Barcelona, Spain.

This new cement sheet, with a surface mass of about 16 kg/m^2 and thickness of 10 mm, constituted of cementitious mortar reinforced by textile waste (TW) nonwoven fabrics as explained deeply in [17]. Figure 1 demonstrates the fabrication process of the panel as well as the flexural test configuration. The optimum panel was made up of the Portland cement paste reinforced by the 6 layers of the reinforcement. Table 1 gathers the mean of the flexural strength, toughness and flexural stiffness of the pre-cracked zone for the optimum cement sheet in both unaged and aged conditions. The aged condition consisted of subjecting the plates to 25 dry-wet cycles, after 28 curing days, in order to estimate the durability of the TW nonwoven fabric within the mortar matrix.

Table 1. Mechanical characteristics of TW cement board composite.

Mechanical properties	unaged sample	Aged sample*
Mean 28-day Flexural Strength [MPa]	15.5	10
Mean Toughness Index [KJ/m^2]	9.7	6.8
Mean Flexural Stiffness [GPa]	11.3	12
*aged sample: after exposure to accelerated aging of wet-dry cycles		

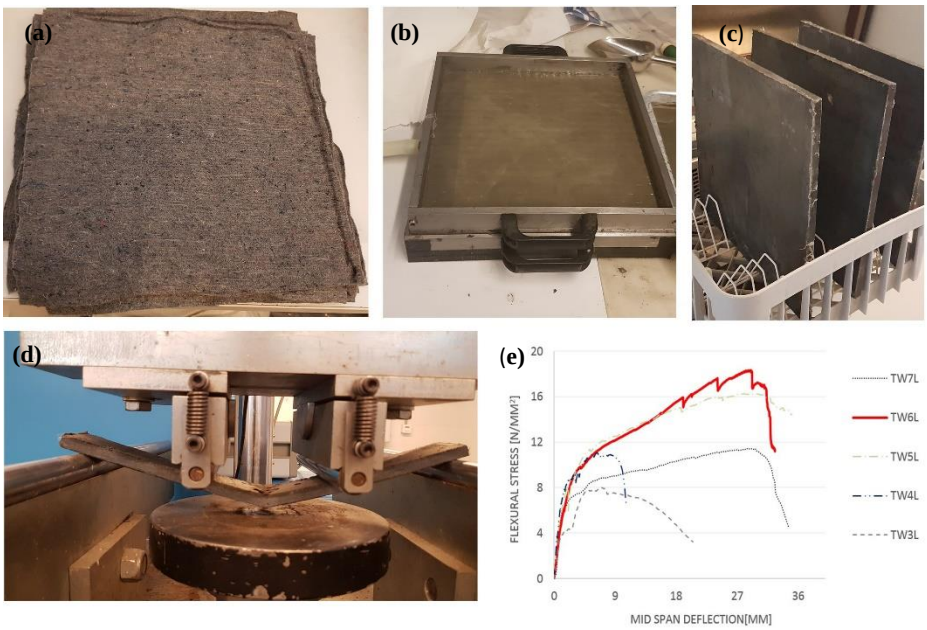

Figure 1. TW composites: a) TW fabric; b) Casting in the mold; c) TW cement boards; d)Flexural configuration; e) Experimental flexural-deflcetion curve

2. Model design

A holistic approach was implemented in this paper to present a general model for the sustainability assessment of cladding panels. To develop the method, data collection and data analysis of cladding panels, particularly oriented to fiber cement sheets, was already done and the model design and model application are in progress. The design of the requirement tree, based on the local characteristics of the case study and its demands, is the first step of the model design. Then, the assignation of weights for indices (requirement, criteria, and indicator) will be evaluated by a group of multidisciplinary experts through the analytical hierarchy process (AHP). Finally, the value function concept is used to transform the results obtained by each indicator to a non-dimensional magnitude value while minimizing the subjectivity in the assessment [23]. Thus, different alternatives could be evaluated and compared through the model and a sustainability index of each one is obtained. In the following parts, the aforementioned steps of MIVES are defined and designed.

2.1. Requirements tree

The requirements tree is a hierarchical diagram in which the various characteristics of the products or processes to be evaluated are organized, at three levels: requirements, criteria and indicators. This requirements tree was developed based on data collected from an extensive literature review and seminars with multidisciplinary experts in this subject. Based on the MIVES concept, indicators should be independent of each other and considered only once [23], so some indicators should be disregarded due to either their lack of representativeness or due to certain overlapping with other indicators already considered.

The preliminary requirement tree of this research was shown in Table 2. As can be seen, the first level of the tree included 4 requirements (R): economic, environmental, social, and technical. The second hierarchical level consisted of 8 criteria (C) and the last level included 14 indicators (I). The *economic requirement* (R_1) measures the estimated investment for the implementation of the cladding façade with the *cost* (C_1) being the determining criterion. The *environmental requirement* (R_2) assesses the environmental

effect of the panels during the life cycle through *emission* (C_2), *resource consumption* (C_3), *and waste* (C_4) *criteria*. The *social requirement* (R_3) considers the health and welfare of people by three criteria: (C_5) *comfort*, (C_6) *safety*, and (C_7) *aesthetic*. Finally, the *technical requirement* (R_4) assesses the mechanical properties of a material by the *reliability* (C_8) criterion.

The *cost* (C_1) includes two indicators: the (I_1) *construction cost* of the external cladding panel including material fabrication, transportation, labor costs, and installation. To estimate this indicator, around 40 composite panels including different fiber cement/mortar boards, ceramics, aluminum panels, and galvanized steel sheets were analyzed. To this end, the online BEDEC database from the Technological Institute of Catalonia (ITeC) [24] was used. The other indicator is (I_2) *maintenance cost* which estimated expected operations such as cleaning, repairing, and replacing during the service life of the panel, usually considered to be 50 years.

The *emission* (C_2) criterion is represented by the indicator of *CO_2 emissions* (I_3) to measure the amount of CO_2 emissions for each cladding panel in the phases of manufacturing and construction. The BEDEC [24] together with The Inventory of Carbon & Energy (ICE) [25] were considered as the reference databases for quantifying this indicator.

The *resource consumption* (C_3) criterion is aimed at quantifying the natural resources consumed, through two indicators. The *energy consumption* (I_4) indicator accounts for the amount of energy consumed during the manufacturing and construction phases. Once more, BEDEC and ICE were considered as a database. The *material consumption* (I_5) considering the amount of raw materials and water used in the fabrication stage, estimated by BEDEC and Environmental Product Declaration (EPD) of materials.

The *waste* (C_4) criterion is assessed by the indicator of *Solid waste management* (I_6) to estimate the amount of waste materials used in the manufacturing phase or the quantity that can be recycled after demolition. A measurable scale of 0 to 20 is used to rate the recyclability of cladding panels through seminars with multidisciplinary engineers and literature reviews.

Comfort (C_5) considers two indicators: (I_7) *acoustic performance*, which evaluates the rate of sound absorption of material by NRC, Noise Reduction Coefficient, a standard rating for how well a material absorbs sound. (I_8) *Thermal performance*, which assesses the thermal conductivity of the different cladding panels, the ability to conduct the heat.

S*afety* (C_6) is meant to assess the security and safety of persons, including occupants or laborers. This includes the indicators of *fire vulnerability* (I_9), which evaluates the durability of the panel against fire, and *risk vulnerability* (I_{10}) which considers the probability of any accidents for persons, the public, and laborers during the construction or assembly of panels. The former will be assessed in min while the latter on a scale of 0 to 10.

The *aesthetic* (C_7) criterion including *Consistency with the surrounding* indicator (I_{10}) assesses the appearance and architectural style of the façade cladding through seminars with multidisciplinary architects. A measurable scale of 0-10 is used to rate the visual quality of the façade panels.

Finally, the *reliability* (C_8) assesses the flexural or tensile resistance of the panels through the *Strength to weight ratio* (I_{12}) parameter. Moreover, the energy absorption and toughness of the panels are measured by the *Toughness and ductility* (I_{13}) indicator to avoid using the brittle material. *Durability* (I_{14}) considers the resilience of the panels in exposure to extreme weather conditions (wet/dry or freeze/thaw cycles).

Table 2. Requirements tree for assessing the façade cladding sustainability.

Requirements	Criteria	Indicators	Units	Function Shape
R_1.Economic	C_1. Cost	I_1.Construction Cost	€/m^2	DC_X
		I_2. Maintenance cost	€/m^2	DC_X
R_2.Environmental	C_2.Emission	I_3. $C0_2$ equivalent emission	Kg/m^2	DC_X
	C_3. Resource consumption	I_4. Energy consumption	MJ/m^2	DC_X
		I_5. Material consumption	Kg/m^2	DC_X
	C_4.Waste	I_6. Solid waste management	Points	I_nC_V
R_3.Social	C_5.Comfort	I_7. Acoustic performance	points	I_nS
		I_8. Thermal performance	m^2 k/w	DS
	C_6.Safety	I_9. Fire vulnerability	min	I_nC_V
		I_{10}. Risk vulnerability	Points	DC_X
	C_7.Aesthetic	I_{11}.Consistency with surrounding	Points	I_nL
R_4.Technical	C_8.Reliability	I_{12}.Strength to weight ratio	Points	I_nC_V
		I_{13}.Toughness and ductility	KJ/m^2	I_nC_V
		I_{14}. Durability	Points	I_nC_V

2.2. Assignation of weights for each parameter

To express the importance of each parameter (requirement, criteria, and indicator) and prioritize them, weights would be assigned. For instance, the weight of I_1 is considered as λ_1=65% while the weight of I_2 is λ_2=35%, showing the greater importance of the former. The weightings of the tree will be assigned based on previous studies and the knowledge of the professors and experts from architecture and civil engineering faculties, namely Universitat Politècnica de Catalunya, involved in the seminar using the analytical hierarchy process (AHP) [26]. The AHP method enables the most consistent weighting judgments and helps

organize the process efficiently, reduce the model complexity and subjectivity, and decrease possible disagreements between the team members [27].

2.3. Establish value functions for each parameter

To homogenize the indicator's units into dimensionless values ranging from 0.0 to 1.0, the value function concept is used. These values, from 0.0 to 1.0, represent the minimum and maximum degree of satisfaction in terms of sustainability, respectively [22], [28]. To determine the satisfaction value for each indicator, first of all, the tendency (increasing or decreasing) of the value function should be defined. An increasing (I_n) function means the decision maker's satisfaction increases with an increase in the measurement variable. In contrast, a decreasing (D) value function shows that an increase in the measurement unit causes a decrease in satisfaction [22].

Secondly, two points that have a satisfaction value of 0.0 (X_{min}) and 1.0 (X_{max}) should be defined for each indicator. These points are usually established according to existing rules and regulations, experience with previous projects, and the value produced by the different alternatives with respect to the indicator. For instance, X_{min} and X_{max} for the I_1 indicator (*construction cost*) are determined as 20.5 and 183 €/m^2 while for I_9 (*fire vulnerability*) are specified as 30 and 200 min.

Afterward, the value function shape, concave, convex, linear, or S-shaped, should be selected [29] in order to connect the two coordinate points, (X_{min}, 0) and (X_{max}, 1) [22]. A concave-shaped (Cv) is used when satisfaction increases rapidly or decreases slightly, while the convex (C_x) one is more suitable when the satisfaction tendency is contrary to the concave curve. linear (L) function is presented for steadily increases/decreases in satisfaction, while an S-shaped (S) function is used if the satisfaction tendency contains a combination of concave and convex functions (see Figure 2).

As can be seen in Table 2, seven indicators have a decreasing tendency including six convex shapes and one S-shaped, while five indicators have increasing concaved shapes. Finally, there is one indicator with an increasing S-shaped and another one with an increasing linear function. Figure 3 demonstrates the function shapes of the I_1 and I_9 indicators as examples. As the satisfaction value of the *construction cost* decreases rapidly with increasing the price, so the convex shape was chosen (Figure 3-a). On the other hand, for *fire vulnerability*, satisfaction increases at first more rapidly when the fire performance of the cladding improves (Figure 3-b). Thus, a concave function could be suitable.

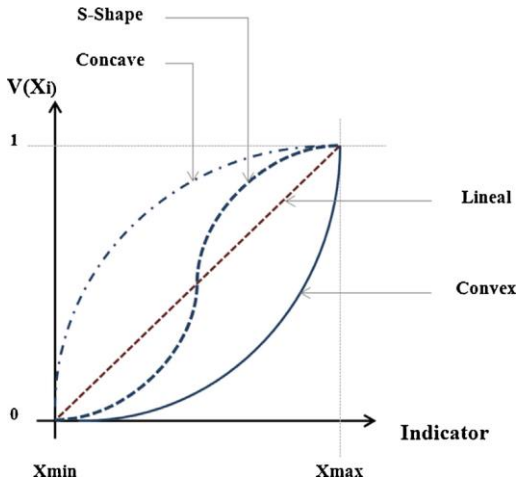

Figure 2. Different value function shapes.

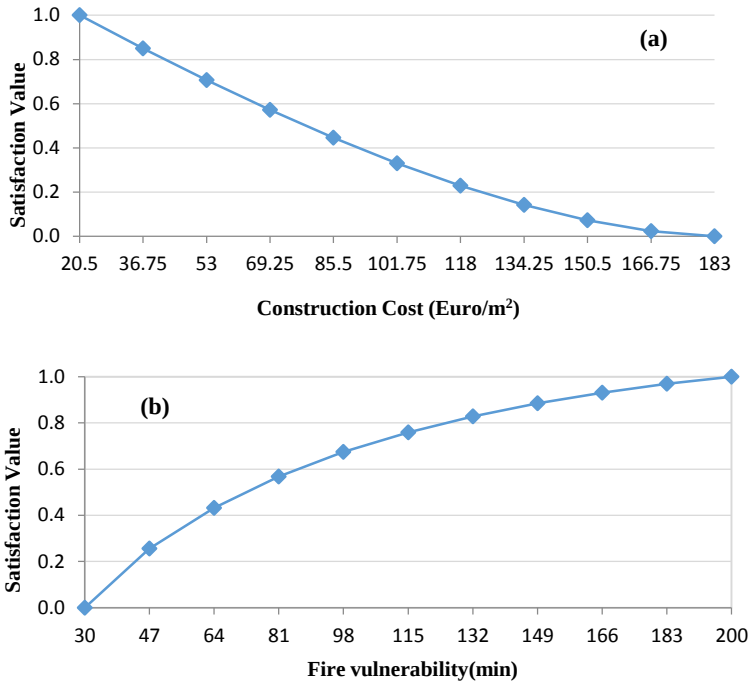

Figure 3. Value function shapes of indicators: a) construction cost; b) fire vulnerability

Finally, the mathematical expression of MIVES, Eq. (1), for obtaining each indicator value satisfaction, V_i, would be applied. To normalize the indicators' values between a range of 0.0 and 1.0 as well as achieving factor B for the previous equation, Eq. (2) is used. The constitutive parameters of the value functions were established based on the scientific literature, existing rules, and regulations, experience with previous projects, and the background of experts (including professors and experts practitioners who attended the seminars). Thus, the sets of indicator values (Vi(xi)) that are between 0.0 and 1.0 is generated.

$$V_i = A + B \cdot [1 - e^{-k_i \cdot (\frac{|X_{Alt_i} - X_{min}|}{c_i})^{p_i}}] \quad (1)$$

$$B = [1 - e^{k_i \cdot (\frac{|X_{max} - X_{min}|}{c_i})^{p_i}}]^{-1} \quad (2)$$

Where:

V_i: *The* satisfaction value of the indicator being evaluated.
A: The response value X_{min} (indicator abscissa), generally A = 0;
B: The factor preventing the function from leaving the range (0.0, 1.0).
X_{Alti}: The indicator abscissa that generates the value, V_i;
X_{min}: The point of minimum satisfaction, with a value of 0.
X_{max}: The point of maximum satisfaction, with a value of 1.
P_i: A shape factor that determines whether the curve is concave or convex, linear or S-shaped;
(*P < 1* the curve is concave; *P > 1* the curve is convex or S-shaped; *P = 1* it is linear).
C_i: The factor that establishes the value of the abscissa for the inflection point in curves with $P_i > 1$;
K_i: The factor that defines the response value to C_i;

For instance, the construction cost of the textile waste fabric reinforced cement boards (X_1) is estimated as 52 €/m^2. Thus, the satisfaction value of this indicator, V_1, is calculated as 0.72.

2.4. Assess the sustainability index (SI)

After the assessment of the satisfaction value of the indicators, the formula that is presented in Eq. (3) should be applied to each tree level. In this equation, the indicator value ($V_i(x_i)$) has previously been determined and the weights (λ_i) are assigned to determine the sustainability value of each branch.

$$SI=\sum \lambda i V_i(x_i) \quad (3)$$

Where:
SI= Sustainability Index;
$V_i(x_i)$: The value function of each indicator, criterion, or requirement;
λ_i: The associated weight.

Thus, the Sustainability Index (SI) of the cladding panel can be computed. Besides calculating the overall sustainability index, this model also makes it possible to calculate economic, social, environmental, and technical satisfaction indexes separately. In this case, the weaknesses and strengths of each alternative can be identified from different points of view. For instance, the satisfaction value of the *economic requirement* (R_1) will be equal to the satisfaction value of the *cost criterion* (C_1) and will be calculated through $\lambda_1 V_1+\lambda_2 V_2$.

3. Summary and Discussion

A new multi-objective approach for the sustainability assessment of the cladding façade panels specifically oriented to the fiber/textile cement board is presented in this research study. This sustainability model, based on the MIVES, uses the value function concept as well as the AHP process to quantify the satisfaction and preferences of the stakeholders and users. The proposed model:

- Considers various indicators in the scope of economic, environmental, social, and technical performances that can be applied to any façade cladding. Nonetheless, the function and the location of the building could affect the final identification and filtration of the indicators.

- Helps decision-makers to compare the sustainability value of all alternatives and choose the optimum solution for cladding panels.

This model is conceptually presented herein, while a real case study, applied on the textile waste fabric reinforced cement boards, is being prepared to serve as an example of application within the context of the Ph.D. thesis of the first author.

Acknowledgment
The authors express their gratitude to the Spanish Ministry of Economy, Industry, and Competitiveness for the financial support received under the scope of the projects CREEF (PID2019-108978RB-C32) and RECYBUILDMAT (PID2019-108067RB-I00).

REFERENCES

[1] O. Pons and G. Wadel, "Environmental impacts of prefabricated school buildings in Catalonia," Habitat Int., vol. 35, no. 4, pp. 553–563, Oct. 2011.

[2] J. L. Gálvez-Martos, D. Styles, H. Schoenberger, and B. Zeschmar-Lahl, "Construction and demolition waste best management practice in Europe," Resour. Conserv. Recycl., vol. 136, pp. 166–178, Sep. 2018.

[3] V. Hartkopf, A. Aziz, and V. Loftness, "Facades facade and Enclosures, Building building for Sustainability," in Encyclopedia of Sustainability Science and Technology, Springer New York, 2012, pp. 3675–3705.

[4] L. J. Fernández, J. Claramunt, A. Llerena, D. Torrens, M. Ardanuy, and J. L. Zamora, "First International Conference on Bio-based Building Materials NONWOVEN FLAX FIBER MATS AND WHITE PORTLAND CEMENT COMPOSITES FOR BUILDING ENVELOPES," Jun. 2015.

[5] J. Claramunt, L. J. Fernández-Carrasco, H. Ventura, and M. Ardanuy, "Natural fiber nonwoven reinforced cement composites as sustainableClaramunt, J., Fernández-Carrasco, L. J., Ventura, H., & Ardanuy, M. (2016). Natural fiber nonwoven reinforced cement composites as sustainable materials for building envelopes. Constructio," Constr. Build. Mater., vol. 115, pp. 230–239, 2016.

[6] M. Ardanuy, J. Claramunt, and R. D. Toledo Filho, "Cellulosic fiber reinforced cement-based composites: A review of recent research," Constr. Build. Mater., vol. 79, pp. 115–128, 2015.

[7] F. Pacheco-Torgal and S. Jalali, "Cementitious building materials reinforced with vegetable fibres: A review," Constr. Build. Mater., vol. 25, no. 2, pp. 575–581, 2011.

[8] A. M. Brandt, "Fibre reinforced cement-based (FRC) composites after over 40 years of development in building and civil engineering," Compos. Struct., vol. 86, no. 1–3, pp. 3–9, 2008.

[9] G. Zani, M. Colombo, and M. Di Prisco, "High performance cementitious composites for sustainable roofing panels," Proc. 10th fib Int. PhD Symp. Civ. Eng., no. February 2015, pp. 333–338, 2014.

[10] G. Promis, T. Q. Bach, A. Gabor, and P. Hamelin, "Failure behavior of E-glass fiber- and fabric-reinforced IPC composites under tension and compression loading," Mater. Struct. Constr., vol. 47, no. 4, pp. 631–645, 2014.

[11] J. Wei and C. Meyer, "Improving degradation resistance of sisal fiber in concrete through fiber surface treatment," Appl. Surf. Sci., vol. 289, pp. 511–523, 2014.

[12] C. Correia, S. Francisco, H. Savastano, and V. Moacyr, "Utilization of vegetal fibers for production of reinforced cementitious materials," no. 2017, 2018.

[13] M. Ramirez, J. Claramunt, H. Ventura, and M. Ardanuy, "Evaluation of the mechanical performance and durability of binary blended CAC-MK/natural fiber composites," Constr. Build. Mater., vol. In progres, 2019.

[14] L. Gonzalez-Lopez, J. Claramunt, Y. Lo Hsieh, H. Ventura, and M. Ardanuy, "Surface modification of flax nonwovens for the development of sustainable, high performance, and durable calcium aluminate cement composites," Compos. Part B Eng., vol. 191, no. February, 2020.

[15] J. Claramunt, H. Ventura, L. J. Fernández-Carrasco, and M. Ardanuy, "Tensile and flexural properties of cement composites reinforced with flax nonwoven fabrics," Materials (Basel)., vol. 10, no. 2, pp. 1–12, 2017.

[16] P. Sadrolodabaee, J. Claramunt, M. Ardanuy, and A. de la Fuente, "Mechanical and durability characterization of a new textile waste micro-fiber reinforced cement composite for building applications," Case Stud. Constr. Mater., vol. 14, p. e00492, Jun. 2021.

[17] P. Sadrolodabaee, J. Claramunt, M. Ardanuy, and A. de la Fuente, "Characterization of a textile waste nonwoven fabric reinforced cement composite for non-structural building components," Constr. Build. Mater., vol. 276, p. 122179, Mar. 2021.

[18] G. K. C. Ding, "Sustainable construction-The role of environmental assessment tools," J. Environ. Manage., vol. 86, no. 3, pp. 451–464, Feb. 2008.

[19] C. Salzer, H. Wallbaum, L. F. Lopez, and J. L. Kouyoumji, "Sustainability of social housing in Asia: A holistic multi-perspective development process for bamboo-based construction in the Philippines," Sustain., vol. 8, no. 2, 2016.

[20] D. Kvočka et al., "Life cycle assessment of prefabricated geopolymeric façade cladding panels made from large fractions of recycled construction and demolition waste," Materials (Basel)., vol. 13, no. 18, 2020.

[21] B. Han, R. Wang, L. Yao, H. Liu, and Z. Wang, "Life cycle assessment of ceramic façade material and its comparative analysis with three other common façade materials," J. Clean. Prod., vol. 99, pp. 86–93, 2015.

[22] B. Alarcon et al., "A Value Function for Assessing Sustainability: Application to Industrial Buildings," Sustainability, vol. 3, no. 1, pp. 35–50, Dec. 2010.

[23] S. M. A. Hosseini, A. De, and O. Pons, "Multi-criteria decision-making method for assessing the sustainability of post-disaster temporary housing units technologies : A case study in Bam , 2003," vol. 20, pp. 38–51, 2016.

[24] "ITeC - Institute of Construction Technology of Catalonia." [Online]. Available: https://itec.cat/. [Accessed: 08-Nov-2020].

[25] G. Hammond and C. Jones, "INVENTORY OF CARBON & ENERGY (ICE) Version 1.6a," 2008.

[26] T. L. Saaty, "How to make a decision: The analytic hierarchy process," Eur. J. Oper. Res., vol. 48, no. 1, pp. 9–26, Sep. 1990.

[27] A. De La Fuente, O. Pons, A. Josa, and A. Aguado, "Multi-criteria decision making in the sustainability assessment of sewerage pipe systems," J. Clean. Prod., vol. 112, pp. 4762–4770, Jan. 2016.

[28] A. Aguado, A. del Caño, M. P. de la Cruz, D. Gómez, and A. Josa, "Sustainability Assessment of Concrete Structures within the Spanish Structural Concrete Code," J. Constr. Eng. Manag., vol. 138, no. 2, pp. 268–276, Feb. 2012.

[29] G. Gilani, O. Pons, and A. de la Fuente, "Towards the Façades of the Future: A New Sustainability Assessment Approach," IOP Conf. Ser. Earth Environ. Sci., vol. 290, no. 1, p. 012075, Jun. 2019.

4. CHAPTER ° IV

RESULTS AND CONCLUSIONS

In this chapter, first, a summary of the research work is carried out emphasizing on the connectivity and coherence among published and submitted papers. Further, the main and specific conclusions derived from this thesis are exposed. Additionally, potential future research lines are included.

4.1 Summary of the thesis and general conclusion

In the preliminary study on the cement composite reinforced with the proposed micro textile waste fiber from residues of the garments and textile industries, composed of 70% cotton and 30% polyester, three different samples with various treatments were made -each including a 6% TW fiber weight fraction cement (Section 3.1). Based on the results obtained from the flexural test carried out after 7 days, the best treatment among the three methods for producing the composite was the use of the intact short TW fibers with the dewatering compression process. This treatment increased the flexural tensile strength and toughness, up to 75 and 55% respectively, in comparison to the other methods. Further, the toughness and energy absorption of this composite was seven times higher than the reference sample without fibers.

After, the mechanical characteristics (flexural and compressive strengths at 7, 28, and 56 days as well as toughness and stiffness) together with durability properties -exposure to wet/dry accelerated aging- of cement paste reinforced with various content of 6 to 10% randomly short TW Fiber was investigated (Section 2.1). The samples were made with the intact short TW fibers with the dewatering compression process. The results were compared with those obtained from Kraft Pulp pine fiber (KP), taken as reference. The main conclusion is the feasibility of using this type of fiber as reinforcement in construction materials with the optimum dosage of 8%. Although the flexural resistance and toughness of the TW composite were lower than KP control by almost 9%, the compressive strength and stiffness together with durability properties proved to be enhanced with respect to the reference composite. However, both composites showed post-cracking performance and improvement in energy absorption suitable for the targeted building components, mainly those non-structural.

After successfully incorporating short fibers as reinforcement for cement-based materials, TW nonwoven fabric produced from this kind of short fibers through card clothing and the needle-punching process was used as internal reinforcement for cement-based matrices (Section 2.2). To this end, the design-oriented flexural properties of a cement-based matrix reinforced with 3 to 7 reinforcement layers of TW laminates were investigated within the context of an extensive experimental program. Flexural tests were carried out after 28 days to characterize the pre-and post-cracking response of these composites. Additionally, tests simulating accelerated aging conditions in addition to SEM and BSEM observations were included to assess the suitability of this material in terms of durability and to provide a preliminary quantification of the post-cracking flexural capacity after inducing damage by means of accelerated aging. The same tests were performed for reference samples with flax nonwoven fabric (FNH). Some of the fabrics of the reference samples were previously undergone the physical treatment of hornification (FH). All the composites showed a remarkable improvement in terms of toughness and post-cracking stress-bearing capacity, six being the optimum number of TW reinforcing layers. Through the analysis of the results, the feasibility of using TW composite as a construction material in non-structural applications was confirmed.

After carrying out the previous two extensive experimental programs involving the use of either fraction of short random TW fibers at 6–10% by weight or nonwoven fabrics in 3–7 laminate layers in the textile waste-reinforcement of cement, the results obtained from those programs were analyzed and compared to identify the optimal composite and applications (Section 2.3). Thereby, flexural resistance in pre-and post-crack, toughness, and stiffness of the resulting composites were assessed in addition to unrestrained drying shrinkage testing. Based on the results of experimental analysis, the feasibility of using this textile waste composite as construction materials in nonstructural applications such as facade cladding, raised floors, and pavements was confirmed. The optimal composite was proven to be that reinforced with six layers of nonwoven fabric, with a flexural strength of 15.5 MPa and a toughness of 9.7 kJ/m^2.

As one of the prospective applications of 6-layer TRM panels reinforced with TW nonwoven fabrics, the sustainability index of this type of material as a façade cladding panel was assessed (Sections 3.2 and

2.4). To this end, fire, thermal, and acoustic tests were performed on this material, and the results were implemented in a model that allows objective assessment of the sustainability performance of building components. This model was designed and developed based on the Spanish integrated value model for sustainability assessment (known as MIVES). To this end, the value function concept and analytic hierarchy process were applied to quantify the satisfaction and preferences (weights) of the stakeholders and users. These methods were calibrated through seminars and interviews with experts. The results demonstrated that the sustainability index of this new material was rather high, in the range of 0.68–0.71 (over 1.00).

In previous studies, the flexural behavior of the textile waste (TW) composite was examined and an optimum number of layers (six) was selected. However, comprehensive studies were yet to be carried out on the improvement in durability against wet-dry and freeze-thaw cycles, or the tensile behavior of this material. Therefore, a new study to develop durable, ductile, and strain-hardening cementitious composites with variable SF content reinforced with TW nonwoven fabric was carried out (Section 5.1). To this end, the effect of Silica Fume (SF) content in the range of 0-30% on the mechanical performance and cement mixture microstructure of the PC matrix was initially evaluated through flexural and compressive tests— at 7 and 28 days— in addition to thermogravimetric analysis (TGA) and X-ray diffraction (XRD) analyses. Thus, the optimum percentage of the SF was selected for composite production. In the next step, the compression-molded laminated composites treated with three distinct SF dosages −the optimum percentage selected, and two reference dosages (0%, 15%, and 30%)−, reinforced with six layers of fabric were produced and tested under the flexural and tensile configuration in different aging conditions —28 curing days, 28 curing days plus 25 wet-dry (WD) or 25 freeze-thaw (FT) accelerating aging cycles. Finally, scanning and backscattered scanning electron microscopy (SEM and BSEM) observations were performed to determine the structure-properties relationships. The results suggested that the composite modified by 30% SF could protect fibers from embrittlement, thereby offering the greatest durability by increasing flexural and tensile resistances by up to 45% and 55%, respectively, as compared to the sample without SF in the wet-dry cycles.

Hence, the general results and outcomes of this study showed that the recycled textile waste fibers from residues of garment industries could be technically feasible to be used as a reinforcement, specifically in a fabric form, in strain-hardening cementitious composite (SHCC) materials with limited structural responsibility (e.g., facade panels, roofing, raised floors, and masonry structures). Indeed, the characterization results of TW fabric composites allowed confirming the potentialities of this material in non-structural applications for building components as an alternative to vegetable or synthetic fiber composites, though the formers presented less mechanical capacity –but sufficient for the target building components. Likewise, from the sustainability point of view, TW reinforcement proved to be a suitable revalorized material for reinforcing cement-based composites.

4.2 Specific conclusions

The following specific conclusions were driven from the whole research work:

- As for the composite reinforced with short randomly textile waste (TW) fibers, compressive and flexural maximum strengths were observed for those composites with 8% of the TW fibers. The flexural stiffness was found to be maximum for composites with 6% of the TW while the maximum toughness was obtained when 10 % of this fiber was used. Based on the standard mechanical requirements for non-structural building components, 8% of the TW fibers resulted in the optimum fiber dosage.

- The results of the accelerated aging tests proved a better mechanical performance (at least 10 %) for the short TW composites with respect to the reference samples, Kraft pulp fibers. The SEM observation results confirmed that this TW fiber was barely affected by the Portlandite contained in the cement.

- As for the composites reinforced with TW or Flax nonwoven fabric, flexural tests' results on unaged specimens confirmed that all composites achieved a post cracking response with the formation of multiple cracking, being requirements to be fulfilled in terms of structural applicability of these composites. Likewise, the results evidenced a clear relationship between the number of reinforcing layers and the post-cracking mechanical properties characterized by an optimum performance when the number of layers ranges from 5 to 6.

- Post-cracking mechanical properties of TW or Flax nonwoven fabric composites subjected to an accelerated aging process were found to be remarkably affected. As a preliminary proposal in terms of design, it is proposed to reduce by a factor of 4.0 the short-term value of MOR so that the degradation due to aging during service conditions can be taken into consideration. It must also be added that those composites reinforced with six layers proved to lead to better mechanical performance after the accelerated aging, especially FH6L (six-layer hornificated flax fabric) and TW6L (six-layer textile waste fabric). Further, SEM and BSEM observations confirmed that the accelerated aging process is associated with an increase in fiber fracture and a decrease in fiber pull-out, especially in vegetable fibers, due to the alkali attack. TW composite had better behavior with respect to FNH (non-hornificated flax fabric) composite since the former was reinforced with both vegetable and synthetic fibers, while the latter was only reinforced with untreated flax fibers.

- As for the comparison between the composites reinforced with short TW fibers (FRC) and those with TW nonwoven fabric form (TRM), the pre-cracking flexural performances of both unaged 6-layer nonwoven TRM and FRM with 8% of fibers were comparable. However, the post-cracking flexural performance and especially the energy absorption capacity of the former were significantly superior (by four times) compared to the latter. The results suggest that randomly distributed short fibers from textile waste have limitations in terms of mechanical performance due to limited cracking capacity and the maximum mixable amount of these fibers.

- Both FRM and TRM composites incorporating TW were subjected to an accelerated aging process that primarily affected the energy absorption of the materials. Nonetheless, the toughness and stiffness of the aged TRM were greater (three times) than the aged FRM. SEM observations confirmed that accelerated aging was associated with an increase in fiber fracture and a decrease in fiber pull-out, especially in vegetable fibers, due to the alkali attack.

- The outcomes of the fire, thermal, and acoustic behavior measurements of the TW6L sample showed that it was appropriate for external facade panels. Fire behavior was evaluated through epiradiator and small-scale fire testing. The TW6L sample did not generate flames and maintained its integrity above 950 °C. The post-fire residual resistance of the TWFRC board was almost six times higher than that of the control plate without fibers. Moreover, the incorporation of TW fiber could improve the thermal and acoustic performance of the plate by 40%.

- As to the sustainability assessment of the TWFRC panel, all the three requirements of sustainability (economic, environmental and social) had an almost equal satisfaction value (a range of 0.65–0.72) for the TW cement board, which indicated that this panel met the needs of sustainable performance in different aspects. Further, the sustainability index of the prefabricated TWFRC facade-cladding panels

for different weighting scenarios was in an acceptable range of 0.68–0.71, particularly for the optimum proposed weight was 0.7 (24% higher than the control plate without fibers).

- The study on the Portland cement (PC) matrix modified with different dosages of silica fume (SF) suggested that the flexural and compressive resistances decreased with the addition of SF at 7 days of curing. However, at 28 days of curing, the difference between variable samples was reduced, indicating the slow reaction of pozzolanic material. Furthermore, TGA and XRD analyses proved that matrices with less than 15% SF presented a large amount of portlandite and were not suitable for improving the durability of the composites. The lowest amount of calcium hydroxide was found in the sample with a 30% SF.

- The results of the flexural tests on the TW composites modified with different dosages of SF showed that wet-dry accelerated aging cycles negatively affected the post-cracking properties of the reinforced composites as compared to the unaged specimens. Nonetheless, composites with 30% SF (C30 sample) presented only slight reductions (< 5%) in their mechanical properties as compared to the unaged specimens. The composite without SF (C0 sample) had a resistance 15% higher in unaged conditions than the C30 sample, with a 40% decrease in the wet-dry cycles.

- The results of the direct tensile tests on the TW composites modified with different dosages of SF revealed that the addition of SF had negligible effects on the mechanical properties in unaged conditions. However, composites with SF exhibited better mechanical properties in aged conditions, especially in wet/dry cycles. Further, SEM and BSEM observations confirmed that the accelerated aging process, mainly wet-dry cycles, leads to an increased fiber fracture ratio and a decreased fiber pull-out strength due to the alkali attack in the C0 sample. Nonetheless, composites containing SF presented a better behavior than the C0 composite, since the amount of calcium hydroxide was significantly reduced (especially in those composites with 30% SF), as confirmed by the TGA study. Thus, the developed PC-based matrix modified with 30% SF prevented fiber embrittlement when submitted to accelerated aging.

4.3 Future perspectives

The outcomes derived from this research are satisfactory and generate expectations for the use of these new composites. However, there are still aspects to be covered through researching and starting from the results presented herein. The following research lines and recommendations are identified:

- Monitoring and controlling (in the industrial environment) the preparation of short recycled textile waste fibers to guarantee stable properties (geometric and mechanical).

- Developing and implementing a method to produce the nonwoven fabric from 100% short TW fibers (without mixing with flax fibers) to improve the sustainability and durability of the material.

- Developing and designing the industrial TW panels with larger dimensions than 300 mm × 300 mm to improve the physical appearance of the panel, specifically as façade cladding elements.

- Using a more eco-friendly type of cement with a lower amount of clinker, thereby lower CO_2 emissions, such as LC^3 (Limestone Calcined Clay Cement) to enhance the sustainability performance.

- Simulating the global mechanical response of TW mortars through numerical analysis and finite elements (using software like Abaqus or Ansys) to explore the structural responsibility.

- Simulating of energy and thermal behavior of the building whose facade is made up of this panel (by software such as IESVE) to shed more light on the environmental sustainability of this material as a façade cladding.

- Producing 3D concrete printing (3DCP) reinforced with these sustainable fibers to explore additive manufacturing technology.

5. APPENDIX :

PAPER OUT OF THE COMPENDIUM - SUBMITTED FOR PUBLICATION

This chapter reproduces a submitted journal paper derived from the last research results in this thesis, however, it is excluded from the official compendium of publications. The paper follows its own numbering of sections, figures, equations, and references.

5.1 Journal paper V:
Effect of accelerated aging and silica fume addition on the mechanical and microstructural properties of hybrid textile waste-flax fabric reinforced cement composites

Submitted to Journal of Cement and Concrete Composites in February 2022

Payam Sadrolodabaee[a*] (payam.sadrolodabaee@upc.edu), Josep Claramunt[b] (josep.claramunt@upc.edu), Monica Ardanuy [c] (monica.ardanuy@upc.edu), and Albert de la Fuente[a] (albert.de.la.fuente@upc.edu)

a: Department of Civil and Environmental Engineering- Universitat Politècnica de Catalunya (BarcelonaTECH)- Barcelona, Spain
b: Department of Agri-Food Engineering and Biotechnology- Universitat Politècnica de Catalunya (BarcelonaTECH)- Barcelona, Spain
c: Department of Material Science and Engineering - Universitat Politècnica de Catalunya (BarcelonaTECH)-Barcelona, Spain
*: Corresponding author

Abstract

The use of more environmentally friendly materials obtained from recycled resources and industrial by-products is gaining increased acceptance in the building sector. Therefore, a cementitious matrix that is made up of supplementary cementitious materials (SCMs) reinforced by recycled fibers may be a promising solution from both a durability and sustainability perspective. This study presents an extensive experimental program carried out on a cement-based composite with Silica Fume (SF), reinforced with recycled textile waste (TW) nonwoven fabric. Initially, the mechanical strength (compression and flexure) of the Portland cement paste substituted with variable SF content (0% to 30%) was characterized. Based on the results, laminate plates having six TW fabric layers impregnated with three different cement pastes −0%, 15%, and 30% SF− were produced, and both the mechanical (flexural and direct tension) and durability (against wet-dry and freeze-thaw cycles) properties of the composite were assessed through testing. Experimental microstructural techniques including thermogravimetric analysis (TGA), X-ray diffraction (XRD), scanning and backscattered scanning electron microscopy (SEM and BSEM) were also used to complement the analysis of the mechanical characterization. The results suggested that the composite modified by 30% SF could protect fibers from embrittlement, thereby offering the greatest durability by increasing flexural and tensile resistances by up to 45% and 55%, respectively, as compared to the sample without SF in the wet-dry cycles. The results and outcomes of this study may serve as the basis for future research on these composites and their potential use in structural applications in the building construction and housing industries.

Keywords: Flax fibers; Freeze-thaw cycles, Textile waste fibers; Supplementary cementitious materials; Textile reinforced cement composites; Wet-dry cycles.

1. Introduction

Fiber-reinforced concrete and mortar composed of a cementitious matrix and a reinforcement system in different forms may be used in a wide range of structural and non-structural applications. However, sustainability is an issue to be addressed in any potential application and function. Recyclability and CO_2 emissions are considered to be some of the main indicators of environmental sustainability in fiber/textile reinforced mortars (FRM/TRM) [1]. To develop more sustainable cementitious building materials, waste and recycled sources, as well as low carbon-embodied materials, are currently being used [2]–[4]. According to previous studies carried out by the authors [5]–[7], recycled textile waste (TW) fibers from clothing waste mixed with vegetable fibers (65% and 35% in mass, respectively) are technically feasible to be used as internal reinforcement (in both short or fabric forms) in cement-based matrices to enhance the toughness and post-cracking behavior for non-structural or low-medium performance structural applications. However, the durability of this type of composites, especially in wet-dry cycles, should be studied in greater detail, given the well-known problem of durability of cement-based composites reinforced with vegetable fibers [6], [8]. Partial weight replacement of Portland cement (PC) matrix with SCMs (supplementary cementitious materials), including pozzolanic and by-products compounds, is a

potential solution to address these durability issues, while simultaneously reducing the carbon footprint derived from clinker production (estimated at approximately 5-7 % of the global CO_2 emissions).

The lack of durability of composites containing natural fibers is mainly due to the presence of calcium hydroxide, $Ca(OH)_2$ in the PC matrix, which degrades the vegetable fibers [9]. To improve durability, certain strategies have been introduced. While some of these strategies modify the fibers through physical and chemical treatments such as hornification [10] or alkaline treatment [11], others modify the matrix to reduce or remove the alkaline compounds, including accelerated carbonation or the use of pozzolanic fillers [12]. The addition of pozzolanic and/or supplementary cementitious materials is intended to transform portlandite (CH) into calcium silicate hydrate (C-S-H) gel. In fact, pozzolanic materials containing a large amount of amorphous silica (SiO_2) and/or alumina (Al_2O_3) promote the pozzolanic reaction during the hydration process, ultimately leading to the replacement of CH by C-S-H [13][14]. Optimized dosages of SCMs to replace cement should be used to ensure the disappearance of portlandite. This optimum dosage is based on matrix composition, curing conditions, and fiber type and content.

According to the literature review, distinct amounts of various SCMs have been used in vegetable fiber FRM/TRM. Fernández et al. [15] used 10 wt.% of sourced silica fume (SF) to achieve a virtual absence of portlandite after autoclaved curing condition in the cement–base reinforced with sisal fibers. Khorami et al. [16] examined the behavior of cement boards reinforced with 8% Kraft pulp waste modified with SF. Their results found that the addition of 3-6% SF by cement weight slightly improved flexural strength, whereas adding more than 6% SF led to a slight reduction of strength as compared to the control specimen. Gutierrez et al. [17] examined the effect of SF, metakaolin (MK), fly ash (FA), and ground granulated blast-furnace slag (GGBS) on cement mortars reinforced with different types of natural and synthetic fibers in the proportion of 2.5% by cement weight. They concluded that the addition of 15% SF or MK improved the composite's performance whereas 15% FA had an adverse effect, probably due to its lower degree of pozzolanic activity. Moreover, they reported that the addition of 70% GGBS offered promising results. Silva et al. [18] managed to improve the durability of the Portland cementitious matrix by incorporating 30% MK and 20% calcined waste crushed clay brick to manufacture composite laminates reinforced with long sisal fibers. Fidelis et al. [19] and Majstorović et al. [20] developed a CH-free matrix by replacing almost 50% of the PC with MK in jute textile-reinforced concrete and flax textile-reinforced composites, respectively.

Other studies have suggested that using SF in the range of 5-45% by cement weight could minimize the loss of toughness of the composites exposed to extreme conditions, while simultaneously improving the impermeability and corrosion resistance [21]–[24]. Toledo Filho et al. [25] studied the long-term durability of cement composites reinforced with sisal and coconut fibers modified by pozzolanic fillers. Their results indicate that the partial replacement of PC by 40% GGBS does not reduce the embrittlement of the fibers with aging, whereas treatment of the matrix by 10% SF was indeed an efficient method. SF consists largely of amorphous (non-crystalline) silicon dioxide, with ultrafine particles (~100 times smaller than cement particles) [26], [27]. As a result of its large surface area (~15 times higher than other pozzolanic materials) and high silica content, SF has been categorized as a highly reactive pozzolanic material, making it a very suitable cementitious material [28]. Numerous studies have reported the favorable impacts of using SF as an SCM in mortar/concrete, including the formation of additional tobermorite-like structure C-S-H gel with a lower calcium-to-silica ratio (Ca/Si) [27], lower permeability, improved pore structures, enhanced interfacial transition zone in concrete, etc. [29]–[31].

To the best of our knowledge, few results are available in the literature regarding the mechanical and durability characterization of PC composites reinforced with nonwoven fabrics made of recycled fibers from the garment industry. In our previous study [4], the flexural behavior of the TW composite was examined and an optimum number of layers (six) was selected. However, comprehensive studies have yet

to be carried out on the improvement in durability against wet-dry and freeze-thaw cycles, or the tensile behavior of this material. Therefore, this work aims to develop durable, ductile, and strain-hardening cementitious composites with variable SF content reinforced with TW nonwoven fabric. To this end, the effect of SF content in the range of 0-30% on the mechanical performance and cement mixture microstructure of the PC matrix was initially evaluated through flexural and compressive tests— at 7 and 28 days— in addition to TGA and XRD analyses. Thus, the optimum percentage of the SF was selected for composite production. In the next step, the compression-molded laminated composites treated with three distinct SF dosages −the optimum percentage selected, and two reference dosages (0%, 15%, and 30%)−, reinforced with six layers of fabric were produced and tested under the flexural and tensile configuration in different aging conditions —28 curing days, 28 curing days plus 25 wet-dry (WD) or 25 freeze-thaw (FT) accelerating aging cycles−. Finally, SEM and BSEM observations were carried out to determine the structure-properties relationships.

2. Experimental Procedure

The considered experimental program (see Figure 1) of this study was classified into two main categories and ten sub-categories, which are described in the following sections.

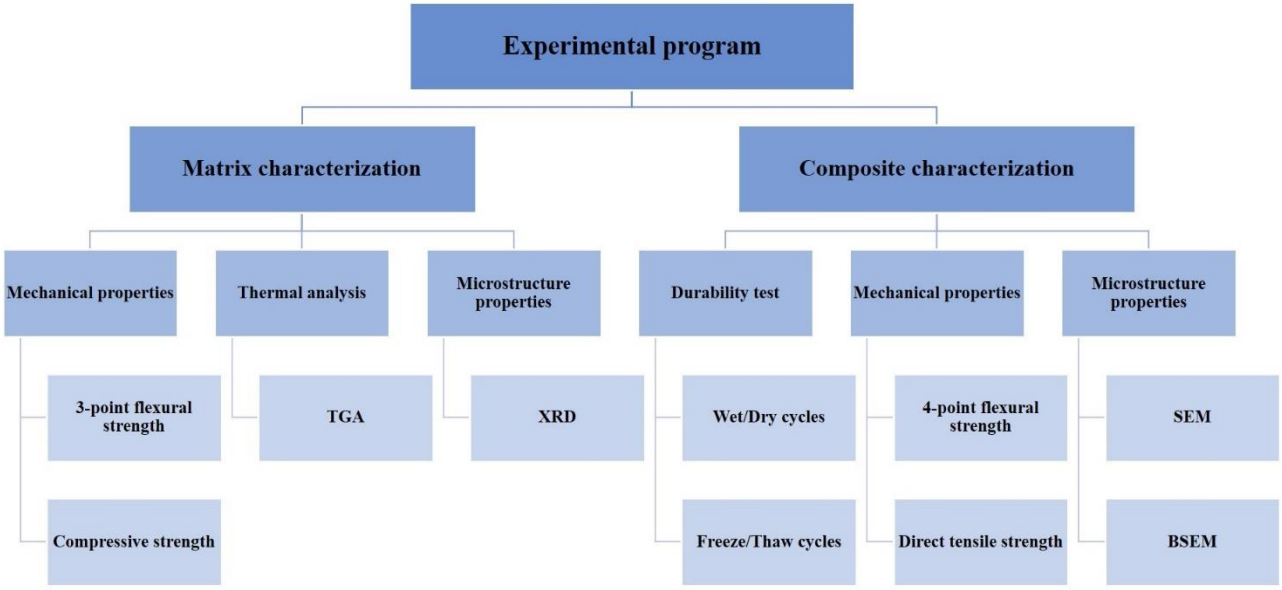

Figure 1. Schematic of the experimental program of this study

2.1 Materials

Portland cement Type I 52.5R with a minimum compressive strength of 52.5 MPa at 28 days according to EN 197-1:2011 standard, supplied by Cementos Molins Industrial, S.A. (Spain) was used to produce the mortars. The chemical composition, as well as the physical and mechanical properties of this cement, are reported in [7]. SF provided by Sika S.A.U. (Barcelona, Spain) with minimum 93.5% SiO_2 content and a density of 2.25g/cm^3, was mixed with the matrix as the pozzolanic addition to reduce the alkalinity of the binder. To improve the fluidity of the matrices and compensate for the adverse impact of SF on the workability of the fresh pastes, a Sika Viscocrete-3425 superplasticizer (SP) based on modified polycarboxylate polymers provided by the aforementioned company, was used.

The hybrid nonwoven fabric, with 1 mm thickness and an areal density of 155 g/m^2, was produced from 65% shredded short recycled TW fibers (by Triturats La Canya S.A., Spain) and 35% long flax fibers (Institut Wlokien Naturalnych, Poland) through card clothing and needle-punching process as described in depth in [4]. Thus, the final fabric, with a tensile rupture load of 2.0 N/g, consisted of approximately 45% cotton, 35% flax, and 20% polyester fibers.

2.2 Matrix preparation and characterization

Six specimens measuring 40 mm × 40 mm × 160 mm per sample were prepared and cured for 7 and 28 days prior to testing under flexure and compression forces. The curing was performed in a humidity chamber with >90% relative humidity (RH) at 20 ± 1 º C. The w/b ratio was fixed at 0.3 for all of the samples and 1%-1.4% SP by binder weight was added to the paste. Table 1 shows the mixed proportions and the designation of the samples based on the SF dosage expressed in percentage of the cement weight.

The mechanical tests, including three-point flexural and compression modes, were performed according to EN 196-1:2005 standard. The span length of the bending test was 100 mm and an INCOTECNIC press equipped with a load cell of 3 KN capacity at a loading rate of 2 mm/min was used. For the compression test carried out on the other halves of the specimens after the bending tests, the same press, equipped with a maximum load cell of 300 kN, was used. The maximum flexural tensile strength (also called the *modulus of rupture* (MOR)) and the compressive strength of the specimens were determined through Equations (1) and (2). Six and twelve specimens per sample were tested for flexure and compression, respectively.

$$MOR_{3p} = \frac{3P_{max}L}{2bh^2} \quad (1)$$

$$f_c = \frac{P_{max}}{bh} \quad (2)$$

Where P_{max} is the maximum associated load recorded, L is the span length, and *b* and *h* are the cross-sectional width and thickness, respectively.

Table 1 – Mix proportions and nomenclature of matrix samples.

Sample	SF0	SF5	SF10	SF15	SF20	SF25	SF30
Cement (g)	2500	2375	2250	2125	2000	1875	1750
SF (g)	0	125	250	375	500	625	750
Water (g)	750	750	750	750	750	750	750
SP (g)	25	25	25	25	35	35	35

The chemical compositions of the SF0 and SF30 samples were determined using an X-ray diffraction (XRD) analysis at various aging times (7 to 270 days) with a diffractometer model D8 Advance of Bruker AXS GMBH (Germany). Data were collected in the range 2θ from 5º to 50º at a resolution of 0.02º and a speed of 1 s/0.02º. The main anhydrous cement phases (C_2S, C_3S, C_3A, and C_4AF) are crystalline and therefore, their detection by XRD is possible, whereas the majority of the hydrated material, such as C-S-H, is amorphous or only partially crystalline [32].

Both TGA and derivative thermogravimetric analysis (DTG) are widely used thermal techniques used to evaluate the reactivity of pozzolanic addition and its reaction with PC to reduce the CH content [32], [33]. In this study, TGA tests were performed on all cement matrices with a thermobalance TGA-SDTA

851e/SF/1100 from Mettler Toledo. Samples containing approximately 20 mg were heated in an open alumina crucible from 25 °C to 950 °C at 10 °C/min with a flux of nitrogen of 50 ml/min. The percentage of CH in each mixture was calculated from the decomposition of portlandite through Equation (3) as previously stated by other authors [20], [34]:

$$CH\ \% = \frac{M_1 - M_2}{M_i} \times \frac{74}{18} \quad (3)$$

Where M_1 and M_2 are the mass of the samples at the start and end of CH decomposition, respectively. M_i represents the initial mass of the sample used in TGA.

2.3 Composite preparation and characterization

The textile-reinforced composite plates were produced based on the hand lay-up and the dewatering techniques (vacuuming and compression), as described in detail in previous works [7], [35]. To summarize, each sample was produced with six layers of nonwoven fabrics (a fiber volume fraction of 15%), which were immersed in matrix paste and stacked as a laminated plate in a drilled mold subjected to vacuum. Then, the sample was pressed under 3.3 MPa and unmolded after 24 h. Curing was carried out for 28 days at >90% RH and 20 ± 1 º C, resulting in a laminated plate with a thickness of approximately 10 mm and a surface mass of 16.6 kg/m^3. For the durability tests, the plates were subjected to the accelerated aging process after the 28-days curing, including 25 WD or 25 FT cycles performed in a CCI automatic climatic chamber (CCI Calidad, Spain), according to EN 12467 standard. Each WD cycle started with an 18-h immersion of the specimens in water at 20 ºC, followed by a 6-h drying at 60 ºC at 60% RH. Each FT cycle extended over 6 hours, in which the temperature was changed between -20 ºC to +20 ºC.

Based on the analyses of the matrices, composites with three different SF mixtures (0%, 15%, and 30%) were produced. The initial w/b ratio was fixed at 1.0, while the final ratio depended on the dewatering technique. For each sample, two plates (300 mm × 300 mm × 10 mm) were produced for flexural and tensile tests. From each of these, six specimens were machined (≈ 300 mm × 45 mm × 10 mm). Table 2 indicates the sample proportions and the composite nomenclature. The number after C reveals the percentage of SF, while WD and FT refer to durability tests: wet-dry and freeze-thaw cycles, respectively.

The mechanical properties of the composites were determined under a four-point flexural test (Figure 2a–c), following RILEM TFR 1 and TFR 4, as well as the uniaxial tensile test (Figure 2d–e), following RILEM TC 232-TDT [36] with modifications in specimen size. For the flexural test, an Incotecnic universal testing machine (Incotecnic Lab-Pre SL, Spain), equipped with a maximum load cell of 3 kN with a crosshead speed of 20 mm/min and a major span of 270 mm, was used. The following parameters were obtained from this test, as previously described in [37], [38]: the modulus of rupture (MOR) as the maximum flexural stress value through Equation (4); the limit of proportionality (LOP) as the breaking stress value of the matrix (first crack strength); the elastic modulus or the flexural stiffness of the pre-cracked zone (E_{1F}) between 60% and 80% of the LOP from the force-displacement curves through Equation (5); the flexural stiffness of the post-cracking zone (E_{3F}) through the previous formula; and finally, the toughness index (I_{GF}) as the specific fracture energy through the area under the force-displacement curve—limited to a deflection of 10% of the support span—divided by the section of the specimen.

For the direct tensile test, the Metrotec universal testing machine (UTM) from the EETAC SHM/CS2 series (Incotecnic Lab-Pre SL, Spain), equipped with a maximum load cell of 30 kN with a crosshead speed of 10 mm/min and clamping length of 180 mm, was used. The following parameters were obtained from this test: the ultimate tensile stress (UTS) as the maximum tensile stress value through Equation (6); the bend over point (BOP) as the breaking stress value of the matrix (first crack strength); the tensile moduli

as the slope of the stress-strain curve in the pre-cracked zone (E_{1T}) and the post-cracking zone (E_{3T}); and finally, the toughness index (I_{GT}) as explained for the flexural test.

$$MOR_{4p} = \frac{P_{max}L}{bh^2} \quad (4)$$

$$E = \frac{23\Delta P.L^3}{108\Delta f.bh^3} \quad (5)$$

$$UTS = \frac{T_{max}}{bh} \quad (6)$$

Where ΔP and Δf are the variations of forces and deflections of two points on the elastic regime or post-cracking regime, T_{max} is the maximum tensile force recorded, and the rest of the parameters are defined according to Equation (1).

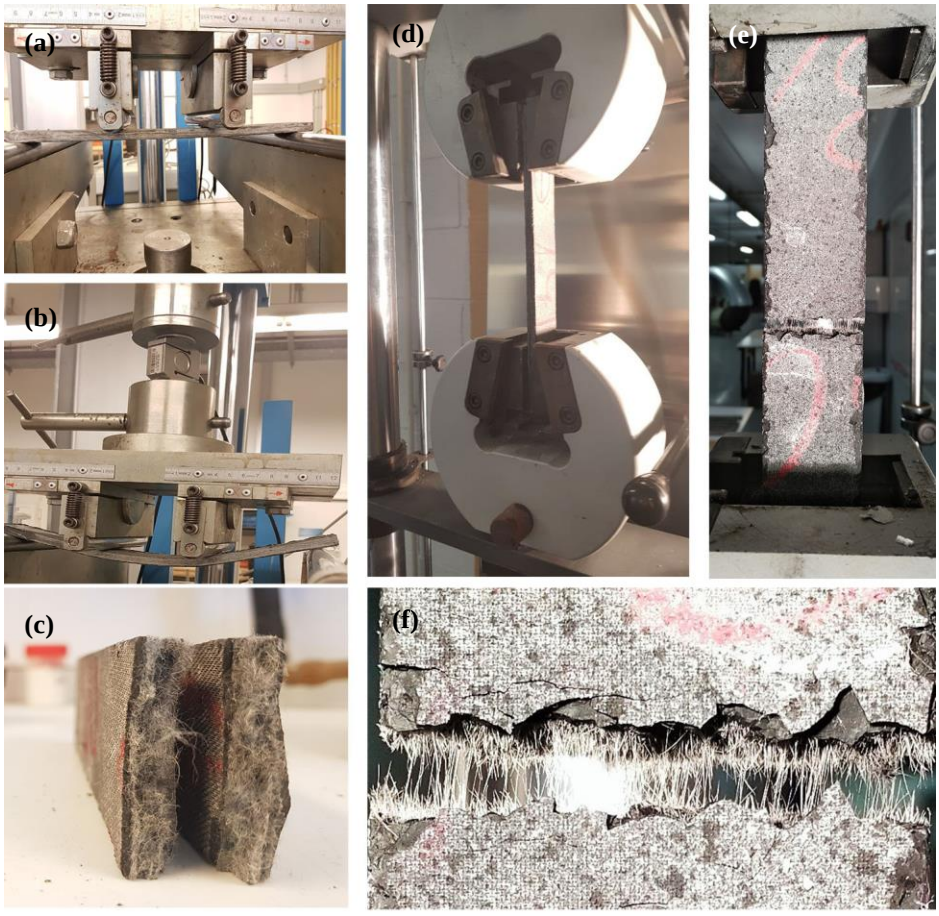

Figure 2. Mechanical tests on the composites: (a) flexural test set-up; (b) specimens under flexural loading; (c) flexural failure surface; (d) tensile test set-up; (e) rupture of the specimen under tension; (f) tensile failure surface .

Table 2 – Mix proportions and nomenclature of TW composite plates.

Sample	C0	C15	C30	C0WD	C15WD	C30WD	C0FT	C15FT	C30FT
Cement (gr)	1500	1275	1050	1500	1275	1050	1500	1275	1050
SF (gr)	0	225	450	0	225	450	0	225	450
Water (gr)	1500	1500	1500	1500	1500	1500	1500	1500	1500
SP (gr)	0	15	15	0	15	15	0	15	15
(w/b) final	0.45	0.55	0.55	0.45	0.50	0.40	0.55	0.55	0.55

Finally, to analyze the microstructure of the composites with a fractured surface, the effects of the accelerated aging cycles as well as the fiber-matrix interface, SEM and BSEM observations were made using a JEOL JSM 6300 (Jeol Ltd., Tokyo, Japan) scanning electron microscope equipped with an energy dispersive X-ray spectrometer (EDS) model Link ISIS-200 (Oxford Instruments, United Kingdom). The hydration reactions of the specimens were frozen by immersion in isopropyl alcohol and specimens were kept under vacuum conditions until analysis. Before BSEM analysis, the specimens were encapsulated in an epoxy resin and polished.

3. Results and Discussion

3.1 Mechanical performance of the matrices

The effects of SF content and curing time on the flexural and compressive strengths of the cement matrix are presented in Figure 3. As for the evolution of the mechanical properties with curing time, all of the samples in both flexural and compression modes presented a slight increase in resistance at 28 days as compared to 7 days. However, this increased rate was greater for those matrices with more than 15% SF, suggesting that the pozzolanic reaction may proceed more slowly than the reaction of the clinker compounds. In other words, although the control sample and those with low SF content reach the majority of their strength at 7 days, others would continue to gradually increase in strength. This type of later pozzolanic reaction in the almost CH-free mixtures had been previously observed by Toledo Filho et al. [39].

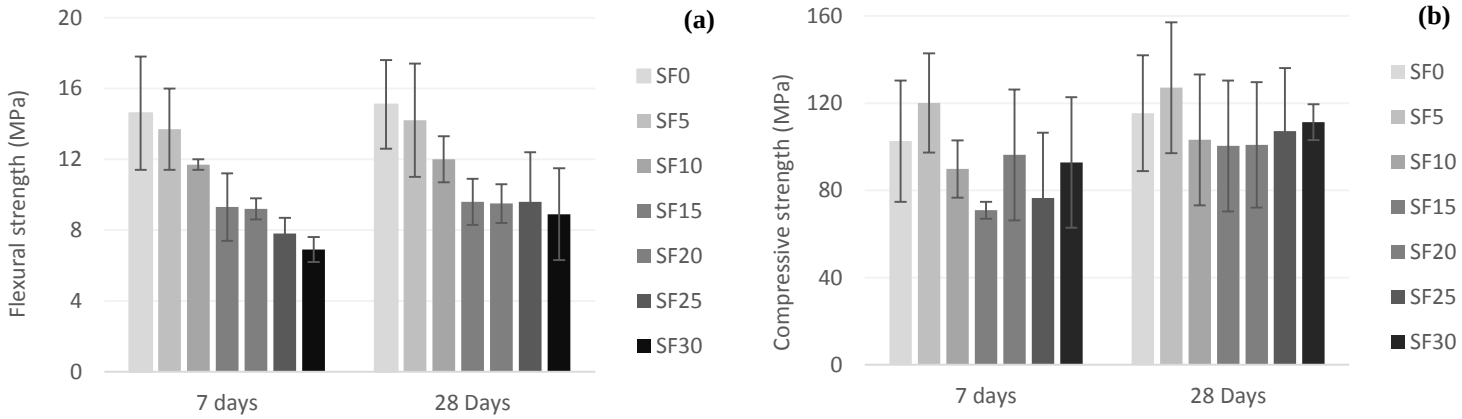

Figure 3. Mechanical results of the matrix: (a) flexural strength; (b) compressive strength

In the bending mode (Figure 3a), the MOR decreased gradually by increasing the SF content at both 7 and 28 days. However, at 28 days, the strength of the SF15 and SF30 samples was almost the same, and the difference with the control sample was reduced as compared to 7 days. This suggested that the pozzolanic materials reacted a bit more slowly and that by increasing the curing time, resistance would be increased.

Indeed, as reported in some studies, the blended pastes would slowly refine pore structures, resulting in increased strength, although their total porosities were equal or even higher as compared to pure PC pastes [36]. However, in the study of [33], adding distinct dosages of MK to the calcium-aluminate cement matrix led to a reduction of MOR with aging after 28 days. Additional and more detailed research on longer curing times with different matrices is necessary to clarify this behavior.

As for compressive strength (Figure 3b), the value of all samples at 28 days was greater than 100 MPa, suggesting that matrix hydration is incomplete at early curing time, due to the low w/b ratio (0.3) and the slow pozzolanic reaction, maintaining a certain amount of unhydrated particles. These particles can be subsequently hydrated, precipitating in porous regions of the matrix, hence filling the pores and increasing the compressive strength.

3.2 Microstructure of the matrices

Figure 4 presents the XRD spectra for the matrices of SF0 and SF30 samples at 7 to 270 curing days. As seen at 7 days for both samples, not all of the cement particles were hydrated and, therefore, the process evolved according to aging and degree of hydration (i.e., the anhydrous phases including C_3S, C_2S, C_3A, and C_4AF were decreasing while the hydrated ones (CH, C-S-H, $CaCO_3$) were increasing, from 7 days to 270 days curing). For the SF0 sample at 270 days, the amount of portlandite decreased due to the carbonation process, which resulted in calcite formation. For the SF30 sample (see Figure 4b), the same hydrated compounds as SF0 were formed. The C-S-H wave was slightly wider as compared to SF0, due to the reaction of SF with calcium. Up to 28 days, the SF0 and SF30 spectra were almost the same, but at 56 and 270 days, the C-S-H had become the majority phase, and at 270 days, the portlandite had virtually disappeared due to the clinker replacement and pozzolanic reaction, which advanced slowly. Indeed, for the SF30 sample, the initial increase in CH content lasted up to 28 days after the onset of PC hydration, after which the CH began to decrease due to the pozzolanic reaction triggered by SF. Thus, based on the XRD analysis, the SF30 sample could decrease the alkalinity of the matrix and increase the C-S-H with aging, especially after 56 days.

As for the TGA, in the cementitious matrix, the mass loss up to 600°C tends to be related to the loss of water and above that temperature, to the release of CO_2. While Portlandite dehydroxylates mainly in the range of 400°C-550°C ($Ca(OH)_2 \rightarrow CaO + H_2O$), calcium carbonate ($CaCO_3$) decomposes above 600°C to CaO and CO_2 [41]. C-S-H phases experience water loss over a wide range of temperatures (specifically 50°C to 400°C) due to the loss of the water in the interlayer and dehydroxylation [33], [40].

Figure 5a shows the amount of CH obtained from TGA and DTG analyses for all the matrices. As seen, the amount of CH decreased almost regularly by increasing the SF, however, the reduction was only significant from the SF15 composite onwards (less than 20% for SF5 and SF10), indicating that 5-10% SF barely decreases the alkalinity of the matrix. Thus, from the SF15 composite onwards, the amount of CH decreased more severely, approximately 38%, reaching its minimum in the SF30 sample, at which point it was reduced by almost 66% with respect to the sample without SF.

Figure 5b-d shows the TGA curves and the corresponding derivatives (DTG) for the SF0, SF15, and SF30 samples, based on weight loss and the exposed temperature. For the SF0 sample (Figure 5b), the DTG curve's main peak was observed in the range of 400°C-600°C, corresponding to the decomposition of CH, which resulted in a water loss of the matrix of almost 45%. A shorter peak was observed between 600°C and 850°C, which may be related to the decomposition of calcite and loss of CO_2 [42], as the presence of calcium carbonate was previously confirmed in XRD results. Some other shorter peaks were observed before 400°C, which can be associated with water loss due to C-S-H decomposition. However, the DTG curves of the SF15 and SF30 samples (Figure 5c,d) have shown no significant peak in the range of temperature related to CH dehydration, confirming the XRD results showing that the amount of CH was

lower as compared to the SF0 sample. The main peaks were observed at less than 200°C, which may be possibly associated with the water loss due to the C-S-H phase decomposition.

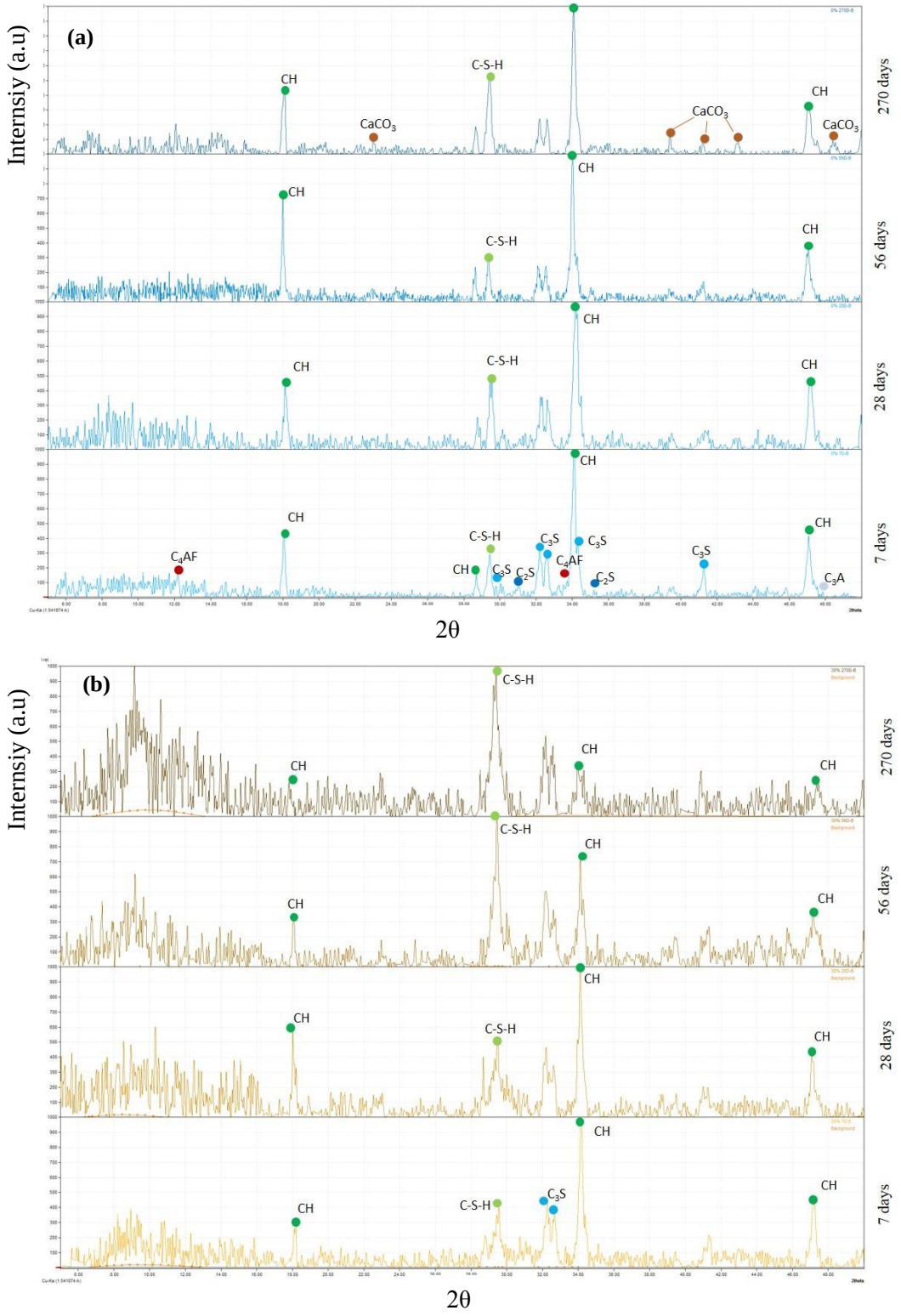

Figure 4. XRD spectra for matrices with distinct SF content at various ages: (a) SF0; (b) SF30 .

.

Thus, XRD and TGA analyses revealed that matrices with less than 15% SF presented a high amount of portlandite and were not suitable for improving the durability of the composites, although they presented a higher mechanical resistance. As for the other composites, according to their mechanical results, the matrices revealed comparable performance at 28 days. Thus, 30% SF sample led to the lowest amount of CH and was therefore selected as the optimum treatment for creating laminated composites. Furthermore, composites having 0% and 15% SF have been produced to compare the effect of portlandite quantity on the accelerated aging cycles.

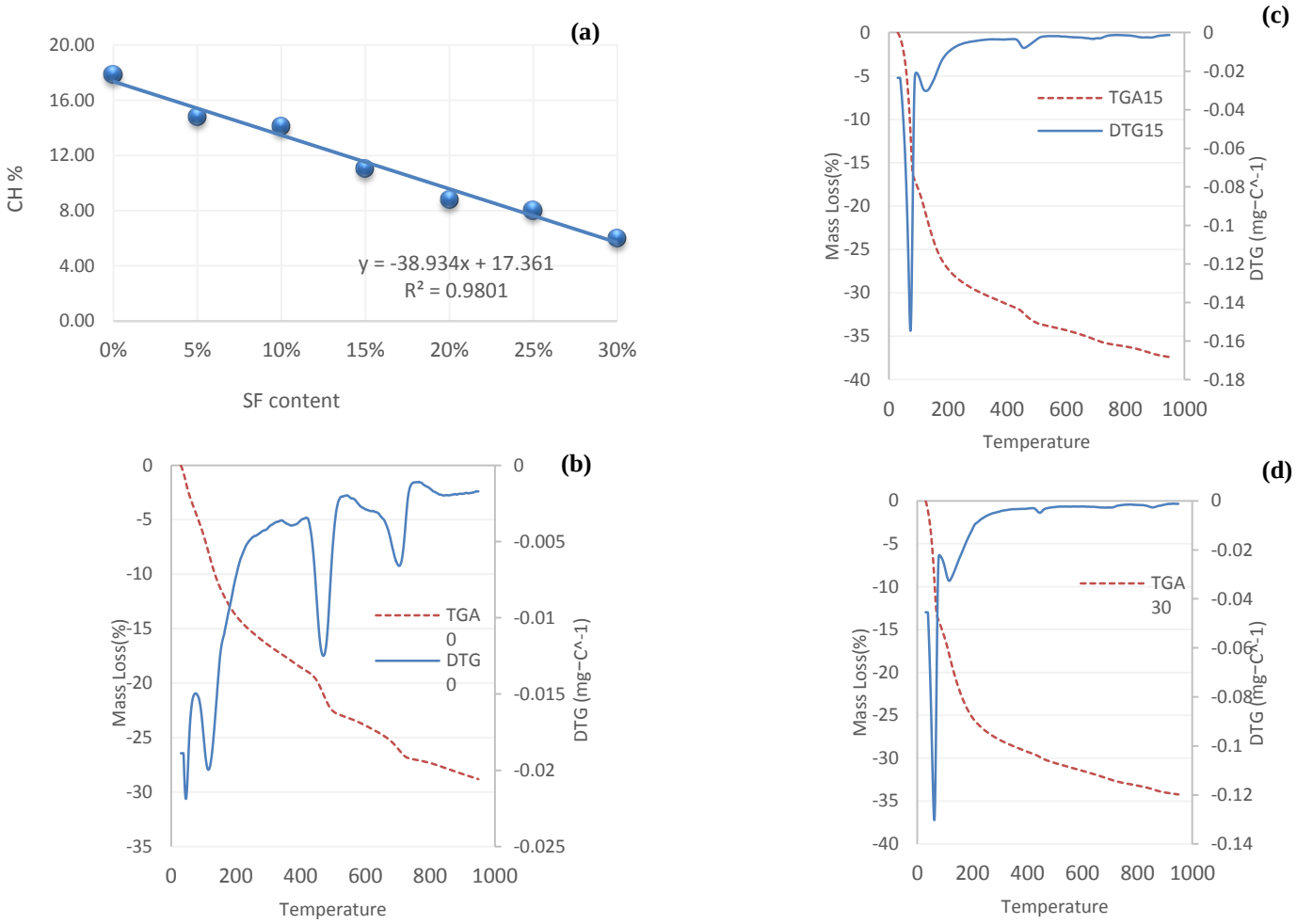

Figure 5. TGA and DTG results: (a): CH content of all samples; (b) SF0; (c): SF15; (d): SF30.

3.3 Flexural performance of the composites

Figure 6 depicts the representative flexural stress-displacement curves of each composite. Likewise, Table 3 presents the mean and CoV of the calculated parameters obtained from the flexural tests. The results shown in Figure 6 confirm that all unaged and aged TW nonwoven fabrics layers presented some extent of strain hardening behavior under flexural configuration, with a high capacity for deformation due to multiple cracking formations (see Figure 7). The cracking phases of the specimens followed the well-known trend including the pre-cracking zone, the transition, or crack propagation zone, and the post-cracking zone [43]. According to the results presented in Table 3 and Figure 8, the LOP decreased slightly when increasing the SF amount in unaged conditions, ranging between 5.2 N/mm^2 and 6.3 N/mm^2. This is in line with the behavior of the materials without reinforcement. Moreover, the LOP value of the composites increased in

aged conditions as compared to the unaged composites. This is more so for those with SF since this parameter was mainly influenced by matrix strength. Hence, the hydration and pozzolanic reaction could further increase said value.

On the other hand, the MOR values presented in Table 3 confirm the flexural-hardening response of all the composites (MOR/LOP > 1.0). In this regard, the cracking triggered the effective contribution of the fiber layers, which controlled the crack opening by bearing tensile stresses across the cracks. Figure 8 shows that in unaged conditions, the MOR value decreased slightly with the addition of SF, although the reinforcement capacity remained constant for all three samples (MOR/LOP ≈ 2.7). This may be due to the reduction of the matrix strength as observed in the LOP values. Nevertheless, in aged conditions, the trend was reversed. For instance, as a result of the pozzolanic additions, the MOR value increased both in WD and FT cycles. As observed in the TGA of the matrices, the addition of SF reduced the amount of CH, which in turn, reduced the degradation and embrittlement of the fibers in accelerated aging conditions. Thus, the reinforcement capacity of the fibers was higher when 30% SF was added, as compared to the C0 sample (e.g. in WD cycles: MOR/LOP = 1.6 for C0, while MOR/LOP = 2.6 for C30).

As for the accelerated aging cycles, WD caused significant damage to the fibers as compared to FT (especially in the C0 composite) as seen in SEM/BSEM observations. The MOR value was reduced by 40% and 24% in WD and FT cycles, respectively, for the C0 composite, whereas said reductions represent only 16% and 4% for the C15 composite. The C30 sample showed equal or even higher MOR (in accelerated aging cycles) than the unaged sample as the fibers almost remained undamaged (see the values of E_{3F} in Table 3) whereas the LOP increased.

The values of toughness (I_{GF}), as a reference parameter for assessing the ductility and energy absorption of the composites, are presented in both Table 3 and Figure 9. The results reveal that I_{GF} follows a similar trend to that obtained for MOR. That is, the C0 sample had the highest I_{GF} value among the unaged composites whereas, in aging conditions, the C30 sample had the highest value. The observed trends for MOR and I_{GF} in this study are in line with other observations in which the effect of SCMs for the wet-dry aged condition was examined through the flexural test for the vegetable-based fiber reinforced mortar composites [25], [37], [39]. In all the studies, the MOR and I_{GF} of the unaged composites were slightly reduced after substituting cement with SCMs (10% SF, 10% MK, and 50% MK/calcined waste, respectively). Furthermore, these parameters decreased significantly for the reference samples −without SCMs− when exposed to WD cycles. Nonetheless, the SCMs in all studies could improve those parameters in aging conditions with respect to aged reference samples.

Table 3– Flexural properties (CoV in %) of all samples

CODE	MOR (N/mm^2)	LOP (N/mm^2)	MOR/LOP	I_{GF} (KJ/m^2)	E_{1F} (GPa)	E_{3F} (GPa)
C0	16.5 (12)	6.3 (19)	2.6	10.1 (12)	11.3 (21)	0.40 (9)
C15	14.9 (15)	5.5 (20)	2.7	8.9 (18)	11.0 (26)	0.37 (28)
C30	14.5 (13)	5.2 (24)	2.8	8.6 (13)	10.8 (22)	0.38 (24)
C0WD	10.0 (27)	6.4 (31)	1.6	6.5 (33)	12.0 (5)	0.15 (24)
C15WD	12.5 (10)	5.9 (12)	2.1	7.7 (13)	11.2 (12)	0.22 (17)
C30WD	14.3 (3)	5.8 (13)	2.4	8.1 (10)	11.0 (8)	0.30 (14)
C0FT	12.5 (15)	6.5 (21)	1.9	7.4 (16)	12.0 (31)	0.27 (30)
C15FT	14.3 (14)	5.9 (22)	2.4	8.2 (20)	11.5 (26)	0.30 (30)
C30FT	15.4 (12)	5.8 (20)	2.7	8.7 (22)	11.1 (22)	0.35 (32)

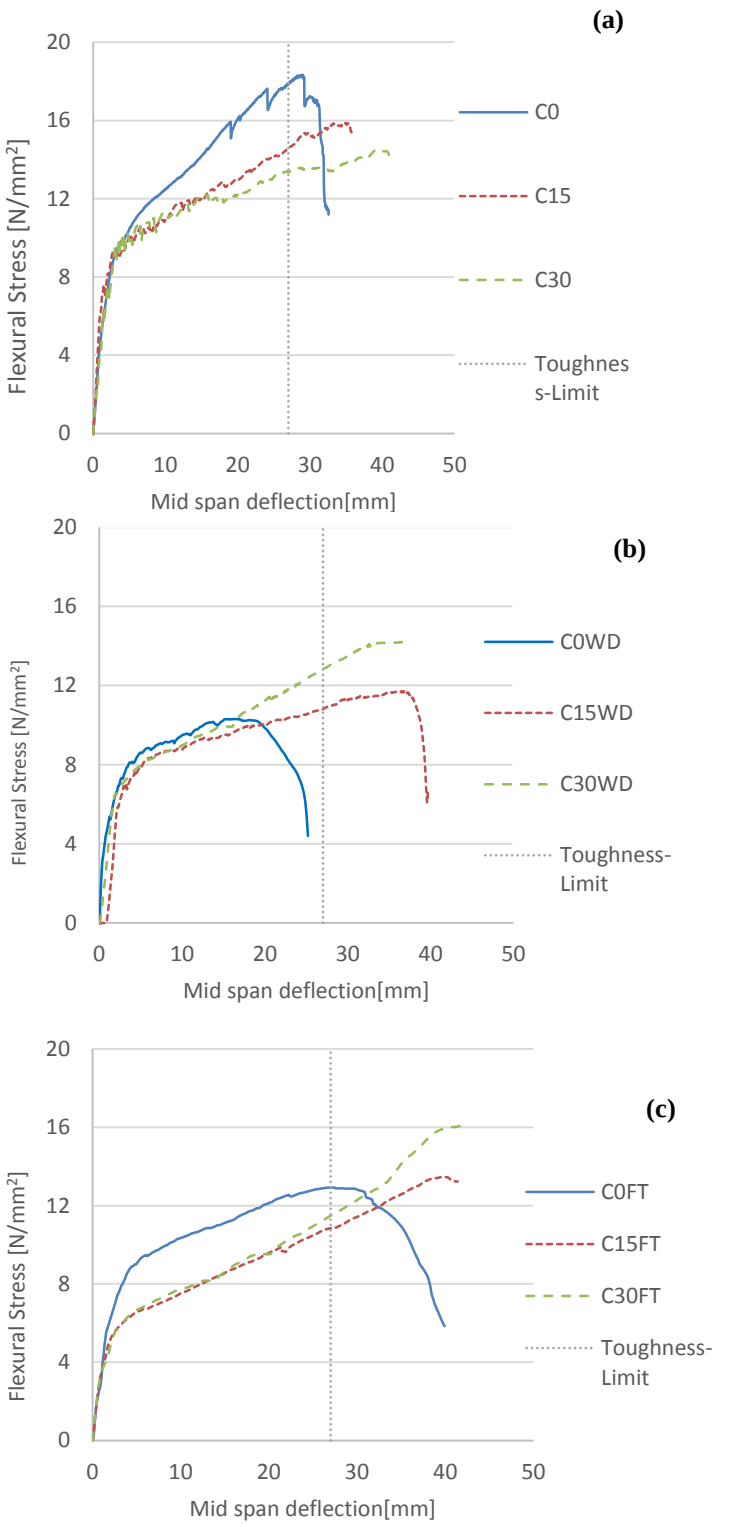

Figure 6. Experimental flexural stress–deflection relationships of TW nonwoven composites in various conditions: (a) unaged; (b) WD aging; (c) FT aging.

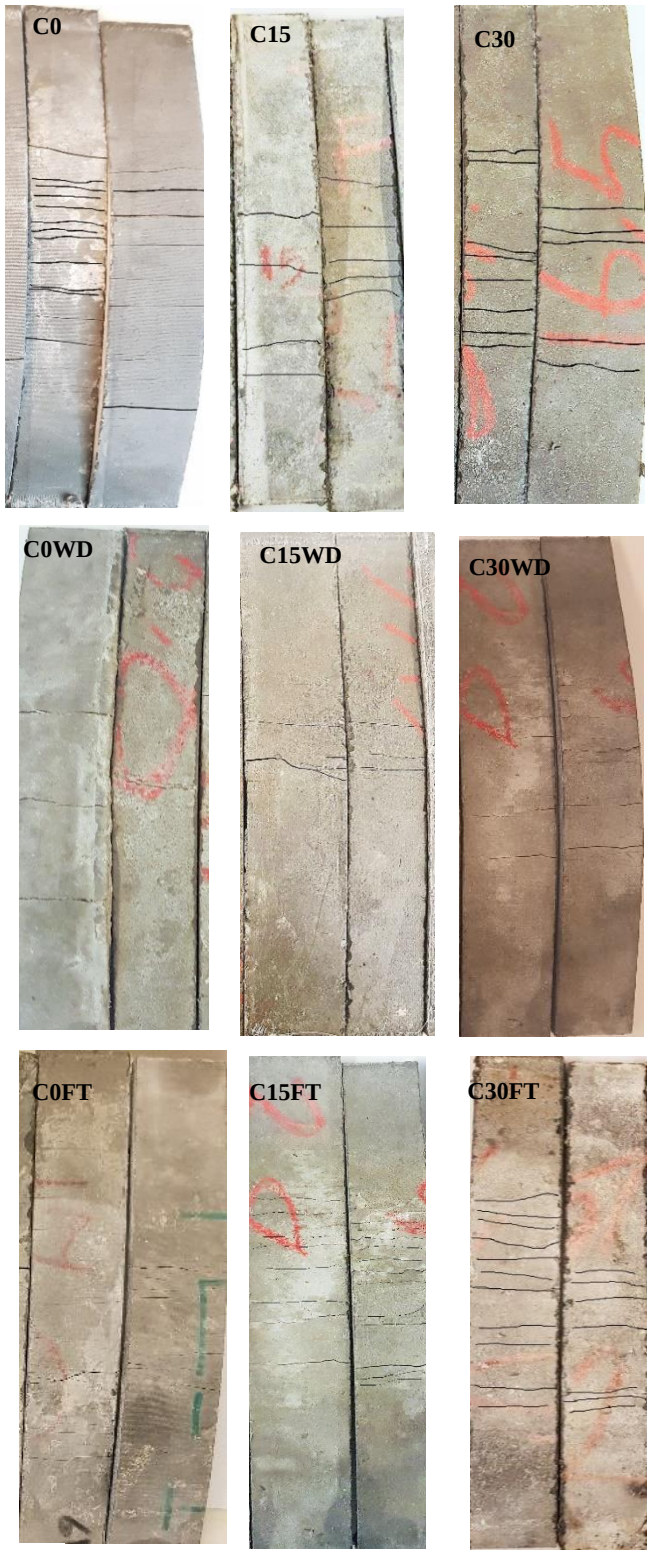

Figure 7. Typical cracking pattern of the composites after the flexural test.

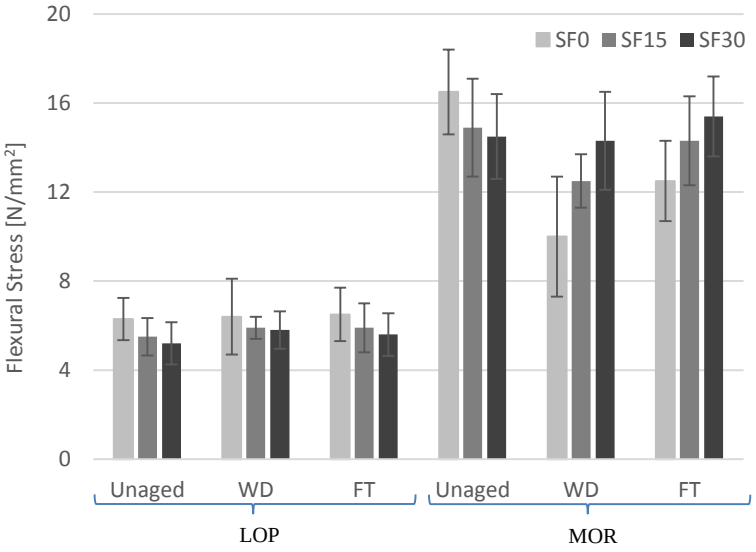

Figure 8. Flexural strength of the nonwoven composites.

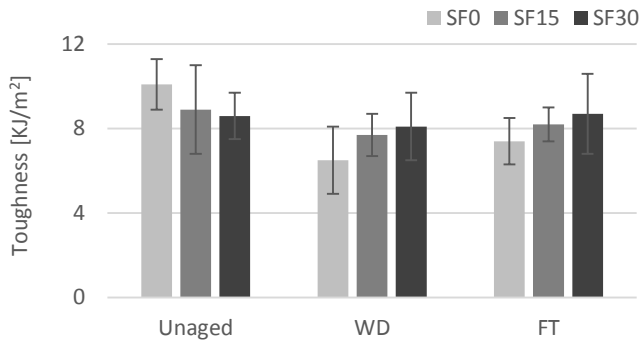

Figure 9. Flexural toughness (I_{GF}) of the nonwoven composites.

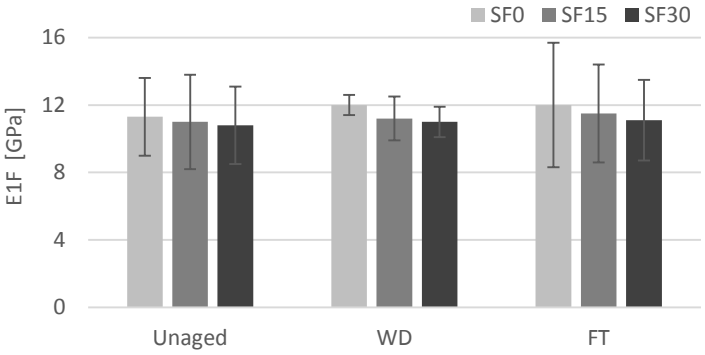

Figure 10. Flexural stiffness of the pre-cracked zone.

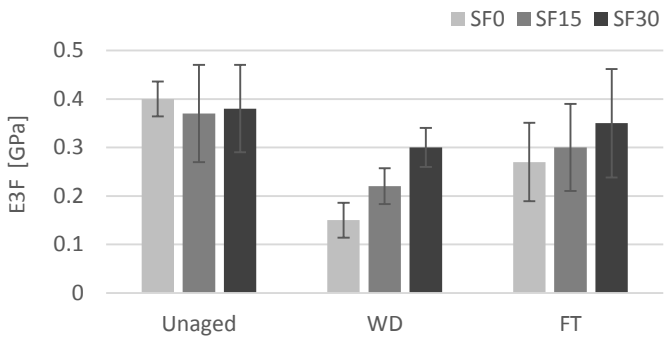

Figure 11. Flexural stiffness of the post-cracked zone.

In this study, although WD cycles negatively affected the toughness of the C0 composite and caused the loss of over 35%, this loss was only 5% for the C30 composite, proving that the remaining CH had an almost negligible effect on fiber degradation. Moreover, the adverse effect of FT cycles was considerably less than WD, confirming that the WD cycles are the most critical durability tests for natural-based fibers, as reported in [8], [44]. Figure 7 reveals that the composites in unaged and FT conditions, had a more uniformly distributed multi-cracking pattern while following the WD cycles, the samples had fewer and wider cracks. This same cracking pattern was reported by Toledo Filho et al. [39] as to the comparison of unaged with WD cycles of sisal reinforced composites. Indeed, under constant environmental conditions, the transfer of OH^- ions or $Ca2^+$ ions from the cement matrix to the fibers is slow. However, exposure to repeated WD cycles causes the capillary pore system of the cement matrix to be consecutively filled and emptied with alkaline pore water, resulting in a faster transfer of the hydration products to the fibers which, in turn, leads to fiber mineralization and embrittlement [45].

Finally, the flexural stiffness of the pre-cracked (E_{1F}) and post-cracked (E_{3F}) zones (see Table 3 and Figures 10-11) were also calculated from the flexural load–midspan deflection curves. As can be seen, the

TW reinforcement is not a governing factor in pre-cracked stiffness ($E_{3F}/E_{1F} \leq 0.04$ in all cases) since the matrix did not crack in this stage. Therefore, the fibers do not effectively contribute to this stiffness. Moreover, E_1 follows almost the same trend as LOP since both parameters are mainly dependent on the matrix characteristics (i.e., after durability tests, the elastic pre-cracking properties (LOP and E_{1F}) remained constant or increased by up to 5% since these mainly depend on the matrix, rather than on fibers). A similar trend, unaltered or even higher amounts for LOP and E_{1F} after the aging of the cement composites, was observed in other research [46], [47].

On the other hand, E_{3F} is governed mainly by the stiffness of the fabrics as the matrix was cracked in the post-cracked regime, and only fibers bear the tensile stresses. As can be seen in Figure 11, WD cycles caused the stiffness of fibers in the C0 composite to degrade significantly (more than 60%) while this amount was half in FT cycles. By adding SF, the degradation of the fibers' stiffness decreased (only 20% and 7% in WD and FT, respectively, for C30) leading to promising results in post-cracking behavior for the C30 sample after aging. Moreover, as seen in Figure 6b, although the aged composite demonstrated strain hardening with multiple cracking behavior, the slope of the post-cracked zones (E_{3F}) was lower than the corresponding unaged composites (Figure 6a), especially as compared to C0 (60%), indicating the loss of the fibers' stiffness due to degradation.

3.4 Tensile performance of the composites

Figure 12 shows the tensile stress-strain curves of the composite samples in both unaged and aged conditions. Likewise, Table 4 presents the mechanical properties obtained from the previous curves. All of the curves in Figure 12 started with the elastic-linear range, in which both the matrix and the fiber behaved linearly. In this first zone, the stiffness of the composite (E_{1T}) is dominated primarily by matrix properties due to the low volume fraction of fibers and lower fiber stiffness with regard to the matrix (less than 20 times). The second zone (cracking stage) was started by an initial crack formation (BOP value) and propagation in the matrix phase. This is where the fibers start to bridge the cracks and thus, the load-carrying capacity continues by occurring multiple cracking behaviors (zone three). Finally, the progressive damage occurred due to the crack widening, which leads to a failure by fiber debonding.

Table 4– Tensile properties (CoV in %) of all nonwoven composites

CODE	UTS (N/mm^2)	BOP (N/mm^2)	UTS/BOP	I_{GT} (KJ/m^2)	E_{1T} (GPa)	E_{3T} (GPa)
C0	6.8 (17)	3.5 (19)	1.9	45.0 (23)	0.20 (22)	0.086 (9)
C15	6.4 (16)	3.4 (20)	1.8	43.2 (18)	0.14 (20)	0.070 (28)
C30	6.5 (4)	3.3 (10)	1.9	50.1 (16)	0.15 (22)	0.080 (20)
C0WD	3.5 (18)	3.2 (8)	1.1	6.7 (28)	0.20 (25)	0.006 (19)
C15WD	4.1 (10)	3.1 (15)	1.3	21.6 (23)	0.17 (22)	0.047 (17)
C30WD	5.5 (5)	3.2 (13)	1.7	32.1 (10)	0.16 (28)	0.055 (24)
C0FT	4.7 (12)	3.7 (21)	1.2	17.6 (34)	0.30 (31)	0.031 (30)
C15FT	5.7 (15)	3.8 (22)	1.5	27.4 (31)	0.20 (26)	0.060 (20)
C30FT	6.9 (28)	4.0 (20)	1.7	47.7 (21)	0.25 (32)	0.069 (32)

The results presented in Table 4 and Figure 13 reveal that the TW fabric was effective in enhancing the post-cracking behavior of the materials (UTS/BOP > 1.0). The addition of SF to the composites in unaged conditions had a negligible effect on all of the mechanical properties. However, this pozzolanic material proved its efficiency in aging cycles. While WD and FT cycles reduced the UTS (50% and 30%, respectively) and toughness (80% and 60%, respectively) of the C0 sample (see Figure 14), the adverse effect of these accelerated aging cycles on the samples containing SF, especially those with 30%, was

noticeably inferior. As for the WD cycles, the C15 sample lost 35% and 50% of its resistance and energy absorption, respectively, while for the C30 sample, said reductions represented only 15% and 36%. Regarding FT, the loss was even less significant (10% and 37% for the C15 sample in UTS and I_{GT}), proving that this type of aging is less critical than WD. The C30 sample demonstrated virtually no mechanical loss in post-cracking parameters after the FT cycles.

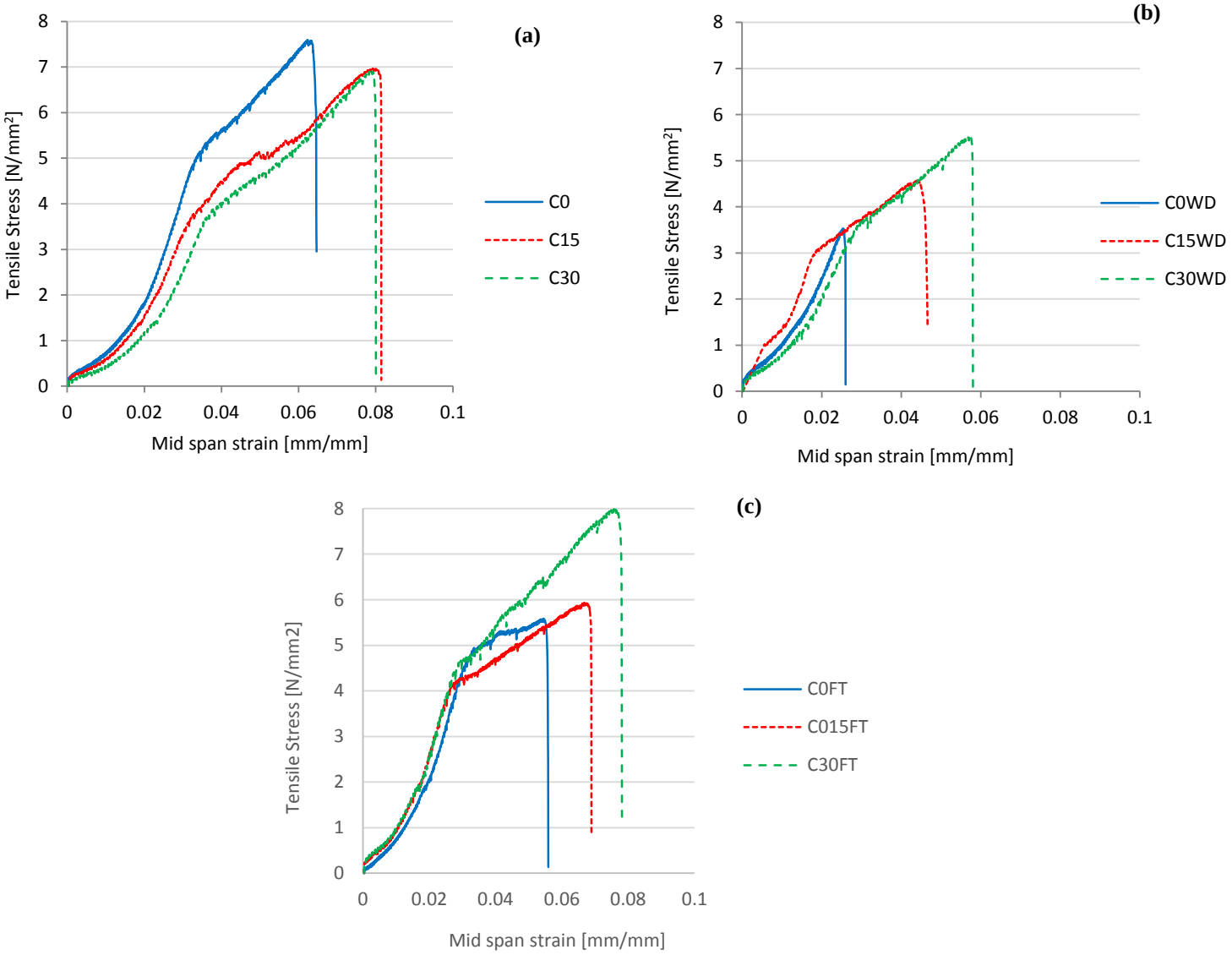

Figure 12. Experimental tensile stress–deflection relationships of TW nonwoven composites in various conditions: (a) unaged; (b) WD aging; (c) FT aging.

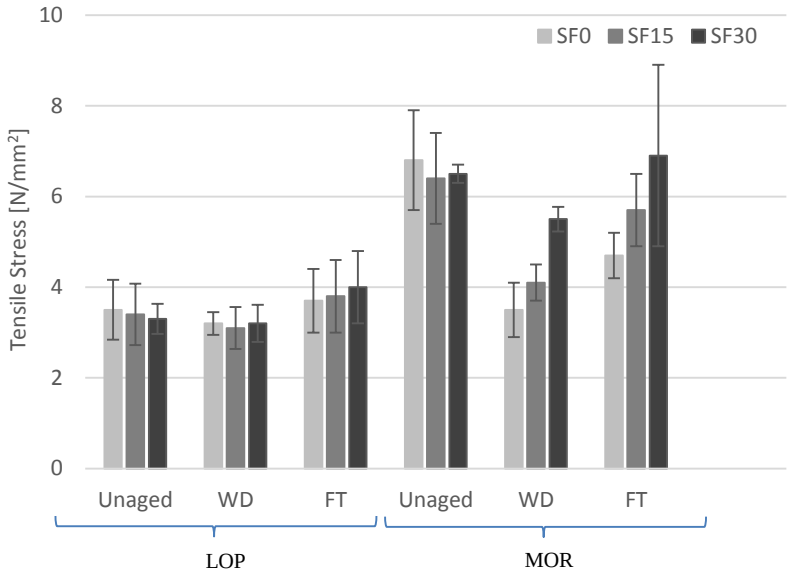

Figure 13. Tensile resistance of the nonwoven composites.

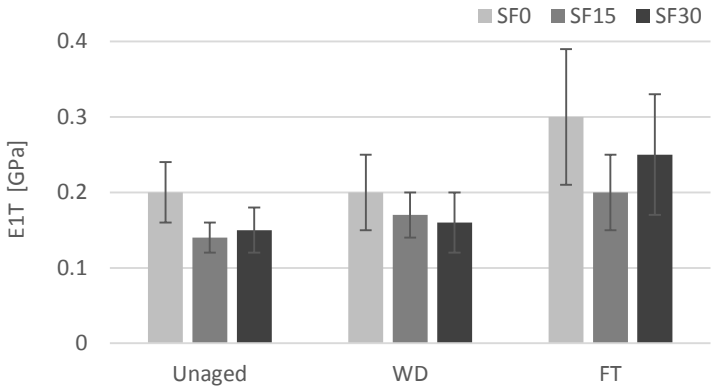

Figure 14. Tensile toughness (I_{GT}) of the nonwoven composites.

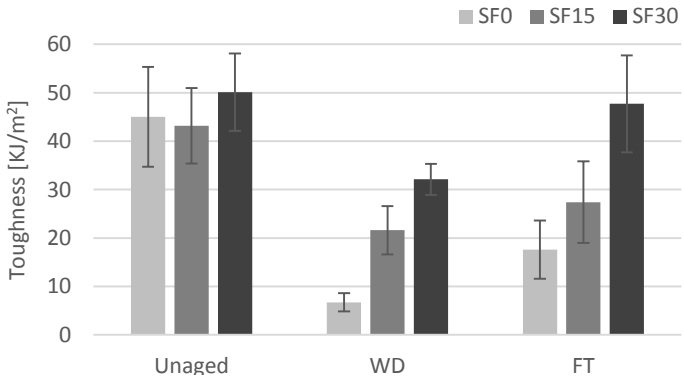

Figure 15. Tensile stiffness of the pre-cracked zone.

The pre-cracking properties including BOP and E_{1T} (see Figure 15) did not change or even improve slightly with aging since the matrix could be hydrated even more during the aging cycles. The addition of SF to the composite did not have a significant effect on these properties.

As seen in Figure 17, E_{3T} was reduced by aging, especially for the C0 sample in WD conditions −almost 90%−, revealing the stiffness degradation of the fiber due to mineralization and migration of CH to the fiber structure. Nevertheless, this loss was less significant for C15 and C30 samples, especially in FT cycles. The C30 composite in FT cycles showed the same mechanical properties as the unaged one since the fiber embrittlement was negligible and the fibers could provide almost the same contribution as in unaged conditions.

As for the comparison between the flexural and tensile performance, Figure 17 shows the amount of ξ for the calculated parameters (e.g. ξ for the maximum resistance will be MOR/UTS) using the C0 composite as a reference since a similar trend was observed for the other samples. The first crack resistance under bending (LOP) occurred on average at stress levels that were 80% higher than those observed for the direct tension test (BOP). A greater discrepancy was noticed for the maximum stresses. Thus, the values reported for MOR are over twice as high as those for UTS. Pre- and post-crack moduli or stiffness were significantly higher for the flexural configuration as well (56.5 and 4.5 times, respectively). The only property that was higher in the tensile configuration was toughness, which was 4.5 times higher in the tensile test. Nonetheless, the general variation trends of all parameters based on aging conditions and SF content were similar in both test configurations. Similar differences between the flexural and tensile resistances were reported in other studies [18], [38].

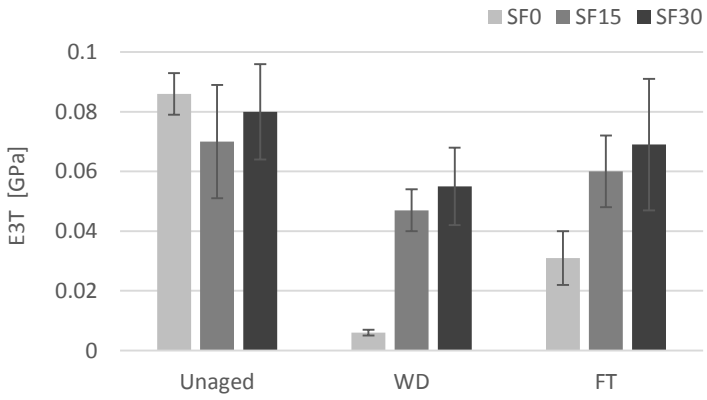

Figure 16. Tensile stiffness of the post-cracked zone.

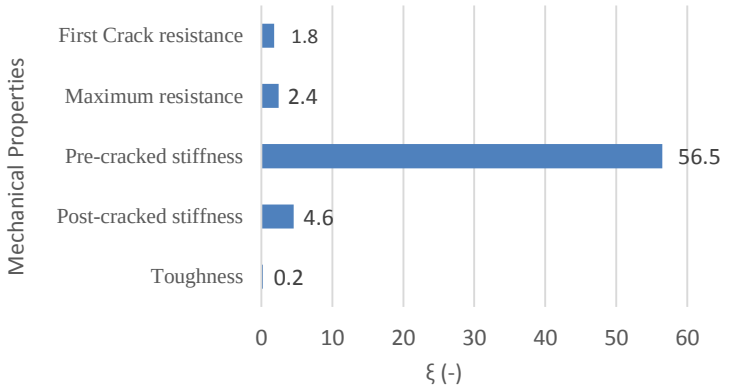

Figure 17. Comparison between flexural and tensile properties for C0 composite

3.5 Microstructure of the composites

Figure 18 shows the scanning electron micrographs of the breaking section of all matrices with nonwoven reinforcement layers. The C0 sample had a very flat and clean breaking surface, in which the fibers protrude slightly from the breaking plane. The matrix was slightly disintegrated in the area of the fibers. The fibers were cut close to the breaking section and the pullout holes (yellow dots) can be detected in addition to the fiber rupture cut right at the edge of the section (yellow arrows). In the C0WD sample, the matrix between the fibers was more significantly disintegrated. The fiber rupture, in addition to the fiber pullout, had a smaller length than that of the unaged sample. In the C0FT sample, no significant differences

were revealed as compared to the C0 sample. There was similar matrix disintegration with a smaller dimension (dotted blue ellipse) along with the fibers cutting a short distance from the breaking section.

In samples with 30% SF, the extraction of the fiber from the fractured section was longer than the corresponding one without SF. Of these, the C30 and C30FT samples were remarkable due to those points where the reinforcing effect of the fibers was hardly damaged and where the matrix areas were trapped and surrounded by fibers (blue arrows). The C30WD sample showed a disintegrated matrix and the fibers were smaller in length. Nonetheless, the pullout holes of the fibers appeared although it is difficult to find fibers cut right at the edge of the section.

Figure 19 shows the SEM image of reinforcement in the C0WD sample. Both natural and synthetic fibers broke without elongation, indicating a brittle break, (i.e., the fibers were easily broken at the anchorage section in the mortar). Figure 19a,b presents the natural cotton fibers where the section revealed concentric fiber layers that were separated from each other by degradation of the hemicelluloses due to the alkalinity of the cement. On the spectra, the deposits in the cotton fibers look like calcium carbonate, derived from the carbonation of calcium hydroxide. Synthetic fibers with a continuous smooth surface can be seen in Figure 19c,d. The type of breakage is similar to that of cellulose fiber. No significant fiber elongation was observed, which would indicate a sudden break. The image above showed cracks perpendicular to the fiber axis. These cracks could be a consequence of fiber deterioration in the extrusion manufacturing process. Synthetic fibers had fewer deposits and spectra indicate that it may be C-S-H, possibly due to the higher hydrophobicity of synthetic fibers as compared to cotton. In WD cycles, the migration of calcium ions from the matrix to the synthetic fibers most likely occurred less often than in the vegetable fibers due to lower water absorption capacity. In general, the natural fibers were more significantly degraded than synthetic fibers in the C0 sample.

In the sample with 30% SF subjected to WD cycles (see Figure 20), most of the fibers keep their length after the sample failure, revealing the good tensile strength and flexibility of the fibers. Vegetable fibers with an almost smooth surface had flakes on the surface and some longitudinal cracks, indicating a superficial degradation that was inferior to that of the C0 sample. No main cracks appear as compared to the COWD sample, and the fiber did not break at the section edge. Moreover, natural fibers retained a large amount of the cement hydration material on the surface, although clearly grouped in granules. Textile waste fibers, on the other hand, appeared to have less hydrated cement compounds on the surface, possibly indicating a lack of adhesion. Most of these fibers had no serious degradation on their surface, although some minor longitudinal cracks were observed. As for the composition of the compounds adhered to the fibers, the spectra indicated the presence of C-S-H with a few traces of calcium hydroxide associated with the addition of 30% silica fume.

Figure 21 presents a general backscattered image of the C0 composite (Figure 21b) with two magnifications: the matrix area (Figure 21a) and the fiber nonwoven area (Figure 21c). Moreover, the EDS analysis of the selected points to detect the different elements making up the material is also presented. As for the matrix, the anhydrous particles of the cement that have not yet been hydrated can be observed. The spectra indicate the presence of calcium and silicon oxides, most likely allite (C_3S) and bellite (C_2S) in SP-a1. The presence of aluminum, as well as silicon, can be detected in SP-a2. This could be an indication of celite (C_3A) in a polyphase particle, along with allite or bellite. Several anhydrous particles of cement (yellow dots in Figure 21a) are evident in the matrix zone. In the fiber zone (Figure 21c) the fibers' ability to absorb and retain moisture generated increased hydration of the cement particles [15]. Thereby, in this area, the anhydrous particles were smaller in size. This phenomenon was most evident around larger diameter fibers, where most particles were less than 1 micron in size. In this case, calcium silicates were detected in SP-c2 and SP-c5, and a ferritic phase (C_4AF), in SP-c3 and SP-c6. As for the hydrated phases, the neutral gray background surrounding the anhydrous particles, amorphous C-S-H was detected in spectra

SP-a3, SP-c4, and SP-c7. In SP-c1, carbon corresponding to the fibers was detected. On the other hand, in Figure 21b the good penetration of the matrix in the structure of the nonwoven was observed, permitting good adhesion to the fibers and ductility.

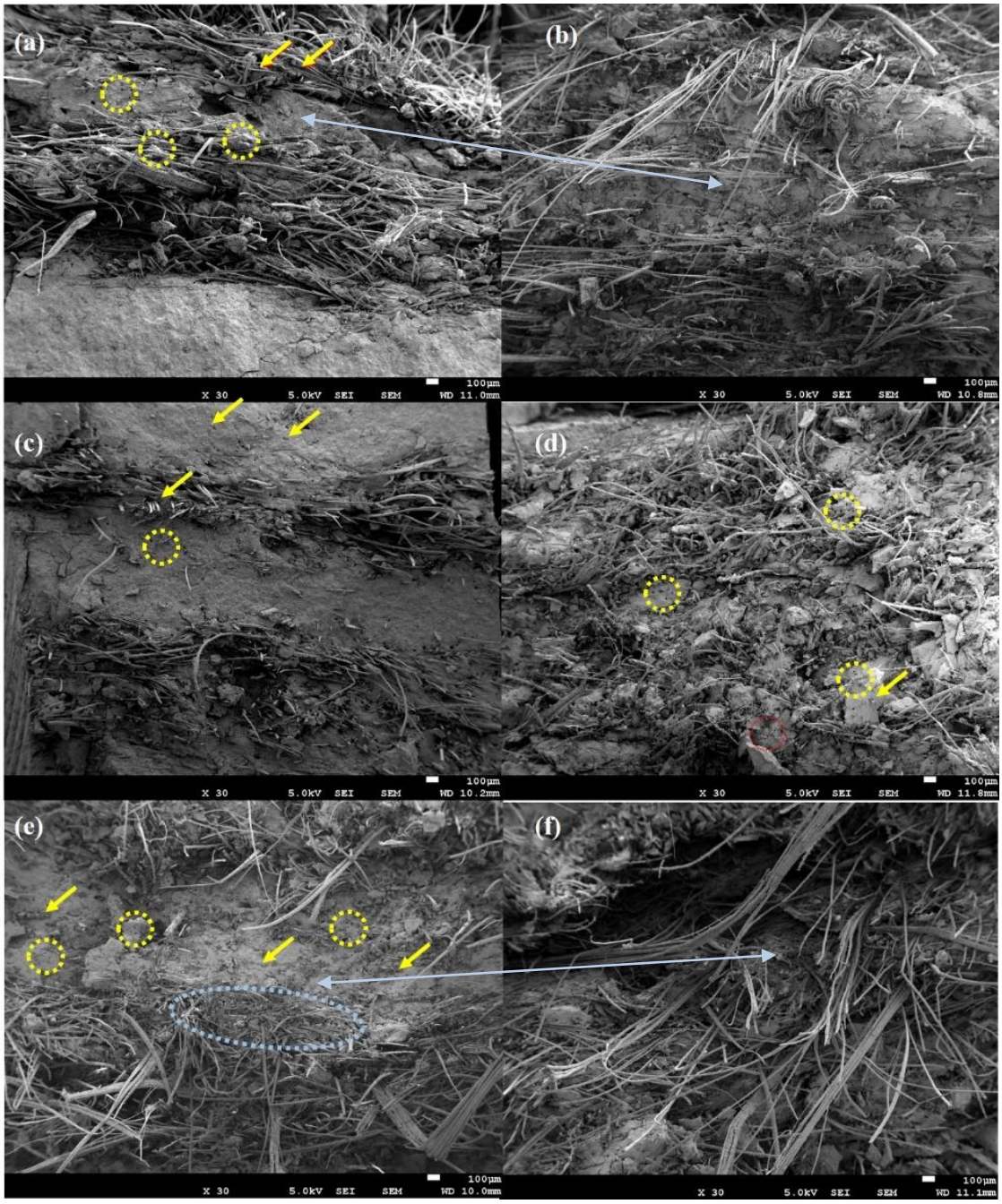

Figure 18. SEM microimages of the fracture surface of all the composites: (a) C0; (b) C30; (c) C0WD; (d) C30WD; (e) C0FT; (f) C30FT.

The main difference between C30 (see Figure 22) and C0 matrices is the unreacted SF particles. In the area of the fibers, given the higher moisture content generated by the vegetable fibers, there was a greater

reaction of the SF particles, leading to the formation of C-S-H (SP-a4 and SP-c4). The same types of anhydrous particles of dicalcium or tricalcium silicates (C_2S and C_3S) were found in SP-a1, SP-a2, SP-c1, and SP-c2. In SP-a3, the presence of silicon, aluminum, calcium, and iron could indicate a polyphasic particle with di-or-tricalcium aluminate fractions, with the presence of C_4AF phases. Moreover, the presence of amorphous areas with calcium and silica with higher oxygen contents indicates that it can be a C-S-H (SP-a5). SP-c3 could indicate an SF particle that has reacted to form C-S-H, given the high presence of Si. Finally, the high carbon content in the fibers was observed in SP-c5.

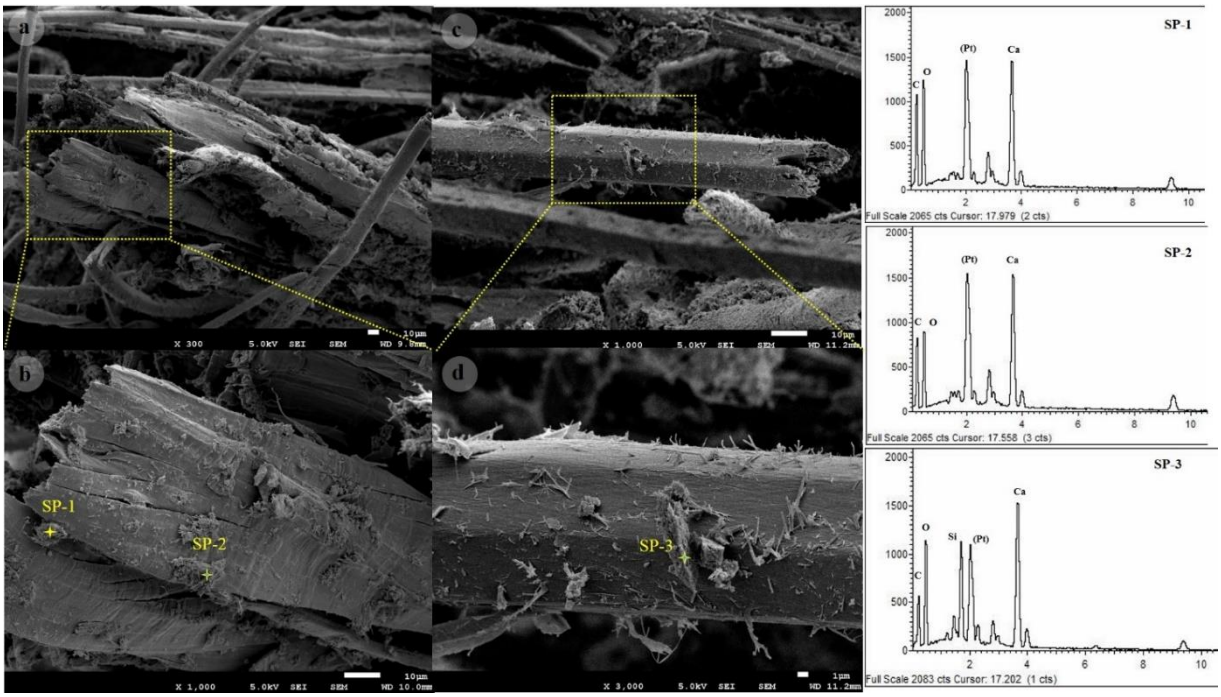

Figure 19. SEM microimages of the fiber surface in the C0WD sample and the corresponding EDS analysis: (a) vegetable fiber; (b) higher magnification of vegetable fiber; (c) synthetic fiber; (d) higher magnification of synthetic fiber

Figure 23 demonstrates the migration content of the Ca ion from the matrix to the fibers as a result of the WD cycles for the composite without SF. Indeed, due to the WD cycles, CH was dissolved in the water and penetrated the pores and fibers. Figure 23a shows a fiber surrounded by the matrix of the C0 composite. Around the fiber, some anhydrous particles are observed, along with the hydrated areas. The fiber, dark in color, was well-detected due to its carbon content (low atomic weight). The map of points for the calcium ion of the C0 sample can be seen in Figure 23b. The fiber was very well-defined and the detection of ions inside the fiber was practically non-existent. Similar details are shown in Figure 23c-d for the C0WD sample after 25 cycles. The matrix is seen to be fully hydrated as a result of its increased exposure to moisture due to WD cycles. The gap between matrix and fiber is also evident as a result of the fiber hornification causing its shrinkage. Furthermore, the boundaries of the fiber are clearer than its interior. Comparing the center of the fibers in the two different conditions −unaged and aged −, the tone of gray in Figure 23c is lighter than that of Figure 23a, indicating the existence of elements with a higher atomic weight. Figure 23d shows how calcium ions can penetrate and deposit on the fiber after aging. The results confirm the findings of Toledo Filho et al. [41], reporting that the degradation of cellulose fibers is a consequence of the accumulation of Ca-rich phases both in and around the fibers after accelerated aging. Indeed, due to the WD cycles, the matrix quickly lost its moisture whereas the fibers retained it and later became dry, given their absorption and retention ability. This resulted in an increased concentration of Ca

ions around the fibers. When the material becomes completely dry, CH precipitates both on and inside the fibers since due to the aging cycles, the pump effect transfers the CH from the matrix zone to the fibers.

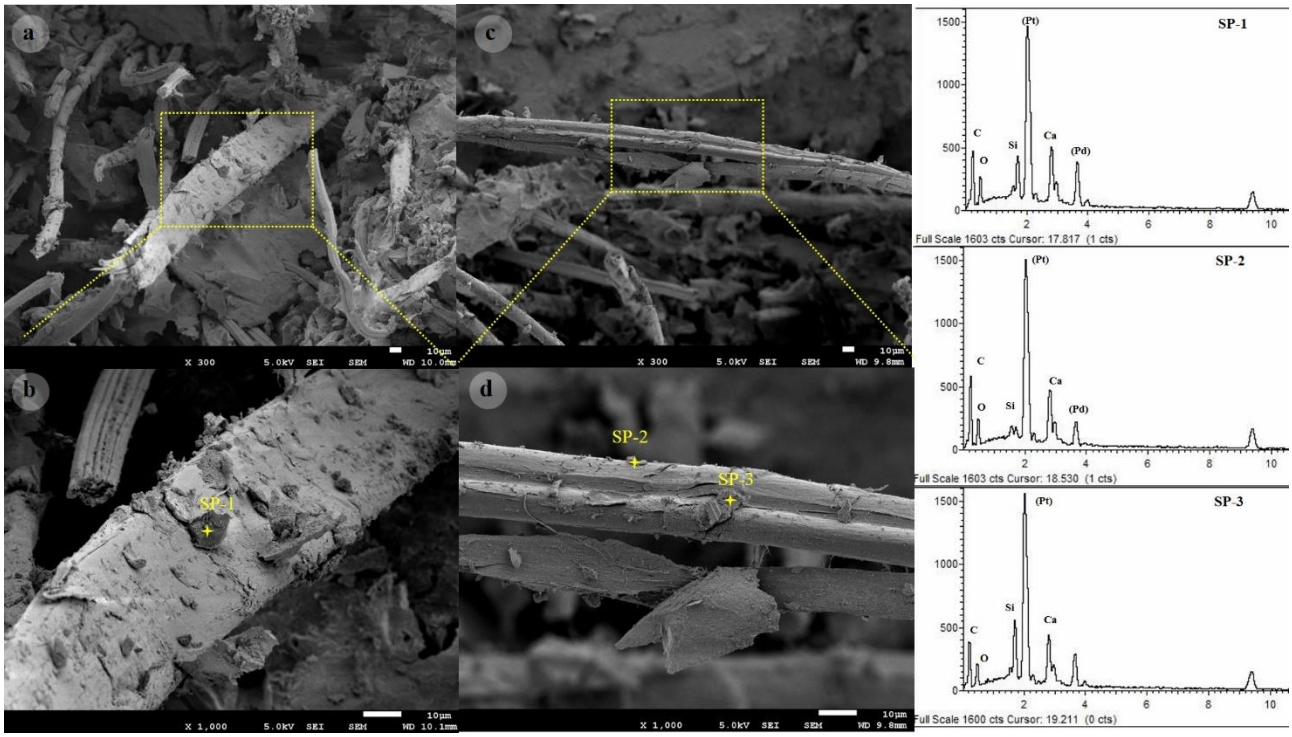

Figure 20. SEM microimages of the fiber surface in the C30WD sample and the corresponding EDS analysis: (a) vegetable fiber; (b) higher magnification of vegetable fiber; (c) synthetic fiber; (d) higher magnification of synthetic fiber

Figure 24 presents the transformation of the matrix after the SF addition and how it affected the fibers after the WD cycles. Figure 24a is a replica of Figure 23c which has been incorporated for the purpose of comparing the two composites from samples C0 and C30, after aging. According to Figure 24c, the area of the matrix in the C30WD sample was almost fully hydrated, as the C0WD one. The fiber has also suffered from shrinkage after the cycles and has been disengaged from the matrix, leaving a certain gap. Figure 24b,d presents a color mix corresponding to the different ions of aluminum, calcium, silicon, and iron (Al, Ca, Si, and Fe, respectively), which are individually presented below as a map of points. As seen for the C0WD sample in Figure 24b, the concentration of Ca ions was very high with the blue tone predominating in the image. On the other hand, for the C30WD sample, with the incorporation of SF, where the majority of CH transforms into C-S-H, the main ion coloration corresponded to the concentration of Si. Therefore, the final image tone is green. Furthermore, the lower solubility of C-S-H reduces the precipitation of the hydration products in the fibers, thereby avoiding serious mineralization which results in constant reinforcing properties. Finally, the ternary triangular diagrams show the transformation of the matrix from Ca-majority to Si-majority, while maintaining the Al concentration.

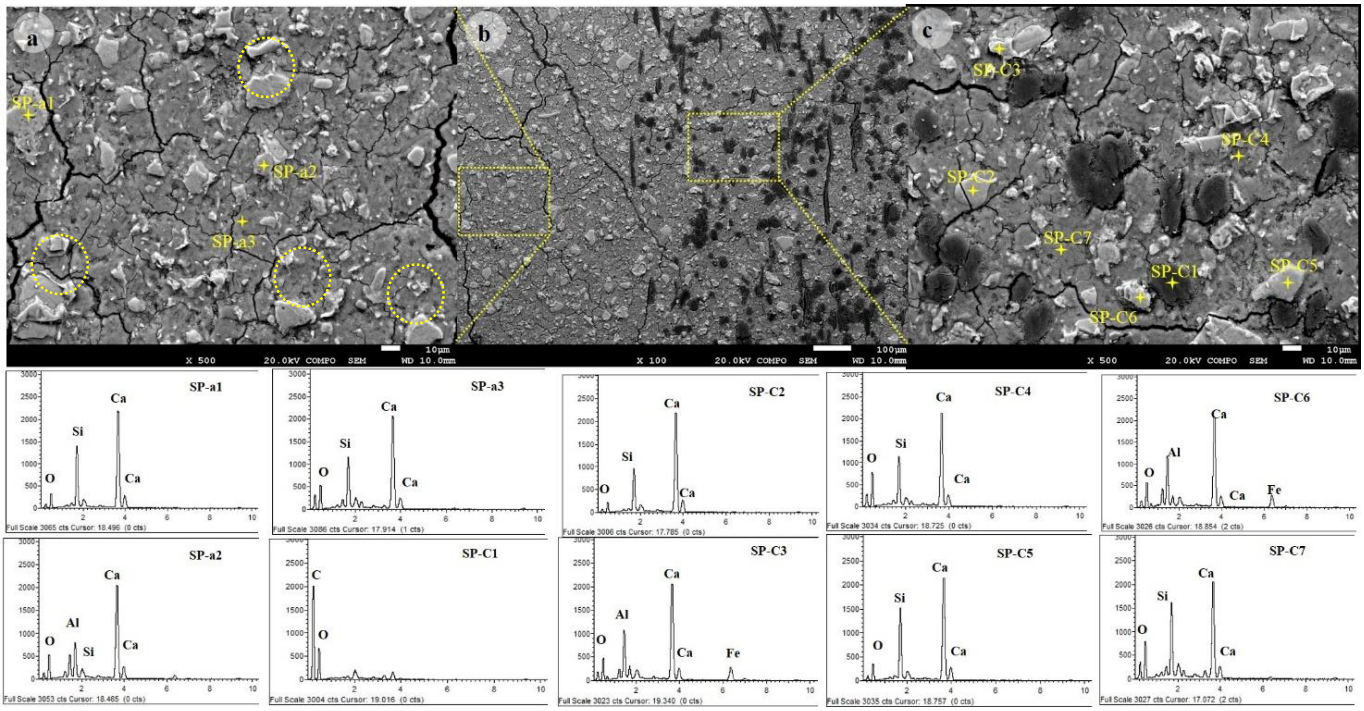

Figure 21. Backscattered images of the C0 and the corresponding EDS analysis: (a) magnification of matrix area; (b) general image of the composite; (c) magnification of the nonwoven area

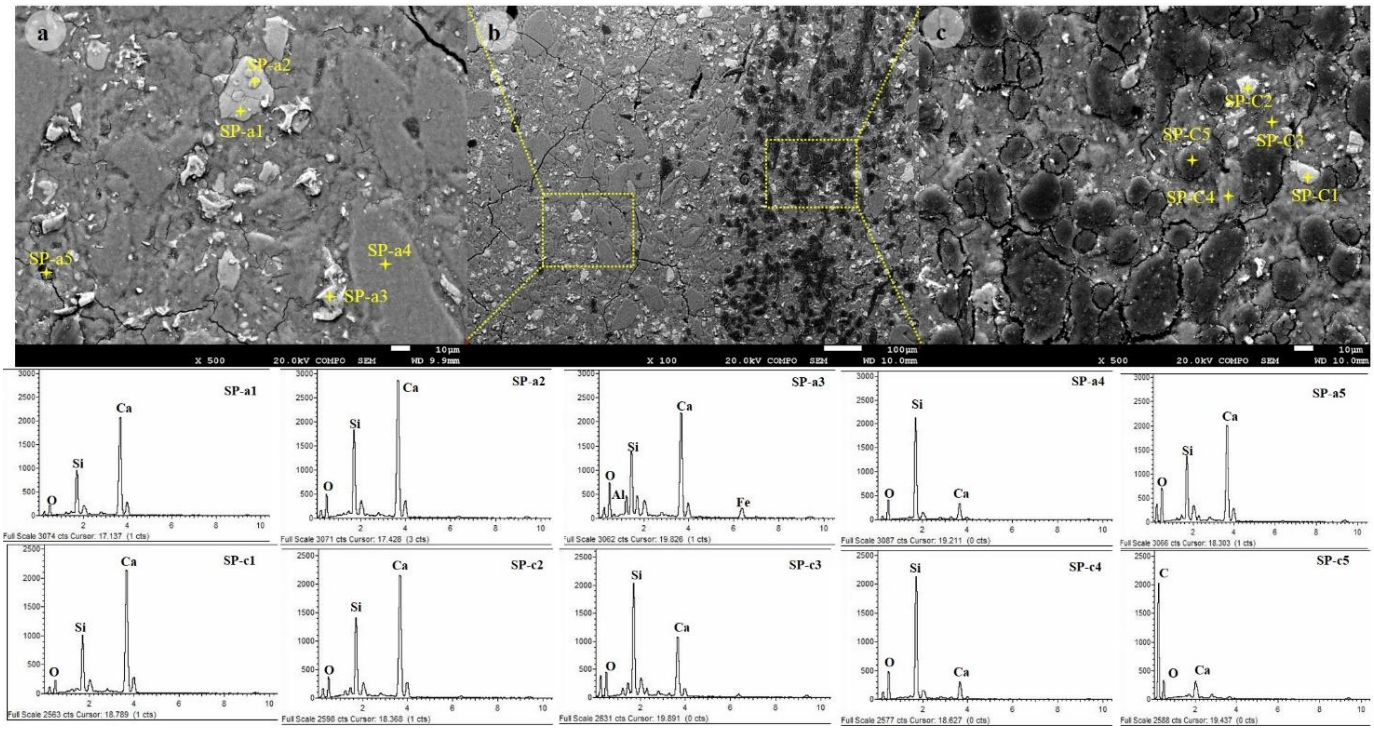

Figure 22. Backscattered images of the C30 and the corresponding EDS analysis: (a) magnification of matrix area; (b) general image of the composite; (c) magnification of the nonwoven area

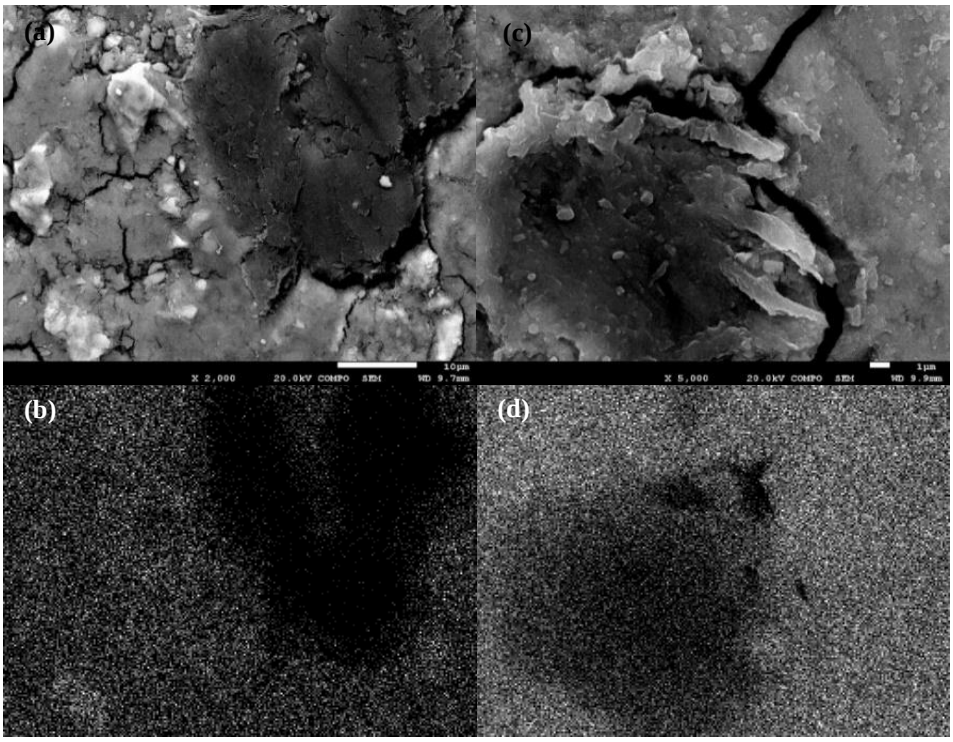

Figure 23. BSEM images of fiber-matrix interfacial zone and dotting map of Ca ion: (a),(b) C0 ; (c),(d) C0WD

4. Conclusions

The main objective of this study was to characterize both design-sensitive mechanical properties (compression, flexure, and direct tension) and durability (against wet-dry and freeze-thaw cycles) of a cement-based −with/without silica fume− textile waste nonwoven fabric reinforcement. The reinforcement is made up of recycled short fibers from the garment industry as well as flax fibers. Cement was replaced by silica fume (SF) by up to 30% to quantify its efficiency in improving the durability of the composite- protection of the fibers.

The following conclusions were made from the experimental program results:

- The study of the matrix suggested that the flexural and compressive resistances decreased with the addition of SF at 7 days of curing. However, at 28 days of curing, the difference between variable samples was reduced, indicating the slow reaction of pozzolanic material. Furthermore, TGA and XRD analyses proved that matrices with less than 15% SF presented a large amount of portlandite and were not suitable for improving the durability of the composites. The lowest amount of calcium hydroxide was found in the C30 sample.

- The results of the flexural tests on the composites showed that wet-dry accelerated aging cycles negatively affected the post-cracking properties of the reinforced composites as compared to the unaged specimens. Nonetheless, composites with 30% SF (C30 sample) presented only slight

reductions (< 5%) in their mechanical properties as compared to the unaged specimens. The composite without SF (C0 sample) had a resistance 15% higher in unaged conditions than the C30 sample, with a 40% decrease in the wet-dry cycles.

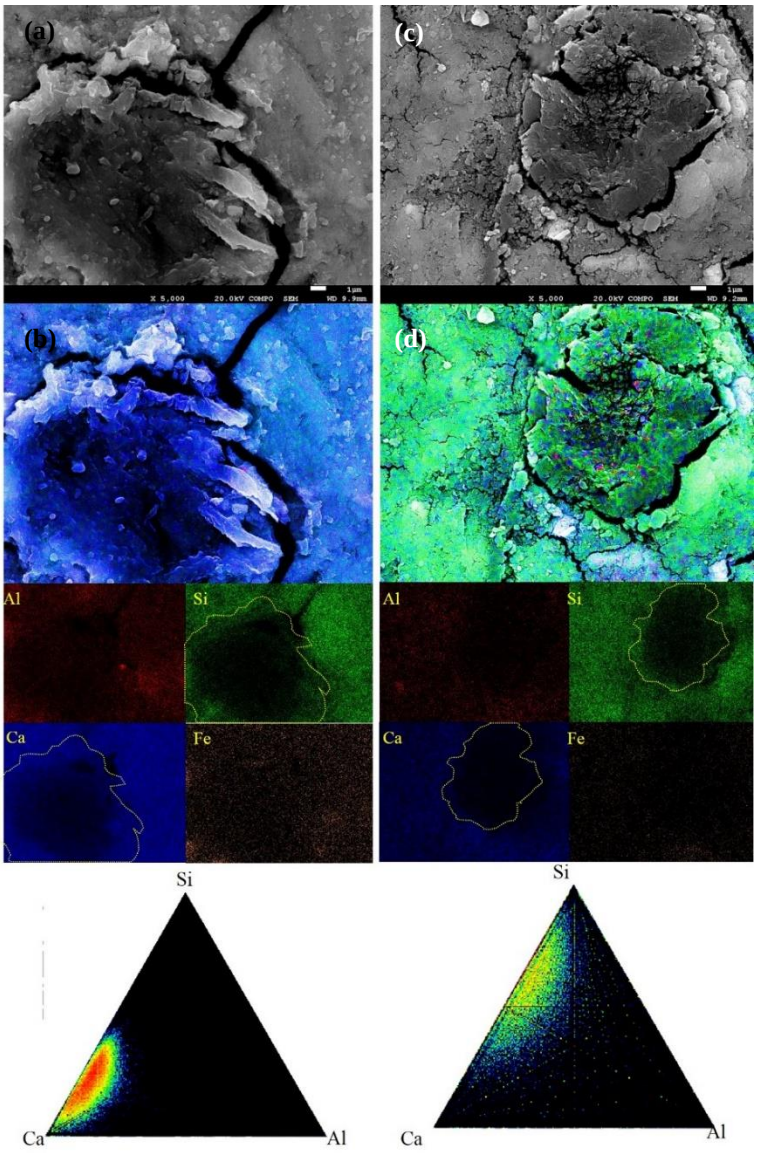

Figure 24. BSEM images of fiber-matrix interfacial zone and dotting map of chemical element: (a),(b) C0WD ; (c),(d) C30WD

- The results of the direct tensile tests on the composites revealed that the addition of SF had negligible effects on the mechanical properties in unaged conditions. However, composites with SF exhibited better mechanical properties in aged conditions, especially in wet/dry cycles.

- SEM and BSEM observations confirmed that the accelerated aging process, mainly wet-dry cycles, lead to an increased fiber fracture ratio and a decreased fiber pull-out strength due to the alkali attack in the C0 sample. Nonetheless, composites containing SF presented a better behavior than the C0 composite, since the amount of calcium hydroxide was significantly reduced (especially in those

composites with 30% SF), as confirmed by the TGA study. Thus, the developed PC-based matrix modified with 30% SF prevented fiber embrittlement when submitted to accelerated aging.

Finally, these characterization results of textile waste composites modified with SF allow us to confirm the potential use of this composite as a durable material for building components with limited structural responsibility, offering enhanced sustainability performance.

Acknowledgments

The authors express their gratitude to the Spanish Ministry of Economy, Industry, and Competitiveness for the financial support received under the scope of the projects RECYBUILDMAT (PID2019-108067RB-I00) and CREEF (PID2019-108978RB-C32).

References

[1] P. Sadrolodabaee, S. M. A. Hosseini, M. Ardunay, J. Claramunt, and A. de la Fuente, "A New Sustainability Assessment Method for Façade Cladding Panels: A Case Study of Fiber/Textile Reinforced Cement Sheets," pp. 809–819, Sep. 2021.

[2] S. Spadea, I. Farina, A. Carrafiello, and F. Fraternali, "Recycled nylon fibers as cement mortar reinforcement," Constr. Build. Mater., vol. 80, pp. 200–209, Apr. 2015.

[3] F. Colangelo, I. Farina, M. Travaglioni, C. Salzano, R. Cioffi, and A. Petrillo, "Innovative Materials in Italy for Eco-Friendly and Sustainable Buildings," Mater. 2021, Vol. 14, Page 2048, vol. 14, no. 8, p. 2048, Apr. 2021.

[4] F. Colangelo, A. Forcina, I. Farina, and A. Petrillo, "Life Cycle Assessment (LCA) of Different Kinds of Concrete Containing Waste for Sustainable Construction," Build. 2018, Vol. 8, Page 70, vol. 8, no. 5, p. 70, May 2018.

[5] P. Sadrolodabaee, J. Claramunt Blanes, M. Ardanuy Raso, and A. de la Fuente Antequera, "Preliminary study on new micro textile waste fiber reinforced cement composite," ICBBM 2021 4th Int. Conf. Bio-based Build. Mater. Barcelona, Catalunya June 16-18, 2021 Proc., pp. 37–42, 2021.

[6] P. Sadrolodabaee, J. Claramunt, M. Ardanuy, and A. de la Fuente, "Mechanical and durability characterization of a new textile waste micro-fiber reinforced cement composite for building applications," Case Stud. Constr. Mater., vol. 14, p. e00492, Jun. 2021.

[7] P. Sadrolodabaee, J. Claramunt, M. Ardanuy, and A. de la Fuente, "Characterization of a textile waste nonwoven fabric reinforced cement composite for non-structural building components," Constr. Build. Mater., vol. 276, p. 122179, Mar. 2021.

[8] J. Claramunt, M. Ardanuy, J. A. García-Hortal, and R. D. T. Filho, "The hornification of vegetable fibers to improve the durability of cement mortar composites," Cem. Concr. Compos., vol. 33, no. 5, pp. 586–595, 2011.

[9] M. Ardanuy, J. Claramunt, and R. D. Toledo Filho, "Cellulosic fiber reinforced cement-based composites: A review of recent research," Constr. Build. Mater., vol. 79, pp. 115–128, 2015.

[10] J. Claramunt, M. Ardanuy, and J. A. García-Hortal, "Effect of drying and rewetting cycles on the structure and physicochemical characteristics of softwood fibres for reinforcement of cementitious composites," Carbohydr. Polym., vol. 79, no. 1, pp. 200–205, 2010.

[11] B. Koohestani, A. K. Darban, P. Mokhtari, E. Yilmaz, and E. Darezereshki, "Comparison of different natural fiber treatments: a literature review," Int. J. Environ. Sci. Technol. 2018 161, vol. 16, no. 1, pp. 629–642, Jul. 2018.

[12] V. da Costa Correia, S. F. Santos, and H. Savastano, “Vegetable fiber as reinforcing elements for cement based composite in housing applications – a Brazilian experience,” MATEC Web Conf., vol. 149, p. 01007, 2018.

[13] S. F. Santos, G. H. D. Tonoli, J. E. B. Mejia, J. Fiorelli, and H. Savastano Jr, “Non-conventional cement-based composites reinforced with vegetable fibers: A review of strategies to improve durability,” Mater. Construcción, vol. 65, no. 317, p. e041, 2015.

[14] L. Dvorkin, V. Zhitkovsky, M. Sonebi, V. Marchuk, and Y. Stepasiuk, “Improving Concrete and Mortar Using Modified Ash and Slag Cements,” Improv. Concr. Mortar Using Modif. Ash Slag Cem., Apr. 2020.

[15] L. Fernández-Carrasco, J. Claramunt, and M. Ardanuy, “Autoclaved cellulose fibre reinforced cement: Effects of silica fume,” Constr. Build. Mater., vol. 66, no. September, pp. 138–145, 2014.

[16] M. Khorami and E. Ganjian, “The effect of limestone powder, silica fume and fibre content on flexural behaviour of cement composite reinforced by waste Kraft pulp,” Constr. Build. Mater., vol. 46, pp. 142–149, 2013.

[17] R. M. de Gutiérrez, L. N. Díaz, and S. Delvasto, “Effect of pozzolans on the performance of fiber-reinforced mortars,” Cem. Concr. Compos., vol. 27, no. 5, pp. 593–598, May 2005.

[18] F. de A. Silva, B. Mobasher, and R. D. T. Filho, “Cracking mechanisms in durable sisal fiber reinforced cement composites,” Cem. Concr. Compos., vol. 31, no. 10, pp. 721–730, 2009.

[19] M. E. A. Fidelis, R. D. Toledo Filho, F. de A. Silva, V. Mechtcherine, M. Butler, and S. Hempel, “The effect of accelerated aging on the interface of jute textile reinforced concrete,” Cem. Concr. Compos., vol. 74, pp. 7–15, Nov. 2016.

[20] F. Majstorović, V. Sebera, M. Mrak, S. Dolenec, M. Wolf, and L. Marrot, “Impact of metakaolin on mechanical performance of flax textile-reinforced cement-based composites,” Cem. Concr. Compos., vol. 126, p. 104367, Feb. 2022.

[21] M. Khorami and E. Ganjian, “Comparing flexural behaviour of fibre-cement composites reinforced bagasse: Wheat and eucalyptus,” Constr. Build. Mater., vol. 25, no. 9, pp. 3661–3667, 2011.

[22] E. Villar-Cociña, L. Rodier, H. Savastano, M. Lefrán, and M. F. Rojas, “A Comparative Study on the Pozzolanic Activity Between Bamboo Leaves Ash and Silica Fume: Kinetic Parameters,” Waste and Biomass Valorization, vol. 11, no. 4, pp. 1627–1634, Apr. 2020.

[23] V. Lilkov, I. Rostovsky, O. Petrov, Y. Tzvetanova, and P. Savov, “Long term study of hardened cement pastes containing silica fume and fly ash,” Constr. Build. Mater., vol. 60, pp. 48–56, 2014.

[24] S. Jianxia, “Durability Design of Concrete Hydropower Structures,” Compr. Renew. Energy, vol. 6, pp. 377–403, Jan. 2012.

[25] R. D. Tolêdo Filho, K. Ghavami, G. L. England, and K. Scrivener, “Development of vegetable fibre-mortar composites of improved durability,” Cem. Concr. Compos., vol. 25, no. 2, pp. 185–196, 2003.

[26] A. I. Nicoara et al., “End-of-Life Materials Used as Supplementary Cementitious Materials in the Concrete Industry,” Mater. 2020, Vol. 13, Page 1954, vol. 13, no. 8, p. 1954, Apr. 2020.

[27] B. Lothenbach, K. Scrivener, and R. D. Hooton, “Supplementary cementitious materials,” Cem. Concr. Res., vol. 41, no. 12, pp. 1244–1256, Dec. 2011.

[28] R. Banar, P. Dashti, A. Zolfagharnasab, A. M. Ramezanianpour, and A. A. Ramezanianpour, "A comprehensive comparison between using silica fume in the forms of water slurry or blended cement in mortar/concrete," J. Build. Eng., vol. 46, p. 103802, Apr. 2022.

[29] A. Mehta and D. K. Ashish, "Silica fume and waste glass in cement concrete production: A review," J. Build. Eng., vol. 29, p. 100888, May 2020.

[30] M. I. Khan and R. Siddique, "Utilization of silica fume in concrete: Review of durability properties," Resour. Conserv. Recycl., vol. 57, pp. 30–35, Dec. 2011.

[31] D. Shen, J. Kang, Y. Jiao, M. Li, and C. Li, "Effects of different silica fume dosages on early-age behavior and cracking resistance of high strength concrete under restrained condition," Constr. Build. Mater., vol. 263, p. 120218, Dec. 2020.

[32] N. C. Collier, "Transition and decomposition temperatures of cement phases - a collection of thermal analysis data," Ceram. - Silikaty, vol. 60, no. 4, pp. 338–343, 2016.

[33] R. Bottom, "Thermogravimetric Analysis," Princ. Appl. Therm. Anal., pp. 87–118, 2008.

[34] R. D. Toledo Filho, F. de A. Silva, E. M. R. Fairbairn, and J. de A. M. Filho, "Durability of compression molded sisal fiber reinforced mortar laminates," Constr. Build. Mater., vol. 23, no. 6, pp. 2409–2420, Jun. 2009.

[35] J. Claramunt, L. Fernández-Carrasco, H. Ventura, and M. Ardanuy, "Natural fiber nonwoven reinforced cement composites as sustainable materials for building envelopes," Constr. Build. Mater., vol. 115, pp. 230–239, 2016.

[36] RILEM Technical Committee 232-TDT (Wolfgang Brameshuber) et al., "Recommendation of RILEM TC 232-TDT: test methods and design of textile reinforced concrete: Uniaxial tensile test: test method to determine the load bearing behavior of tensile specimens made of textile reinforced concrete," Mater. Struct. Constr., vol. 49, no. 12, pp. 4923–4927, May 2016.

[37] M. Ramirez, J. Claramunt, H. Ventura, and M. Ardanuy, "Evaluation of the mechanical performance and durability of binary blended CAC-MK/natural fiber composites," Constr. Build. Mater., vol. In progres, 2019.

[38] J. Claramunt, H. Ventura, L. J. Fernández-carrasco, and M. Ardanuy, "Tensile and Flexural Properties of Cement Composites Reinforced with Flax Nonwoven Fabrics," Materials (Basel)., pp. 1–12, 2017.

[39] R. D. Toledo Filho, F. de A. Silva, E. M. R. Fairbairn, and J. de A. M. Filho, "Durability of compression molded sisal fiber reinforced mortar laminates," Constr. Build. Mater., vol. 23, no. 6, pp. 2409–2420, Jun. 2009.

[40] S. Goto, K. Suenaga, T. Kado, and M. Fukuhara, "Calcium Silicate Carbonation Products," J. Am. Ceram. Soc., vol. 78, no. 11, pp. 2867–2872, Nov. 1995.

[41] "A Practical Guide to Microstructural Analysis of Cementitious Materials," A Pract. Guid. to Microstruct. Anal. Cem. Mater., Oct. 2018.

[42] K. S. P. Karunadasa, C. H. Manoratne, H. M. T. G. A. Pitawala, and R. M. G. Rajapakse, "Thermal decomposition of calcium carbonate (calcite polymorph) as examined by in-situ high-temperature X-ray powder diffraction," J. Phys. Chem. Solids, vol. 134, pp. 21–28, Nov. 2019.

[43] M. Saidi and A. Gabor, "Iterative analytical modelling of the global behaviour of textile-reinforced cementitious matrix composites subjected to tensile loading," Constr. Build. Mater., vol. 263, p. 120130, 2020.

[44] M. Ardanuy, J. Claramunt, J. A. García-Hortal, and M. Barra, “Fiber-matrix interactions in cement mortar composites reinforced with cellulosic fibers,” Cellulose, vol. 18, no. 2, pp. 281–289, Apr. 2011.

[45] R. D. Tolêdo Filho, K. Scrivener, G. L. England, and K. Ghavami, “Durability of alkali-sensitive sisal and coconut fibres in cement mortar composites,” Cem. Concr. Compos., vol. 22, no. 2, pp. 127–143, Apr. 2000.

[46] J. Claramunt, L. J. Fernández-Carrasco, H. Ventura, and M. Ardanuy, “Natural fiber nonwoven reinforced cement composites as sustainableClaramunt, J., Fernández-Carrasco, L. J., Ventura, H., & Ardanuy, M. (2016). Natural fiber nonwoven reinforced cement composites as sustainable materials for building envelopes. Constructio,” Constr. Build. Mater., vol. 115, pp. 230–239, 2016.

[47] P. Sadrolodabaee, J. Claramunt, M. Ardanuy, and A. de la Fuente, “A Textile Waste Fiber-Reinforced Cement Composite: Comparison between Short Random Fiber and Textile Reinforcement,” Mater. 2021, Vol. 14, Page 3742, vol. 14, no. 13, p. 3742, Jul. 2021.